Characterisation of the interactions of RGL1; a negative regulator of gibberellin signalling

A thesis presented in partial fulfilment of the requirements for the degree of

Doctor of Philosophy

in

Biochemistry

Massey University, Palmerston North

New Zealand.

David John Sheerin

2010

Abstract

The gibberellins are a family of phytohormones that promote many aspects of plant development. Central to the function of gibberellins are the DELLA regulatory proteins. The DELLA proteins actively repress cell differentiation and elongation, but are degraded upon perception of gibberellin, thus relieving repression of gibberellin responses. The GID1-family gibberellin receptors and DELLA-specific F-box proteins are essential for the gibberellin-induced degradation of the DELLA proteins. Importantly, the direct interaction between gibberellin-bound GID1-family gibberellin receptors and the N-terminal domain of DELLA proteins is a prerequisite for proteasomal degradation through recruitment of the F-box proteins. To increase understanding of gibberellin signalling, I have characterised a gibberellin-dependent GID1-DELLA-F-box protein signalling switch in *Arabidopsis thaliana*. First, I have characterised a suite of anti-DELLA antibodies for detection of four endogenous *A. thaliana* DELLA proteins, GIBBERELLIC ACID-INSENSITIVE (GAI), REPRESSOR OF GA1-3 (RGA), RGA-LIKE-1 (RGL1), and RGA-LIKE-2 (RGL2). Using these monoclonal antibodies against the conserved motifs of DELLA proteins, I showed that residues Asp/Glu/Leu/Leu within the signature DELLA motif are not essential for interaction of RGL1 with GID1A. Further, *in vitro* interaction assays allowed modelling a two-step conformational change within the N-terminal domain of RGL1 upon interaction with gibberellin-bound GID1A. Together with interaction assays in yeast two- and three-hybrid systems, these experiments provided three clues to the mechanism of GID1A-RGL1-SLY1 gibberellin signalling switch: i) N- to C- inter-domain interactions of RGL1 regulate its accessibility to SLY1; ii) the N-terminal domain of RGL1 undergoes conformational rearrangement upon interaction with gibberellin-GID1A; iii) the conformational changes of the N-terminal domain of RGL1 primes the C-terminal domain for the recruitment of SLY1. I have also isolated two novel RGL1-interacting proteins, the myrosinase THIOGLUCOSIDE GLUCOHYDROLASE-2 (TGG2) and GERMIN-LIKE-PROTEIN-1 (GLP1), through affinity-purification from nuclear extract and mass spectrometry fingerprinting. Neither protein has yet been implicated in gibberellin signalling. Therefore, the identification of these novel components may help resolve several uncharacterised aspects of gibberellin signalling.

Acknowledgments

I would like to thank my supervisors, Dr Jasna Rakonjac, Dr William Jones, and Dr Toshi Foster for their advice and guidance. I would also like to thank the other members of both the Helipad lab and the Plant and Food Research Immunology group for their helpful support.

I am grateful to Julian Spagnuolo who assisted in the optimisation of quenching conditions used for deuterium exchange mass spectrometry. I also thank members of Prof. Nicholas Harberd's research group at the John Innes Centre for supplying *A. thaliana* plant material and reagents for the determination of monoclonal antibody specificity.

This project was supported by grants from the Foundation for Research Science and Technology (No. C06X0207) and the Agricultural and Marketing Research and Development Trust (No. 20585).

Table of contents

Abstract ii

Acknowledgements iii

List of figures vii

List of tables ix

Abbreviations x

Chapter 1. Introduction 1

1.1 DELLA proteins 2

1.2 Structure and function of the DELLA proteins 6

1.3 Transcriptional regulation mediated by DELLA proteins 8

1.4 A signal transduction pathway for gibberellin perception 12

1.4.1 Production of bioactive gibberellins 13

1.4.2 Perception of bioactive gibberellins 15

1.4.3 Nuclear localised gibberellin receptors 17

1.4.4 Gibberellin-induced DELLA protein degradation 22

1.5 Additional gibberellin signalling components 26

1.6 Phytohormone cross-signalling 28

1.7 An integrated model for gibberellin signalling 30

1.8 Statement of problem and significance 32

1.9 Hypothesis 33

Chapter 2. Material and methodology 34

2.1 Materials and reagents 34

2.2 General methodology 35

2.2.1 Molecular biology 35

2.2.2 Protein electrophoresis 36

2.2.3 Western blotting 36

2.3 *Escherichia coli* strains and growth conditions 37

2.4 *Saccharomyces cerevisiae* strains and culture conditions 37

2.5 *Arabidopsis thaliana* lines and growth conditions 38

2.6 Total *Arabidopsis thaliana* protein extraction 38

2.7 *Arabidopsis thaliana* nuclear protein extraction 38
2.8 Preparation of Rabbit polyclonal antisera 39
2.9 Anti-DELLA monoclonal antibodies 39
2.10 Construction of recombinant plasmids 40
2.11 Yeast two- and three-hybrid interaction reporter assays 41
2.12 Recombinant protein expression and purification 42
2.13 *in vitro* interaction experiments 43
2.13.1 Analysis of association and dissociation kinetics 44
2.14 Deuterium exchange mass spectrometry 44
2.15 Affinity purification of RGL1-interacting proteins 45
2.16 Mass spectrometry fingerprinting 45

Chapter 3. Characterisation of antibodies against *Arabidopsis thaliana* DELLA proteins 59
3.1 Detection of endogenous *Arabidopsis thaliana* DELLA proteins 62
3.1.1 Identification of endogenous *Arabidopsis thaliana* DELLA proteins 65
3.2 Mapping of anti-DELLA antibody epitopes 75

Chapter 4. Characterisation of the interactions of RGL1 78
4.1 Characterisation of the gibberellin-dependent GID1A:RGL1 interaction 80
4.1.1 Requirement of the DELLA and TVHYNP motifs 84
4.1.2 Effects of bioactive gibberellins on interaction strength 86
4.1.3 DELLA and TVHYNP motif competition analysis 89
4.1.4 Characterisation of interaction kinetics 98
4.2 Gibberellin-dependent recruitment of SLY1 to RGL1 108
4.2.1 RGL1 inter-domain interactions 110
4.3 Prediction of the surface accessibility of Q272 116
4.3.1 Prediction of the RGL1 GRAS domain tertiary structure 118

Chapter 5. Identification of novel RGL1-interacting proteins 120
5.1 Affinity purification of RGL1-interacting proteins 121
5.2 Identification of isolated RGL1-interacting proteins 123

Chapter 6. Discussion 130
6.1 Detection of endogenous *Arabidopsis thaliana* DELLA proteins 130
6.2 Contacts of the Asp/Glu/Leu/Leu α-helix of RGL1 are not essential for the GID1A/GA_4:RGL1 interaction 132
6.3 The N-terminal DELLA domain of RGL1 undergoes conformational changes upon interaction with gibberellin-bound GID1A 134
6.4 GID1A/GA_4 recruits SLY1 to RGL1 through alteration of the conformational state to RGL1 135
6.5 Novel RGL1-interacting proteins 140

Conclusions and future directions 143

Appendix A 146
Appendix B 149
Appendix C 156

References 158

List of figures

Figure 1.1. Gibberellin signalling mutant phenotypes. 3

Figure 1.2. DELLA protein domain organisation. 7

Figure 1.3. Gibberellin biosynthetic pathway. 14

Figure 1.4. Structural basis of the DELLA-GID1A interaction. 21

Figure 1.5. Nuclear molecular switch model. 24

Figure 1.6. A model for DELLA integrated signalling. 31

Figure 3.1. Stabilisation of *A. thaliana* endogenous DELLA proteins. 64

Figure 3.2. Characterisation of the affinity-purified anti-RGL1 polyclonal antibody R1PC. 66

Figure 3.3. Detection of endogenous DELLA proteins in lines competent in gibberellin biosynthesis. 68

Figure 3.4. Characterisation of the monoclonal antibody BC9. 69

Figure 3.5. Characterisation of the monoclonal antibody AD7. 71

Figure 3.6. Characterisation of the monoclonal antibody AB8. 72

Figure 3.7. Characterisation of the monoclonal antibody BB7. 73

Figure 3.8. Partial mapping of anti-DELLA monoclonal antibody epitopes. 76

Figure 4.1. Gibberellin-dependent *A. thaliana* GID1A-C:DELLA interactions. 82

Figure 4.2. Gibberellin uptake by *S. cerevisiae*. 83

Figure 4.3. Characterisation of the gibberellin-dependent GID1A:RGL1 interaction. 85

Figure 4.4. Comparison of the GA_3- and GA_4-dependent GID1A-C:RGL1 interaction *in vitro*. 88

Figure 4.5. Mapping of RGL1 residues essential for interaction with GID1A. 90

Figure 4.6. GID1A-mediated competition of monoclonal antibody binding to the N-terminal RGL1 DELLA domain. 95

Figure 4.7. Structural prediction of the RGL1 N-terminal DELLA domain when in complex with GID1A. 97

Figure 4.8. Kinetic characterisation of the gibberellin-dependent GID1A:$RGL1^{1-137}$ interaction. 99

Figure 4.9. Surface accessibility mapping of $RGL1^{1-137}$. 101

Figure 4.10. Conformational change kinetic modelling of the gibberellin-dependent GID1A:RGL1$^{1-137}$ interaction. 103
Figure 4.11. Characterisation of MBP-GID1A aggregation. 105
Figure 4.12. Gibberellin-dependent recruitment of SLY1 to RGL1. 109
Figure 4.13. Domain analysis of the gibberellin/GID1A-dependent recruitment of SLY1 to RGL1. 111
Figure 4.14. Spatial domain separation affects on gibberellin/GID1A-dependent recruitment of SLY1 to RGL1. 114
Figure 4.15. Conservation of the VHIID motif and downstream Q272 amongst *A. thaliana* GRAS proteins. 117
Figure 4.16. Prediction of the RGL1 GRAS domain tertiary structure. 119
Figure 5.1. Affinity purification of RGL1 N-terminal domain interacting proteins. 122
Figure 5.2. Alignment of closely related GLP protein sequences. 128
Figure 5.3. Evaluating an *in vivo* GLP1:RGL1 interaction. 129
Figure 6.1. Proposed model of gibberellin-dependent recruitment of SLY1 to RGL1. 138

Figure A.1. Immobilised RGL1 N-terminal domain binding capacity. 146
Figure A.2. Gibberellin saturation of GID1A. 147
Figure A.3. Gibberellin-dependent binding of RGL1$^{1-137}$ to immobilised GID1A. 148

List of tables

Table 2.1 *Escherichia coli* strains 47
Table 2.2 *Saccharomyces cerevisiae* strains 48
Table 2.3 *Arabidopsis thaliana* lines 53
Table 2.4 Plasmids 54
Table 2.5 Oligonucleotides 56
Table 3.1 Antibody specificity for recombinant *A. thaliana* DELLA proteins 61
Table 3.2 Antibody specificity for endogenous *A. thaliana* DELLA proteins 74
Table 4.1 Two-state conformational change model 107
Table 5.1 Mass spectrometry analysis of RGL1 interacting protein p24 125
Table 5.2 Mass spectrometry analysis of RGL1 interacting protein p64 126

Abbreviations

3-AT	3-amino-1,2,4- trizol
ABA	abscisic acid
cDNA	complementary deoxyribonucleic acid
cGMP	cyclic guanosine monophosphate
Col-0	Columbia-0
CPS	*ent*-copalyl diphosphate synthase
CTR1	*Arabidopsis thaliana* CONSTITUTIVE TRIPLE RESPONSE-1
D1	*Oryza sativa* DWARF-1
D27	27 residue synthetic DELLA motif peptide
DMSO	dimethyl sulfoxide
DTT	1,4-dithiothreitol
EDTA	ethylene-diamine-tetra-acetic acid
EIN3	*Arabidopsis thaliana* ETHYLENE INSENSITIVE-3
GA_1	gibberellin A1
GA_3	gibberellin A3
GA_4	gibberellin A4
GA1	*Arabidopsis thaliana* GA REQUIRING 1 (CPS)
GA2ox	GA2-OXIDASE
GA3ox	GA3-OXIDASE
GA20ox	GA20-OXIDASE
GAI	*Arabidopsis thaliana* GIBBERELLIC ACID-INSENSITIVE
GARE	gibberellic acid responsive element
LC-ESI-MS/MS	liquid chromatography electrospray ionisation quadrapole-time-of-flight coupled mass spectrometry
LC-MS	liquid chromatography coupled mass spectrometry
GID1	*Oryza sativa* GIBBERELLIN-INSENSITIVE DWARF-1
GID1A	*Arabidopsis thaliana* GID1-LIKE-A
GID1B	*Arabidopsis thaliana* GID1-LIKE-B
GID1C	*Arabidopsis thaliana* GID1-LIKE-C
GID2	*Oryza sativa* GIBBERELLIN-INSENSITIVE DWARF-2
GFP	*Aequorea victoria* GREEN FLUORESCENT PROTEIN

GLP1	*Arabidopsis thaliana* GERMIN-LIKE-PROTEIN-1
$GLP1^{\Delta SS}$	GLP1, lacking N-terminal secretion signal sequence
GST	*Schistosoma japonica* GLUTATHIONE S-TRANSFERASE
GUS	*Escherichia coli* β-D-GLUCURONIDASE
HA	*Influenza* HAEMAGGLUTININ epitope tag
HEPES	4-(2-hydroxyethyl)-1-piperazineethanesulfonic acid
HGP	heterotrimeric G-protein
HIS3	*Saccharomyces cerevisiae* IMIDAZOLEGLYCEROL-PHOSPHATE DEHYDRASE
HSIMYB	*Hordeum vulgare* SPY INTERACTING MYB
HSINAC	*Hordeum vulgare* SPY INTERACTING NAC
IAA	indole-acetic acid
IPTG	isopropylthio-β-D-galactoside
Ler	Landsberg *erecta*
MBP	*Escherichia coli* MALTOSE BINDING PROTEIN
MBP-β-gal	MBP- fusion to β-GALACTOSIDASE-α
MG132	proteasome inhibitor Z-Leu-Leu-Leu-al
O-GlcNAc	*O*-linked *N*-acetyl glucosamine
$OD_{420/600}$	optical density measured at either 420 or 600 nm
ONPG	*O*-nitrophenyl-β-D-galactopyranoside
PAGE	poly-acrylamide gel electrophoresis
PBS	phosphate buffered saline
PCR	polymerase chain reaction
PEG-4000	poly-ethylene glycol-4000
PHOR1	*Solanum tuberosum* PHOTOPERIOD-RESPONSIVE-1
PIF3	*Arabidopsis thaliana* PHYTOCHROME INTERACTING FACTOR-3
PIF4	*Arabidopsis thaliana* PHYTOCHROME INTERACTING FACTOR-4
PMSF	phenyl-methyl-sulfonyl-fluoride
RGA	*Arabidopsis thaliana* REPRESSOR OF GA1-3
RGL1	*Arabidopsis thaliana* RGA-LIKE-1
$RGL1^{\Delta DELLA}$	17 residue DELLA motif deletion of RGL1
$RGL1^{\Delta TVHYNP}$	18 residue TVHYNP motif deletion of RGL1

$RGL1^{Q272R}$	glutamine 272-arginine replacement of RGL1
RGL2	*Arabidopsis thaliana* RGA-LIKE-2
RGL3	*Arabidopsis thaliana* RGA-LIKE-3
SCF	SKP-CULLIN-F-BOX E3 Ubiquitin ligase complex
SDS	sodium dodecyl sulfate
SHI	*Arabidopsis thaliana* SHORT-INTERNODES
SLN1	*Hordeum vulgare* SLENDER-1
SLR1	*Oryza sativa* SLENDER RICE-1
SLY1	*Arabidopsis thaliana* SLEEPY-1
$SLY1^{E138K}$	glutamic acid 138 lysine replacement of SLY1
SPY	*Arabidopsis thaliana* SPINDLY
T21	21 residue synthetic TVHYNP motif peptide
TGG2	*Arabidopsis thaliana* THIOGLUCOSIDE GLUCOHYDROLASE-2
TRIS	tris (hydroxymethyl) aminomethane
Tween-20	polysorbate-20
YFP	YELLOW FLUORESCENT PROTEIN (GFP mutant)

Chapter 1

Introduction

The world is faced with an ever growing need of plant crops for food. Furthermore, these plants are also desired as a source of renewable fuel. Arable land is limited; therefore, new approaches to enable increased yields or the use of infertile land must be developed. Understanding how plants respond to their environment will be crucial for the substantial increases in crop production that are required to meet the world's needs.

High yield crop lines were previously selected for with limited knowledge of the processes involved in plant responses to their environment and those that regulate the storage of nutrients. There is potential for further advances in crop production through understanding these mechanisms. These advances may allow tailoring of plants to the environment; thus relieving pressures on the use of fresh water and non-renewable resources.

Amongst many genetic elements linked to increasing the yields of grain are genes encoding components of gibberellin signalling. Gibberellin is a phytohormone that controls various aspects of plant development; including seed germination, stem and root elongation, and floral development (Fleet and Sun, 2005; Swain and Singh, 2005). More recently this pathway has been shown to be involved in plant responses to many environmental conditions; including light and salt stress (Achard *et al.*, 2006; Achard *et al.*, 2007b).

Gibberellins, including gibberellic acid (GA_3), are tetracyclic diterpenoids produced by plants and also by some plant-associated fungi and bacteria (Hedden *et al.*, 2001). Gibberellins were first isolated from the fungus *Gibberella fujikuroi*, which causes foolish seedling disease (*Bakanae*) in rice, where stems elongate uncontrollably and collapse. There are 136 different gibberellic acids identified to date, numbered in order of their discovery (http://www.plant-hormones.info/gibberellins.htm). However, only a

few gibberellic acids are biologically active; other forms include precursors of biosynthesis and catabolically inactivated products (Hedden and Phillips, 2000). The major active gibberellins produced by plants are GA_1, and GA_4, while the most agriculturally used is GA_3, produced by a fungus *G. fujikuroi* (Eriksson *et al*., 2006; Fei *et al.*, 2004; Talon *et al.*, 1990; Yang *et al.*, 1995).

Following the 'green revolution' a number of enhanced yield crop lines were found to have mutations that reduce the sensitivity of plants to gibberellins (Peng *et al.*, 1999). Prominent amongst these 'green revolution' genes are a family now known to encode the DELLA proteins, named after a conserved amino acid motif (Peng *et al.*, 1997; Peng *et al.*, 1999). Hence, DELLA genes have been labelled as 'green revolution genes' (Peng *et al.*, 1997). There has been substantial research to understand how these genes function in plant development in the hope of increasing crop yields further, and more recently to create stress-resistant plants.

1.1 DELLA proteins

Research on the functions of gibberellins resulted in the identification of the *Arabidopsis thaliana DELLA* gene *GIBBERELLIC ACID INSENSITIVE* (*GAI*) (Peng *et al.*, 1997). The *gai-1* mutation results in dwarf plants similar to gibberellin-deficient mutants, exhibiting broad dark green leaves, low germination frequencies, and are late in forming an underdeveloped inflorescence (Figure 1.1) (Koornneef *et al.*, 1985). However, unlike gibberellin-deficient mutants, the *gai-1* phenotype cannot be rescued by treatment with exogenous bioactive gibberellins (Koornneef *et al.*, 1985). This would imply that *GAI* is a positively acting component of gibberellins signal transduction pathway. However, further research revealed *GAI* is in fact a negative regulator, and that the *gai-1* in frame deletion mutation is a gain-of-function mutation (Peng *et al.*, 1997).

Figure 1.1. Gibberellin signalling mutant phenotypes. Comparison of mature *Arabidopsis thaliana* plants: A, semi-dwarf phenotype, either gibberellin-deficient or insensitive; B, severe dwarf phenotype, gibberellin-insensitive; C, slender phenotype, constitutive gibberellin signalling. Scale indicates 5 cm (Wen and Chang, 2002; image reproduced with permission from the American Society of Plant Biologists, www.plantcell.org Copyright American Society of Plant Biologists).

DELLA genes have been characterised in several plant species; including rice (*Oryza sativa*) *SLENDER RICE-1* (*SLR1*), and barley (*Hordeum vulgare*) *SLENDER-1* (*SLN1*) (Fu *et al.*, 2002; Ikeda *et al.*, 2001; Silverstone *et al.*, 1998; Silverstone *et al.*, 1997). However, *DELLA* genes function differently in Bryophytes and Lycophytes, and are reported to have evolved a role in gibberellin signalling during land plant development (Yasumura *et al.*, 2007). The Eudicotyledons analysed thus far, including *A. thaliana*, encode multiple DELLA proteins that may function redundantly. Alternatively, multiple DELLA genes could allow these plants to respond in more complex ways to environmental stimulus.

In addition to the aforementioned *GAI*, *A. thaliana* encodes four other *DELLA* genes: *REPRESSOR OF GA1-3* (*RGA*), *REPRESSOR OF GA1-3-LIKE-1* (*RGL1*), *REPRESSOR OF GA1-3-LIKE-2* (*RGL2*), and *REPRESSOR OF GA1-3-LIKE-3* (*RGL3*) (Lee *et al.*, 2002; Silverstone *et al.*, 1998; Silverstone *et al.*, 1997; Wen and Chang, 2002). The biological functions of the five *A. thaliana DELLA* genes have been investigated through T-DNA insertion lines. However, among the five individual *DELLA* disruption lines, only loss of either *RGA* or *RGL2* have perceptible effects on plant development (Tyler *et al.*, 2004). Loss of *RGL2* in the gibberellin-deficient *ga1-3* (*GA REQUIRING-1*) background allows gibberellin-independent germination, whereas loss of *RGA* partially rescues the dwarf phenotype of *ga1-3* vegetative tissues (Lee *et al.*, 2002; Tyler *et al.*, 2004). Immuno-detection of both RGA and RGL2 protein levels in imbibed seeds revealed that RGA is highly abundant when compared to RGL2, yet loss of *RGA* does not affect germination phenotypes, indicating a unique role for *RGL2* in seed germination (Tyler *et al.*, 2004).

DELLA T-DNA insertion lines have been crossed into both wild-type and gibberellin-deficient (*ga1-3*) genetic backgrounds (Cheng *et al.*, 2004; Tyler *et al.*, 2004). The rescue of dwarfed vegetative growth resulting from lack of gibberellins is mediated by the loss of both *RGA* and *GAI* in combination (Cheng *et al.*, 2004; Dill *et al.*, 2001; King *et al.*, 2001). This correlates with the restraint model, which states that DELLA proteins actively repress gibberellin responses until gibberellin-induced degradation relieves this repression (Hardtke, 2003; King *et al.*, 2001; Peng *et al.*, 1997; Richards *et al.*, 2001).

Gibberellin deficiency also results in infertility through arrest of floral development in *A. thaliana* (Cheng *et al.*, 2004). Detailed analysis of floral phenotype in lines lacking multiple *DELLA* genes has revealed that specifically stamen elongation and microsporogenesis fail to progress past floral stage 10 (Cheng *et al.*, 2004; Smyth *et al.*, 1990). In these plants stamen cells fail to elongate, and microspores fail to correctly undergo mitotic divisions following meiosis (Cheng *et al.*, 2004). A similar phenotype of arrested anther development is observed in gibberellin-deficient rice, where tapetal cells surrounding the microspores fail to undergo programmed cell death and instead expand and interfere with microspore division (Aya *et al.*, 2009).

By rescue of gibberellin-deficient floral developmental defects by deletion of *DELLA* genes in *A. thaliana*, it has been shown that *GAI*, *RGA*, *RGL1* and *RGL2* are each involved in repressing this stage of development (Cheng *et al.*, 2004; Tyler *et al.*, 2004). The disruption of these four *DELLA* genes is sufficient to rescue floral development and plant fertility, whilst the deletion of both *RGA* and *RGL2* is sufficient for partial rescue of fertility (Cheng *et al.*, 2004; Tyler *et al.*, 2004).

The functions of these *DELLA* genes in *A. thaliana* in developmental responses to gibberellin are consistent with their expression patterns (Tyler *et al.*, 2004). *RGA* is expressed in most tissues at constitutive levels, consistent with this genes functions in vegetative growth, seedling development, and floral development (Tyler *et al.*, 2004). *RGA* is also the most highly expressed of the *DELLA* genes, and is the only *DELLA* gene that shows any perceptible differences in vegetative growth as a single *DELLA* loss-of-function mutation (Tyler *et al.*, 2004). *GAI* has effects on most stages of development similar to *RGA*, particularly vegetative tissues, albeit to a small extent in comparison to *RGA*, consistent with its comparatively lower level of expression in many tissues (Tyler *et al.*, 2004). *RGL2* transcript is most abundant in imbibed seeds, and in floral tissues, whilst *RGL1* is most abundant in floral tissues (Tyler *et al.*, 2004). Unlike *RGA* and *GAI*; *RGL1*, *RGL2*, and *RGL3* show tissue specific expression. *RGL1* expression localises to the ovule and developing anthers, as shown by *in situ* hybridisation, whilst *RGL2* is expressed in the radicle for approximately 24 hours following imbibition of seeds (Lee *et al.*, 2002; Wen and Chang, 2002). *RGL3* expression is primarily localised to germinating seeds alongside *RGL2* (Tyler *et al.*, 2004).

Altogether, the current experimental evidence suggests that the *DELLA* genes are partially functionally redundant, but do have different tissue expression patterns. However, the resolution of these techniques is limited to plant organs. Yet unidentified differences in distribution of individual DELLA proteins amongst tissues within organs likely account for developmental functions of specific DELLA proteins.

1.2 Structure and function of the DELLA proteins

The *DELLA* genes encode proteins that belong to the GRAS protein family, which is unique to plants (Pysh *et al.*, 1999). The GRAS proteins are named after the first sequenced members (GAI, RGA, and SCARECROW), and are putative transcription regulators based on limited similarities to the mammalian nuclear receptors (Pysh *et al.*, 1999). The DELLA subfamily of the GRAS proteins is further characterised by an N-terminal DELLA domain that is highly variable, with the exception of two highly conserved motifs: DELLA, and TVHYNP (Figure 1.2). The rice genome encodes only one *DELLA* gene, *SLR1*; the lack of redundancy in this organism allowed genetic dissection of the roles DELLA protein domains and key motifs in gibberellin signalling.

Deletion analysis of *SLR1* has shown that the DELLA and TVHYNP motifs, and a non conserved spacer separating them, are all required for gibberellin perception, as deletions of these regions resulted in gibberellin-insensitive plants (Itoh *et al.*, 2002). Deletion of a region rich in serine and theronine residues within the non-conserved N-terminal DELLA domain also resulted in dwarf plants. However, these plants are still able to perceive gibberellin, suggesting a possible role in perception of other regulatory signals. Conversely, deletion mutations of regions of the C-terminal highly conserved GRAS domain resulted in recessive slender phenotypes, corresponding to constitutive gibberellin responses (Itoh *et al.*, 2002). A non-standard leucine zipper (leucine heptad repeat) predicted within the GRAS domain may have functions in homo-dimerisation, though no DELLA-DELLA interactions have been confirmed (Itoh *et al.*, 2002). It is more likely the putative leucine zipper mediates interactions of DELLA proteins with as yet unknown binding partners

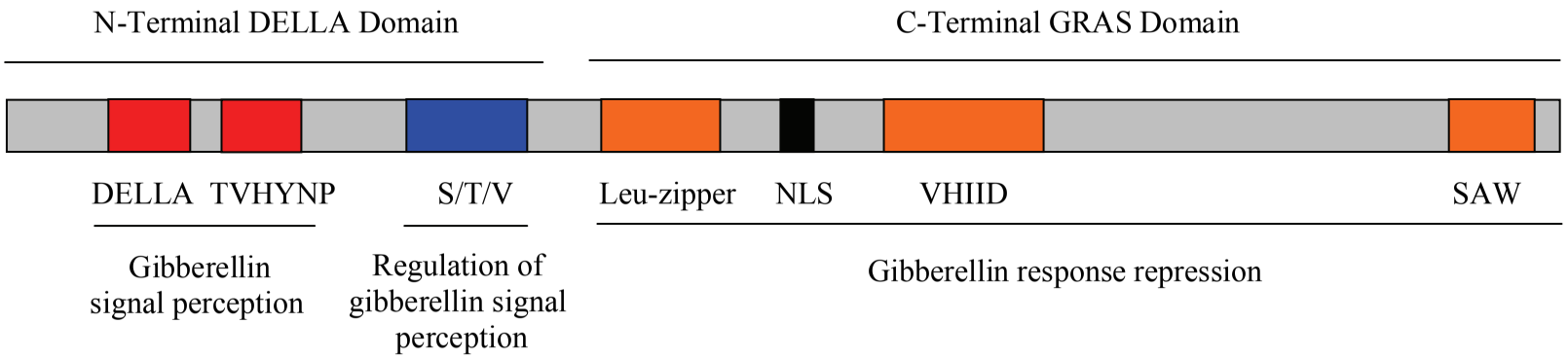

Figure 1.2. DELLA protein domain organisation. The DELLA N-terminal domain is required for gibberellin perception, whereas the C-terminal GRAS domain is required for repression of gibberellin responses. Conserved motifs, DELLA and TVHYNP, are essential for gibberellin perception (red). The serine/threonine rich region, poly S/T/V, enhances gibberellin perception (blue). Leu-zipper, VHIID, and SAW motifs, are essential for repressive function (orange). NLS, nuclear localisation signal. (Itoh *et al.*, 2002; Pysh *et al.*, 1999).

The first isolated DELLA gene mutation, *gai-1*, is an in-frame deletion of the DELLA motif (Peng *et al.*, 1997). Similar mutations have also been introduced into *RGA* and *RGL1* to study the functions of these genes (Silverstone *et al.*, 1998; Wen and Chang, 2002). These mutations act as dominant repressors of gibberellin signalling, and render plants insensitive to gibberellins (Peng *et al.*, 1997; Silverstone *et al.*, 1998; Wen and Chang, 2002).

Transgenic plants expressing GREEN FLOURESCENT PROTEIN (GFP) recombinant fusions to DELLA proteins have shown DELLA proteins to be nuclear localised (Dill *et al.*, 2001; Fleck and Harberd, 2002; Itoh *et al.*, 2002; Silverstone *et al.*, 2001; Wen and Chang, 2002). These GFP fusions have also revealed that DELLA proteins are degraded soon after gibberellin perception (Dill *et al.*, 2001; Itoh *et al.*, 2002; Silverstone *et al.*, 2001). However, DELLA proteins lacking the leucine zipper region are not degraded on gibberellin perception, yet they do not repress gibberellin responses, suggesting roles of this region in both gibberellin perception, and repressive activities (Itoh *et al.*, 2002).

1.3 Transcriptional regulation mediated by DELLA proteins

MicroArrays have revealed changes in expression of large sets of genes following gibberellin treatment of gibberellin-deficient *A. thaliana* mutants (Cao *et al.*, 2006; Hou *et al.*, 2008; Nemhauser *et al.*, 2006; Zentella *et al.*, 2007). Comparisons between wild-type, gibberellin-deficient mutants, and multiple DELLA gene deletions have revealed subsets affected by the degradation of DELLA proteins (Cao *et al*., 2006; Nemhauser *et al.*, 2006). A gain-of-function mutant form of *RGA*, $rga^{\Delta 17}$; fused to the glucocorticoid receptor, was used to further define early DELLA-responsive genes important for seedling development (Zentella *et al.*, 2007). The glucocorticoid receptor fusion retains the protein to the endoplasmic reticulum, preventing DELLA protein function, until release induced using dexamethasone (Aoyama and Chua, 1997). From a dataset of 475 genes differentially expressed by seedlings treated with dexamethasone to induce $rga^{\Delta 17}$ function, only 14 genes are in common with those differentially expressed within 1 hour

gibberellin treatment (Zentella *et al.*, 2007). Several genes known to function in gibberellin biosynthesis (*GIBBERELLIC ACID-20-OXIDASE-2*, *GA20ox2* and *GIBBERELLIC ACID-3-OXIDASE-1, GA3ox1*), and gibberellin perception (*GIBBERELLIN-INSENSITIVE-DWARF-1-LIKE-A*, *GID1A*; and *GIBBERELLIN-INSENSITIVE-DWARF-1-LIKE-B*, *GID1B*) are upregulated via RGA function (Zentella *et al.*, 2007). Furthermore, TAP-tagged RGA was found to be associated with the promoter regions of 8 of the 14 identified targets in chromatin-immunoprecipitation experiments (Zentella *et al.*, 2007). Thus DELLA proteins may directly bind promoter elements, or more likely interact with transcription factors to regulate transcription.

Similar expression experiments have been used to investigate DELLA downstream targets during floral development, using a glucocorticoid receptor fusion of RGA to repress constitutive responses in a *ga1-3*, *rgl2-1*, *rga-t2* background (Hou *et al.*, 2008). Comparison of 806 RGA-regulated genes in floral tissues again revealed small overlap with previous studies of gibberellin and DELLA deficient mutants; interestingly only 29 target genes overlapped with RGA regulated genes in seedling tissues, confirming the presence of unique tissue-dependent transcriptional targets (Cao *et al.*, 2006; Hou *et al.*, 2008; Zentella *et al.*, 2007). Floral targets appear to largely regulate changes in metabolism important for stamen and pollen development (Hou *et al.*, 2008). Changes in expression of target genes, detected by *in situ* hybridisation, localise to just these tissues, consistent with the developmental roles of gibberellin signalling (Hou *et al.*, 2008).

More complex analysis of the targets of gibberellin signalling in rice floral development shows most regulatory effects are mediated through relief of DELLA protein repression (Aya *et al.*, 2009). A total of 390 genes were identified as being upregulated and 480 genes downregulated in floral tissues in response to gibberellin, determined by comparison of wild-type and a gibberellin-deficient rice mutant, *cps1-1* (*ENT-COPALYLY DIPHOSPHATE SYNTHASE-1*) (Aya *et al.*, 2009). Two mutations, *gid2-5* (*GIBBERELLIN-INSENSITIVE-DWARF-2*) and *gid1-4* (*GIBBERELLIN-INSENSITIVE-DWARF-1*), both blocking gibberellin-induced SLR1 degradation, generated expression patterns closely matching that resulting from *cps1-1* (Aya *et al.*, 2009). These results show that almost all roles of gibberellin in rice floral development are mediated by DELLA protein functions; this is in contrast to *A. thaliana* where only 67 % of

gibberellin upregulated and 44 % of down-regulated genes were attributed to *DELLA* gene function (Aya *et al.*, 2009; Cao *et al.*, 2006). The *A. thaliana* gene expression datasets are likely biased due to the presence of a functional *RGL3* gene; hence, not all DELLA-dependent regulation was abolished in these plants, possibly accounting for the observed differences between rice and *A. thaliana* based experiments (Cao *et al.*, 2006).

Although DELLA proteins have not yet been shown to interact with DNA directly, they have been found to interact with PHYTOCHROME INTERACTING FACTOR-3 AND -4 (PIF3, and PIF4) (de Lucas *et al.*, 2008; Feng *et al.*, 2008). PIF3 and PIF4 are basic helix-loop-helix (bHLH) class transcription factors involved with far-red light perception (Chen *et al.*, 2004). PIF proteins are inactivated through direct binding of far-red light activated phytochrome phyB, during etiolation (Chen *et al.*, 2004). *In vivo* split YELLOW FLUORESCENT PROTEIN (YFP) and yeast two-hybrid assays show that RGA can also interact directly with either PIF3 or PIF4 (de Lucas *et al.*, 2008; Feng *et al.*, 2008). Furthermore, the presence of RGA inhibits the binding activity of PIF3 and PIF4 for their target genes in chromatin-immunoprecipitation and electromobilty shift assays; this is accompanied by inhibition of reporter fusions to gibberellin-dependent genes (de Lucas *et al.*, 2008; Feng *et al.*, 2008). This is the first reported function of a DELLA protein as a regulator of a transcription factor thus far. However, it is likely that similar mechanisms are involved in DELLA-dependent regulation of many other gibberellin-regulated genes.

In the aleurone tissue of seeds, the effect of gibberellins is required to release nutrients for germination. The enzymes required for the breakdown of stored nutrients include α-amylases, the expression of which is upregulated in response to gibberellins (Kaneko *et al.*, 2004). This event has been shown to be mediated by the gibberellin upregulated expression GAMYB transcription factors (Gubler *et al.*, 2002; Gubler *et al.*, 1995). GAMYB was identified in barley as having gibberellin-induced expression in aleurone cells by measuring mRNA levels from plants treated with gibberellins, or the gibberellin biosynthesis inhibitor paclobutrazol (Gubler *et al.*, 2002). Barley GAMYB is also upregulated in the absence of *de novo* protein synthesis, and is even upregulated in response to the translation inhibitor cyclohexamide (Gubler *et al.*, 1995). Therefore, GAMYB activation is both transcription and translation independent. Barley GAMYB has been shown to bind directly to a gibberellic acid-responsive-element (GARE,

TAACAA) within the promoter region of α-amylase encoding genes and activate their expression (Gubler *et al.*, 1995). Importantly, GAMYB induction is repressed by a DELLA gain-of-function mutation, *sln1-d* (Gubler *et al.*, 2002).

GAMYBs have also been found to function in gibberellin-dependent floral development during short days. Barley GAMYB, and two *A. thaliana* homologues GAMYB33 and GAMYB65, are required for correct anther development (Millar and Gubler, 2005; Murray *et al.*, 2003). Histochemical visualisation of the localisation of GAMYB33 and GAMYB65 using promoter:GUS fusions revealed that expression localises to developing tissues including anthers in floral tissue and the radicle in imbibed seeds (Millar and Gubler, 2005).

The role of rice *GAMYB* in gibberellin-dependent seed germinations floral development was also studied in microArray expression studies. Rice plants with null mutations of *GAMYB* arrest during floral development with similar phenotypes to gibberellin-deficient mutants (Aya *et al.*, 2009). Comparison of GAMYB regulated genes revealed a similar gene set to those regulated by gibberellin, and those requiring DELLA-dependent signalling (Aya *et al.*, 2009; Tsuji *et al.*, 2006). A large portion of gibberellin-induced genes in rice flowers were found to require *GAMYB* for up-regulation (Aya *et al.*, 2009). In a similar fashion, gibberellin-induced genes in aleurone also require *GAMYB*, however when datasets are compare there is almost no overlap between aleurone and floral tissue data (Tsuji *et al.*, 2006). Furthermore, *GAMYB* activates expression of gibberellin-induced genes in anthers by direct binding to promoter element, as shown by gel-shift assays (Aya *et al.*, 2009). GAMYB function *in vivo* was confirmed by way of overexpression of a glucocorticoid receptor fusion enabling 3-10 fold induction of target genes in the absence of *de novo* protein synthesis (Aya *et al.*, 2009). Together this data clearly show that GAMYBs function downstream of DELLA proteins in Poaceae, though this is not as clear in *A. thaliana*.

The micro RNA (miRNA) miR159 has been shown to function in regulation of gibberellin responses in *A. thaliana* (Achard *et al.*, 2004; Tsuji *et al.*, 2006). miR159 was shown to target a conserved region within *A. thaliana GAMYB* mRNA. Gibberellin increases the abundance of miR159, which in turn targets *GAMYB* mRNA for degradation (Achard *et al.*, 2004). miR159 has been proposed to act as a feed back loop

to regulate *GAMYB*, as GAREs are present within its parent RNA promoter. However, it has also been suggested that miR159 may have important functions in determining tissue specificity of *GAMYB* expression (Achard *et al.*, 2004; Millar and Gubler, 2005).

GAMYBs appear to function downstream of the DELLA proteins. Therefore, it was unclear why changes in their expression were not detected in global gene expression studies (Cao *et al.*, 2006). Although they are regulated by miR159 at a post-transcriptional level, this should affect GAMYB mRNA abundance. The identification of methylation based regulation involving the 1st intron within GAMYB genes has revealed a method of gibberellin-dependent regulation, but the processes involved are not yet known (Washio and Morikawa, 2006). It is possible that known GAMYBs are only upregulated at specific stages of development such as seed germination and floral initiation. Other MYB genes were up-regulated in these seedling and floral datasets. Therefore, specific MYB up-regulation may act as a mechanism for tissue specific responses. Alternatively, it is possible that DELLA proteins may regulate GAMYB function through post-translational processes either directly or in-directly.

1.4 A signal transduction pathway for gibberellin perception

Gibberellins are produced by plants through a biosynthetic pathway from geranyl-geranyl-diphosphate, an intermediate of the isoprenoid biosynthetic pathway (Figure 1.3) (Hedden and Phillips, 2000). Regulation of the production of bioactive gibberellins is primarily mediated through expression of the final catabolic enzymes required for activation and inactivation, GA20ox (GA20-OXIDASE)/GA3ox (GA3-OXIDASE) and GA2ox (GA2-OXIDASE), respectively (Hedden and Phillips, 2000).

Many components of the gibberellin signal transduction pathway have been identified through characterisation of mutant plant lines. Plants lines insensitive to exogenously applied bioactive gibberellins indicate a mutation in an essential component of the transduction pathway (Peng *et al.*, 1997). Mutations resulting in constitutive gibberellin

responses, but not elevated bioactive gibberellin levels, were also identified; indicating possible negative regulators of the signal transduction pathway (Peng *et al.*, 1997).

1.4.1 Production of bioactive gibberellins

Knowledge of the sites of bioactive gibberellin production is important for understanding how they function in plant development. Although exogenously applied gibberellins result in systemic responses, whether endogenously produced bioactive gibberellins are actively transported is unclear as no transporters have yet been identified. Several approaches have been used to determine the sites of bioactive gibberellin production. Chromatography studies revealed that gibberellin production is limited to developing tissues (Ogawa *et al.*, 2003). Accurate mapping of expression of GA3-oxidase, required for the final step of bioactive GA_1 or GA_4 synthesis, was performed using *A. thaliana* promoter:GUS reporter lines; these experiments indicated bioactive gibberellins are produced in or adjacent to perceptive tissues (Kaneko *et al.*, 2003).

A. thaliana encodes four *GA3-oxidase* genes, *GA3ox1-4* (Mitchum *et al.*, 2006). Detailed analysis of the expression *GA3ox1-4* has revealed that the expression of each is primarily localised to the tissues of gibberellin perception (Mitchum *et al.*, 2006). *GA3ox1* is the dominant enzyme in most tissues, *GA3ox2* functions during seed germination and vegetative tissue development, *GA3ox3* is expressed in flowers and siliques, and *GA3ox4* in developing and germinating seeds (Hou *et al.*, 2008; Mitchum *et al.*, 2006). *GA3-oxidase* expression is primarily localised to dividing cells within elongating zones during development of these tissues (Itoh *et al.*, 1999; Itoh *et al.*, 2001; Kaneko *et al.*, 2003).

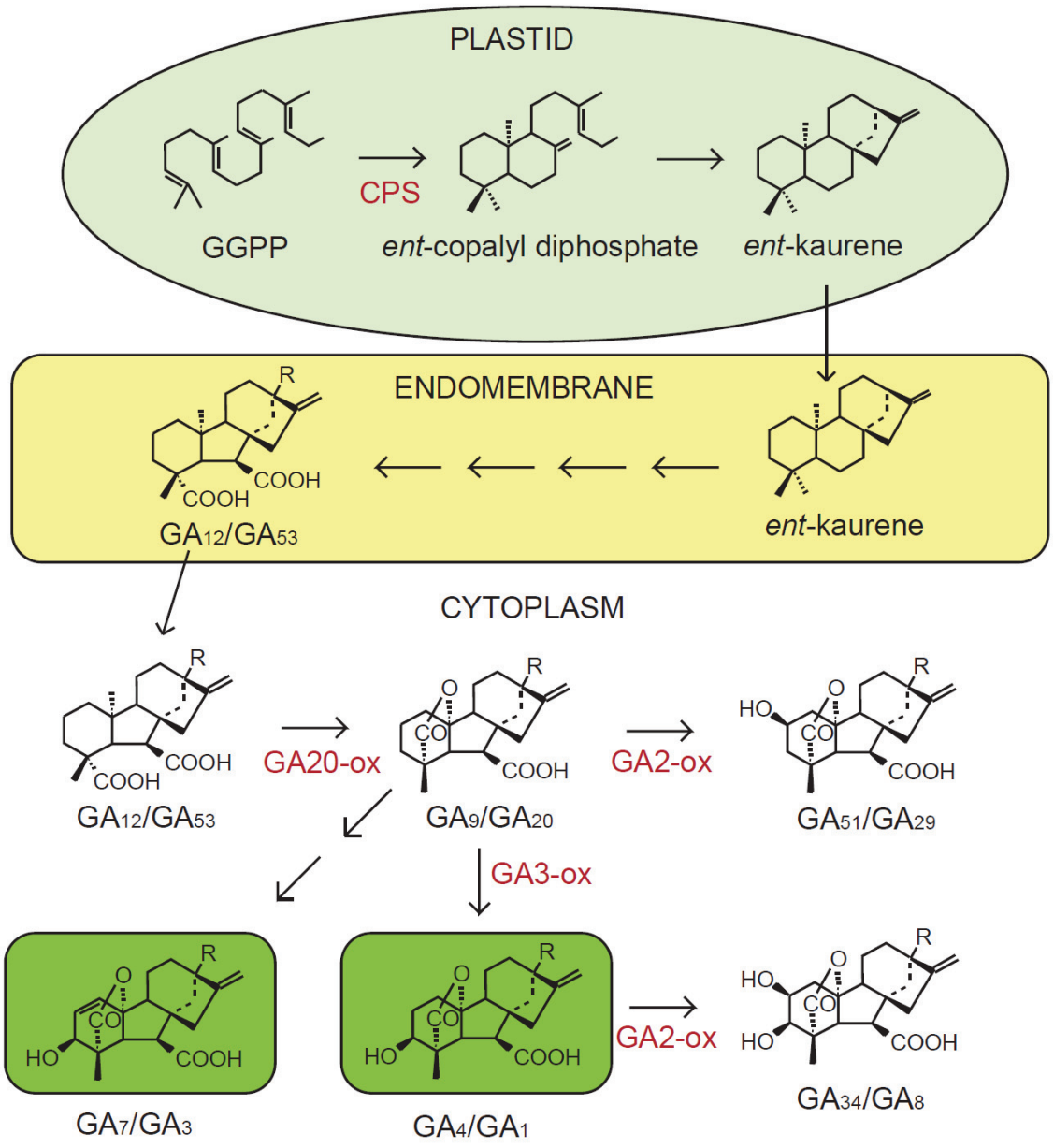

Figure 1.3. Gibberellin biosynthetic pathway. Gibberellin synthesis begins with synthesis of *ent*-kaurene from geranyl-geranyl-diphosphate in the plastid, starting with *ent*-copalyl diphosphate synthase (CPS). Conversion of *ent*-kaurene to GA_{12}/GA_{53} occurs at the endomembrane. Final activation of gibberellins by GA20-oxidase (GA20ox), and GA3-oxidase (GA3ox) occurs in the cytoplasm. Biologically active gibberellins are highlighted in green. GA_4 and GA_1 are further catabolised by GA2-oxidase (GA2ox). R= H/OH respectively (Hedden and Phillips, 2000).

Interestingly the early stages of gibberellin biosynthesis, which occur within the plastid, can take place in different cells to those where the active forms are synthesised (Mitchum *et al.*, 2006). In *A. thaliana* the expression sites of ent-copalyl diphosphate synthase (CPS) and two GA3-oxidases, *GA3ox1* or *GA3ox2*, as determined by promoter:GUS lines, were clearly separated in root tissues (Mitchum *et al.*, 2006).

The concentrations of bioactive gibberellins are highly regulated. Expression of GA20-oxidase, GA3-oxidase, and GA2-oxidase are controlled by feedback mechanisms, and by signalling pathways of other phytohormones. GA20-oxidase expression levels are repressed by bioactive gibberellins, likely due to loss of DELLA-mediated activation upon gibberellin perception (Phillips *et al.*, 1995; Xu *et al.*, 1995; Zentella *et al.*, 2007) . The final enzyme for activation of gibberellins, GA3-oxidase, is upregulated by light-induced signalling and DELLA protein-meditated transcriptional activation (Chiang *et al.*, 1995; Yamaguchi *et al.*, 1998; Zentella *et al.*, 2007). A third target of regulation is the catabolism of bioactive gibberellins by GA2-oxidase, which is upregulated in response to bioactive gibberellins by a yet unknown mechanism (Thomas *et al.*, 1999).

1.4.2 Perception of bioactive gibberellins

There is limited evidence for perception of bioactive gibberellins at the plasma membrane in aleurone tissue. Extracellular application of the bioactive gibberellin GA_3 was found to be sufficient for induction of gibberellin inducible α-amylase expression in barley (Gilroy and Jones, 1994). In contrast, micro-injection of GA_3 into aleurone cells was not sufficient, indicating a requirement of perception at the plasma membrane (Gilroy and Jones, 1994). However, to date no plasma membrane localised receptor has been characterised. Given that a nuclear-localised receptor for gibberellins has been identified and well characterised, these events at the plasma membrane could be an artifact of the procedures used, though it is possible multiple sites of gibberellin perception are required for some responses.

Genetic studies suggest that a heterotrimeric G protein (HGP) may have a role in gibberellin signalling (Ueguchi-Tanaka *et al.*, 2000). Analyses of completely sequenced genomes of *O. sativa* and *A. thaliana* have identified only one putative HGP complex made of an α, a β and two γ subunits (Kato *et al.*, 2004). This is in contrast to mammals whose genomes encode for many different heterotrimeric G-protein complexes (Offermanns, 2003). The HGP appears to function in almost every plant hormone signalling pathway (Ullah *et al.*, 2002). *DWARF-1* (*D1*) is a rice gene encoding the α subunit of the HGP (Ueguchi-Tanaka *et al.*, 2000). The *D1* mutant, *d1*, has a partial gibberellin-insensitive dwarf phenotype (Ueguchi-Tanaka *et al.*, 2000). However, the rice *d1* null mutation does not affect gibberellin-induced post-transcriptional activation of α-amylase, suggesting the HGP only functions in some gibberellin responses (Nanjo *et al.*, 2004). Global analysis of transcription also revealed sensitivity to gibberellin remains in the *d1* mutant; however, induction of gibberellin responsive genes was to a smaller magnitude than in wild-type rice (Bethke *et al.*, 2006). As the HGP is has been implicated in the signalling pathways of many phytohormones, it may be possible that the effects of the *d1* mutation on gibberellin signalling are due to effects on phytohormone cross-signalling, and not a direct involvement in perception of gibberellins.

Several secondary effectors, including cGMP (cyclic guanosine monophosphate), Ca^{2+} and Calmodulin, have been implicated in gibberellin signalling in the cytoplasm. The levels of cGMP were shown to rise upon gibberellin treatment of aleurone (Penson *et al.*, 1996). This cGMP increase was demonstrated to be required, but not sufficient for gibberellin-dependent induction of the target genes (Penson *et al.*, 1996). Furthermore the guanylyl cyclase inhibitor LY83583 which lowers cGMP levels, prevents induction of gibberellin-inducible α-amylase genes in aleurone (Gomez-Cadenas *et al.*, 2001).

The increase of the cytoplasmic Ca^{2+} concentration and activation of Calmodulin have also been implicated in gibberellin signalling. Calmodulin mRNA and protein concentration were shown to be rapidly increased upon gibberellin signalling, but by definition this is an indirect induction as it requires *de novo* protein synthesis (Schuurink *et al.*, 1996). It is likely that Calmodulin is required for delayed gibberellin-dependent responses. The cytoplasmic concentration of Ca^{2+} in aleurone cells greatly increases on gibberellin treatment and this is required for activation of gibberellin-

induced genes (Gilroy, 1996). One cytoplasmic protein kinase from barley, CALCIUM DEPEDENT PROTEIN KINASE-1 (CDPK1) has been shown to mediate gibberellin-dependent regulation of vacuolar functions via Ca^{2+}; however, its effect is downstream of transcriptional regulation, so it is part of the gibberellin response, not gibberellin signalling (McCubbin *et al.*, 2004).

Together these plasma membrane and cytoplasmic events reveal a complex, and yet unclear role in perception of gibberellins. As the HGP and cytoplasmic Ca^{2+} are important for many plant hormone signalling pathways they may function as an important site for integration of these signals.

1.4.3 Nuclear localised gibberellin receptors

One of several gibberellin-insensitive mutants isolated in rice, *gid1*, was shown to encode a novel gibberellin signalling component, *GID1* (Ueguchi-Tanaka *et al.*, 2005). The *gid1-1* mutation could only be propagated as a heterozygote, as homozygotes for this recessive mutation have a severe gibberellin-deficient phenotype, including infertility that cannot be rescued by exogenous gibberellins (Ueguchi-Tanaka *et al.*, 2005). *GID1* sequence indicates that it encodes a protein similar to hormone sensitive lipases (HSL), but lacks a conserved histidine residue that forms part of the Ser/Asp/His catalytic triad (Osterlund, 2001; Ueguchi-Tanaka *et al.*, 2005). Interestingly, using competition assays, GID1 was shown to bind biologically active gibberellins, including GA_1, GA_4, and GA_3 (Ueguchi-Tanaka *et al.*, 2005). Although GID1 has the highest binding affinity for GA_4 amongst biologically active gibberellins, GA_3 has a greater effect *in planta* (Ueguchi-Tanaka *et al.*, 2005; Ueguchi-Tanaka *et al.*, 2007). This discrepancy is accounted for by a double bond at the 2' carbon of GA_3 increasing its stability through inhibiting catabolism by GA2-oxidase, which normally inactivates GA_1 and GA_4 (Ueguchi-Tanaka *et al.*, 2005; Ueguchi-Tanaka *et al.*, 2007).

Rice GID1 is primarily nuclear localised, and is not translocated between sub-cellular compartments upon gibberellin signalling, as shown by a recombinant GFP-GID1

fusion (Ueguchi-Tanaka *et al.*, 2005). Furthermore, *GID1* is required for responses to gibberellin, and has thus been defined as a nuclear gibberellin receptor (Ueguchi-Tanaka *et al.*, 2005). This contradicts previous studies indicating involvement of plasma membrane and cytoplasmic events, though these have been proposed as only being involved in some gibberellin responses, and could function as regulatory mechanisms from other stimuli (Ueguchi-Tanaka *et al.*, 2005).

A. thaliana encodes three *GID1* homologs: *GID1A*, *GID1B*, and *GID1C* (Griffiths et al., 2006; Nakajima et al., 2006). GID1A-C show high homology to rice GID1 with 60-63 % amino acid sequence similarity, and between 67-85 % similarity with each other, GID1A and GID1C being the most similar (Nakajima *et al.*, 2006). GID1A-C bind biologically active gibberellins in a similar fashion to rice GID1, while other closely related *A. thaliana* esterases have no binding activity (Nakajima *et al.*, 2006). Of the three *A. thaliana* GID1-like proteins, recombinant GID1B has the highest affinity for bioactive gibberellins, whilst GID1A has the slowest dissociation rate (Nakajima *et al.*, 2006).

A. thaliana GID1A-C all function as gibberellin receptors *in planta*, as shown by rescue of gibberellin signalling in *gid1-1* rice by transgenic overexpression (Nakajima *et al.*, 2006). Furthermore, a triple deletion mutant of *A. thaliana* is required for a complete gibberellin-insensitive phenotype, showing that they are at least partially redundant in function (Griffiths *et al.*, 2006; Iuchi *et al.*, 2007). A double mutant, lacking both *GID1A* and *GID1C* has a partial dwarf phenotype, indicating these two genes to be the most functionally important (Griffiths *et al.*, 2006; Iuchi *et al.*, 2007). The *A. thaliana GID1A-C* genes do show some tissue specific expression during development; *GID1A* is the most abundant in most plant tissues, with very high levels in dormant seeds, whilst *GID1B* in expressed in vegetative tissues, particularly roots tissues (Griffiths *et al.*, 2006). *GID1C* is expressed at a comparatively low level, which is in contrast to its greater role in development than *GID1B* (Griffiths *et al.*, 2006). This has been attributed to possible specific roles during development. However, in light of the discovery of DELLA mediated activation of *GID1A* and *GID1B* transcription, the phenotype differences in *gid1a-c* mutations could also be a result of alterations in feed-back regulation of expression (Griffiths *et al.*, 2006; Zentella *et al.*, 2007).

GID1 gibberellin receptors are required for the degradation of the DELLA proteins, explaining how they are required for gibberellin signalling (Ueguchi-Tanaka *et al.*, 2005). The rice *gid1-1* mutation results in the accumulation of SLR1, which is normally degraded in response to gibberellin (Ueguchi-Tanaka *et al.*, 2005). In line with the requirement of GID1 for gibberellin-dependent DELLA protein degradation, SLR1 levels remain high in *gid1-1* mutant even following exogenous gibberellin treatment (Ueguchi-Tanaka *et al.*, 2005). In an *A. thaliana* triple *gid1a-c* knockout mutant, the RGA protein abundance is elevated to a similar level as in the gibberellin-deficient mutant *ga1-3*, but is not reduced on exogenous gibberellin treatment (Griffiths *et al.*, 2006).

Recombinant GID1 and SLR1, expressed in *E. coli*, have been shown to directly interact *in vitro* in the presence of biologically active gibberellins (Ueguchi-Tanaka *et al.*, 2005; Ueguchi-Tanaka *et al.*, 2007). Furthermore, this interaction has been shown *in vivo* in yeast two-hybrid interaction experiments, and *in planta*, using split YFP-fusions of GID1 and SLR1 (Ueguchi-Tanaka *et al.*, 2005; Ueguchi-Tanaka *et al.*, 2007).

All fifteen combinations of GID1A-C and the five *A. thaliana* DELLA proteins have been reported to interact *in vivo* in the presence of biologically active gibberellins in yeast two-hybrid reporter experiments (Feng *et al.*, 2008; Griffiths *et al.*, 2006). Split-YFP fusions of GID1C and RGA have been reported to interact within the plant nucleus in the presence of gibberellins (Feng *et al.*, 2008). *A. thaliana* DELLA proteins have also been successfully co-immunoprecipitated from plant extracts of over-expressing plant lines through their interaction with either recombinant *E. coli* expressed GID1A or GFP-GID1A-C fusions over-expressed *in planta* (Feng *et al.*, 2008; Wang *et al.*, 2009).

Deletion analysis of GID1, and the DELLA proteins SLR1, RGA and GAI, has been used to discover regions important for gibberellin-dependent interactions of these proteins. Deletion of motifs or domains of SLR1 in yeast two-hybrid assays and *in planta* split-YFP experiments revealed that both the conserved DELLA and TVHYNP motifs are essential for interaction with GID1 (Ueguchi-Tanaka *et al.*, 2007). Furthermore, *in vitro* gel filtration experiments revealed that the N-terminal DELLA domain with intact DELLA and TVHYNP motifs is sufficient for interaction with GID1 (Ueguchi-Tanaka *et al.*, 2007). Deletion analysis of GID1 revealed that all but a small

portion of the N-terminal sequence is required for binding both gibberellins and SLR1 (Ueguchi-Tanaka *et al.*, 2007). The regions important for either gibberellin binding or interaction with SLR1 have been mapped in detail by alanine replacement scanning (Ueguchi-Tanaka *et al.*, 2007). When compared to a predicted folding structure, these regions clustered around the predicted binding pocket and 'lid' structure (Ueguchi-Tanaka *et al.*, 2007).

Deletion studies of *A. thaliana* DELLA proteins have given similar results to SLR1, though some possible differences have been reported. Interaction with GID1A in yeast two-hybrid assays requires both the DELLA and TVHYNP motifs of RGA (Griffiths *et al.*, 2006). However the TVHYNP motif of GAI has been reported to not be required, perhaps due to differences between the DELLA proteins, or unexplained artefacts resulting through large deletions (Willige *et al.*, 2007).

Although no structure of a full length DELLA protein has yet been described, the structures of both gibberellin-bound rice GID1, and part of the N-terminal domain of the *A. thaliana* DELLA protein GAI in complex with GID1A have been solved. Interestingly, these structures confirm that gibberellin binds within what would be the catalytic pocket of an esterase fold (Figure 1.4) (Murase *et al.*, 2008; Shimada *et al.*, 2008). Furthermore, GID1 and GID1A possess a flexible N-terminal 'lid' that closes over the bound gibberellin, trapping it within the binding pocket (Murase *et al.*, 2008; Shimada *et al.*, 2008). The opposite face of the lid forms a hydrophobic surface, enabling interaction of GID1A with the N-terminal domain of the DELLA protein GAI (Murase *et al.*, 2008). Although the N-terminal domain of GAI appears to be unstructured in absence of binding partners, based on circular dichroism spectra, both the conserved DELLA and TVHYNP motifs obtain secondary and tertiary structure upon binding to GID1A (Murase *et al.*, 2008). The N-terminal domain of GAI forms two main helices, αB and αD, corresponding to conserved regions within the DELLA and TVHYNP motifs, respectively, that pack against each other in a parallel orientation (Figure 1.4B). The short DELL αA helix, or 'thumb', angles down to fill a hydrophobic pocket. The αC helix and the TVHYNP sequence form a loop that interacts with the lid of GID1A.

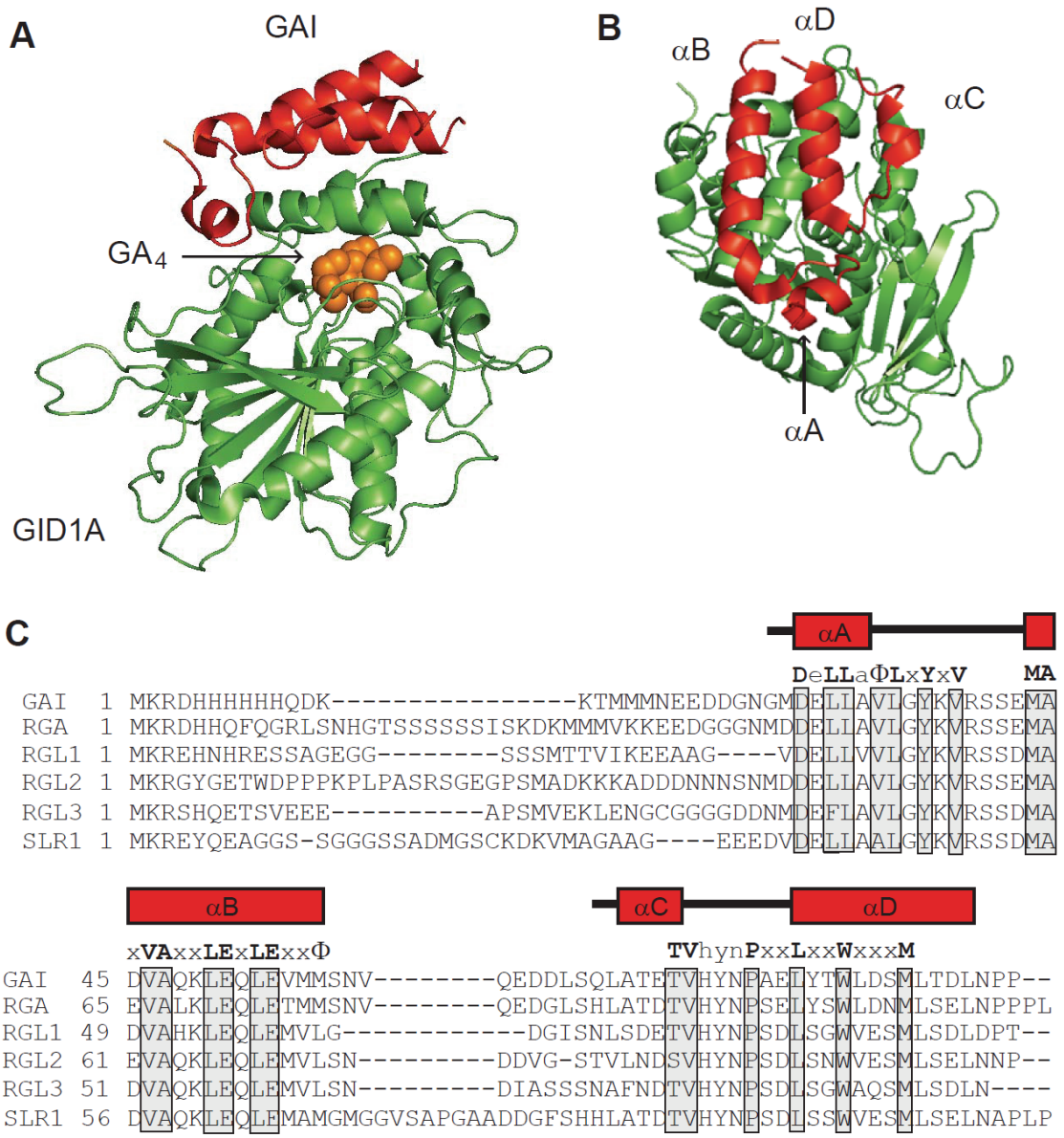

Figure 1.4. Structural basis of the DELLA-GID1A interaction. A. Side view of GA_4-bound GID1A (green) in complex with the GAI N-terminal domain (red). **B**. Top view showing GAI α-helices A-D. **C**. N-terminal domain alignment showing conserved GID1A interacting residues (highlighted) and secondary structure; α-helices A-D, red; loop, black. The diagram was made using coordinates from the PDB entry 2ZSI (Murase *et al.*, 2008)

The steps involved in formation of the GID1A: GAI complex are as yet unknown; the GAI N-terminal domain is possibly unstructured when unbound, but must either have transient secondary structure, or fold upon interaction with the hydrophobic surface of GID1A. Furthermore, the involvement of only this short region of GAI is consistent with most deletion analysis experiments, but it is unclear whether other regions of GAI would normally form part of this complex in an intact protein. Interestingly, the interaction of GID1A or GID1 with DELLA proteins is sufficient to abolish DELLA protein repressive functions, as shown by rescue of plant growth by GID1 overexpression in genetic backgrounds that prevent DELLA protein degradation (*sly1*, *gid2*, see next section) (Ariizumi *et al.*, 2008; Ueguchi-Tanaka *et al.*, 2008). This effect suggests the GID1-DELLA interaction has large effects on the whole DELLA protein conformation, and the function of the C-terminal GRAS domain, not just the N-terminal DELLA domain.

1.4.4 Gibberellin-induced DELLA protein degradation

The gibberellin-insensitive mutation of rice *GID2*, and an *A. thaliana* mutation of *SLEEPY* (*SLY1)* have been characterised to be null mutations of genes encoding a homologous F-box protein (McGinnis *et al.*, 2003; Sasaki *et al.*, 2003). F-box proteins represent an obligatory component of a SCF (SKP-CULLIN-F-BOX) E3 Ubiquitin ligase complex that targets specific proteins for degradation by the proteasome (Kipreos and Pagano, 2000). An F-box protein acts to specifically bind cognate target proteins for recruitment to the E3 complex.

Both *SLY1* in *A. thaliana* and *GID2* in rice are required for normal gibberellin responses. Null mutants have severe dwarf phenotypes that cannot be rescued by exogenous gibberellins. *A. thaliana* does encode a second homolog, *SNEEZY* (*SNY*), but this gene is poorly expressed, and cannot compensate for *SLY1* null mutations unless over-expressed (Strader *et al.*, 2004). *SLY1* and *GID2* null mutants accumulate high levels of DELLA proteins; hence the DELLA proteins are targeted for degradation by these two F-box proteins (Dill *et al.*, 2004; Fu *et al.*, 2004; Gomi *et al.*, 2004). A

mutation of *SLY1*, *gar2*, was isolated that rescued the dwarf phenotype of the dominant *gai-1* mutation in *A. thaliana* (Swain *et al.*, 2004). *gar2* has been determined to be a gain-of-function single amino acid mutation of SLY1 (Dill *et al.*, 2004; Fu *et al.*, 2004).

Yeast 2-hybrid interaction systems have been used to show that both SLY1 and GID2 can bind to DELLA proteins (Dill *et al.*, 2004; Fu *et al.*, 2004; Gomi *et al.*, 2004; Tyler *et al.*, 2004). Furthermore, recombinant GLUTATHIONE S-TRANSFERASE (GST)-fusions of either SLY1 or GID2 were used to pull-down endogenous DELLA proteins *in vitro* from plant extracts (Fu *et al.*, 2004; Gomi *et al.*, 2004). Further analysis of the regions of the DELLA protein required for interaction have indicated that SLY1 interacts with a region within the C-terminal GRAS domain including the putative leucine zipper (Dill *et al.*, 2004). In pull-down experiments wild-type SLY1 and GID2 could only bind with high affinity to phosphorylated GAI and SLR1 protein, respectively (Fu *et al.*, 2004; Gomi *et al.*, 2004). In contrast, the gain-of-function SLY1 mutant protein, sly1^{gar2}, was able to bind with high affinity to both unphosphorylated and phosphorylated DELLA proteins in pull-down experiments (Fu *et al.*, 2004).

The interaction experiments of the *A. thaliana* and rice nuclear GID1-family gibberellin receptors and the F-box proteins SLY1 and GID2 lead to the proposal of a nuclear localised molecular switch (Figure 1.5) (Griffiths *et al.*, 2006; Harberd *et al.*, 2009). As GID1-family gibberellin receptors interact with the N-terminal DELLA domain of DELLA proteins, and this is essential for induced degradation of the DELLA proteins, it is likely that this event is the trigger for recruitment of F-box proteins SLY1/GID2 to the DELLA proteins. In yeast three-hybrid experiments, gibberellin-bound GID1A allowed SLY1 to interact with RGA, fitting this proposed model (Griffiths *et al.*, 2006). However the exact mechanism of this recruitment is yet to be discovered.

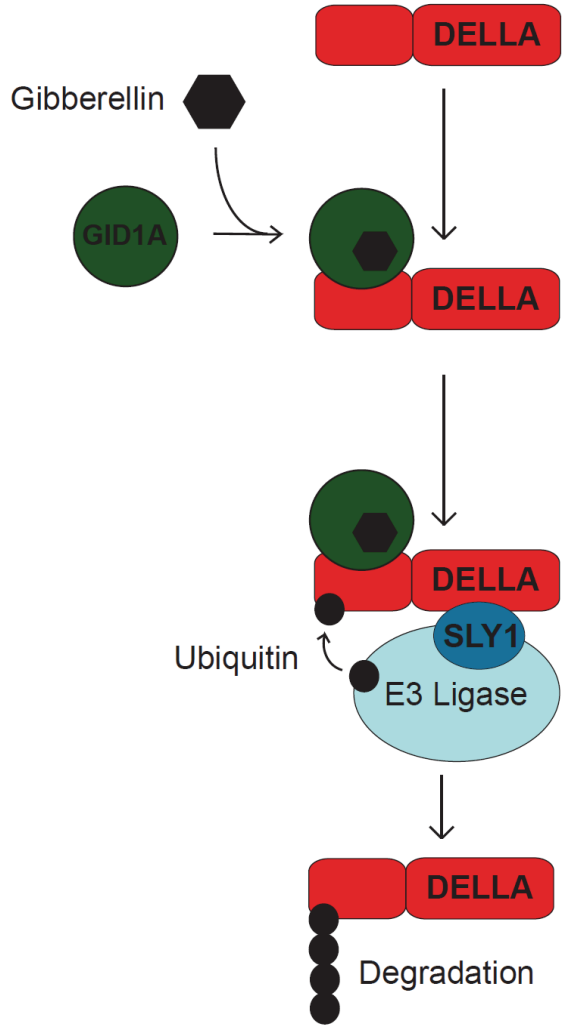

Figure 1.5. Nuclear molecular switch model. When gibberellin receptors GID1A-C (green) bind bio-active gibberellin they bind the N-terminal DELLA domain of DELLA proteins (red). This enables the F-box protein SLY1 (blue) to recruit an E3 Ubiquitin ligase to the DELLA protein, resulting in poly-Ubiquitination of the DELLA protein. Poly-Ubiquitin tagged DELLA proteins are subsequently degraded by the proteasome (Griffiths *et al.*, 2006; Harberd *et al.*, 2009).

Additional events appear to be necessary *in planta* for this three-protein molecular switch to function. DELLA proteins have been reported to be post-translationally modified, with multiple serine residues within the N-terminal DELLA domain being phosphorylated (Fu *et al.*, 2004; Gomi *et al.*, 2004; Itoh *et al.*, 2005). Furthermore, phosphorylation of either *A. thaliana* GAI or rice SLR1 increased the strength of interaction with SLY1 and GID2 in pull-down assays (Fu *et al.*, 2004; Gomi *et al.*, 2004). In contrast, *in planta* and cell free systems developed to study DELLA protein degradation indicate that protein dephosphorylation is required (Hussain *et al.*, 2007; Wang *et al.*, 2009). The nature of the phosphorylation signal remains obscure, given that no protein kinase or phosphatase has yet been identified as implicated in gibberellin signalling and the phosphorylation state of DELLA proteins is yet to be well characterised. It is possible that phosphorylation of the DELLA proteins, or other signalling components is an important site for regulation by other cell signalling events.

Characterisation of the phosphorylation status of SLR1 has revealed that phosphorylation targets on DELLA proteins are primarily serine residues in the serine and threonine rich region within the DELLA N-terminal domain (Itoh *et al.*, 2005). However, phosphorylation of these residues is not a result of gibberellin signalling, as it occurs in tissues lacking bioactive gibberellins (Itoh *et al.*, 2005). Other possible phosphorylation targets may be aspartic acid (D), threonine (T), histidine (H), or tyrosine (Y), all of which are present in the DELLA and TVHYNP motifs. Phosphorylated DELLA proteins have a higher affinity for the F-box proteins; this is in agreement with genetic evidence that the poly S/T/V region is involved in increasing the effect of the gibberellin signal (Fu *et al.*, 2004; Itoh *et al.*, 2002).

Amino acid replacement in a tobacco cell culture has been used to mimic phosphorylation of amino acids to determine those that are important for gibberellin induced DELLA protein degradation. Replacement of 12 serine residues and 5 threonine residues throughout both the N- and C-terminal domains that are conserved amongst DELLA proteins revealed that phosphorylation of threonine residues within the C-terminal GRAS domain may be important for protein stabilisation (Hussain *et al.*, 2005). However, the results of this replacement strategy could be interpreted as the conserved residues being essential for protein-protein interactions and may not normally be targets of phosphorylation. The serine/threonine phosphatase inhibitors okadaic acid

and cypermethin blocked gibberellin-induced RGL2 degradation, however serine/threonine kinase inhibitors did not (Hussain *et al.*, 2005). Similarly protein phosphatase inhibitors, but not kinase inhibitors stabilised MALTOSE-BINDING PROTEIN (MBP)-RGA fusion in an *in vitro* cell-free system (Wang *et al.*, 2009). This is contradictory to phosphorylated forms binding with stronger affinity to *A. thaliana* SLY1 or rice GID2.

Phosphorylation of tyrosines has been found to be important for the gibberellin-induced degradation of DELLA proteins (Hussain *et al.*, 2007). A mixture of tyrosine kinase inhibitors was sufficient for stabilising RGL2 against gibberellin-induced degradation in a tobacco cell culture system (Hussain *et al.*, 2007). However, the target tyrosine residues are as yet unclear as the mutated Y residues are conserved and have been shown to form direct contacts with gibberellin-bound GID1-family gibberellin receptors, required for gibberellin-induced degradation.

Altogether, the role of phosphorylation and dephosphorylation is still unclear. The exact sites are yet to be mapped, and to date no kinase or phosphatase has been shown to specifically target DELLA proteins or be functionally important to gibberellin signalling.

1.5 Additional gibberellin signalling components

The potato (*Solanum tuberosum*) protein encoded by *PHOTOPERIOD-RESPONSIVE-1* (*PHOR1*) has been identified to be translocated from the cytoplasm to nucleus upon gibberellin signalling (Amador *et al.*, 2001). Downregulation of *PHOR1* expression by antisense mRNA produces gibberellin-resistant dwarf potato plants, implicating an important role in gibberellin signalling (Amador *et al.*, 2001). PHOR1 has homology to an ARM repeat protein, ARMADILLO, from Drosophila. ARMADILLO is a regulator of gene expression involved in segment polarity and tissue differentiation in Drosophila, so if there is functional conservation between invertebrates and plants, PHOR1 may regulate gene expression on gibberellin signal perception (Amador *et al.*, 2001).

PHOR1 was shown to be expressed in most tissues, and is also upregulated during short days, when gibberellins are required for flowering. PHOR1 has been suggested to be a positive regulator of gibberellin signalling and may be a U-box protein, a class of proteins that little is known about (Monte *et al.*, 2003). U-box proteins may act as E4 ubiquitin ligases that bind Ubiquitinated proteins and aid their poly-Ubiquitination. Alternatively, they may act as an E3 ubiquitin ligase involved in targeted protein degradation. GFP-PHOR1 acquires nuclear localisation upon gibberellin treatment, making it a possible candidate for a gibberellin signal carrier from cytoplasm to nucleus, if either membrane or cytoplasmic gibberellin receptor exists. There are three *A. thaliana PHOR1* homologues, *HIM1, 2, 3* (also known as *PUB28, 29, 27*) (Monte *et al.*, 2003). However, there is currently no reported research on how or if they function in gibberellin signalling in *A. thaliana*.

SHORT-INTERNODES (*SHI*) is a gene of *A. thaliana* that is implicated in gibberellin signalling. A 35S:GUS fusion of functional *SHI* demonstrated a gibberellin-insensitive dwarf phenotype, suggesting that the SHI protein acts to repress gibberellin signalling (Fridborg *et al.*, 1999; Fridborg *et al.*, 2001). *SHI* is normally expressed in most tissues at a low level, but is upregulated in root and shoot primordia (Fridborg *et al.*, 2001). Null mutants have a normal phenotype, possibly due to genetic/functional redundancy. *SHI* belongs to a family of at least 9 genes, including *LATERAL ROOT PRIMORDIUM* (*LRP*). The proteins encoded by genes in this family contain a putative Zn^{2+} binding RING finger motif similar to a mammalian protein, COP1, but with several significant differences in the domain (Fridborg *et al.*, 2001). COP1 functions as a component of the SCF E3 ubiquitin ligase that targets proteins for degradation (Freemont, 2000). This suggests that SHI may be part of an SCF E3 complex, possibly including SLY1, involved in gibberellin signalling. However, overexpression results indicate that SHI may interfere with the function of an SCF E3 complex, though this could be an artifact of overexpression. SHI and its homologues carry a C-terminal domain named IGGH that is unique to plants, and so are named IGGH proteins (Fridborg *et al.*, 2001).

The putative *O*-linked *N*-acetyl glucosamine (*O*-GlcNac) transferase SPINDLY (SPY) has been implicated in having roles in gibberellin signalling. Null mutations of *SPY* result in tall slender plant, similar to constitutive gibberellin signalling mutants (Swain

et al., 2001; Swain *et al.*, 2002). Overexpression of SPY was also found to interfere with seed germination, suggesting a role in repressing gibberellin signalling (Swain *et al.*, 2002). SPY has been proposed to function in gibberellin signalling by post-translational modification of DELLA proteins through *O*-glucosylation of serine or threonine residues to increase their repressive functions (Shimada *et al.*, 2006; Silverstone *et al.*, 2007). However, use of glucocorticoid receptor fusions, allowing retention in the cytoplasm, reveals that SPY only functions in gibberellin regulation of cytokinin responses within the cytoplasm (Maymon *et al.*, 2009). This is not consistent with phenotypical observations; therefore, it is likely SPY operates in gibberellin signalling at several stages. It is possible that interaction between gibberellin and cytokinin signalling functions independently of DELLA protein function.

SPY has been shown to bind to two transcription factors in barley, SPY INTERACTING NAC (HSINAC) a member of the NAC class transcription factors, and SPY INTERACTING MYB (HSIMYB) (Robertson, 2004). HSINAC has been shown to be down-regulated on gibberellin signalling. HSIMYB interacts with the promoter of an α-amylase gene as a complex with SPY to repress this gibberellin-induced gene expression (Robertson, 2004). These interactions further indicate that SPY class proteins function during several aspects of gibberellin signalling, in both the nucleus and cytoplasm.

1.6 Phytohormone cross-signalling

Evidence of substantial cross-signalling between plant hormones is emerging, revealing the complex ways plants develop and respond to environmental stimuli. Auxin, ethylene, abscisic acid (ABA), brassinosteroids, jasmonates, and cytokinins have all been shown to regulate gibberellin signalling, though only auxin and ethylene have yet been shown to affect DELLA protein function (Weiss and Ori, 2007).

Auxins are a major class of phytohormones, controlling both cell division and differentiation. Auxin is primarily produced in developing young tissues and is

transported throughout the plant in a polar fashion, generating a gradient that is essential for determining correct cell function. Auxin control of root development has been shown in part to require regulation of gibberellin signalling (Fu and Harberd, 2003). In *A. thaliana* the DELLA genes *GAI* and *RGA* are important for correct root development including control of cell elongation (Fu and Harberd, 2003). Experiments investigating the stability of GFP-RGA reveal that auxin is required for normal gibberellin-induced degradation of RGA (Fu and Harberd, 2003).

A possible mechanism of this de-stabilisation is regulation of bioactive gibberellin levels. The gibberellin biosynthetic gene GA1-oxidase expression is down-regulated, whist gibberellin inactivating enzymes are upregulated, in root tissues of *Pisum sativum* L. (Pea) treated with the auxin transport inhibitor 1-*N*-naphthylthalamic acid (NPA) (Weston *et al.*, 2009). These results could explain the de-stabilising effect of auxin on the DELLA proteins; however, more conclusive research is required to exclude other possible mechanisms such as regulation of DELLA protein phosphorylation. The complexity is that DELLA proteins bind in complex to activate the promoters of GA20ox and GA3ox genes, required for gibberellin biosynthesis (Zentella *et al.*, 2007). Therefore, reduced DELLA protein levels may be the cause of altered gibberellin biosynthesis noted in Pea.

A second major phytohormone, the gas ethylene, has also been shown to regulate gibberellin signalling during important developmental stages. Ethylene is well known for its role in fruit ripening and leaf dehiscence, but it is also essential for correct development during flowering and seed germination (Achard *et al.*, 2007a). In contrast to auxin, ethylene stabilises DELLA proteins, as shown by the stabilisation of a GFP-RGA fusion in gibberellin treated root tips (Achard *et al.*, 2007a). This effect has been shown to be developmentally important in apical hook formation, and in root elongation (Achard *et al.*, 2007; Achard *et al.*, 2003; Vriezen *et al.*, 2004). The mechanism of stabilisation is not yet clear, although it is dependent on CTR1 (CONSTITUTIVE TRIPLE RESPONSE-1) and EIN3 (ETHYLENE-INSENSITIVE-3), key proteins involved in ethylene signalling. The regulation of floral transition by ethylene is also DELLA-dependent, resulting in control the floral identity genes *LFY* (*LEAFY*) and *SOC1* (*SUPPRESSOR OF OVEREXPRESSION OF CO 1*) (Achard *et al.*, 2007a). DELLA proteins were stabilised against excess levels of exogenous GA_3, suggesting

that this stabilising effect is not simply mediated through regulation of production or inactivation of bioactive gibberellins (Achard *et al.*, 2007a).

1.7 An integrated model for gibberellin signalling

A central molecular switch has been proposed as the controlling mechanism of gibberellin action of plant development (Figure 1.6). In this model DELLA proteins regulate gene expression, mediated by regulation of transcription factors (for example, inactivation of PIF3 and PIF4).

Upon biosynthesis within the cytoplasm, or uptake into the cell, biologically active gibberellins enter the nucleus where they are bound by the GID1 gibberellin receptors. Liganded GID1-family proteins can then bind directly to the N-terminal DELLA domain of DELLA proteins. This both inactivates the transcriptional regulation activity of DELLA protein, and targets them for degradation. Degradation is mediated by the F-box SLY1, a component of a DELLA-specific E3 Ubiquitin ligase that poly-Ubiquitinates targeted DELLA proteins, tagging them for degradation by the proteasome. SLY1 cannot interact with the DELLA proteins, unless triggered by regulatory signals including binding of liganded GID1 to the DELLA proteins. The exact mechanism of SLY1 recruitment to DELLA proteins by GID1/gibberellin is yet to be shown.

Other effectors also regulate the degradation of the DELLA proteins. Auxin “sensitises” whilst ethylene protects DELLA from gibberellin-induced degradation. The mechanism is not yet known, though post-translational modification of the DELLA proteins is a likely required. DELLA proteins are often phosphorylated in planta, and phosphorylated forms are more readily bound by SLY1 and thus degraded. Phosphorylation of serine residues stabilises against degradation, whilst phosphorylation of tyrosine residues appears essential for degradation. However, the protein kinases and phosphatases involved as yet remain unknown.

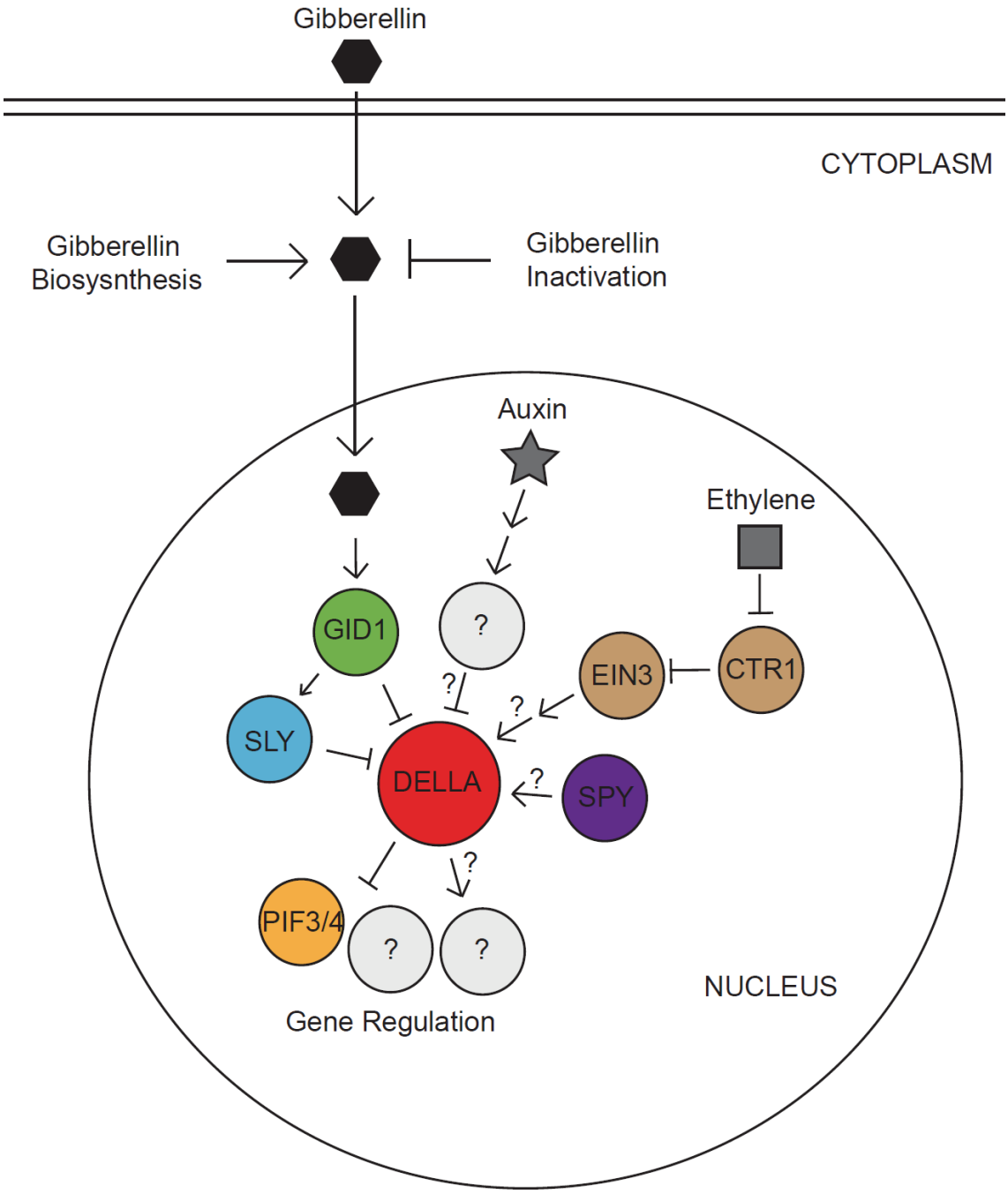

Figure 1.6. A model for DELLA integrated signalling. Exogenous and intracellular gibberellins enter the nucleus where they activate GID1-mediated DELLA inactivation and subsequent SLY1-dependent degradation. Auxin represses DELLA function via increased susceptibility to gibberellin-induced degradation by an as yet unknown mechanism. Ethylene signalling through CTR1 and EIN3 stabilises DELLA proteins against degradation through an undefined interaction. DELLA proteins regulate transcription via inactivation of PIF3/4 and activation of other unknown transcription factors. SPY increases the effects of DELLA proteins on gene regulation through an unresolved mechanism.

1.8 Statement of problem and significance

Many modern crop lines possess mutated alleles of DELLA genes. Furthermore, these mutations consist of in-frame deletions of the N-terminal region of the encoded protein. These gain-of-function mutations enhance the growth-repressive functions of the encoded DELLA protein. As a result, the elongation of stems is partially repressed, allowing plants to invest more resources into fruit, seeds, and grain.

Recent molecular and structural studies have revealed that the deleted region normally interacts directly with the GID1-like gibberellin receptors. The binding of liganded GID1-like proteins to the N-terminal DELLA domains in turn targets the DELLA proteins for degradation: thereby relieving their repressive activities on plant growth.

DELLA protein degradation requires recruitment of a third protein, SLY1 or GID2; F-box class protein that forms part of a larger E3-Ubiquitin ligase. This complex adds a poly-ubiquitin chain to the target protein, tagging it for recognition for degradation by the proteasome. The mechanism by which GID1 gibberellin receptors predispose the binding of DELLA proteins to the F-box proteins, which is the key step in committing DELLA protein to degradation, is yet unclear.

Environmental stimuli and plant effectors other than gibberellin are also known to regulate the degradation of the DELLA protein. As yet, only a few of the plant cell components involved have been discovered, and the mechanisms by which they function have not been characterised. Combining further knowledge of how the turn-over of DELLA proteins is regulated could lead to key advances in control of plant architecture in order to obtain stress resistant plants with greater crop yields.

This study aims to characterise interactions of the DELLA protein RGL1, of a model plant *Arabidopsis thaliana* and in this way further increase the fundamental knowledge of gibberellin-mediated plant developmental mechanisms.

1.9 Hypothesis

At the onset of this work, I hypothesised that in *A. thaliana* the GID1-family gibberellin receptor GID1A mediates recruitment of the F-box protein SLY1 to the DELLA protein RGL1 in the absence of other components. Furthermore, I propose this interaction is mediated through conformational changes within RGL1. Other signals are able to affect the stability of DELLA proteins, thus I hypothesise that these signals are mediated by as yet unknown proteins interacting directly with the DELLA proteins.

Aims

a) To dissect the gibberellin-dependent interactions between GID1A, RGL1, SLY1.

b) To identify novel proteins interacting with the N-terminal DELLA domain of RGL1.

Chapter 2

Materials and methodology

2.1 Materials and reagents

Analytical grade chemicals: 3-amino-1,2,4- trizol (3-AT), ammonium persulfate, ethdium bromide, gibberellin A3 (GA_3), gibberellin A4 (GA_4), ethanolamine, 1-ethyl-3-(3-dimethylaminopropyl)carbodiimide (EDC), β-octyl-glucopyranoside, *O*-nitrophenyl-β-D-galactopyranoside (ONPG), sodium chloride, sodium dodecyl sulfate (SDS), Z-Leu-Leu-Leu-al (MG132), general use protease inhibitor cocktail (P2714 - AEBSF; Aprotin, Bestatin HCl, E-64, EDTA, Leupeptin hemisulfate), and tetra-methyl-ethylene-diamine (TEMED) were sourced from Sigma, Missouri, USA. Ammonium sulfate, dimethyl sulfoxide (DMSO), glycine, (4-(2-hydroxyethyl)-1-piperazineethanesulfonic acid (HEPES), maltose, 2-mercaptoethanol, *N*-hydroxy-succinimide (NHS), potassium orthophosphate, potassium chloride, and polysorbate-20 (Tween 20) were supplied by BDH, Poole, United Kingdom. Magnesium sulfate, sodium di-hydrogen orthophosphate, di-sodium orthophosphate, hydrochloric acid, acetic acid, potassium hydroxide, and poly-ethylene glycol-4000 (PEG-4000) were obtained from Merck, Darmstadt, Germany. Ethylene-diamine-tetra-acetic acid (EDTA), sodium hydroxide, and sucrose were sourced from APS, New South Wales, Australia. Ampicillin, 1,4-Dithiothreitol (DTT), kanamycin, and phenyl-methyl-sulfonyl-fluoride (PMSF) were supplied by Roche Applied Bioscience, Basel, Switzerland. Acrylamide and bis-Acrylamide were obtained from Bio-rad, California, USA. Tricine and electrophoresis grade agarose were sourced from USB, Ohio, USA and Bioline, London, United Kingdom respectively tris (hydroxymethyl) aminomethane (Tris) was supplied by Invitrogen, California, USA. Isopropylthio–β-D-galactoside

(IPTG) was obtained from EMB biosciences, Darmstadt, Germany. Glycerol was supplied by Scientific Supplies, Auckland, New Zealand.
Bacteriological grade media: peptone and 2x yeast extract/tryptone (2xYT) were obtained from BD, New Jersey, USA. Yeast nitrogen base and synthetic dropout amino acid mixtures were sourced from Clontech, California, USA. Tryptone, yeast extract, and D-glucose were supplied by Merck, Darmstadt, Germany. Bacteriological grade agarose was obtained from Oxoid, Hampshire, United Kingdom.

2.2 General methodology

2.2.1 Molecular biology

PCR amplification was performed using Primestar DNA polymerase (Takara-Bio, Shiga, Japan), according to manufacturer's instructions. Restriction endonucleases were supplied by Roche Applied Bioscience, Basel, Switzerland, or New England Biolabs, Massachusetts, USA, and used according to manufacturer's instructions. DNA fragments were separated by size for identification, quantification, and purification using agarose gel electrophoresis (Sambrook and Russell, 2001). 0.7-1.0 % w/v agarose, gels were run in 40 mM Tris:acetate pH 8.0, 1 mM EDTA (TAE). DNA concentrations were determined by fluorometry (Qubit, Invitrogen, California, USA). DNA fragments were ligated using T4 DNA ligase (Roche Applied Bioscience, Basel, Switzerland), using 1 Unit to ligate 100 ng DNA for 16 hours at 16 °C. Ligated DNA was subsequently transformed into chemically competent *Escherichia coli* using a previously described heat shock method and transfomants were selected for on appropriate antibiotics (Sambrook and Russell, 2001).

2.2.2 Protein electrophoresis

Denatured proteins were separated by 10 % w/v acrylamide sodium dodecyl sulfate-poly-acrylamide gel electrophoresis (SDS-PAGE), as previously described (Laemmli, 1970). For the separation of native proteins, samples were separated by 3-12 % w/v acrylamide gradient blue-native-PAGE (Invitrogen, California, USA; (Schagger, 2001)). Tricine-SDS-PAGE was performed for the separation of affinity-purified proteins as previously described (Schagger and Von Jagow, 1987), with reduction of the total acrylamide concentration to 8 % w/v acrylamide, and modification of the bis-acrylamide/acrylamide ratio from 6 to 3 %. Proteins were detected by staining with either coomassie brilliant blue G250 (Simply-Blue Safe-stain; Invitrogen, California, USA), or with SYPRO ruby gel stain (Bio-Rad, California, USA).

2.2.2 Western blotting

Western blotting was performed as previously described (Sambrook and Russell, 2001). Un-stained proteins separated by poly-acrylamide gel electrophoresis were transferred to polyvinylidene fluoride membrane (Millipore, Massachusetts, USA) in ice-cold 100 mM Tris, 100 mM glycine, 10 % v/v methanol at 300 mA for 1 hour. Membranes were equilibrated and blocked in 10 mM Na_2HPO_4, 2 mM KH_2PO_4, 137 mM NaCl, 2.7 mM KCl, pH 7.4 (phosphate buffered saline, PBS), supplemented with 0.02 % v/v Tween-20, and 5 % w/v non-fat milk powder as a blocking agent. Membranes were incubated for 16 hours at 4 °C with 1 μg/mL primary antibody in PBS, 0.02 % v/v Tween-20, 5 % w/v non-fat milk powder. Following washes in PBS, 0.02 % v/v Tween-20, and a 1 hour incubation with Horse radish peroxidase labelled secondary antibodies (Sigma A5278 or A8275 at 1:20000 dilution) in PBS, 0.02 % v/v Tween-20, 5 % w/v non-fat milk powder, membranes were washed and developed using ECL^{Plus} detection reagent (GE Healthcare, Pennsylvania, USA), and visualised using X-ray film. Proteins separated by

blue native-PAGE were probed with 0.1 μg/mL primary and 1:200000 secondary antibodies, and developed using ECL^{Advance} (GE Healthcare, Pennsylvania, USA) and detected using an Intelligent-dark box-II (Fujifilm, Tokyo, Japan).

2.3 *Escherichia coli* strains and growth conditions

All bacterial strains used in this work are listed in Table 2.1. Strains TG1 and TOP10 (Invitrogen, California, USA), used for cloning recombinant plasmids, were propagated in 2xYT medium at 37 °C. The protein expression strain, TUNER, was propagated in 25 g/L tryptone, 7.5 g/L yeast extract, 3 g/L NaCl, 2 g/L D-glucose, 20 mM Tris/HCl pH 7.5. Media was supplemented with either ampicillin (100 μg/mL), or kanamycin (50 μg/mL) as appropriate for transformed strains. Bacterial strains were stored by addition of DMSO to overnight cultures to a final concentration of 7 % v/v and freezing at -80 °C.

2.4 *Saccharomyces cerevisiae* strains and culture conditions

All *Saccharomyces cerevisiae* strains used in this thesis are listed in Table 2.2. The strain CG1945 was cultured in 10 g/L yeast extract, 20 g/L peptone, 20 g/L D-glucose (YPD) or synthetic dropout media: 26.7 g/L minimal nitrogen base, 20 g/L D-glucose, 0.6 g/L complete amino acid mixture. Strains transformed with recombinant plasmids were cultured in synthetic dropout media: 26.7 g/L minimal nitrogen base, 20 g/L D-glucose, 0.6 g/L appropriate amino acid mixture. Solid media plates were made by the addition of 20 g/L bacteriological grade agarose. Liquid cultures were incubated overnight at 30 °C unless noted otherwise and aerated by shaking at 300 rpm. *S. cerevisiae* strains grown on solid media were incubated at 30 °C for 3-4 days. Yeast strains were stored by addition of sterile glycerol to overnight cultures to a final concentration of 25 % v/v and freezing at -80 °C.

2.5 *Arabidopsis thaliana* lines and growth conditions

All *Arabidopsis thaliana* lines used are listed in Table 2.3. *A. thaliana* seeds were either grown as previously described (Peng *et al.*, 1997), or stratified at 4 °C for 4 days in half-strength Murashige and Skoog media supplemented with Gamborg's vitamins (Sigma, Missouri, USA) and transferred to moistened seed-raising mix for germination (for wild-type *A. thaliana* Col-0). Plants were grown under long-day conditions: 16 hours light/ 8 hours darkness at 25 °C.

2.6 Total *Arabidopsis thaliana* protein extraction

Inflorescence tissue of 4-5 week old *A. thaliana* was frozen in liquid nitrogen upon collection and stored at -80 °C. Frozen tissue was subsequently crushed using a pellet pestle in ice cold extraction buffer: 50 mM HEPES:KOH pH 7.4, 400 mM NaCl, 1 mM EDTA, 20 μM MG132, at approximately 3 μL per mg of tissue. Insoluble debris was removed by centrifuged at 20000 x g for 30 min at 4 °C. The supernatant, containing extracted proteins, was stored at -80 °C until use.

2.7 *Arabidopsis thaliana* nuclear protein extraction

Nuclei were isolated based on a previously described method, modified for use with *A. thaliana* inflorescence tissue (Busk and Pages, 1997). Inflorescence tissue collected from 4-5 week old wild-type *A. thaliana* Columbia was ground in liquid nitrogen using a mortar and pestle. Ground tissue was then suspended in nuclei isolation buffer: 20 mM HEPES:KOH pH 7.8, 1 mM DTT, 0.2 mM PMSF, 1.0 % w/v PEG-4000, protease inhibitor cocktail (1 vial/L), and filtered through 25 μM pore cloth. Filtrate was then

centrifuged at 4000 x g for 20 min at 4 °C. The pellet was then resuspended in nuclei isolation buffer, layered on a 1.5 M sucrose cushion and centrifuged 12000 x g for 10 min at 4 °C. Pelleted nuclei were then lysed by resuspension in hypotonic lysis buffer: 20 mM HEPES:KOH pH 7.8, 1 mM EDTA, 1 mM DTT, 0.2 mM PMSF, protease inhibitor cocktail (1 vial/L), and subsequent freezing at -80 °C. Further fractions of nuclear proteins were extracted by sequential low (100 mM NaCl) and high (1 M NaCl) salt extractions. All three protein fractions were pooled at a ratio of 100:40:5, giving a final NaCl concentration of 50 mM.

2.8 Preparation of Rabbit polyclonal antisera

An anti-RGL1$^{1-137}$ Rabbit polyclonal antibody was previously obtained from a Rabbit immunised with a purified recombinant maltose binding protein (MBP) fusion to the N-terminal DELLA domain of RGL1 (MBP-RGL1$^{1-137}$) (Sheerin, 2005). The immunoglobulin fraction was separated from serum by ammonium sulfate precipitation, and dissolved in PBS as previously described (Harlow and Lane, 1988). Anti-RGL1 antibodies were affinity purified against a recombinant THYRODOXIN-A fusion of RGL1 (TrxA-RGL1$^{1-137}$), immobilised by cross-linking to Amino-link plus resin (Pierce, Illinois, USA). The unbound immunoglobulin fraction was subsequently used for affinity purification of anti-MBP antibodies, using purified recombinant MBP-β-galactosidase-α (MBP-β-gal) cross-linked to Amino-link plus resin.

2.9 Anti-DELLA monoclonal antibodies

Several anti-DELLA antibodies were developed and supplied by William Jones, Plant and Food Research, New Zealand. These mouse monoclonal antibodies: BC9, AD7, AB8, and BB7 were raised against recombinant N-terminal domains of *A. thaliana* DELLA proteins. The mouse monoclonal antibody 6C8 was raised against a synthetic

peptide, consisting of 12 amino acid residues spanning the N-terminal portion of the DELLA motif.

2.10 Construction of recombinant plasmids

All bacterial and yeast plasmids used in this thesis are detailed in Table 2.4. *RGA* (At2g01570), *RGL1* (At1g66350), *RGL2* (At3g03450), *SLY1* (At4g24210) and *GLP1* (At1g72610) coding sequences were PCR amplified from *A. thaliana* Columbia genomic DNA. *GID1A* (At3g05120), *GID1B* (At3g63010), and *GID1C* (At5g27320) coding sequences were PCR amplified from *A. thaliana* Columbia cDNA.

RGA and *RGL2* coding sequences were cloned into the *NcoI*/*XmaI* sites of pACT2 (yeast two-hybrid system vector) to generate pDJS010, and pDJS008 respectively. *RGL1* was cloned into *XmaI/SacI* –cleaved pACT2 to obtain pDJS006. $rgl1^{\Delta DELLA}$ (deletion of residues 32-48; (Peng *et al.*, 1997)), $rgl1^{\Delta TVHYNP}$ (deletion of residues 68-85; (Itoh *et al.*, 2002)), and $rgl1^{Q272R}$ (nucleotide 815A→G; (Muangprom *et al.*, 2005)) were generated by ligation-mediated PCR mutagenesis and cloned into the *XmaI/SacI* site of pACT2 to obtain pJB04, pJB05, and pJB06 respectively (Ali and Steinkasserer, 1995; Buchanan, 2007). The domain interruption of *RGL1* using in frame *mGFP* (between nucleotides 411 and 412 of *RGL1*, spaced by codons for three glycine residues at each joint) was constructed by overlap extension in two stages to combine the three fragments and cloned into the *XmaI/SacI* site of pACT2 to generate pDS041 (Higuchi *et al*., 1988). $rgl1^{1-137}$ was generated by PCR and cloned into *XmaI/SacI* –cleaved pACT2 to obtain pDJS042.

SLY1 coding sequence was cloned into the *EcoRI*/*BamHI* sites of pGADT7 (yeast two-hybrid system vector), and within the first multiple cloning site of pBridge (yeast three-hybrid system vector) under the constitutive *ADH1* promoter (*pADH1*) to obtain pDJS024, and pDJSDJS020. $sly1^{E138K}$ (nucleotide G412→A) was generated by amplification using a mutagenic reverse amplification primer (Table 2.5), and cloned into *EcoRI*/*BamHI*-cleaved pGADT7, and pBridge under *pADH1* to generate pJB03 and pJB01.

GID1A, *GID1B* and *GID1C* were cloned into the *EcoRI*/*BamHI* sites of pGBKT7 to obtain pDJS013, pDJS014, and pDJS015 respectively. *GID1A* was sub-cloned from the *EcoRI/SalI* sites within pGBKT7 into the *EcoRI/SalI* of pMALc2x (MBP-fusion expression vector) to generate pDJS027. *GID1B* and *GID1C* were sub-cloned from the *EcoRI/PstI* sites within pGBKT7 into the *EcoRI/PstI* of pMalc2x to generate pDJS034 and pDJS035 respectively. *GID1A* was also cloned into the *NotI* site within the second multiple cloning site of pBridge (tertiary Haemagglutinin (HA) tag fusion expression under the control of the *MET25* promoter; *pMET25*) to obtain pDJS021. pDJS020 and pJB01, with *SLY1* or $sly1^{E138K}$ coding sequences in the *EcoRI*/*BamHI* sites of the first multiple cloning site, were further modified by inserting *GID1A* into the *NotI* site within the second multiple cloning site to obtain pDJS023 and pJB02, respectively. .

GLP1 was cloned into *EcoRI*/*BamHI*-cleaved pGBKT7 to generate pDJS039. $GLP1^{\Delta SS}$ (deletion of nucleotides 1-51) was generated through PCR amplification with an alternative forward primer, and cloned onto the *EcoRI*/*BamHI* sites of pGBKT7 to obtain pDJS040.

Oligonucleotides (synthesized by Invitrogen, California, USA) are listed in Table 2.5. All constructs were confirmed by dideoxy nucleotide sequencing (Allan Wilson Centre Genome Services, Massey University, Palmerston North, New Zealand).

2.11 Yeast two-hybrid interaction reporter assays

Yeast two- and three-hybrid reporter assays were performed using previously described protocols (yeast two-hybrid system-3 manual; Clontech, California, USA), modified to enable assaying the requirement for the phytohormone gibberellin. The yeast reporter strain, *S. cerevisiae* CG-1945, was used for all interaction experiments. Preparation of competent yeast cells and transformation were performed using the Frozen-EZ yeast transformation kit (Zymo Research, California, USA). *HIS3* (*IMIDAZOLEGLYCEROL-PHOSPHATE DEHYDRASE*) reporter expression was assayed by growth on synthetic

dropout minimal medium (minus histidine, leucine, and serine), containing 0, 1, 2, 5, 10, 30, or 60 mM 3-AT, supplemented with 0, 1, 10, or 100 µM GA_3 in 200 µM HEPES/KOH pH 7.8. A modified culture preparation protocol was performed for β-galactosidase assays: overnight cultures in synthetic dropout medium (minus leucine and serine) were diluted to OD_{600nm} = 0.10 in medium supplemented with 100 µM GA_3 (or 1 nM -10 µM GA_3/GA_4 for dose-response experiments) in 200 µM HEPES/KOH pH 7.8, or 200 µM HEPES/KOH pH 7.8. Cultures were incubated at 30 °C with rotational agitation (250 rpm) for exactly 20 hours, 1.5 mL of the ~ OD_{600nm} = 0.6 cultures were harvested by centrifugation at 10000 x g for 10 min. The resulting cell pellets were resuspended in 300 µL 100 mM Na_2HPO_4/NaH_2PO_4 pH 7.0, 10 mM KCl, 1 mM $MgSO_4$, 50% v/v Y-Per protein extraction reagent (Pierce, Illinois, USA), protease inhibitor cocktail (1 vial/L), and vortexed for 15 min at room temperature. Liquid ONPG assays were performed in triplicate from three transformants, for a total of nine assays, according to the Clontech yeast two-hybrid system-3 instruction manual.

2.12 Recombinant protein expression and purification

An N-terminal MBP-fusion of the RGL1 N-terminal DELLA domain (MBP-$RGL1^{1-137}$) was expressed as previously described (Sun *et al.*, 2008). MBP-GID1A-C fusions were expressed from pMALc2x constructs; pDJS027, pDJS034, and pDJS035 respectively, and purified as described in the pMAL system manual (New England Biolabs, Massachusetts, USA), except protein expression was induced at 20 °C with 100 µM IPTG for 4 hours. The cells were harvested by centrifugation and resuspended in ice cold 10 mM HEPES/NaOH pH 7.5, 125 mM NaCl, 0.1% v/v Triton X-100, 0.1% w/v octyl-β-D-glucopyranoside, 1 mM EDTA, 1 mM DTT, protease inhibitor cocktail (1 vial/L) to an OD_{600nm} of 50, followed by subsequent lysis by addition of 100 µg/mL Chicken Lysozyme (Roche Applied Bioscience, Basel, Switzerland) and 0.2 units/mL DNAse I (Fermentas, Ontario, Canada). MBP-GID1A-C fusion proteins were affinity purified using immobilised amylose resin (New England Biolabs, Massachusetts, USA), and concentrated using 100 kDa cut-off Vivaspin centrifugal concentrators (Sartorius, Aubagne, France) to remove products of partially degradation, yet retain the majority of

the 80 kDa active recombinant protein. MBP-tag (MBP-β-gal, expressed from the unmodified vector pMALc2x) was prepared as described in the pMAL system manual except bacteria were resuspended and lysed as above, and amylose affinity-purified protein was concentrated using 5 kDa cut-off Vivaspin centrifugal concentrators (Sartorius, Aubagne, France). Protein concentrations were determined by fluorometry (Qubit; Invitrogen, California, USA).

2.13 *in vitro* interaction experiments

Interactions were monitored by surface plasmon resonance using a Biacore X instrument (GE Healthcare, Pennsylvania, USA). Affinity purified anti-MBP rabbit polyclonal antibodies were cross-linked to a CM5 chip, according to manufactures instructions, and subsequently used to capture ligands: purified *E. coli*-expressed MBP-RGL1$^{1-137}$ and MBP-tag control. Any remaining MBP-binding sites were blocked by saturation with purified MBP tag. Binding of purified recombinant MBP-GID1A-C to both MBP-tag and MBP-RGL1$^{1-137}$ (flow cell 1 and 2 respectively) was assayed and background binding of MBP-GID1A-C to captured MBP-tag was subtracted from all binding curves. Assays were performed at 25 °C in HBS-EP (GE Healthcare, Pennsylvania, USA), at a flow rate of 10 µL/min. 70 µL volumes of samples were injected, hence duration of association was 7 min (420 s). MBP-tag and MBP-RGL1$^{1-137}$ were applied at 500 nM; MBP-GID1A at 100-1600 nM (kinetic studies); MBP-GID1A-C at 200 nM (binding assays) or 100 nM (competition assays); and monoclonal antibodies at 500 nM (competition assays). GA_3 and GA_4 were added to MBP-GID1A-C samples at 100 µM in binding assays, or 5 µM GA_4 in competition assays, 30 min prior to injection. Gibberellins were absent from all other solutions.

Binding, in fmol/mm^2, of either monoclonal antibodies or MBP-GID1A in competition experiments refers to the total analyte bound at the end of the 420 s association phase. Values were subjected to the following transformations: binding of the analyte (MBP-GID1A or monoclonal antibody) to the control flow cell (MBP-tag) was subtracted; furthermore, to account for gradual loss of anti-MBP from the chip, binding was

standardised to daily interaction controls (MBP-GID1A +/- GA_4). Binding is expressed in response units, 1 RU = 1 pg/mm^2 and further converted to fmol/mm^2, using the following molecular mass values: antibodies, M = 150 kDa; MBP-GID1A, M = 81.6 kDa.

2.13.1 Analysis of association and dissociation kinetics

Concentration-dependent aggregation of recombinant GID1A/GA_4 was observed; hence surface plasmon resonance saturation experiments, using monoclonal antibody BC9 as a reference, were used to determine that the GID1A/GA_4:RGL1$^{1-137}$ complex is 1:1, and that MBP-GID1A cannot aggregate significantly at the chip surface (Appendix A). I defined the active GID1A/GA_4 concentration as equal to the concentration of GID1A present in possible monomer and dimer fractions, which were quantified by blue-native-PAGE and densitometry of corresponding bands in 100 nM, 200 nM and 400 nM samples. Densitometry of 800 nM and 1600 nM samples was not reliable and these concentrations were excluded from model fitting. Association and dissociation data were simultaneously fitted to a two-state, conformational change model for interaction using BiaEvaluation software version 3.1 (GE Healthcare, Pennsylvania, USA).

2.14 Deuterium exchange mass spectrometry

Deuterium exchange mass spectrometry was performed as previously described (Englander *et al.*, 2003). Purified recombinant MBP-RGL1$^{1-137}$ was incubated with 90 % v/v deuterated water for 0, 10, 100, 1000, 3000, or 60000 s at 0 ºC in PBS pH 7.4. Deuterium exchange was quenched using low pH by addition of glycine to 1M. Samples were stored at -80 ºC until digestion with pepsin. Peptides were subsequently separated and analysed by coupled liquid-chromatography-mass spectrometry (LC-MS). Peptide data were assigned to MBP-RGL1$^{1-137}$ sequence using MassLynx software (Waters, Massachusetts, USA). Assigned peptides were assessed for quality by

closeness of fit to predicted peptide monoisotopic data, using a software based cut-off of 2.99. Low quality peptides and duplicate assignments were removed from the peptide pool following further scoring by user for clear monoisotopic peaks. The percentage of backbone amines exchanged for each quality peptide was calculated by comparison to the undeuterated (0 %) and full deuteration (60000 s, 100 %).

2.15 Affinity purification of RGL1-interacting proteins

A procedure for affinity purification of plant proteins that interact with the N-terminal domain of RGL1 was previously developed (Sheerin, 2005). This procedure was altered to improve yield of affinity isolated proteins, including up-scaling the quantity of plant tissue used, and using columns with syringe attachments for rapid washing of the columns. Affinity columns were prepared using purified MBP-β-gal or MBP-RGL1$^{1-137}$ cross-linked to amino link plus resin (Amino link plus kit, Pierce, Illinois, USA) through lysine residues. Plant nuclear extract, prepared as described above from 10 g inflorescence tissue, was incubated with 20 µL MBP-RGL1$^{1-137}$-coated resin for 2 hours at 4 °C with gentle agitation (Nutator: Labnet, New Jersey, USA). Unbound extract and resin were separated by gentle pressure applied to a micro column (Micro spin columns, Pierce, Illinois, USA), and subsequent rapid washing (approximately 1 mL/min) using 2 x 500 µL ice cold 20 mM HEPES/ KOH pH 7.8, 50 mM NaCl, 1 mM EDTA, 1 mM DTT, 0.2 mM PMSF, complete protease inhibitor cocktail (1 vial/L) . Proteins were eluted by boiling resin in 20 µL 2 x SDS-PAGE loading buffer for 3 min, and separated by Tricine-SDS-PAGE, and visualised by SYPROruby staining.

2.16 Mass spectrometry fingerprinting

Protein bands were excised from tricine-SDS-PAGE gels stained with SYPROruby gel stain. Gel fragments were desiccated under vacuum and sent to the Mass Spectrometry Facility, University of Auckland, New Zealand, for analysis of tryptic digests by

electrospray ionisation-quadrapole-time-of-flight coupled mass spectrometry (LC-ESI MS/MS). Mass fingerprint data was analysed using MASCOT (Matrix Science, London, United Kingdom), searching the entire Swissprot protein sequence database with a parent peptide cut-off of +/- 1 Da, and +/- 0.1 Da for fragmentation data. Unassigned peptides were de-novo sequenced using PEAKS (Bioinformatics Solutions, Ontario, Canada), a database of all possible peptide fingerprints, and searched against the non-redundant (nr) protein databases using BLAST (Altschul *et al.*, 1990).

Table 2.1 ***Escherichia coli*** **strains**

Strain	Genotype	Reference
TUNER	*F- ompT hsdS(rBmB-) gal dcm lacY1*	EMD biosciences, California, USA
TG1	*K12 Δ(lac-pro) supE44 thi hsdR 5 F' traΔ36 proA+B+ lacIq lacZΔM14*	
TOP10	*F- mcrA* Δ(*mrr-hsdRMS-mcrBC*) ϕ80*lacZΔM15* Δ*lacX74 recA1 araD139* Δ(*ara-leu*)*7697 galU galK rpsL* (*Str*^{R}) *endA1 nupG*	Invitrogen, California, USA
K1915	TUNER, pPMB7235 (MBP-RGL1$^{1-137}$), Amp^{R}	(Sheerin, 2005)
K1918	TUNER, pMALc2x, Amp^{R}	This study
K2057	TUNER, pDJS027 (MBP-GID1A), Amp^{R}	This study
K2123	TUNER, pDJS034 (MBP-GID1B), Amp^{R}	This study
K2124	TUNER, pDJS035 (MBP-GID1C), Amp^{R}	This study

Table 2.2 ***Saccharomyces cerevisiae*** **strains**

Strain	Genotype	Reference
CG1945	*MATa ura3-52 his3-200 ade2-101 lys2-801 trp1-901 leu2-3 112 gal4-542 gal80-538 cyhr2 LYS2 : : GAL1uas-GAL1tata-HIS3 URA3 : : GAL4 17-mers (x3) -CYC1tata-lacZ*	(Feilotter *et al.*, 1994)
SC011	CG1945, pGBKT7, pACT2	(Sheerin, 2005)
SC050	CG1945, pBRIDGE, pACT2	(Sheerin, 2005)
SC058	CG1945, pGBKT7, pGADT7	(Sheerin, 2005)
SC004	CG1945, pGBK-p53, pGAD-T-antigen	(Sheerin, 2005)
SC023	CG1945, pGBKT7, pDJS010 (AD-RGA)	(Sheerin, 2005)
SC015	CG1945, pGBKT7, pDJS006 (AD-RGL1)	(Sheerin, 2005)
SC063	CG1945, pGBKT7, pJB04 (AD-rgl1$^{\Delta DELLA}$)	This study
SC064	CG1945, pGBKT7, pJB05 (AD-rgl1 $^{\Delta TVHYNP}$)	This study
SC065	CG1945, pGBKT7, pJB06 (AD-rgl1 ^{Q272R})	This study
SC019	CG1945, pGBKT7, pDJS008 (AD-RGL2)	(Sheerin, 2005)
SC066	CG1945, pGBKT7, pDJS024 (AD-SLY1)	This study
SC067	CG1945, pGBKT7, pJB03 (AD-sly1^{E138K})	This study
SC051	CG1945, pBRIDGE, pDJS006 (AD-RGL1)	This study
SC091	CG1945, pBRIDGE, pJB04 (AD-rgl1$^{\Delta DELLA}$)	This study
SC092	CG1945, pBRIDGE, pJB05 (AD-rgl1$^{\Delta TVHYNP}$)	This study
SC093	CG1945, pBRIDGE, pJB06 (AD-rgl1^{Q272R})	This study
SC031	CG1945, pDJS013 (BD-GID1A), pACT2	This study
SC032	CG1945, pDJS014 (BD-GID1B), pACT2	This study
SC033	CG1945, pDJS015 (BD-GID1C), pACT2	This study
SC060	CG1945, pDJS020 (BD-SLY1), pACT2	This study
SC061	CG1945, pJB01 (BD-sly1^{E138K}), pACT2	This study
SC087	CG1945, pDJS021 (HA-GID1A), pACT2	This study
SC052	CG1945, pDJS023 (BD-SLY1, HA-GID1A), pACT2	This study
SC062	CG1945, pJB02 (BD-sly1^{E138K}, HA-GID1A), pACT2	This study

Table 2.2 continued

Strain	Genotype	Reference
SC094	CG1945, pDJS039 (BD-GLP1), pACT2	This study
SC095	CG1945, pDJS040 (BD-GLP1$^{\Delta SS}$), pACT2	This study
SC038	CG1945, pDJS013 (BD-GID1A), pDJS010 (AD-RGA)	This study
SC039	CG1945, pDJS014 (BD-GID1B), pDJS010 (AD-RGA)	This study
SC040	CG1945, pDJS015 (BD-GID1C), pDJS010 (AD-RGA)	This study
SC041	CG1945, pDJS013 (BD-GID1A), pDJS006 (AD-RGL1)	This study
SC042	CG1945, pDJS014 (BD-GID1B), pDJS006 (AD-RGL1)	This study
SC043	CG1945, pDJS015 (BD-GID1C), pDJS006 (AD-RGL1)	This study
SC068	CG1945, pDJS013 (BD-GID1A), pJB04 (AD-rgl1$^{\Delta DELLA}$)	This study
SC069	CG1945, pDJS013 (BD-GID1A), pJB05 (AD-rgl1$^{\Delta TVHYNP}$)	This study
SC070	CG1945, pDJS013 (BD- GID1A), pJB06 (AD-rgl1^{Q272R})	This study
SC044	CG1945, pDJS013 (BD- GID1A), pDJS008 (AD-RGL2)	This study
SC045	CG1945, pDJS014 (BD- GID1B), pDJS008 (AD-RGL2)	This study
SC046	CG1945, pDJS015 (BD- GID1C), pDJS008 (AD-RGL2)	This study
SC071	CG1945, pDJS013 (BD-GID1A), pDJS024 (AD-SLY1)	This study
SC072	CG1945, pDJS013 (BD-GID1A), pJB03 (AD-sly1^{E138K})	This study

Table 2.2 continued

Strain	Genotype	Reference
SC056	CG1945, pDJS020 (BD-SLY1), pDJS006 (AD-RGL1)	This study
SC056	CG1945, pDJS020 (BD-SLY1), pDJS006 (AD-RGL1)	This study
SC073	CG1945, pDJS020 (BD-SLY1), pJB04 (AD-rgl1$^{\Delta DELLA}$)	This study
SC074	CG1945, pDJS020 (BD-SLY1), pJB05 (AD-rgl1$^{\Delta TVHYNP}$)	This study
SC075	CG1945, pDJS020 (BD-SLY1), pJB06 (AD-rgl1^{Q272R})	This study
SC079	CG1945, pJB01 (BD-sly1^{E138K}), pDJS006 (AD-RGL1)	This study
SC080	CG1945, pJB01 (BD-sly1^{E138K}), pJB04 (AD-rgl1$^{\Delta DELLA}$)	This study
SC081	CG1945, pJB01 (BD-sly1^{E138K}), pJB05 (AD-rgl1$^{\Delta TVHYNP}$)	This study
SC082	CG1945, pJB01 (BD-sly1^{E138K}), pJB06 (AD-rgl1^{Q272R})	This study
SC057	CG1945, pDJS021 (HA-GID1A), pDJS006 (AD-RGL1)	This study
SC088	CG1945, pDJS021 (HA-GID1A), pJB04 (AD-rgl1$^{\Delta DELLA}$)	This study
SC089	CG1945, pDJS021 (HA-GID1A), pJB05 (AD-rgl1$^{\Delta TVHYNP}$)	This study
SC090	CG1945, pDJS021 (HA-GID1A), pJB06 (AD-rgl1^{Q272R})	This study
SC053	CG1945, pDJS023 (BD-SLY1, HA-GID1A), pDJS006 (AD-RGL1)	This study
SC076	CG1945, pDJS023 (BD-SLY1, HA-GID1A), pJB04 (AD-rgl1$^{\Delta DELLA}$)	This study

Table 2.2 continued

Strain	Genotype	Reference
SC077	CG1945, pDJS023 (BD-SLY1, HA-GID1A), pJB05 (AD-rgl1$^{\Delta TVHYNP}$)	This study
SC078	CG1945, pDJS023 (BD-SLY1, HA-GID1A), pJB06 (AD-rgl1^{Q272R})	This study
SC083	CG1945, pJB02 (BD-sly1^{E138K}, HA-GID1A), pDJS006 (AD-RGL1)	This study
SC084	CG1945, pJB02 (BD-sly1^{E138K}, HA-GID1A), pJB04 (AD-rgl1$^{\Delta DELLA}$)	This study
SC085	CG1945, pJB02 (BD-sly1^{E138K}, HA-GID1A), pJB05 (AD-rgl1$^{\Delta TVHYNP}$)	This study
SC086	CG1945, pJB02 (BD-sly1^{E138K}, HA-GID1A), pJB06 (AD-rgl1^{Q272R})	This study
SC096	CG1945, pDJS039 (BD-GLP1), pDJS006 (AD-RGL1)	This study
SC097	CG1945, pDJS040 (BD-GLP1$^{\Delta SS}$), pDJS006 (AD-RGL1)	This study
SC098	CG1945, pGBKT7, pDJS041 (AD-RGL1^{N}-GFP-RGL1^{C})	This study
SC099	CG1945, pDJS013 (BD-GID1A), pDJS041 (AD-RGL1^{N}-GFP-RGL1^{C})	This study
SC100	CG1945, pBRIDGE, pDJS041 (AD-RGL1^{N}-GFP-RGL1^{C})	This study
SC101	CG1945, pDJS020 (BD-SLY1), pDJS041 (AD-RGL1^{N}-GFP-RGL1^{C})	This study
SC102	CG1945, pJB01 (BD-sly1^{E138K}), pDJS041 (AD-RGL1^{N}-GFP-RGL1^{C})	This study
SC103	CG1945, pDJS021 (HA-GID1A), pDJS041 (AD-RGL1^{N}-GFP-RGL1^{C})	This study
SC104	CG1945, pDJS023 (BD-SLY1, HA-GID1A), pDJS041 (AD-RGL1^{N}-GFP-RGL1^{C})	This study

Table 2.2 continued

Strain	Genotype	Reference
SC105	CG1945, pJB02 (BD-sly1^{E138K}, HA-GID1A), pDJS041 (AD-RGL1^{N}-GFP-RGL1^{C})	This study
SC106	CG1945, pGBKT7, pDJS042 (AD-rgl1$^{1-137}$)	This study
SC107	CG1945, pDJS039 (BD-GLP1), pDJS042 (AD-rgl1$^{1-137}$)	This study
SC108	CG1945, pDJS040 (BD-GLP1$^{\Delta SS}$), pDJS042 (AD-rgl1$^{1-137}$)	This study

Table 2.3 ***Arabidopsis thaliana*** **lines**

Genotype	Background	Reference
Wild-type, Col-0	Columbia	
Wild-type, Ler	Landsberg-*erecta*	
ga1-3,	Landsberg-*erecta*	(Koornneef and Vanderveen, 1980)
gai-t6	Landsberg-*erecta*	(Peng *et al.*, 1997)
rga-t2	Landsberg-*erecta*	(Lee *et al.*, 2002)
rgl1-1	Landsberg-*erecta*	(Lee *et al.*, 2002)
rgl2-1	Landsberg-*erecta*	(Lee *et al.*, 2002)
rgl3-1	Landsberg-*erecta*	Nicholas Harberd, unpublished
gai-t6, *rga-t2*, *rgl1-1*, *rgl2-1*	Landsberg-*erecta*	(Achard *et al.*, 2006)
gai-t6, *rga-t2*, *rgl1-1*, *rgl2-1*, *rgl3-1*	Landsberg-*erecta*	Nicholas Harberd, unpublished
ga1-3, *gai-t6*, *rga-t2*, *rgl1-1*, *rgl2-1*	Landsberg-*erecta*	(Cao *et al.*, 2005)
ga1-3, *rga-t2*, *rgl1-1*, *rgl2-1*	Landsberg-*erecta*	(Cao *et al.*, 2005)
ga1-3, *gai-t6*, *rgl1-1*, *rgl2-1*	Landsberg-*erecta*	(Cao *et al.*, 2005)
ga1-3, *gai-t6*, *rga-t2*, *rgl2-1*	Landsberg-*erecta*	(Cao *et al.*, 2005)
ga1-3, *gai-t6*, *rga-t2*, *rgl1-1*	Landsberg-*erecta*	(Cao *et al.*, 2005)

Table 2.4 Plasmids

Name	Description	Reference
pMALc2x	*pLAC:MALE*$_{(\Delta \text{ signal sequence})}$, *Amp*^{R}, *Col E1 ori*	New England Biolabs, Massachusetts, USA
pACT2	*pADH1:GAL4*$^{(768\text{-}881)}$*-HA*, *LEU2*, Amp^{R}, *Col E1 ori*, *2μ ori*	(Li *et al.*, 1994)
pGBKT7	*pADH1:GAL4*$^{(1\text{-}147)}$*-c-myc*, *TRP1*, Kan^{R}, *f1 ori*, *2μ ori*	Clontech, California, USA (Louvet *et al.*, 1997)
pGADT7	*pADH1:GAL4*$^{(768\text{-}881)}$*-HA*, *LEU2*, Amp^{R}, *pUC ori*, *2μ ori*	Clontech, California, USA
pBRIDGE	*pADH1:GAL4*$^{(1\text{-}147)}$, *pMET25:HA*, *TRP1*, Amp^{R}, *Col E1 ori, 2μ ori*	Clontech, California, USA (Tirode *et al.*, 1997)
pGBKT7-p53	murine *p53*$^{(72\text{-}390)}$ in pGBKT7, *TRP1*, Kan^{R}	Clontech, California, USA
pGADT7-T	SV40 large T-antigen$^{(84\text{-}708)}$ in pGADT7, *LEU2*, Amp^{R}	Clontech, California, USA
pPMB7235	*RGL1*$^{(\text{nt1-411})}$ in pMALc2x, Amp^{R}	(Sun *et al.*, 2008)
pDJS027	*GID1A* in pMALc2x, Amp^{R}	This study
pDJS034	*GID1B* in pMALc2x, Amp^{R}	This study
pDJS035	*GID1C* in pMALc2x, Amp^{R}	This study
pDJS006	*RGL1* in pACT2, *LEU2*, Amp^{R}	(Sheerin, 2005)
pJB04	*rgl1*$^{(\Delta 94\text{-}144)}$ in pACT2, *LEU2*, Amp^{R}	(Buchanan, 2007)
pJB05	*rgl1*$^{(\Delta 202\text{-}255)}$ in pACT2, *LEU2*, Amp^{R}	(Buchanan, 2007)
pJB06	*rgl1*$^{(\text{A815T})}$ in pACT2, *LEU2*, Amp^{R}	(Buchanan, 2007)
pDJS008	*RGL2* in pACT2, *LEU2*, Amp^{R}	(Sheerin, 2005)
pDJS010	*RGA* in pACT2, *LEU2*, Amp^{R}	(Sheerin, 2005)
pDJS013	*GID1A* in pGBKT7, *TRP1*, Kan^{R}	This study
pDJS021	*GID1A* in pBRIDGE (*pMET25*), *TRP1*, Amp^{R}	This study
pDJS014	*GID1B* in pGBKT7, *TRP1*, Kan^{R}	This study

Table 2.4 continued

Name	Description	Reference
pDJS015	*GID1C* in pGBKT7, *TRP1*, Kan^R	This study
pDJS020	*tSLY1* in pBRIDGE (*pADH1*), *TRP1*, Amp^R	This study
pDJS024	*SLY1* in pGADT7, *LEU2*, Amp^R	This study
pJB01	$sly1^{(G412A)}$ in pBRIDGE (*pADH1*), *TRP1*, Amp^R	(Buchanan, 2007)
pJB03	$sly1^{(G412A)}$ in pGADT7, *LEU2*, Amp^R	(Buchanan, 2007)
pDJS023	pBRIDGE, *SLY1* (*pADH1*), *GID1A* (*pMET25*), *TRP1*, Amp^R	This study
pJB02	pBRIDGE, $sly1^{(G412A)}$ (*pADH1*), *GID1A* (*pMET25*), *TRP1*, Amp^R	(Buchanan, 2007)
pDJS039	*GLP1* in pGBKT7, *TRP1*, Kan^R	This study
pDJS040	$GLP1^{(\Delta 1\text{-}51)}$ in pGBKT7, *TRP1*, Kan^R	This study
pDJS041	$RGL1^{(1\text{-}411)}$-*GFP*-$RGL1^{(412\text{-}1533)}$ in pACT2, *LEU2*, Amp^R	This study
pDJS042	$rgl1^{(1\text{-}411)}$ in pACT2, *LEU2*, Amp^R	This study

Table 2.5 **Oligonucleotides**

Sequence	Details
GGTCGTCAGACTGTCGATGAAGCC	pMALc2x, forward vector insert sequencing primer
CGCCAGGGTTTTCCCAGTCACGAC	pMALc2x, reverse vector insert sequencing primer
TTTAATACGACTCACTATAGGGC	pGBKT7, forward vector insert sequencing primer
TAAGAGTCACTTTAAAATTTGTAT	pGBKT7, reverse vector insert sequencing primer
TTTAATACGACTCACTATAGGGC	pGADT7, forward vector insert sequencing primer
GCGGGGTTTTTCAGTATCTAC	pGADT7, reverse vector insert sequencing primer
TCATCGGAAGAGAGTAG	pBridge, forward vector insert sequencing primer, first multiple cloning site
CGTTTTCCTAAGAGTCAC	pBridge, reverse vector insert sequencing primer, first multiple cloning site
TTGGGGAACTGTGGTGGTTG	pBridge, forward vector insert sequencing primer, second multiple cloning site
CCGTATTACCGCCTTTGAGT	pBridge, reverse vector insert sequencing primer, second multiple cloning site
GGAATTCATGGCTGCGAGCGATGAAG	*GID1A*, forward: *EcoRI*
CGGGATCCGTTAACATTCCGCGTTTACAAAC	*GID1A*, reverse: *BamHI*

Table 2.5 continued

Sequence	Details
ATAAGAATGCGGCCGCTATGGCTGCGAGCGATGAAG	*GID1A*, forward: *NotI*
ATAAGAATGCGGCCGCTATTAACATTCCGCGTTTACAAAC	*GID1A*, reverse: *NotI*
GGAATTCATGGCTGGTGGTAACGAAGT	*GID1B*, forward: *EcoRI*
CGGGATCCGCTAAGGAGTAAGAAGCACAGG	*GID1B*, reverse: *BamHI*
GGAATTCATGGCTGGAAGTGAAGAAGTT	*GID1C*, forward: *EcoRI*
CGGGATCCGTCATTGGCATTCTGCGTTTAC	*GID1C*, reverse: *BamHI*
CGGAATTCATGAAGCGCAGTACTACCGAC	*SLY1*, forward: *EcoRI*
CGCGGATCCGTTATTTGGATTCTGGAAGAGGTC	*SLY1*, reverse: *BamHI*
CGCGGATCCGTTATTTGGATTCTGGAAGAGGTCTCTTAGTGAAACTCATCT TCTTGTAG	*SLY1*, reverse, mutagenic primer G412→A: *BamHI*
CGGAATTCATGTTGCGTACTATCTTCCTCTTATC	*GLP1*, forward: *EcoRI*
CGGAATTCTCTGTTCAAGATTTCTGTGTCGCA	$GLP1^{\Delta Signal\ Sequence}$, forward: *EcoRI*
CGCGCGGGATCCCTTAGCCAGTTCCTCCAAGAACAC	*GLP1*, reverse: *BamHI*
ATCGGAGTTATCCTCTACGGGTGGCGAATGAGTAAAGGAGAAGAAC	*GFP*, forward for overlap extension
GAATCCAAAACCACCACAGAGCGACCCCCTCCTTTGTATAGTTCATCCAGC	*GFP*, reverse for overlap extension
GTTCTTCTCCTTTACTCATTCCGCCACCCGTAGAGGATAACTCCGAT	$RGL1^{(411)}$, reverse for overlap extension
GCATGGATGAACTATACAAAGGAGGGGTCGCTCTGTGGTGGTTTTGGATTC	$RGL1^{(412)}$, forward for overlap extension

Table 2.5 continued

Sequence	Details
TCCCCCGGGTATGAAGAGAGAGCACAACCACC	*RGL1*, forward: *XmaI*
CGAGCTCGTTACGTAGAGGATAACTCCGATTCAA	*RGL1*$^{(411)}$, reverse: *SacI*
CGAGCTCGTTATTCCACACGATTGATTCGCC	*RGL1*, reverse: *SacI*

Chapter 3

Characterisation of antibodies against *Arabidopsis thaliana* DELLA proteins

Insertion mutant analysis of multiple *A. thaliana DELLA* genes has revealed the individual *DELLA* genes to be partially functionally redundant (Cheng *et al.*, 2004; Dill *et al.*, 2001; King *et al.*, 2001; Lee *et al.*, 2002). Furthermore, insertion mutants have been crossed into a gibberellin-deficient *ga1-3* background to rescue gibberellin signalling and to allow developmental functions to be attributed to subsets of the *A. thaliana DELLA* genes (Cheng *et al.*, 2004; Tyler *et al.*, 2004). The expression patterns for the five *A. thaliana DELL*A genes throughout development have been well characterised, and are consistent with the observed developmental functions of each *DELLA* gene (Tyler *et al.*, 2004). However, the DELLA proteins are known to be regulated at the post-translational level. Therefore, assigning specific functions to individual *DELLA* genes cannot be entirely based upon expression data.

The DELLA proteins are normally present at a very low level in plant tissues. Hence, transgenic constructs to overexpress DELLA protein fusions have provided the majority of information about the behaviour of the DELLA proteins thus far (Dill *et al.*, 2001; Silverstone *et al.*, 2001; Wen and Chang, 2002). A significant disadvantage to this approach is that DELLA protein overexpression retards plant development and therefore observations may not reflect events within wild-type plants. With the exception of rice SLR1, endogenous DELLA proteins have only been detected in plants lines deficient in gibberellin-dependent DELLA protein degradation (Dill *et al.*, 2004; Itoh *et al.*, 2002). Therefore, in an effort to achieve detection of the low-abundance endogenous *A. thaliana* DELLA proteins, a series of anti-DELLA antibodies were developed by the Plant Immunology group, lead by W. Jones, at Plant and Food Research, Palmerston North, New Zealand.

The anti-DELLA monoclonal antibodies, BC9, AD7, AB8, and BB7 were raised against recombinant *A. thaliana* N-terminal DELLA domains. This domain is overall highly variable; however it encompasses two conserved motifs, DELLA and TVHYNP, that define the DELLA protein family. Because of its general variability, this domain is most likely region to generate antibodies specific to individual DELLA proteins. I have also generated an affinity-purified polyclonal antibody, R1PC, against this region of the DELLA protein RGL1 (Sheerin, 2005).

The specificities of the monoclonal antibodies BC9, AD7, AB8, and BB7 for recombinant forms of all five *A. thaliana* DELLA proteins have been determined *in vitro* (Table 3.1; W. Jones, unpublished). BC9 acts as a universal anti-DELLA antibody: binding strongly to all five recombinant *A. thaliana* DELLA proteins. AD7 recognises RGL1, RGL2, and RGL3, but neither GAI nor RGA. The monoclonal antibodies AB8 and BB7 are highly specific, recognising only individual DELLA proteins: RGL1 and RGL2, respectively. The specificity of the polyclonal antibody R1PC has been examined by immunoblot for four of the five recombinant DELLA proteins, excluding RGL3, and recognises all of these proteins (Sheerin, 2005).

Table 3.1 Antibody specificity for recombinant *A. thaliana* DELLA proteins

Antibody	GAI	RGA	RGL1	RGL2	RGL3
R1PC	+	+	+	+	nd[§]
BC9	+	+	+	+	+
AD7	-	-	+	+	+
AB8	-	-	+	-	-
BB7	-	-	-	+	-

+, Recombinant protein detected by immunoblot

-, No reaction detected by immunoblot

§ nd, Not done.

3.1 Detection of endogenous *Arabidopsis thaliana* DELLA proteins

Transgenic plant lines expressing GFP-fusions to DELLA proteins have shown the DELLA proteins to be nuclear localised. However, probing nuclear extract prepared from wild-type inflorescence tissue by immunoblotting with R1PC failed to detect any endogenous proteins, even though this fraction should be enriched in DELLA proteins (Sheerin, 2005).

Published reports have shown that some endogenous DELLA proteins are present at detectable levels in crude extracts prepared from the gibberellin-deficient *A. thaliana* mutant *ga1-3*, where gibberellin-induced degradation is limited (Dill *et al.*, 2001; Silverstone *et al.*, 2001). However, initial trials using BC9, AD7, or the polyclonal antibody R1PC to probe crude *ga1-3* lysates, failed to detect any endogenous DELLA proteins (data not shown). Therefore it is likely that the endogenous DELLA proteins are degraded during extraction from tissues, for both crude preparations and nuclear extracts.

To overcome this problem of DELLA protein degradation during protein extraction, I developed an extraction method based upon two previously described methods that were successful for the detection of endogenous DELLA proteins. As I intended for extracts to be used in immuno-precipitation and protein:protein interaction experiments, I used a simple extraction protocol using a moderate salt concentration as has been previously used for SLR1 extraction from rice (Itoh *et al.*, 2005). Furthermore, I included the proteasome inhibitor, MG132, which has been previously shown to increase the abundance of extracted DELLA proteins (Hussain *et al.*, 2005; Wang *et al.*, 2009).

DELLA proteins were extracted from gibberellin-deficient *A. thaliana ga1-3* inflorescence tissue in a neutral pH buffer containing 400 mM NaCl and the proteasome inhibitor, MG132. Extract of the quadruple *DELLA* mutant; *gai-t6*, *rga-t2*, *rgl1-1*, *rgl2-1,* that possess T-DNA insertions within four of the five *A. thaliana DELLA* genes, was

used as a control. Endogenous DELLA proteins present in these extracts were probed by immunoblot with the polyclonal antibody R1PC, as this antibody very likely recognises multiple epitopes, and as such is unlikely to be blocked by putative *in planta* post-translational modifications.

The simple extraction procedure allowed detection of a faint protein band of approximately 60 kDa in size, consistent with the calculated molecular mass of the *A. thaliana* DELLA proteins that range from 56.7 to 64.0 kDa (Figure 3.1). In the presence of the proteasome inhibitor MG132, a strong pair of bands was detected, even after incubation of the extract at 4 °C for 120 min. However, even as little as 30 min at 4 °C in the absence of MG132, the time taken to prepare the extract, was sufficient for the majority of the DELLA proteins to be degraded. The degradation of the DELLA proteins upon extraction from tissue occurs even in the gibberellin-deficient *ga1-3* mutant. Hence, the mechanism for this proteasomal degradation of DELLA proteins upon tissue damage is likely gibberellin-independent.

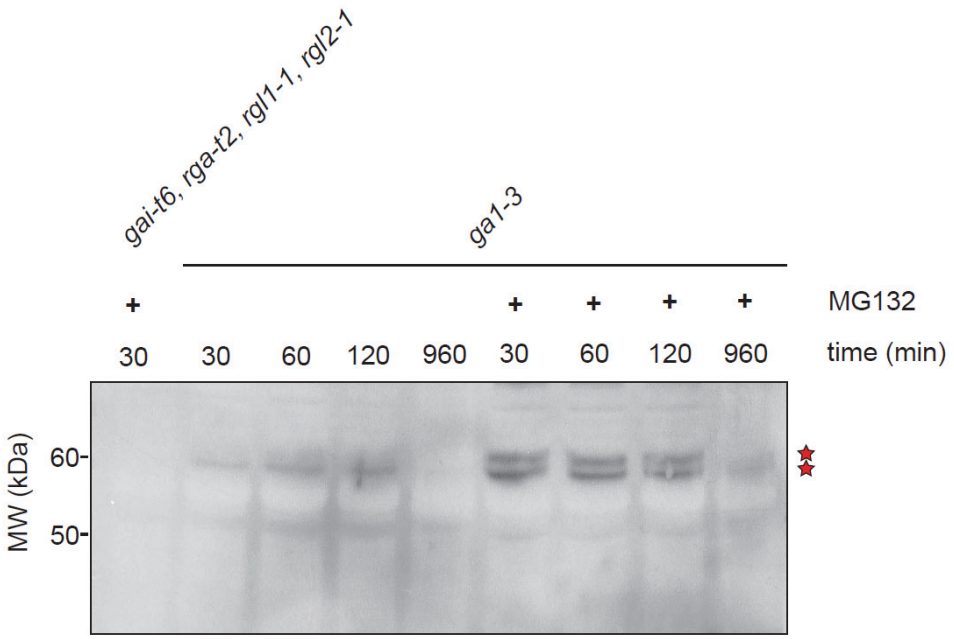

Figure 3.1. Stabilisation of *A. thaliana* endogenous DELLA proteins. Endogenous DELLA proteins were detected in total *A. thaliana* protein extracts by immunoblot using affinity purified anti-RGL1 polyclonal antibody R1PC. Inflorescence tissue extracts were incubated at 4 °C for 30 - 960 min, with the addition of either 0.5 % v/v DMSO, or 20 µM proteasome inhibitor MG132 in 0.5 % v/v DMSO. Extracts prepared from *DELLA* gene quadruple T-DNA insertion mutant, *gai-t6*, *rga-t2*, *rgl1-1*, *rgl2-1*; negative control, and the gibberellin-deficient mutant *ga1-3*. Red stars indicate proteins detected in *ga1-3* extracts at expected molecular weights for RGA, 64 kDa and RGL2, 60.5 kDa.

3.1.1 Identification of endogenous *Arabidopsis thaliana* DELLA proteins

Previous reports have shown only GAI, RGA, and RGL2 to be present at detectable levels, and only in the DELLA protein degradation-deficient *ga1-3* or *sly1-10* backgrounds (Dill *et al.*, 2004; Tyler *et al.*, 2004). Therefore, to fully characterise the specificity of the anti-DELLA antibodies for endogenous DELLA proteins, extracts from gibberellin-deficient *DELLA* T-DNA insertion lines were probed. As all five *A. thaliana* DELLA proteins are of similar molecular weight, they migrate in close proximity when separated by SDS-PAGE, making distinction of individual DELLA proteins difficult. Furthermore, DELLA proteins are predicted to be post-translationally modified; which may alter mobility on SDS-PAGE gels, or even block the binding of probing antibodies. Therefore, to allow precise determination of which DELLA proteins could be detected, plant lines retaining only a single wild-type DELLA gene were investigated. These lines additionally retained a functional copy of *RGL3*. However, *RGL3* is only expressed at a very low level and so RGL3 is not expected to be present at a detectable level (Tyler *et al.*, 2004).

The affinity purified polyclonal antibody R1PC detects all *A. thaliana* DELLA proteins in plant extracts, with the exception of RGL3 (Figure 3.2). GAI, RGA, and RGL2 were detected as single bands with mobilities consistent with their calculated molecular weights of 58.9, 64.0, and 60.5 kDa respectively. In the *ga1-3*, *gai-t6*, *rga-t2*, *rgl2-1* line, where only *RGL1* and *RGL3* remain uninterrupted, two bands of differing mobilities were detected: one at the expected size for RGL1, 56.7 kDa, and one of slower mobility similar to RGL2. As these detected proteins only appeared in extracts from the *ga1-3*, *gai-t6*, *rga-t2*, *rgl2-1* mutant line, this would indicate that both are forms of RGL1. The slower mobility form could be a post-translational modification specific to RGL1 that is as yet unknown. However, a simple explanation is that this line retains a functional copy of *RGL2*.

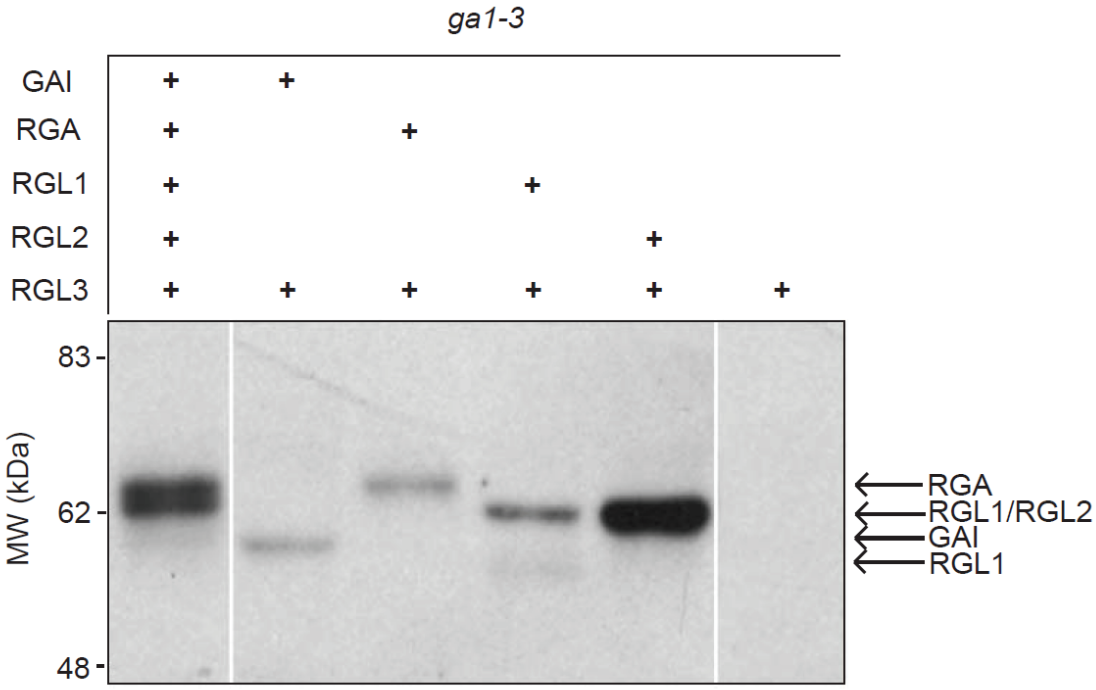

Figure 3.2. Characterisation of the affinity-purified anti-RGL1 polyclonal antibody R1PC. Immunoblot analysis of total *A. thaliana* protein extracts prepared from inflorescence tissue. Detection of individual DELLA proteins in extracts from the gibberellin-deficient *ga1-3* mutant, lacking multiple DELLA genes. Extracts prepared from combinations of *gai-t6*, *rga-t2*, *rgl1-1*, and *rgl2-1*. GAI, RGA, RGL1, and RGL2 with calculated molecular weights of 58.9, 64.0, 56.7, and 60.5 kDa respectively, are indicated. Extracts were prepared from three inflorescences in 100 µL; 5 µL of each extract was loaded per lane.

Interestingly, RGL2 appeared to be highly abundant in extracts prepared from plants devoid of other intact DELLA genes. This effect could be due to cessation of floral development at a stage where RGL2 accumulates; alternatively, other DELLA proteins may regulate the abundance of RGL2. Further experimentation is required to investigate this observation.

As expected, DELLA proteins were less abundant in a background where gibberellins are synthesised at normal levels (Figure 3.3). RGL2 is the only DELLA protein clearly identifiable, in extracts from wild-type and single *DELLA* gene deletion mutants, and absent from *rgl2-1*. Intriguingly, RGL2 is again highly abundant in one extract, produced from the *rgl1-1* mutant line. Therefore, *RGL1*, but not other DELLA proteins, appears to affect the expression level of *RGL2,* or the RGL2 protein level.

The universal anti-DELLA monoclonal antibody BC9 detected four endogenous DELLA proteins, similar to those detected by R1PC, in extracts prepared from *ga1-3* multiple *DELLA* gene deletion mutants (Figure 3.4A). In the *ga1-3*, *gai-t6*, *rga-t2*, *rgl2-1* line, where R1PC detected two forms of RGL1 with differing mobilities, BC9 only detected the slower mobility form. The slow mobility form of RGL1 may either be in high abundance in the *ga1-3* background, or bound by BC9 with a greater affinity than are other forms (another possibility, as mentioned above, is that this line may retained a functional copy of *RGL2*). An accumulation of RGL2 in the *ga1-3*, *gai-t6*, *rga-t2*, *rgl1-1* line was detected by BC9, confirming this same observation for R1PC.

BC9 was more sensitive than R1PC in detecting endogenous *A. thaliana* DELLA proteins in wild-type and single DELLA gene T-DNA insertion mutants (Figure 3.4B). GAI, RGA, and RGL2 were all detectable in these tissues. The slow mobility form of RGL1 was not detectable in the *rgl2-1* mutant, and if it is present in other lines it would be masked by RGL2 which shares a similar mobility. Therefore, it is unclear whether RGL1 was detectable using this antibody in gibberellin producing plant tissues. In the *rgl1-1* deletion mutant, BC9 (similarly to R1PC) detected a high abundance of DELLA proteins, in particular RGA and RGL2 in comparison to the level identified in other single mutants and the wild-type.

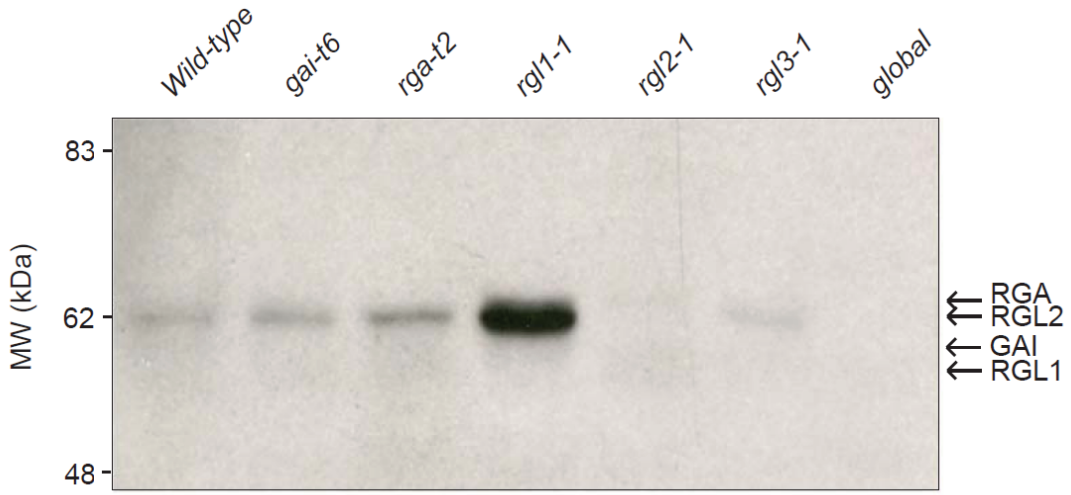

Figure 3.3. Detection of endogenous DELLA proteins in lines competent in gibberellin biosynthesis. Immunoblot analysis of total *A. thaliana* protein extracts prepared from inflorescence tissue. Detection of endogenous DELLA proteins in plant lines functional in production of gibberellins, but lacking individual *DELLA* genes. *global*: complete DELLA disruption mutant, *gai-t6*, *rga-t2*, *rgl1-1*, *rgl2-1*, *rgl3-1*. GAI, RGA, RGL1, and RGL2 with calculated molecular weights of 58.9, 64.0, 56.7, and 60.5 kDa respectively, are indicated. Extracts (100 µL) were each prepared from a total of three inflorescences; 5 µL of each extract was loaded per lane.

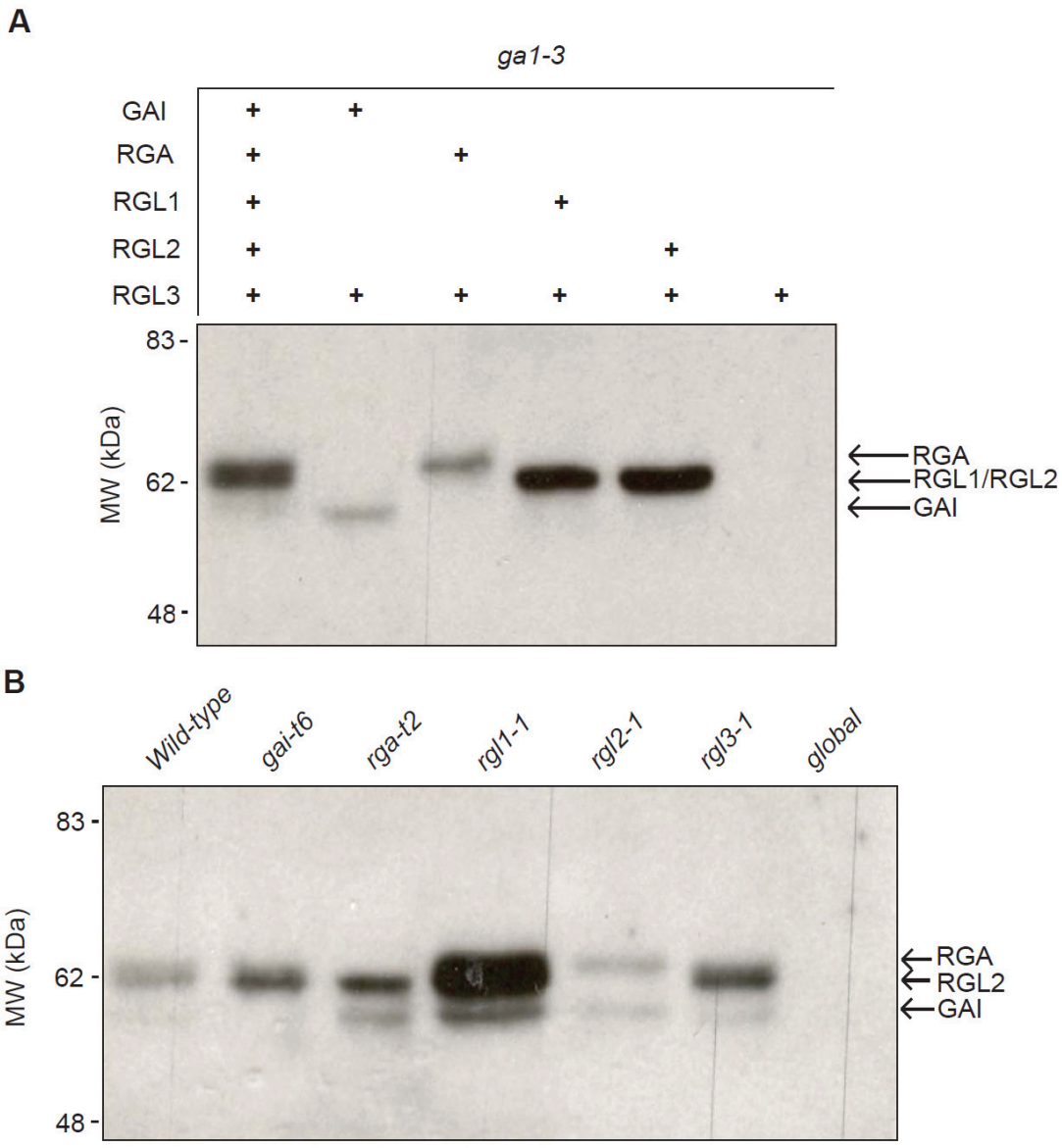

Figure 3.4. Characterisation of the monoclonal antibody BC9. Immunoblot analysis of total *A. thaliana* protein extracts prepared from inflorescence tissue. **A**. Detection of individual DELLA proteins in extracts from the gibberellin-deficient *ga1-3* mutant, lacking multiple DELLA genes. Extracts prepared from combinations of *gai-t6*, *rga-t2*, *rgl1-1*, and *rgl2-1*. **B**. Detection of endogenous DELLA proteins in plant lines functional in production of gibberellins, but lacking individual *DELLA* genes. *global*: complete DELLA disruption mutant, *gai-t6*, *rga-t2*, *rgl1-1*, *rgl2-1*, *rgl3-1*. GAI, RGA, RGL1, and RGL2 with calculated molecular weights of 58.9, 64.0, 56.7, and 60.5 kDa respectively, are indicated. Extracts (100 µL) were each prepared from a total of three inflorescences; 5 µL of each extract was loaded per lane.

AD7, a monoclonal antibody specific for RGL1, RGL2, and RGL3, detected several forms of both RGL1 and RGL2 in the *ga1-3* multiple DELLA deletion mutants (Figure 3.5A). A protein with a mobility matching that expected for RGL3, 57.3 kDa, was weakly detected in the *ga1-3*, *gai-t6*, *rga-t2*, *rgl1-1*, *rgl2-1* line. However, a line possessing the *rgl3-1* mutation in a *ga1-3* background was not available to confirm the identity of this protein. Two major forms of RGL1 were detected, similar to the mobilities detected by R1PC. Furthermore, two low abundance faster mobility forms of RGL1 were detected; these have an apparent molecular weight smaller than calculated for RGL1 and hence are likely degradation products. Two forms of RGL2 were detected in extracts prepared from a *ga1-3* background retaining only *RGL2* as a functional DELLA gene (Figure 3.5A). These two forms of RGL2 are likely the full length, and a partially degraded form. In wild-type tissues only RGL2 was detectable, and RGL2 was again more abundant in the *rgl1-1* T-DNA insertion line.

The monoclonal antibody AB8 is specific for RGL1, and this antibody was able to detect a single protein matching the predicted molecular weight of RGL1 in both wild-type and gibberellin-deficient tissue (Figure 3.6). Thus the combination of BC9, AD7, and AB8 may distinguish these two different forms of RGL1 in plant extracts. The monoclonal antibody BB7 is specific for RGL2; it detected a protein matching the predicted molecular weight of RGL2 in the gibberellin-deficient background but not in wild-type tissues (Figure 3.7). The protein detected appears to be slightly smaller in molecular weight than the RGL2 as detected with other antibodies, though this result needs to be confirmed. It is possible that the major portion of RGL2 is normally post-translationally modified, and this modification could block binding of BB7.

In summary, I have confirmed the specificities of the monoclonal antibodies BC9, AD7, AB8, and BB7 using endogenous *A. thaliana* DELLA proteins, summarised in Table 3.2 below. Furthermore, I have shown that wild-type levels of GAI, RGA, RGL1, and RGL2, although low, can be detected using this set of monoclonal antibodies.

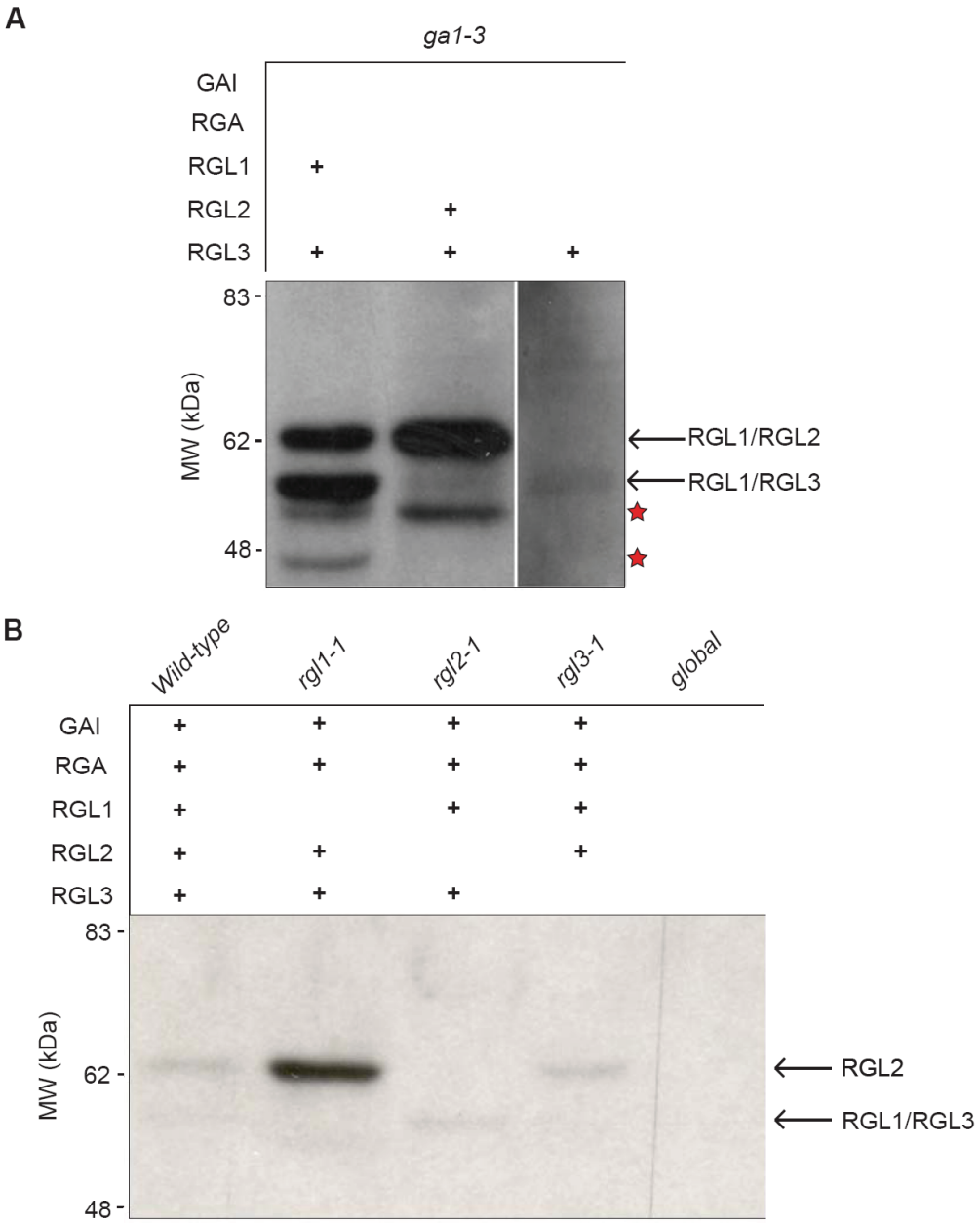

Figure 3.5. Characterisation of the monoclonal antibody AD7. Immunoblot analysis of total *A. thaliana* protein extracts prepared from inflorescence tissue. **A**. Detection of individual DELLA proteins in extracts from the gibberellin-deficient *ga1-3* mutant, lacking multiple DELLA genes. Extracts prepared from combinations of *gai-t6*, *rga-t2*, *rgl1-1*, and *rgl2-1*. **B**. Detection of endogenous DELLA proteins in plant lines functional in production of gibberellins, but lacking individual *DELLA* genes. *global*: complete DELLA disruption mutant, *gai-t6*, *rga-t2*, *rgl1-1*, *rgl2-1*, *rgl3-1*. RGL1, RGL2, and RGL3, with calculated molecular weights of 56.7, 60.5, and 57.3 kDa respectively, are indicated. Extracts (100 µL) were each prepared from a total of three inflorescences; 5 µL of each extract was loaded per lane. Red stars indicate possible degraded forms of RGL1 and RGL2.

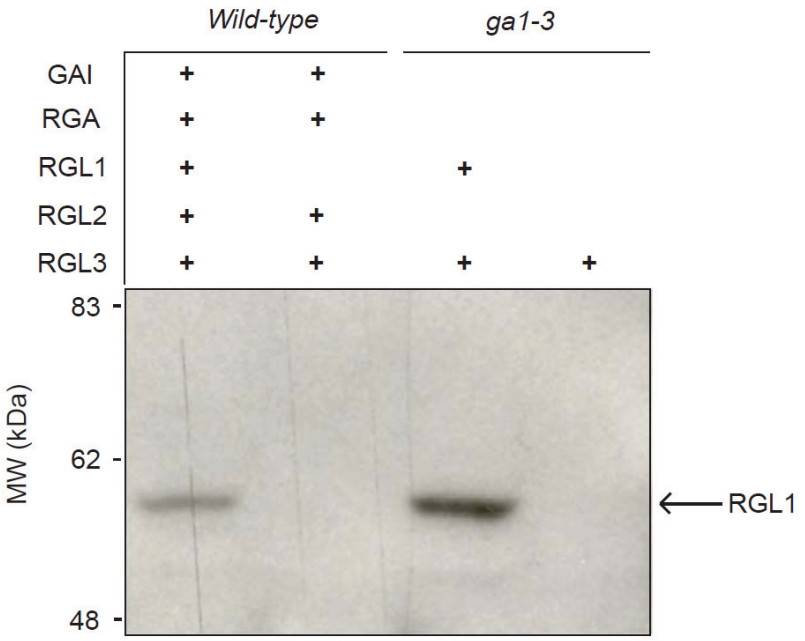

Figure 3.6. Characterisation of the monoclonal antibody AB8. Immunoblot analysis of total *A. thaliana* protein extracts prepared from inflorescence tissue. Detection of RGL1 in extracts from wild-type *A. thaliana*, *rgl1-1*, or the gibberellin-deficient *ga1-3* mutant, retaining RGL1 as the single functional DELLA gene. RGL1, with a calculated molecular weight of 56.7 kDa, is indicated. Extracts (100 µL) were each prepared from a total of three inflorescences; 5 µL of each extract was loaded per lane.

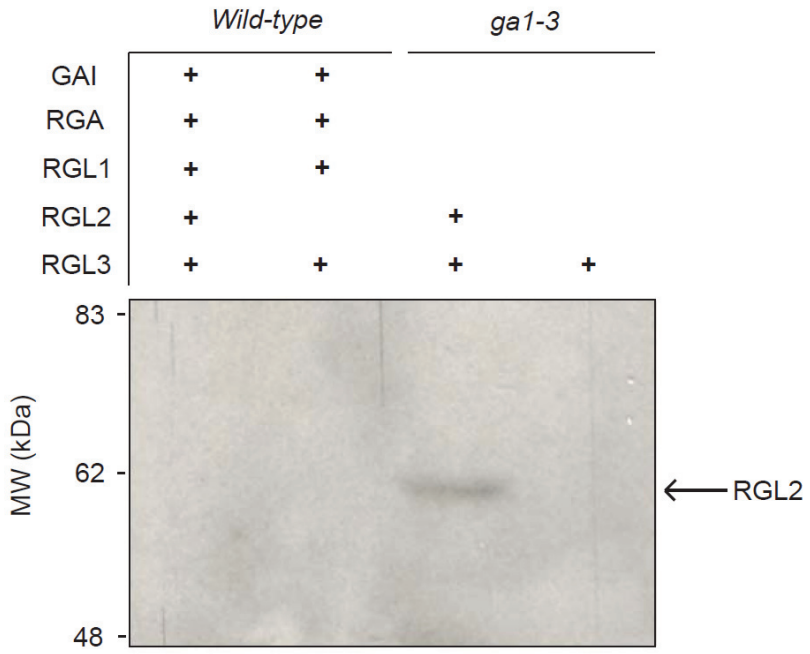

Figure 3.7. Characterisation of the monoclonal antibody BB7. Immunoblot analysis of total *A. thaliana* protein extracts prepared from inflorescence tissue. Detection of RGL2 in extracts from wild-type *A. thaliana*, *rgl2-1*, or the gibberellin-deficient *ga1-3* mutant, retaining RGL2 as the single functional DELLA gene. RGL2, with a calculated molecular weight of 60.5 kDa, is indicated. Extracts (100 µL) were each prepared from a total of three inflorescences; 5 µL of each extract was loaded per lane.

Table 3.2. Antibody specificities for endogenous *A. thaliana* DELLA proteins

Antibody	GAI	RGA	RGL1[§]	RGL1*[§]	RGL2	RGL3
R1PC	+	+	+	+	+	-
BC9	+	+	-	+	+	-
AD7	-	-	+	+	+	+[†]
AB8	-	-	+	-	-	-
BB7	-	-	-	-	+[‡]	-

§. Expected and low mobility (*) forms of RGL1.

+, Endogenous protein detected by immunoblot.

-, Not detected by immunoblot

†. Detection not confirmed.

‡. Epitope likely blocked by post-translational modification.

3.2 Mapping of anti-DELLA antibody epitopes

For use of monoclonal antibodies in pull-down and interaction assays, knowledge of the epitopes to which they bind is important. For example, it needs to be considered whether the antibody will compete with another interacting protein, or if it may be blocked by post-translational modifications.

The monoclonal antibody BC9 had been characterised as binding to the epitope VxxYxVR, located within the conserved DELLA motif, through alanine replacement scanning by William Jones (Figure 3.8A; Sun *et al*., 2010). To elucidate whether the monoclonal antibodies AD7 or AB8 also bind to the DELLA motif I designed an *in vitr*o binding assay, using surface plasmon resonance and competition using synthetic peptides, to detect the binding specificities of monoclonal antibodies to the immobilised N-terminal DELLA domain of RGL1 ($RGL1^{1-137}$). In competition assays, hundred fold excess of peptides were incubated with antibodies, prior to measuring antibody binding to $RGL1^{1-137}$. The synthetic peptide, D27, that spans the DELLA motif of RGL1, was bound by the monoclonal antibody BC9, consistent with the previously mapped epitope of BC9, preventing interaction of this monoclonal antibody with immobilised $RGL1^{1-137}$ (Figure 3.8B).

To establish whether the epitopes of the monoclonal antibodies AD7 or AB8 are located within the conserved DELLA or TVHYNP motifs, similar peptide competition experiments were performed. Binding of the monoclonal antibody AD7 to the immobilised $RGL1^{1-137}$ was prevented by T21, a synthetic peptide matching the TVHYNP motif of RGL1, by not by D27 (Figure 3.8C). The AD7 epitope has subsequently been mapped by alanine replacement scanning to be HYNPSDLxxW by William Jones (Figure 3.8A; Sun *et al*., 2010). Neither D27 nor T21 inhibited binding of the third monoclonal antibody, AB8, to $RGL1^{1-137}$ (Figure 3.1C). Hence, the RGL1-specific AB8 must bind an epitope outside these regions.

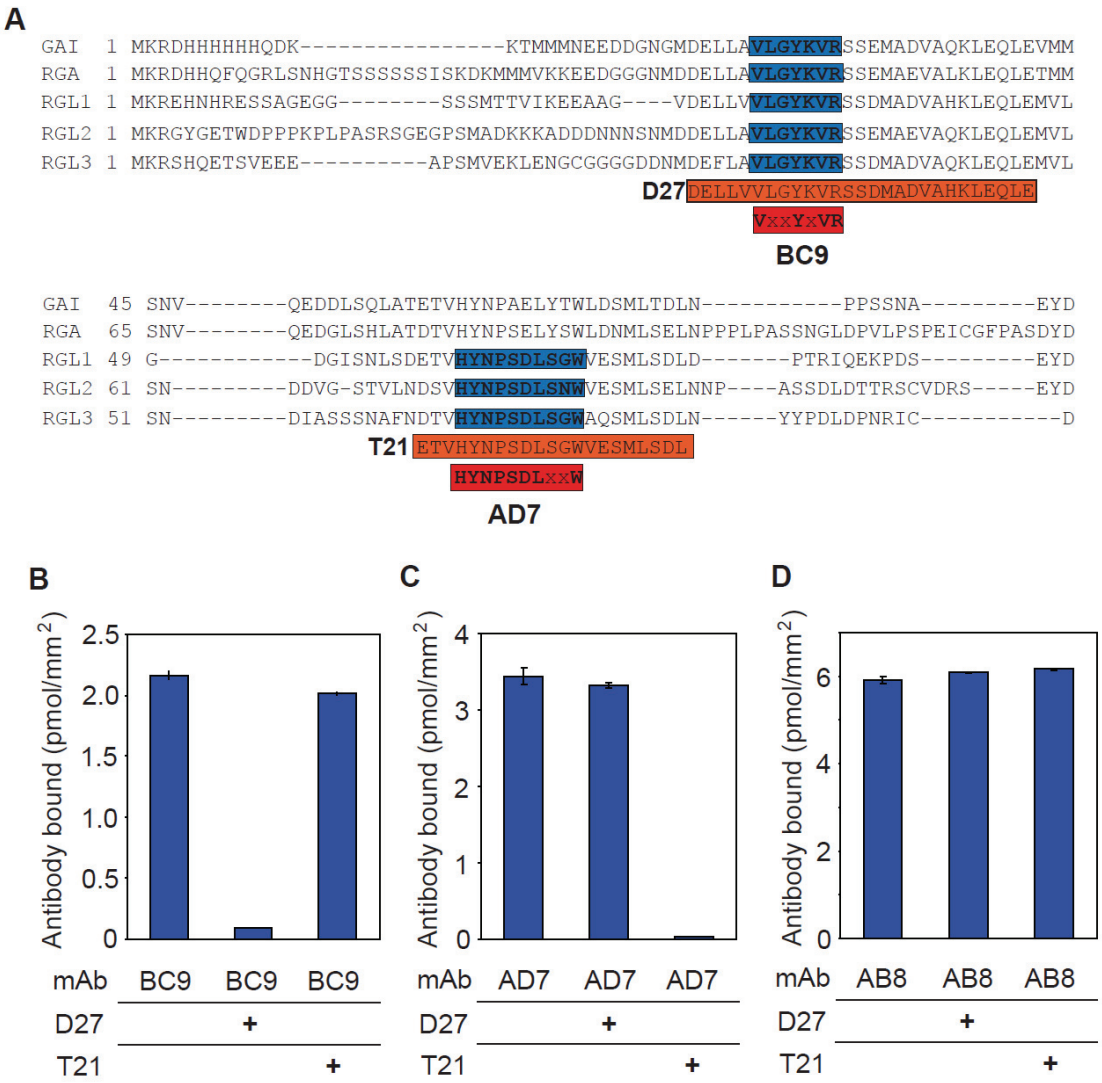

Figure 3.8. Mapping of anti-DELLA monoclonal antibody epitopes.

A. Alignment of *A. thaliana* N-terminal DELLA primary sequences, including synthetic peptides D27 and T21 and the epitopes for monoclonal antibodies (mAb) BC9 and AD7. **B-D**. Surface plasmon resonance detection of monoclonal antibodies, BC9 (B), AD7 (C), and AB8 (D) bound to an immobilised N-terminal DELLA domain of RGL1 ($RGL1^{1-137}$). The amount of antibody bound after 420 s-continuous flow of 100 nM monoclonal antibody is shown. Synthetic peptides D27 and T21 were added to the antibody solutions 30 min prior to the $RGL1^{1-137}$ binding assay. Results are the average of two replicate experiments, showing +/- one standard deviation.

In summary, the characterised suite of anti-DELLA antibodies recognises a multitude of targets throughout the RGL1 N-terminal domain. These antibodies recognise both the conserved DELLA (BC9) and TVHYNP (AD7) motifs, and a non-conserved epitope outside these regions (AB8). I have confirmed the specificities of the monoclonal antibodies BC9, AD7, AB8, and BB7 for their *in planta* target DELLA proteins. Furthermore, I have assisted in the mapping of the epitopes of several of these monoclonal antibodies.

Chapter 4

Characterisation of the interactions of RGL1

GRAS proteins of the DELLA family are nuclear localised repressors of gibberellin responses (Itoh *et al.*, 2002; Peng *et al.*, 1997). Upon cell perception of gibberellin, the DELLA proteins undergo degradation (Dill *et al.*, 2004; Fu *et al.*, 2002; Fu *et al.*, 2004; Gomi *et al.*, 2004). This gibberellin-dependent loss of the DELLA proteins relieves their active repression of growth responses, defining a central mechanism for gibberellin signalling.

Two other groups of proteins are known to be essential for gibberellin-induced DELLA protein degradation. These are the GID1 family proteins, and a member of the F-box protein family. The GID1 family proteins are nuclear-localised gibberellin receptors that have been shown to directly bind biologically active gibberellins (Griffiths *et al.*, 2006; Iuchi *et al.*, 2007; Nakajima *et al.*, 2006; Ueguchi-Tanaka *et al.*, 2005). Gibberellin-liganded GID1 family proteins interact directly with the N-terminal DELLA domain of DELLA family proteins, whereas non-liganded GID1-family proteins cannot (Griffiths *et al.*, 2006; Ueguchi-Tanaka *et al.*, 2005; Ueguchi-Tanaka *et al.*, 2007).

The second component of gibberellin signalling that has been shown to be essential for gibberellin-induced DELLA protein degradation is a DELLA-specific F-box protein. F-box family proteins direct E3 Ubiquitin ligases to specific target proteins, resulting in poly-ubiquitination and degradation by the proteasome. This explains the mechanism by which DELLA proteins are degraded. However, the DELLA specific F-box proteins SLY1 and GID2 cannot interact with their target DELLA proteins in the absence of an uncharacterised gibberellin-induced signal (Dill *et al.*, 2004; Fu *et al.*, 2004; Gomi *et al.*, 2004). Therefore, multiple components must act together in the gibberellin-induced degradation of the DELLA proteins.

At the beginning of this thesis project, I have hypothesised that the binding of gibberellin-liganded GID1 family proteins to the DELLA proteins is the gibberellin-induced signal that allows the DELLA specific F-box proteins to bind and target the DELLA proteins for degradation. Indeed, since the outset of this work, the *A. thaliana* GID1 family protein GID1A has been reported to increase the strength of interaction between the F-box protein SLY1 and the DELLA protein RGA (Griffiths *et al.*, 2006). Knowledge of the mechanism of this interaction between gibberellin signalling components is paramount to establishing how other phytohormones and environmental stimuli may be integrated.

The DELLA protein RGL1 is one of five encoded by *A. thaliana*. Insertion mutant analysis has shown RGL1 to function partially redundantly in floral development with two other *A. thaliana* DELLA proteins: RGA and RGL2. Furthermore, RGL1 has been shown to be degraded *via* the proteasome in response to gibberellin (Hussain *et al.*, 2007; Wang *et al.*, 2009). To determine the mechanism of gibberellin induced DELLA protein degradation I have characterised the interaction between the *A. thaliana* gibberellin receptor GID1A and the DELLA protein RGL1. Furthermore, I have investigated the process by which gibberellin-liganded GID1A induces the recruitment of SLY1 to RGL1.

4.1 Characterisation of the gibberellin-dependent GID1A:RGL1 interaction

The *A. thaliana* genome encodes a total of five DELLA proteins (GAI, RGA, RGL1, RGL2, and RGL3) and three GID1 family gibberellin receptors (GID1A, GID1B, and GID1C) (Griffiths *et al.*, 2006; Iuchi *et al.*, 2007; Lee *et al.*, 2002; Nakajima *et al.*, 2006; Peng *et al.*, 1997; Silverstone *et al.*, 1997; Wen and Chang, 2002). To establish whether the three *A. thaliana* GID1 family gibberellin receptors interact with RGL1 in a similar fashion to other DELLA proteins, I incorporated these proteins into a yeast two-hybrid system alongside two other DELLA proteins, RGA and RGL2, all of which have partial functional redundancy (Tyler *et al.*, 2004). Furthermore, the functions and interactions of RGA have been well characterised.

In the yeast two-hybrid system, GID1A-C each interacted with each DELLA proteins only in the presence of gibberellins (Figure 4.1). *HIS3* reporter growth assays, where yeast was grown on histidine-lacking media supplemented with the bioactive gibberellin GA_3, revealed some differences in affinities. A weak gibberellin-independent interaction between GID1B and RGL1 was observed; it remains to be determined whether this is biologically relevant. This assay also demonstrated a gibberellin-dependent interaction between GID1B and RGA that was much greater at low gibberellin concentrations than those of other interacting pairs. The distinctively weakest gibberellin-dependent interaction was observed between GID1C and RGL2. Whether these observed differences in affinities are real and of biological importance, or are artefacts of the yeast two-hybrid system remains to be resolved.

Gibberellins are not normally transported into *S. cerevisiae*, the organism used in yeast two-hybrid assays. Hence, it is unlikely *S. cerevisiae* possesses a mechanism to uptake gibberellins efficiently. This could drastically affect results of yeast two-hybrid assays as internal concentrations of gibberellins in the *S. cerevisiae* nucleus, where interactions take part, are likely much lower than those incorporated in the assays. To investigate this, I assayed reporter strains that had been grown in liquid media containing bioactive gibberellins for either 3 or 24 hours.

For reporter strains assayed at the same stage of growth, those incubated with gibberellins for 24 hours resulted in a much stronger (12 - 1343 fold) induction of the *LACZ* reporter in comparison to incubation with gibberellins for only 3 hours (Figure 4.2). The GID1B:RGL1 pair again appears to weakly interact in the absence of gibberellins, though whether this is of biological importance is yet to be established (Figure 4.2B). Interestingly, when incubated with bioactive gibberellins for 24 hours, eight of the nine gibberellin-dependent interactions (excluding GID1A:RGL2) were of similar strength (47 - 70 Miller Units). The gibberellin-dependent interaction between GID1A and RGL2 was somewhat stronger, at 136 Miller Units. These results are consistent with gibberellin uptake of *S. cerevisiae* being limited, and thus all further yeast two-hybrid assays are performed using a 20 hour incubation with bioactive gibberellins. Furthermore, it can be concluded that differences in affinities between GID family protein - DELLA pairs are likely small.

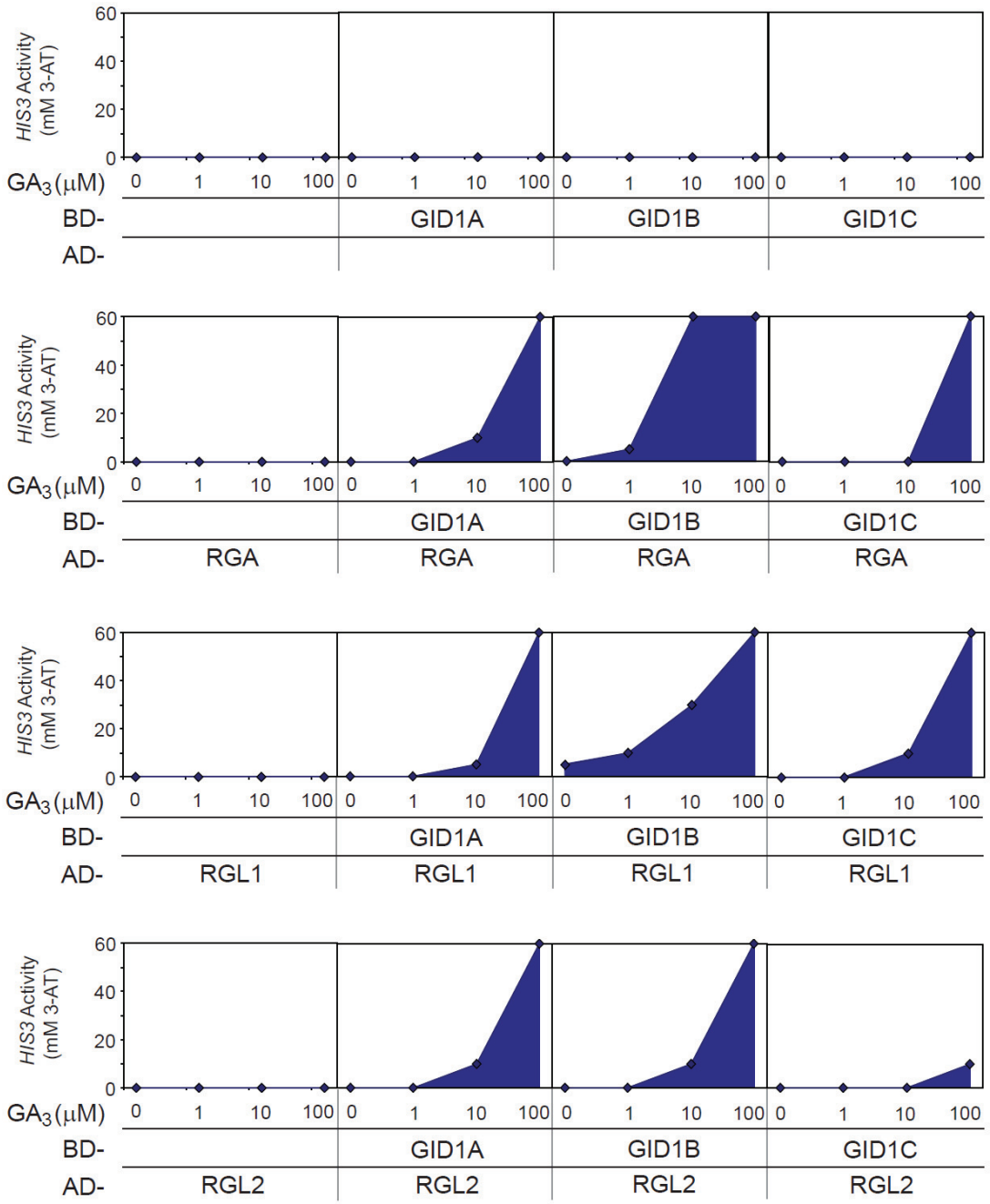

Figure 4.1. Gibberellin-dependent *A. thaliana* GID1A-C:DELLA interactions. Yeast two-hybrid assays for interaction between GAL4 DNA binding domain (BD-) fusions of GID1A-C and GAL4 activation domain (AD-) fusions of *A. thaliana* DELLA proteins RGA, RGL1, and RGL2. *HIS3* reporter assay, measured by growth on media lacking histidine and containing the histidine biosynthesis inhibitor 3-AT. Growth assayed at discrete concentrations of 3-AT: 0, 1, 2, 5, 10, 30, or 60 mM, in the presence of 0, 1, 10, or 100 μM gibberellin GA_3. The maximum concentration of 3-AT upon which *S. cerevisiae* transformants were able to grow is plotted.

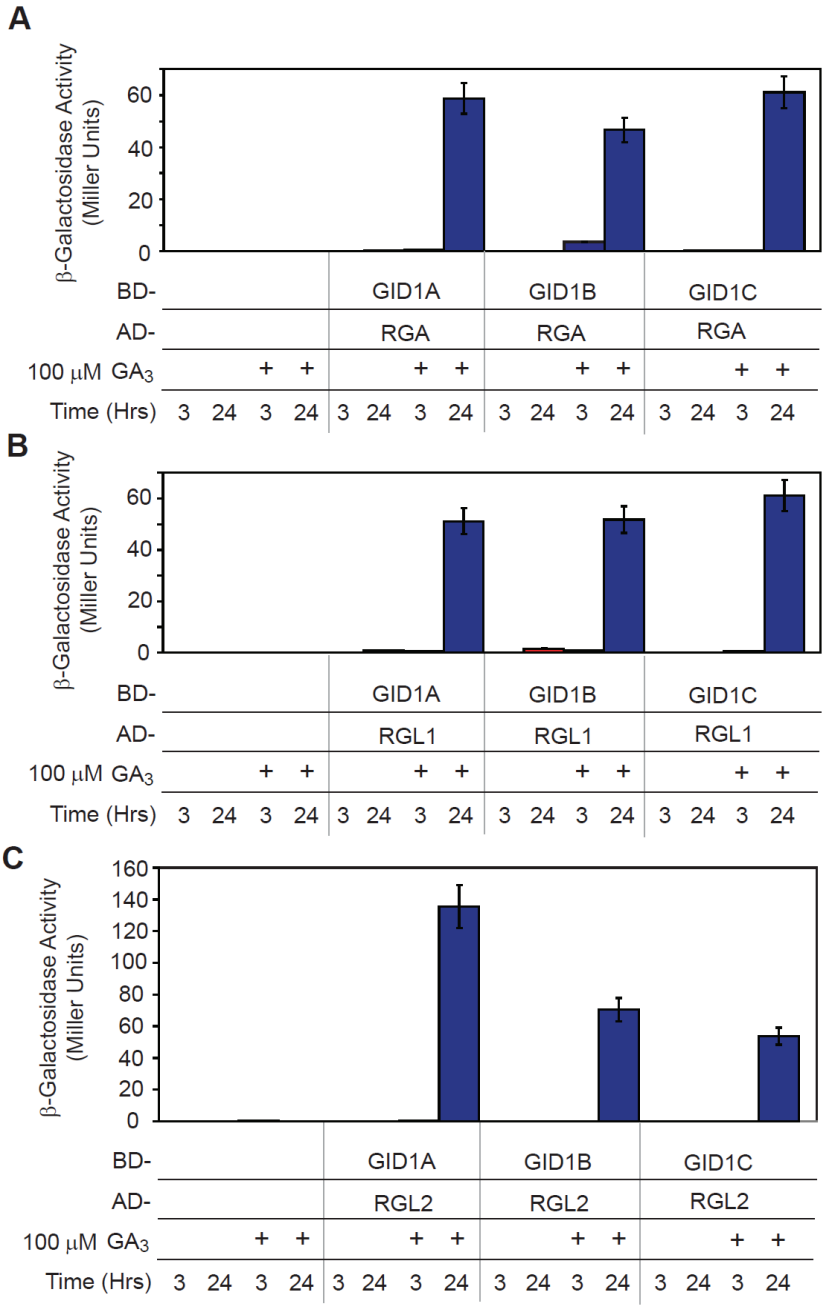

Figure 4.2. Gibberellin uptake by *S. cerevisiae*. Yeast two-hybrid assays for interaction between GAL4 DNA binding domain (BD-) fusions of GID1A-C and GAL4 activation domain (AD-) fusions to *A. thaliana* DELLA proteins RGA, RGL1, and RGL2. **A-C.** *LACZ* (β-galactosidase) reporter assay for the interaction between GID1A-C and either RGA (**A**), RGL1 (**B**), or RGL2 (**C**). 100μM gibberellin GA_3 was added to cultures either 3, or 24 hours prior to the assaying of exponentially growing cultures. Interaction in the absence of gibberellins is shown in red, whereas interaction in the presence of gibberellin GA_3 is shown in blue. Results are the averages of nine assays; error bars are showing +/- one standard deviation.

4.1.1 Requirement of the DELLA and TVHYNP motifs

A number of in-frame deletion mutations within DELLA-encoding genes have been reported to cause a characteristic gibberellin-insensitive dwarf phenotype in plants (Itoh *et al.*, 2002; Muangprom *et al.*, 2005; Peng *et al.*, 1997) (detailed in Appendix B). These mutations all localise to the two conserved regions within the N-terminal DELLA domain; though there is one exception, a single glutamine-arginine substitution within the C-terminal GRAS domain downstream of the conserved VHIID motif (Muangprom *et al.*, 2005).

The conserved DELLA and TVHYNP motifs, both located within the N-terminal domain, have been reported to be essential for a gibberellin-dependent interaction between GID1 family gibberellin receptors and the DELLA proteins SLR1 and RGA (Griffiths *et al.*, 2006; Ueguchi-Tanaka *et al.*, 2007). Furthermore, the N-terminal DELLA domains of both SLR1 and RGA are sufficient for the interaction with gibberellin-liganded GID1 family gibberellin receptors (Griffiths *et al.*, 2006; Ueguchi-Tanaka *et al.*, 2007).

Although several DELLA proteins have been well studied, there have been relatively few reports on the characterisation of RGL1. Hence, further analysis was required to establish that RGL1 interacts with gibberellin-liganded GID1A in a similar fashion to that reported for other DELLA proteins. Three mutations; *gai-1*, *rga-d*, and $slr1^{\Delta TVHYNP}$, have been reported to result in gibberellin-insensitive dwarf phenotypes (Itoh *et al.*, 2002; Koornneef *et al.*, 1985; Muangprom *et al.*, 2005; Peng *et al.*, 1997). To investigate the effects of these mutations upon the gibberellin-dependent interaction between GID1A and RGL1, equivalent mutations were constructed for RGL1, and introduced into a yeast two-hybrid system by Jeremy Buchanan (Buchanan, 2007) (Figure 4.3A) (sequences presented in Appendix B). I performed both *HIS3* and *LACZ* reporter assays to determine the effects of these dwarfing mutations upon the gibberellin-dependent interaction of RGL1 with GID1A (Figure 4.3B, data not shown).

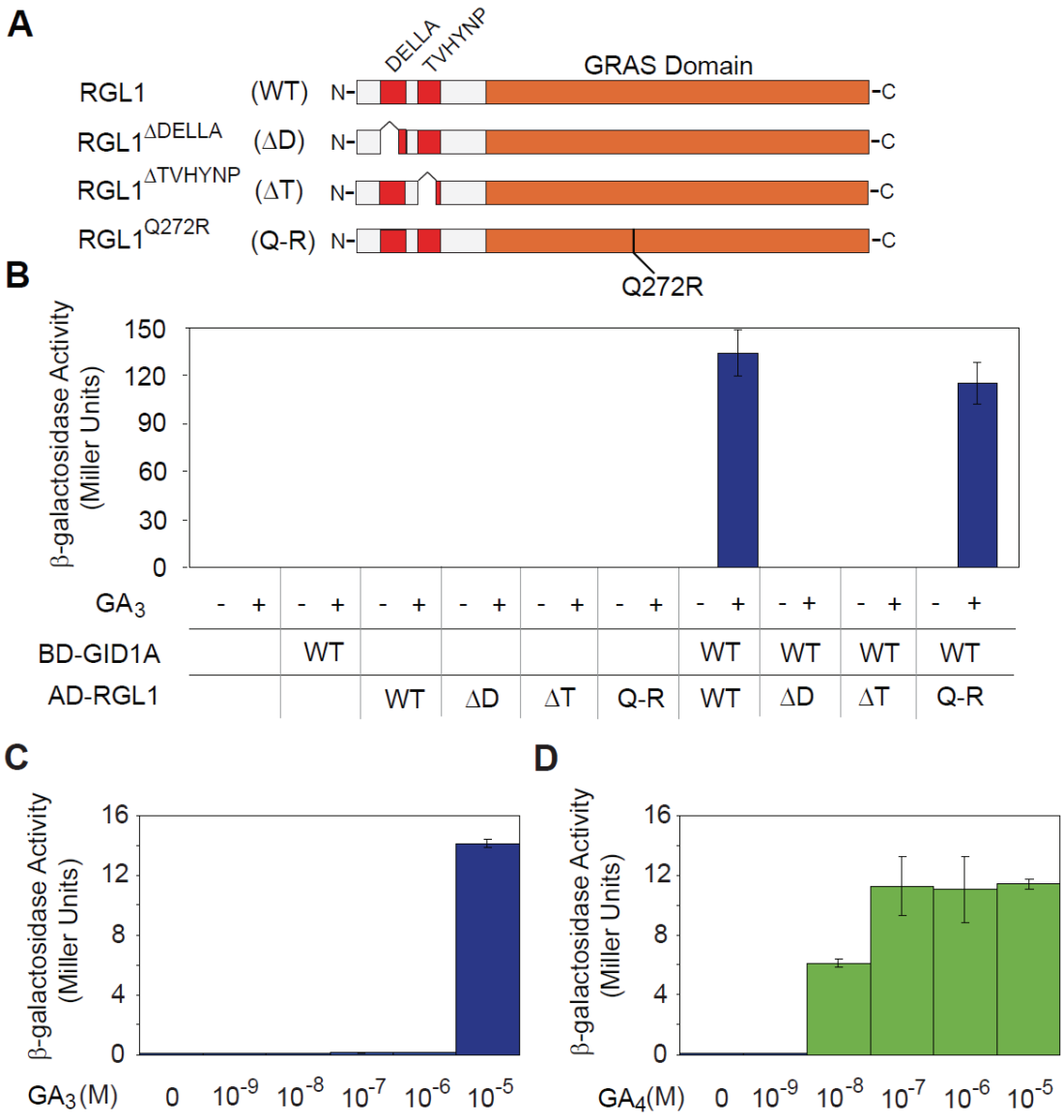

Figure 4.3. Characterisation of the gibberellin-dependent GID1A:RGL1 interaction. A. Schematic representation of the domain structure of RGL1, including investigated DELLA dwarfing mutations. **B-D.** *LACZ* (β-galactosidase) reporter assays. **B.** Interaction between a GAL4 DNA binding domain (BD-) fusion of GID1A and GAL4 activation domain (AD-) fusions of RGL1 (WT), rgl1$^{\Delta DELLA}$ (ΔD), rgl1$^{\Delta TVHYNP}$ (ΔT), and rgl1^{Q272R} (Q-R). Interactions performed in the presence of either 0 or 100 μM gibberellin GA_3 **C-D.** Interaction between BD-GID1A and AD-RGL1 in the presence of 1 nM - 10 μM gibberellins GA_3 (**C**) or GA_4 (**D**). Results are the averages of nine assays, with error bars showing +/- one standard deviation. Expression of all forms of RGL1 was confirmed by western blot of yeast extracts (data not shown).

For RGL1, as has been previously reported for the DELLA proteins RGA and SLR1, deletion of either of the conserved DELLA or TVHYNP motifs abolished the gibberellin-dependent interaction between GID1A and RGL1 (Figure 4.3B) (Griffiths *et al.*, 2006; Ueguchi-Tanaka *et al.*, 2007). Introduction of the glutamine-arginine replacement within the C-terminal GRAS domain (Q272R) into RGL1 resulted in no disruption of the gibberellin-dependent interaction with GID1A when compared to wild-type (Figure 4.3B). This mutation is known to result in gibberellin-insensitive dwarf plants through blocking the F-box protein SLY1 from binding, and thus blocking DELLA protein degradation (Muangprom *et al.*, 2005). The Q272R mutation lies within the C-terminal GRAS domain, that has been reported as not being essential for gibberellin-dependent interaction between GID1A and RGA (Griffiths *et al.*, 2006).

4.1.2 Effects of bioactive gibberellins on interaction strength

The major biologically important gibberellin in *A. thaliana*, GA_4, binds to the gibberellin receptors GID1A-C with a much higher affinity than does GA_3 and a much lower dose is required for eliciting biological responses (Nakajima *et al.*, 2006). However, it has not been resolved whether the affinity of gibberellin-liganded GID1-family proteins for the DELLA proteins is affected by the particular gibberellin bound to the receptor.

The gibberellin-dependent interaction between GID1A and RGL1 was detected in the yeast two-hybrid system at concentrations as low as 10 μM for the gibberellin GA_3, and as low as 10 nM for GA_4 (Figure 4.3C,D). This result, where GA_4 promotes interaction at a concentration three orders of magnitude below that of GA_3, is consistent with previously published results for other gibberellin receptor:DELLA combinations (Nakajima *et al.*, 2006; Ueguchi-Tanaka *et al.*, 2005; Ueguchi-Tanaka *et al.*, 2007).

To resolve whether the observed dose response difference between GA_3 and GA_4 was due to differing kinetics of binding of these hormones to GID1A or interaction of liganded GID1A with RGL1, I applied an *in vitro* real-time binding assay (Figure 4.4). High of concentrations of GA_3 and GA_4 were used to saturate recombinant GID1A prior to interaction with RGL1, and thereby eliminate the effect of different affinities of these two phytohormones for their receptor (a comparison of 0, 5, and 100 μM gibberellin is included in Appendix A). The N-terminal DELLA domain of RGL1 (residues 1-137) was used in these experiments, as recombinant full-length RGL1 expressed in *E. coli* is insoluble, and therefore non-functional.

Characteristics of both the association and dissociation between immobilised $RGL1^{1-137}$ and either GID1A/GA_3 or GID1A/GA_4 were similar, with GA_4 resulting in a slightly higher association rate (Figure 4.4A). The remaining two *A. thaliana* gibberellin receptors, GID1B and GID1C, behaved similarly: the difference between GA_4- and GA_3-liganded GID1C was slightly more pronounced than that for GID1A, whereas the kinetics for GA_3- and GA_4-liganded GID1B were almost identical (Figure 4.4B,C). The strength of interaction cannot be reliably compared between GID1A, GID1B, and GID1C as the proportion of active recombinant protein may differ. These findings show that different gibberellins bound to GID1A-C have, if any, only a minor effect on the kinetics of GID1/GA-DELLA protein interactions.

In summary, these *in vitro* real-time binding experiments indicate that the biological responses to GA_3 and GA_4 are largely limited by reported differences in the association and dissociation kinetics of gibberellins to GID1A-C (Nakajima *et al.*, 2006).

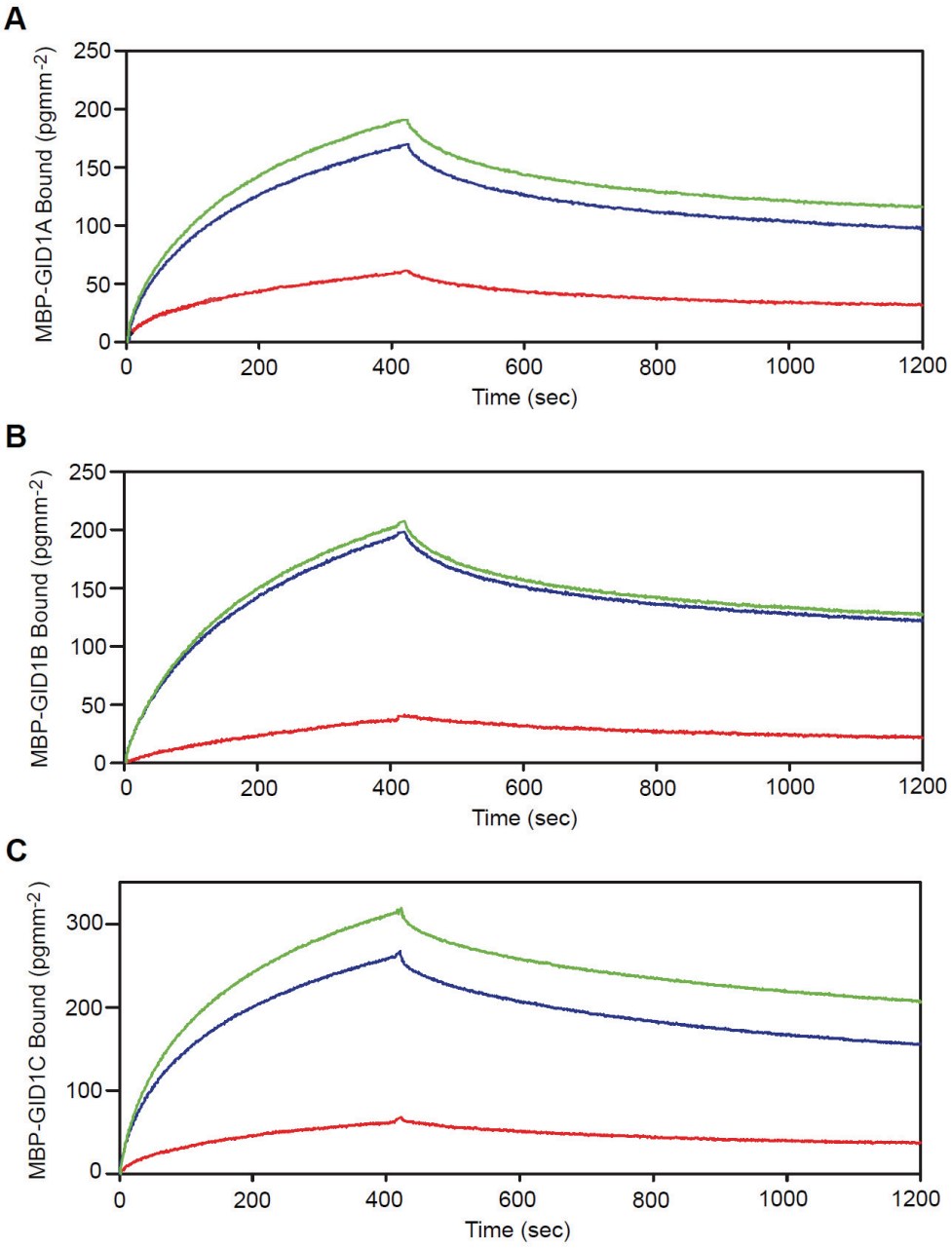

Figure 4.4. Comparison of the GA_3- and GA_4-dependent GID1A-C:RGL1 interaction *in vitro*. Association of recombinant GID1A (**A**), GID1B (**B**), or GID1C (**C**), with an immobilised N-terminal DELLA domain of RGL1 (residues 1-137). The mass binding from a continuous flow of 200 nM GID1A-C during association (0-420 s), and dissociation (420-1200 s) was monitored by surface plasmon resonance. Interactions were performed in the presence of either 100 µM GA_3 (blue), 100 µM GA_4 (green), or no gibberellin (red). Gibberellins were incubated with GID1A-C for 30 min prior to the binding assays, and were excluded from solution during the dissociation phase. The mass of GID1A-C is shown in pg bound per mm^2 of surface area. Simultaneous binding to a control flow cell lacking RGL1 was subtracted from all plots.

4.1.3 DELLA and TVHYNP motif competition analysis

Determining the regions of the N-terminal DELLA domain required for interactions with GID1-like gibberellin receptors by in-frame deletions can result in structural changes outside the investigated region, thus confounding interpretation of the essential components of this interaction. A high-resolution structure for the GID1A/GA_4:GAI^{11-113} complex has been reported, indicating the contacting residues (Figure 4.5A) (Murase *et al.*, 2008). However, no competition experiments, in the context of the intact N-terminal domain have yet been reported. Therefore, it is not yet known which residues are essential for interaction with gibberellin-liganded GID1 family proteins.

Competition of the GID1A/GA_4 interaction with the N-terminal DELLA domain of RGL1 by synthetic peptides spanning the DELLA and TVHYNP motifs was applied to the *in vitro* interaction assay (Figure 4.5). In this experiment, the capture of GID1A/GA_4 was monitored by surface plasmon resonance in real time in the presence or absence of trialled peptides. The 27 residue DELLA motif (capped) peptide, D27; Ac(N)-DELLVVLGYKVRSSDMADVAHKLEQLE-(C)NH_2, and 21 residue TVHYNP motif peptide, T21; Ac-(N)ETVHYNPSDLSGWVESMLSDL(C)-NH_2, span all conserved residues that form direct contacts between GAI and GID1A in the GID1A/GA_4:GAI^{11-113} complex (Figure 4.5A) (Murase *et al.*, 2008). Neither peptide, nor the combination of both, significantly inhibited GID1A binding (Figure 4.5B). The D27 peptide matching the conserved DELLA motif did inhibit GID1A binding to a small extent, approximately 7.5% ($P < 0.90$, Student's t-test), but only at a high concentration of 10μM, 100-fold in excess of the GID1A concentration. This indicates that these motifs, independently, are insufficient to interact with liganded GID1A with any significant affinity.

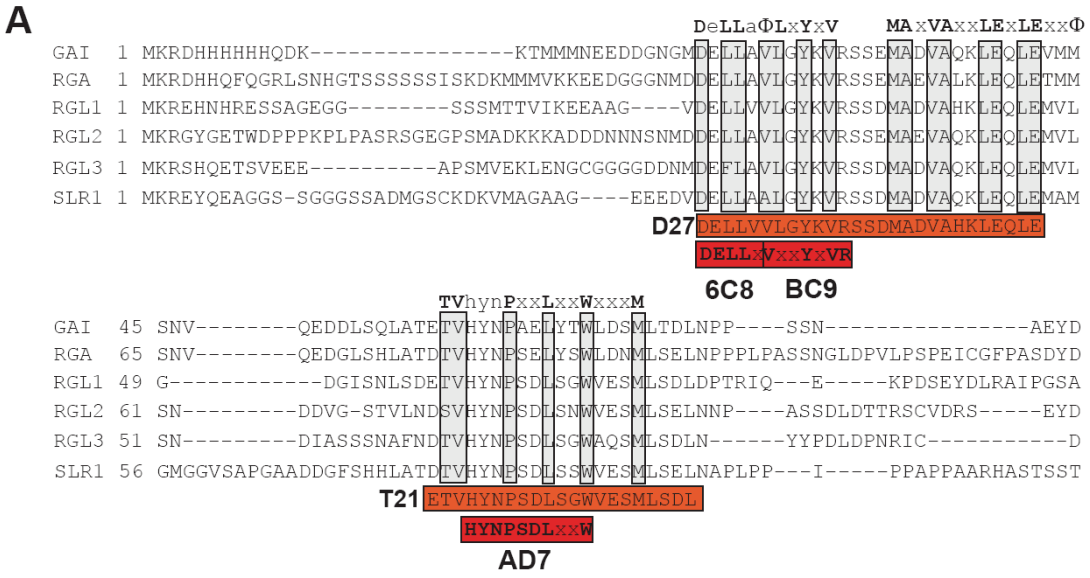
A
DeLLaΦLxYxV
MAxVAxxLExLExxΦ
GAI 1 MKRDHHHHHHQDK----------KTMMMNEEDDGNGMDELLAVLGYKVRSSEMADVAQKLEQLEVMM
RGA 1 MKRDHHQFQGRLSNHGTSSSSSSISKDKMMMVKKEEDGGGNMDDELLAVLGYKVRSSEMAEVALKLEQLETMM
RGL1 1 MKREHNHRESSAGEGG--------SSSMTTVIKEEAAG----VDELLVVLGYKVRSSDMADVAHKLEQLEMVL
RGL2 1 MKRGYGETWDPPPKPLPASRSGEGPSMADKKKADDDNNNSNMDDELLAVLGYKVRSSEMAEVAQKLEQLEMVL
RGL3 1 MKRSHQETSVEEE----------APSMVEKLENGCGGGGDDNMDEFLAVLGYKVRSSDMADVAQKLEQLEMVL
SLR1 1 MKREYQEAGGS-SGGGSSADMGSCKDKVMAGAAG----EEEDVDELLAALGYKVRSSDMADVAQKLEQLEMAM
D27 DELLVVLGYKVRSSDMADVAHKLEQLE
DELLxVxxYxVR
6C8
BC9
TVhynPxxLxxWxxxM
GAI 45 SNV--------QEDDLSQLATETVHYNPAELYTWLDSMLTDLNPP----SSN----------AEYD
RGA 65 SNV--------QEDGLSHLATDTVHYNPSELYSWLDNMLSELNPPPLPASSNGLDPVLPSPEICGFPASDYD
RGL1 49 G----------DGISNLSDETVHYNPSDLSGWVESMLSDLDPTRIQ---E-----KPDSEYDLRAIPGSA
RGL2 61 SN---------DDVG-STVLNDSVHYNPSDLSNWVESMLSELNNP----ASSDLDTTRSCVDRS-----EYD
RGL3 51 SN---------DIASSSNAFNDTVHYNPSDLSGWAQSMLSDLN------YYPDLDPNRIC----------D
SLR1 56 GMGGVSAPGAADDGFSHHLATDTVHYNPSDLSSWVESMLSELNAPLPP---I-----PPAPPAARHASTSST
T21 ETVHYNPSDLSGWVESMLSDL
HYNPSDLxxW
AD7
B
Competitor
GA4
-
-
-
+
D27
+
T21
+
D27/T21
+
0
1
2
3
4
MBP-GID1A bound (fmol/mm2)
C
Competitor
GA4
-
-
-
+
AB8
+
6C8
+
6C8
Saturated
+
BC9
+
AD7
+
0
2
4
6
8
mAb bound (fmol/mm2)
0
1
2
3
4
MBP-GID1A bound (fmol/mm2)

Figure 4.5. Mapping of RGL1 residues essential for interaction with GID1A. **A.** ClustalW alignment of *A. thaliana* DELLA protein N-terminal primary sequences including *O. sativa* SLR1. GID1A interacting residues, as reported for GAI, are indicated above the alignment (Larkin *et al.*, 2007; Murase *et al.*, 2008). Synthetic peptides D27 and T21, spanning the conserved DELLA and TVHYNP motifs, are indicated below the alignment. The contact residues for monoclonal antibodies 6C8, BC9 and AD7 are also indicated below the alignment. **B-C.** Surface plasmon resonance detection of GID1A binding to an immobilised N-terminal DELLA domain of RGL1 (residues 1-137). The amount of GID1A bound after 420 s from a continuous flow of 100 nM GID1A is shown. **B.** Competition of binding, using synthetic peptides D27 and T21 in solution with GID1A. 5 μM gibberellin GA_4 and synthetic peptides; D27, and T21, were added to GID1A solutions 30 min prior to $RGL1^{1-137}$ binding assays. **C.** Monoclonal antibody-mediated competition of the GID1A/GA_4:$RGL1^{1-137}$ interaction. Monoclonal antibodies were first bound to immobilised $RGL1^{1-137}$ (420 sec of continuous flow). The chip was then exposed to GID1A. Graph to the left, the quantity of each competing monoclonal antibody (mAb) bound to $RGL1^{1-137}$ prior to binding of GID1A. Graph to the right, the amount of GID1A bound to the chip containing $RGL1^{1-137}$-mAb complex. An additional approach for antibody binding was incorporated for 6C8. $RGL1^{1-137}$ and 6C8 were incubated together for 30 min prior to capture on the chip surface, thus, allowing 6C8 saturation. Results are the averages of two replicate assays (excluding 6C8 saturation assay), with error bars showing +/- one standard deviation. Simultaneous binding to a control flow cell lacking RGL1 was subtracted from all plots.

To compete out regions within the intact N-terminal DELLA domain I took advantage of the suite of anti-DELLA protein monoclonal antibodies, described in Chapter 3. In addition, the monoclonal antibody 6C8 was included. 6C8 was raised against a 12 residue DELLA motif peptide by W. Jones (Plant and Food Research, New Zealand). The epitope of this antibody has been determined through alanine replacement scanning to target the DELL residues within the characteristic DELLA motif (from now on referred to as Asp/Glu/Leu/Leu for clarity; W. Jones, unpublished). The three anti-RGL1 monoclonal antibodies, whose epitopes overlap with GID1A contact residues; 6C8, BC9, and AD7, were used to probe the requirement of their target epitopes for the GID1A/GA_4:$RGL1^{1-137}$ interaction. (Figure 4.5A,C). A fourth monoclonal antibody, AB8, specific for RGL1 and shown to bind outside the DELLA and TVHYNP motifs (Chapter 3) was used as a negative control.

To determine the requirement of the antibody-targeted residues of RGL1 for the formation of the GID1A/GA_4:$RGL1^{1-137}$ complex, I introduced monoclonal antibodies into the *in vitro* surface plasmon resonance detection system. Monoclonal antibodies were pre-complexed with $RGL1^{1-137}$ on the chip surface. Therefore, if a monoclonal antibody interacts with a region of the N-terminal domain of RGL1 that is essential for interaction with GID1A/GA_4, then the subsequent association of GID1A/GA_4 will be abolished. Alternatively, a bound monoclonal antibody can sterically hinder access to nearby spatial regions. However, due to the flexible nature of the RGL1 N-terminal domain (see section 4.14), steric hindrance is expected to be limited.

The antibody AB8, that has an epitope outside the DELLA and TVHYNP motifs, inhibited the binding of GID1A/GA_4 by approximately 25% (Figure 4.5C). The exact nature of the reduced binding of GID1A/GA_4 is not known. This antibody was not expected to interfere with GID1A binding due to its epitope lying outside the GID1A interacting regions. Furthermore, AB8 does not block binding of RGL1 to plant endogenous GID1C in ELISA experiments (Sun *et al*., 2010). However, due to the presence of the large antibody molecules (approximately twice the molecular weight of the recombinant GID1A protein) at the chip surface, interference could be attributed to reduced spatial access at the chip surface.

Interestingly, the monoclonal antibody 6C8 inhibited GID1A/GA_4 association to a similar extent to AB8 (Figure 4.5C), suggesting that the 6C8 epitope is not essential for the GID1A/GA_4:$RGL1^{1-137}$ interaction. This was unexpected, given that 6C8 targets the DELLA motif residues Asp/Glu/Leu/Leu, three of which form direct contacts between GAI^{11-113} and GID1A/GA_4 in the high resolution crystal structure (Murase *et al.*, 2008). The quantity of 6C8 present as a competitor was lower in comparison to AB8. This was in part due to the lower affinity of 6C8 for $RGL1^{1-137}$ (K_D of 4.5 x 10^{-8} mol/L), compared to 1.2 x 10^{-9} mol/L for AB8 (William Jones, unpublished). As a result, only a portion of available RGL1 sites were blocked using this experimental design. The monoclonal antibody BC9 possesses an epitope immediately adjacent to that of 6C8 in the RGL1 primary sequence (Figure 4.5A). Unlike 6C8, when used as a competitor, BC9 almost completely abolishes the gibberellin-dependent interaction between GID1A/GA_4 and immobilised $RGL1^{1-137}$ (Figure 4.5C). This indicates the BC9-epitope, VxxYxVR within the conserved DELLA motif, includes residues that are essential for the GID1A/GA_4:$RGL1^{1-137}$ complex to form. Importantly, the quantity of BC9 bound to $RGL1^{1-137}$ as a competitor was similar to that used for 6C8. This supports the observation that the 6C8 epitope is not essential for the GID1A/GA_4: $RGL1^{1-137}$ interaction, as the quantity bound should be sufficient to act as a competitor. As an alternative approach, the 6C8 binding capacity was increased through pre-saturation of $RGL1^{1-137}$ prior to capture on the chip surface. Although the exact quantity of antibody cannot be directly measured, the mass of $RGL1^{1-137}$:6C8 can. At least 3.7 fmol/mm^2 of 6C8 was bound using this approach; this is based on the total $RGL1^{1-137}$:6C8 mass bound compared to the $RGL1^{1-137}$ binding capacity of the chip, thus an equivalent amount to that of BC9. Lastly, when the TVHYNP motif-specific monoclonal antibody AD7 was pre-complexed with immobilised $RGL1^{1-137}$, GID1A/GA_4 association was abolished in a similar fashion to BC9 (Figure 4.5C). This indicates that the targeted region within the TVHYNP motif is also essential for the GID1A/GA_4:$RGL1^{1-137}$ complex to form.

To confirm the direct competition between monoclonal antibodies and GID1A/GA_4, a reversed experiment was performed. Similar to the antibody mediated competition, GID1A/GA_4 was pre-complexed with the immobilised N-terminal domain of RGL1 and monoclonal antibody association measured. However, saturation of the immobilised $RGL1^{1-137}$ with GID1A was not feasible due to the aggregation of GID1A at high

concentrations. An $RGL1^{1-137}$ occupancy of 16 % was used, though the maximum accessibility at the chip surface was determined to be only 25 % for BC9 and 40 % for AB8 (based on saturation of monoclonal antibody binding; Appendix A). Therefore, if GID1A/GA_4 binding site availability matches BC9, approximately 65% of interaction-available RGL1 molecules were occupied by GID1A/GA_4. The difference in availability of binding sites to various antibodies could be accounted for by the immobilisation strategy. As the $RGL1^{1-137}$ recombinant protein is anchored through an N-terminal fusion, distal regions towards the C-terminus will be more available at the chip surface.

As expected, AB8 binding to RGL1 and pre-complexed GID1A/GA_4:$RGL1^{1-137}$ was similar (Figure 4.6A). Likewise, 6C8 binding was not inhibited (Figure 4.6B). One of the two antibodies that competed out GID1A/GA_4 interaction with immobilised $RGL1^{1-137}$, BC9, had a greatly reduced association to the RGL1 pre-complexed with GID1A/GA_4 (Figure 4.6C). The second GID1A/GA_4 competing antibody, AD7, also exhibited a strong reduction in binding to the GID1A/GA_4:$RGL1^{1-137}$ complex in comparison to $RGL1^{1-137}$. These results are consistent with the VxxYxVR and HYNPSDLxxW residues, of the DELLA and TVHYNP motifs respectively, including essential residues for the GID1A/GA_4:$RGL1^{1-137}$ interaction. Furthermore, this also supports the observation that the Asp/Glu/Leu/Leu residues within the DELLA motif are not essential for the GID1A/GA_4:$RGL1^{1-137}$ interaction

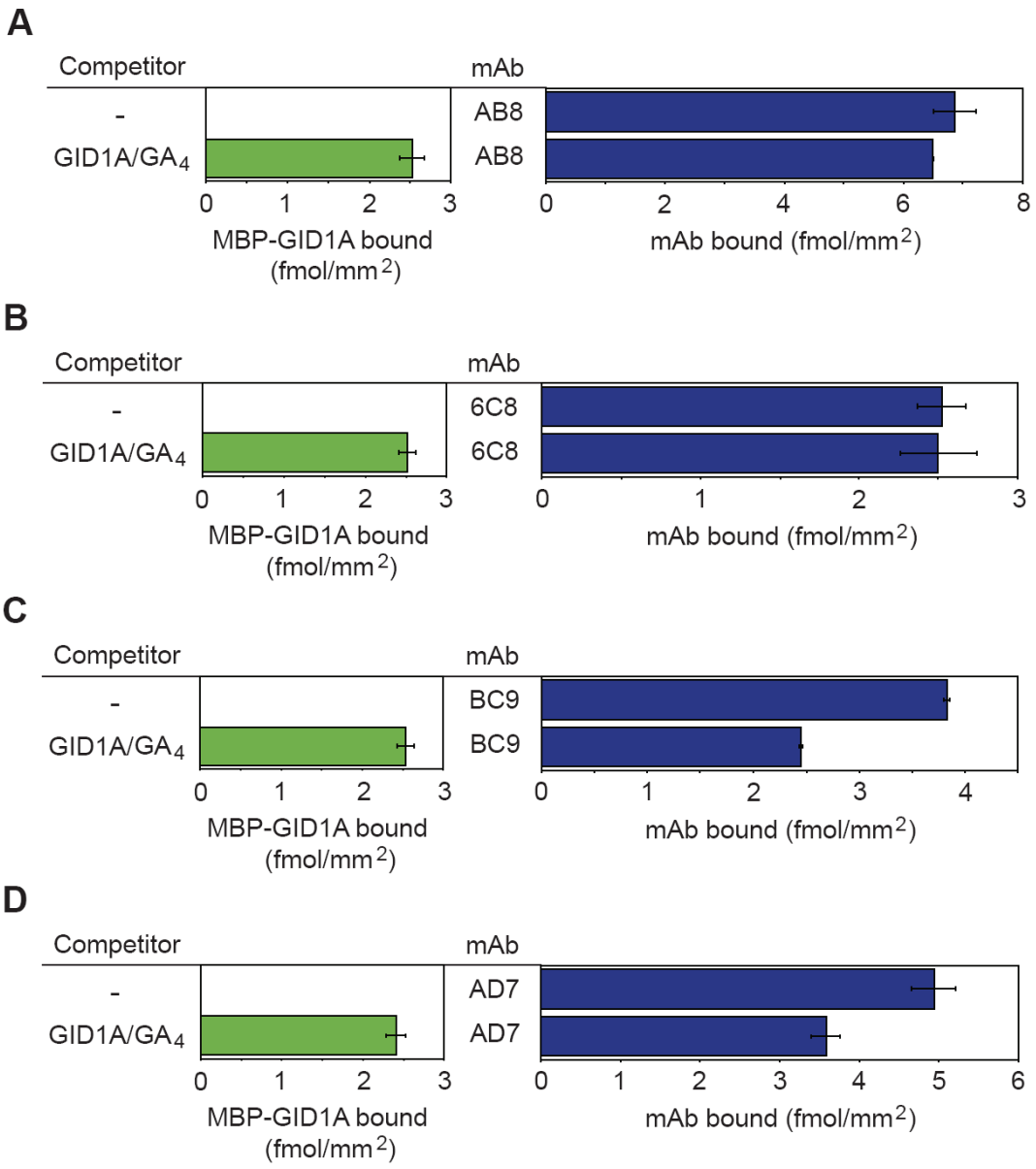

Figure 4.6. GID1A-mediated competition of monoclonal antibody binding to the N-terminal RGL1 DELLA domain. A-D. Surface plasmon resonance detection of monoclonal antibody binding to an immobilised N-terminal DELLA domain of RGL1 (residues 1-137): AB8 (**A**), 6C8 (**B**), BC9 (**C**), and AD7 (**D**). Left: The amount (fmol/mm^2) of GID1A/GA_4 bound to immobilised $RGL1^{1-137}$ prior to monoclonal antibody binding. Right: the amount of monoclonal antibody bound (fmol/mm^2) following 420 s of association from a continuous 500 nM solution. GID1A/GA_4 binding to $RGL1^{1-137}$ was performed immediately prior to assaying antibody association. 100 nM solutions GID1A were incubated at room temperature for 30 min following the addition of 5 μM gibberellin GA_4. Results are the averages of two replicate assays, with error bars showing +/- one standard deviation.

The antibodies 6C8 and BC9 bind the residues Asp/Glu/Leu/Leu and VxxYxVR, respectively (William Jones, unpublished). These epitopes are immediately adjacent in the primary sequence of RGL1 and both contain GID1A-interacting residues, based on the GID1A/GA_4:$GAI^{11\text{-}113}$ high resolution structure (Figure 4.5A) (Murase *et al.*, 2008). To visualise these epitopes in respect to the tertiary structure of $RGL1^{1\text{-}137}$, this domain of RGL1 was modelled using SwissModel (Figure 4.7A). The presented model was generated from the coordinates of $GAI^{11\text{-}113}$ in the high resolution GID1A/GA_3:$^{GAI11\text{-}113}$ structure. The Asp/Glu/Leu/Leu residues are predicted to form a short α-helix, making contacts with both the GID1A core domain and the N-terminal extension that covers the GID1A gibberellin binding pocket (Murase *et al.*, 2008). Occupying of this region through interaction with an antibody would be unlikely to interfere with other regions of the GID1A/GA_4: $RGL1^{1\text{-}137}$ interface, and so would be expected to only weaken the interaction (Figure 4.7B). Furthermore, RGL1 has a valine residue in place of an alanine in the context of the DELLA residues. This hydrophobic valine residue may make the αA helix structure unstable as it is exposed on the surface of the complex. In contrast to 6C8, the monoclonal antibodies BC9 and AD7 both bind epitopes that form loops between the helices αA and αB, or αC and αD, respectively. These loops are rich in GID1A interacting residues: V, Y, and V within the BC9 epitope; and P, L, and W within the AD7 epitope. Furthermore, the binding of an antibody to these regions would likely also inhibit formation of the tertiary structure of the DELLA domain upon binding to GID1A/GA_4.

These results indicate that the Asp/Glu/Leu/Leu residues of RGL1 are not essential for interaction with GID1A/GA_4, whilst both the VLGYKVR and HYNPSDLSGW regions (DELLA and TVHYNP motifs respectively) are absolutely required for interaction with GID1A/GA_4.

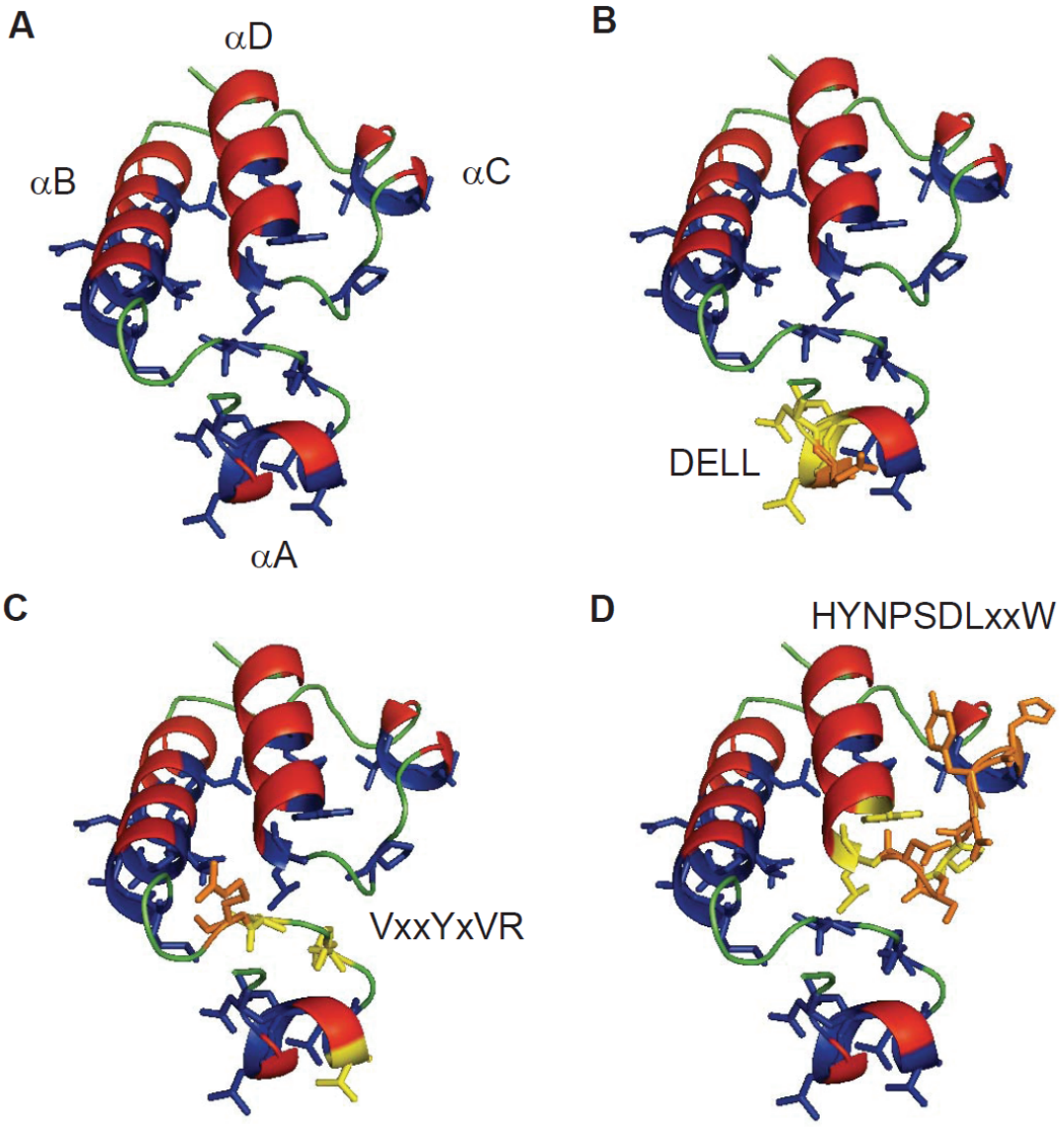

Figure 4.7. Structural prediction of the RGL1 N-terminal DELLA domain when in complex with GID1A. A. Predicted RGL1$^{1\text{-}137}$ tertiary structure, modelled from the GID1A/GA_4:GAI$^{11\text{-}113}$ crystal structure using SwissModel (PDB 2ZSI; (Arnold *et al.*, 2006; Murase *et al.*, 2008)). Secondary structure is highlighted in red, α-helices, and green, random coil. Conserved residues that form direct interactions between GAI and GID1A are shown in blue (Murase *et al.*, 2008). **B-D.** RGL1$^{1\text{-}137}$ model, indicating monoclonal antibody epitopes; 6C8 (**B**), BC9 (**C**), and AD7 (**D**). Antibody epitopes are highlighted in orange and yellow. Orange indicates a residue that also forms a direct GAI-GID1A interaction, whereas yellow residues do not.

4.1.4 Characterisation of interaction kinetics

Although a crystal structure for GID1A/GA_4:GAI^{11-113} has been solved, the mechanism by which this complex forms has not yet been shown (Murase *et al.*, 2008). The measurement of individual association and dissociation phases of an interaction through surface-plasmon resonance enables modelling of the interaction kinetics. Therefore, the gibberellin-dependent interaction between GID1A/GA_4 and the RGL1 N-terminal DELLA domain, $RGL1^{1-137}$, was measured over a range of GID1A concentrations from 100 nM through to 1600 nM (Figure 4.8A,B). To investigate the possibility that the GID1A/GA_4: $RGL1^{1-137}$ interaction follows a complex interaction model, rather than a simple 1:1 Langmuir ($A + B \leftrightarrow AB$) mechanism, association and dissociation data were transformed (Figure 4.8C,D). Neither a Scatchard plot, R/dt *vs* R, of association data, nor a $\ln(R_0/R)$ *vs* t plot of the dissociation phase produced linear plots; these results indicate that the interaction data does not fit Langmuir kinetics (Karlsson *et al.*, 1991; Morton *et al.*, 1995; O'Shannessy, 1994).

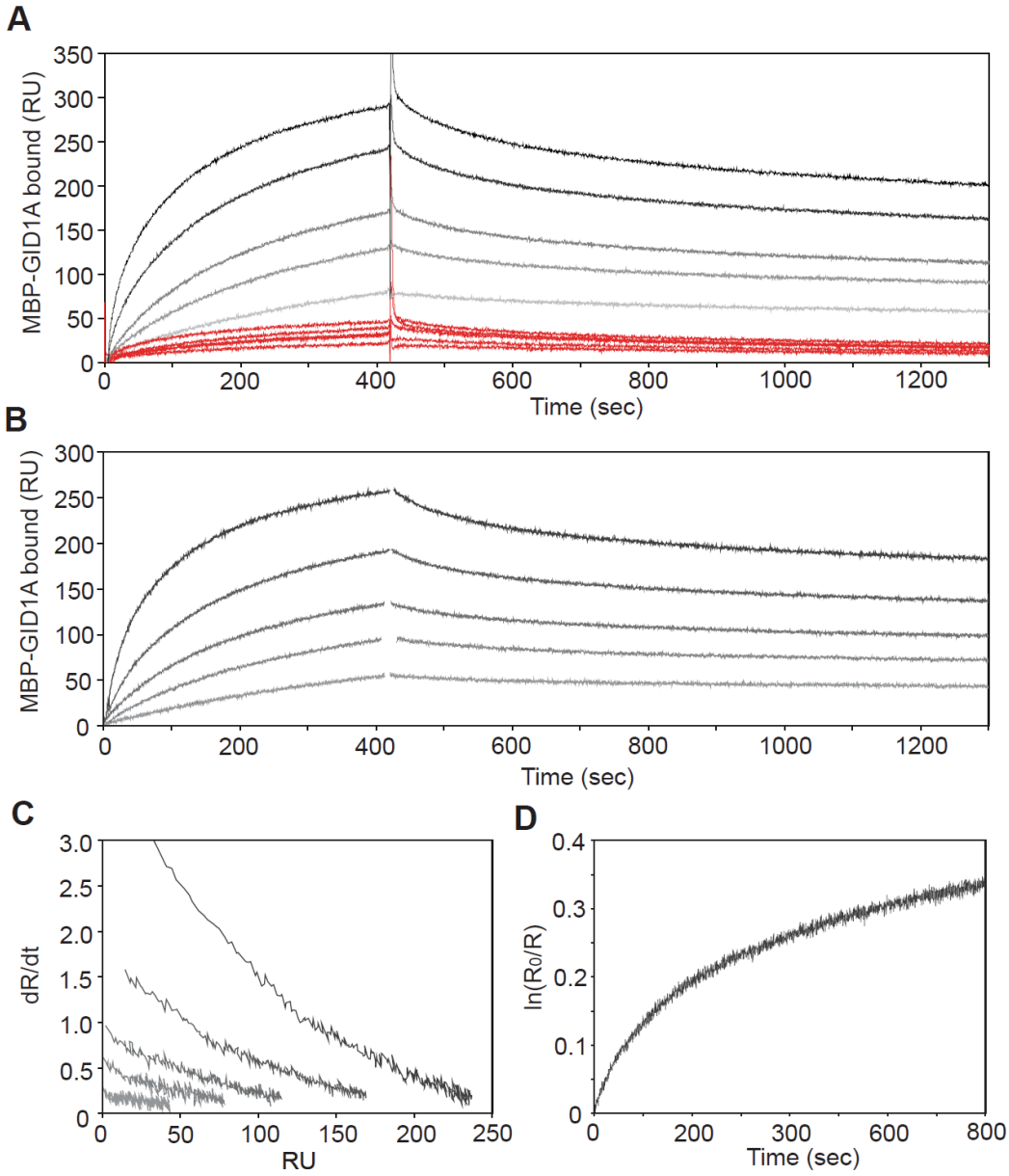

Figure 4.8. Kinetic characterisation of the gibberellin-dependent GID1A:RGL1$^{1-137}$ interaction. A. Surface plasmon resonance-detected association (0-420 sec) of recombinant GID1A from a continuous flow with immobilised RGL1$^{1-137}$, and subsequent dissociation (420-1300 s). Interaction assays were performed in the presence (grey) or absence (red) of gibberellin GA_4 for 100, 200, 400, 800, and 1600 nM solutions of GID1A. 100 µM GA_4 was added to GID1A solutions 30 min prior to assay, and was absent from solution during dissociation. **B.** GA_4-dependent association and dissociation, calculated by subtraction of binding in the absence of gibberellins. **C.** Scatchard plot (dR/dt *vs.* R) of the GA_4-dependent association phase where R = Response Units (RU) and t = time (s). **D.** $\ln(R_0/R)$ *vs* time linearisation transformation of the dissociation phase, shown for 1600 nM GID1A.

These results indicate that the GID1A/GA_4: $RGL1^{1-137}$ interaction involves a complex mechanism. Comparison of previously reported high resolution structures for the GID1A/GA_4: GAI^{11-113} complex and free GID1/GA_4 reveal that the GID1 tertiary structure is almost identical (Murase *et al.*, 2008; Shimada *et al.*, 2008). Therefore, the tertiary structure of the liganded GID1-like proteins is not affected by their binding to the N-terminal DELLA domain.

The N-terminal DELLA domain of GAI was reported to have defined secondary and tertiary structure within the GID1A/GA_4:GAI^{11-113} complex, whereas circular dichroism measurements indicated a lack of structure in the absence of liganded GID1A (Murase *et al.*, 2008). To establish whether $RGL1^{1-137}$ is unstructured in the absence of GID1A/GA_4, I determined the solvent accessibility through deuterium exchange mass spectrometry (Figure 4.9). Even within 10 s, the shortest exposure measured, greater than 90 % of RGL1 N-terminal DELLA domain peptide backbone amides were exchanged with Dueterium. This is typical for random coil, or unstructured proteins, indicating a lack of secondary structure within this domain. In contrast, the MBP moiety of the fusion is resistant to deuterium exchange. The exchange map of MBP is consistent with high resolution structures of this protein, validating the exchange data for the unstructured N-terminal domain of RGL1 (PDB 2ZXT; Kawano *et. al*, unpublished). Therefore, experimental evidence indicates that the N-terminal DELLA domain must undergo conformational changes ether prior or upon interaction with the gibberellin receptor GID1A.

One possible model for the N- terminal DELLA domain interaction with GID1A/GA_4 involves the N-terminal domain obtaining a complex tertiary structure prior to interaction with GID1A/GA_4. This conformational change would need to be transient, as it was not observed in the surface accessibility map of $RGL1^{1-137}$. This model would explain the non-Langmuir characteristics observed for the of association phase. However, this model is not consistent with the non-Langmuir dissociation that was observed. It is possible that some transient structure formation may occur, but this cannot account for the entirety of the complex kinetics that were observed.

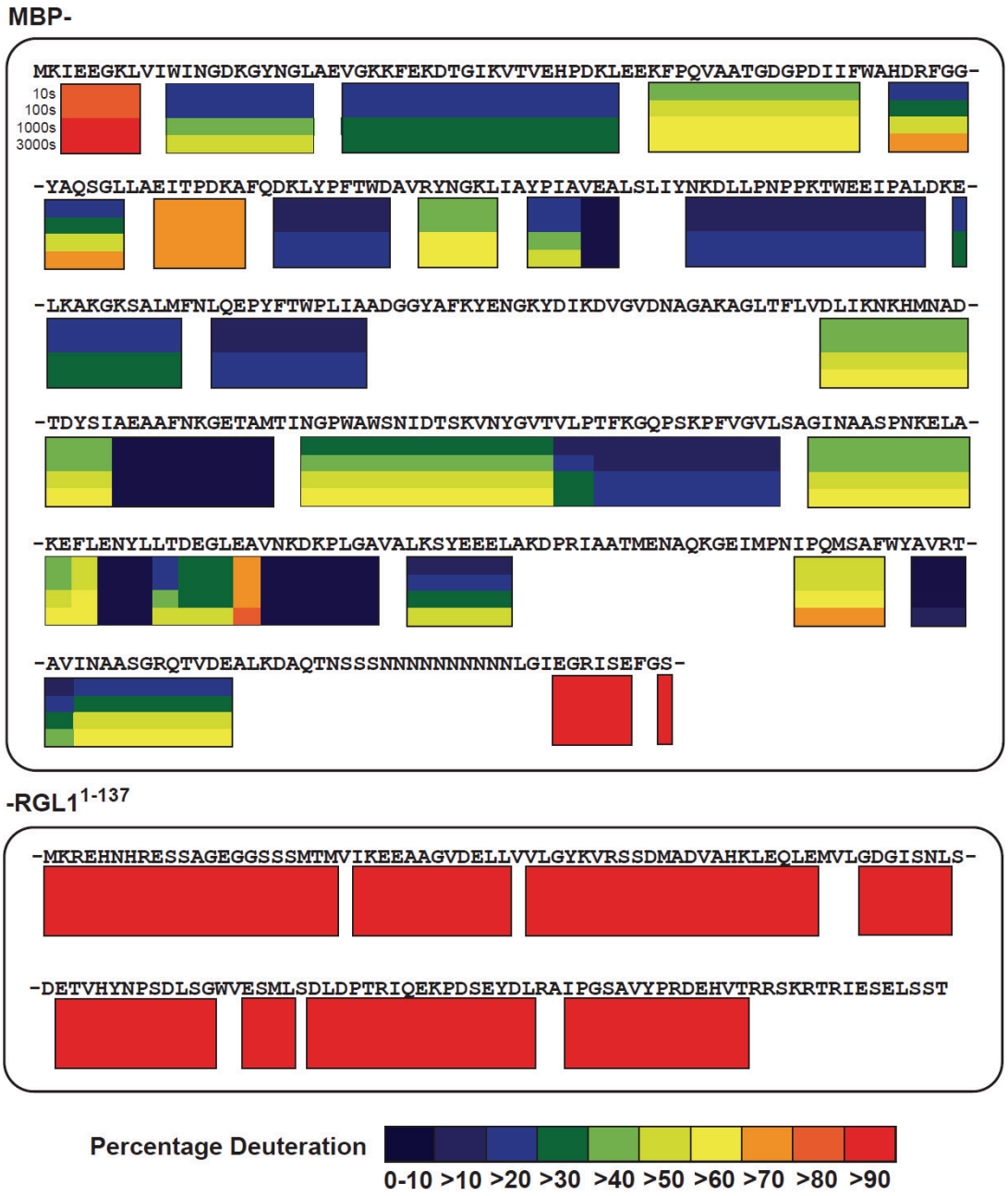

Figure 4.9. Surface accessibility mapping of RGL1$^{1-137}$. Deuterium exchange mass spectrometry analysis of recombinant RGL1$^{1-137}$ fusion to MALTOSE BINDING PROTEIN (MBP). Native recombinant protein was subjected to a time course exposure to deuterium, followed by pepsin digest and mass spectrometry analysis to determine the extent of deuteration of peptides (Englander *et al.*, 2003). The percentage deuteration, in comparison to a 16 hour exposure, is indicated below the sequence for 10, 100, 1000, and 3000 sec exposures. The percentage of residues deuterated is represented by a colour scale.

I modelled the association and dissociation to a two-state conformational change model; A + B ↔ AB ↔ AB* (Figure 4.10). Due to concentration-dependent aggregation of recombinant GID1A, and as such a non-linear relationship between functional GID1A and total recombinant protein concentration, each concentration dataset was modelled separately. As can be seen from the residual plots, this model is a good fit at lower GID1A concentrations where aggregation is minimal, yet only a reasonable fit at higher GID1A concentrations. Slight inconsistencies between the data and the model may be due to aggregation effects, or other complexities of the interaction such as transient secondary structure formation in RGL1.

The N-terminal DELLA domain of RGL1 does not aggregate, allowing accurate determination of the active concentration. Therefore, a reversed experiment was performed, where $RGL1^{1-137}$ association and dissociation to and from immobilised GID1A was measured (Appendix A). However, only approximately 2-3 % of the immobilised GID1A was functional in binding $RGL1^{1-137}$. Furthermore, rapid dissociation of a portion of the immobilised MBP-GID1A from the chip surface generated a large baseline drift. Together these complications generate large errors in kinetic data, precluding obtaining data useful for kinetic characterisation.

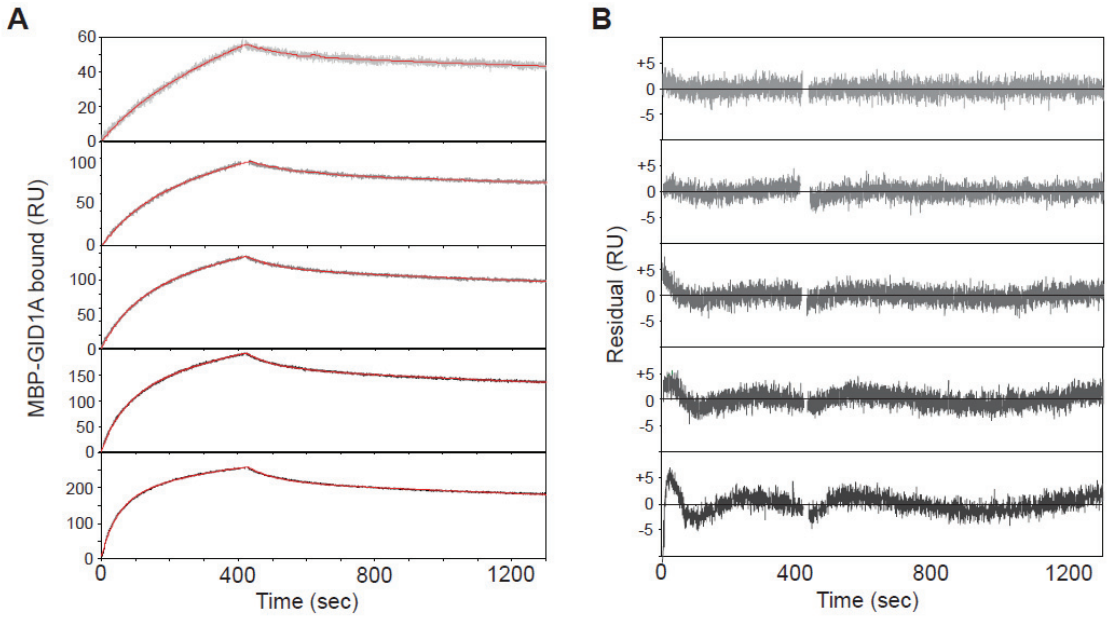

Figure 4.10. Conformational change kinetic modelling of the gibberellin-dependent GID1A:RGL1$^{1-137}$ interaction. A. Gibberellin-dependent association and dissociation data for the interaction between GID1A and immobilised RGL1$^{1-137}$, detected by surface plasmon resonance. Interactions were performed for 100, 200, 400, 800, and 1600 nM solutions of GID1A (top to bottom). A calculated two-state kinetic model was fitted to individual curves, indicated in red, using BiaEvaluation software version 3.1. **B.** Residual plot for variance in response units (RU), of the kinetic data from the calculated model for each GID1A concentration.

Attempts were made to determine the active concentration of GID1A in purified MBP-GID1A solutions. Using an *in vitro* depletion assay, coupled with detection and quantification of unbound protein via immuno-dot-blot; no significant portion of recombinant protein was active at any concentration (100 - 1600 nM MBP-GID1A; data not shown; error of +/- 24 %).

As an alternative approach to determine the active recombinant GID1A concentration, the extent of aggregation was quantified through native gel electrophoresis (Figure 4.11). What is likely dimeric MBP-GID1A appeared to be the most abundant, whilst monomeric MBP-GID1A was a minor fraction. MBP-GID1A is expected to aggregate through the hydrophobic N-terminal DELLA-interacting region, based on the observed aggregation within the reported rice GID1 hexamer high resolution structure (Shimada *et al.*, 2008). Therefore, aggregates cannot interact with RGL1. Dimeric MBP-GID1A appears to be in equilibrium with monomeric MBP-GID1A as the abundance of monomeric MBP-GID1A was noted to increase in the presence of $RGL1^{1-137}$, thus the abundance of monomeric through to dimeric MBP-GID1A was used as the active GID1A concentration. This was calculated to range from 10.5 % through to 9.1 % for MBP-GID1A concentrations of 100-400 nM; higher concentrations were excluded due to saturation of the quantification signal (Figure 4.11B).

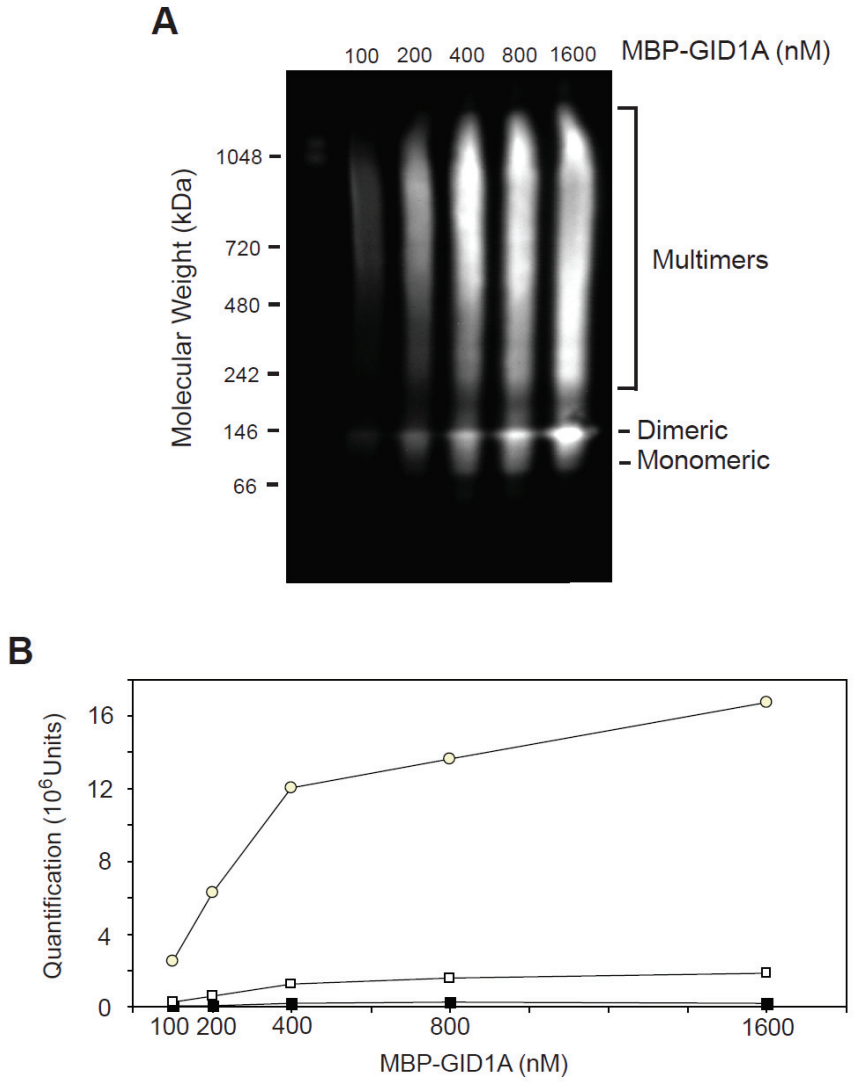

Figure 4.11. Characterisation of MBP-GID1A aggregation. A. Detection of various mobility forms of purified recombinant MBP-GID1A separated by blue-native-PAGE. 100, 200, 400, 800, and 1600 nM solutions of MBP-GID1A were separated and detected by immunoblot with an anti-MBP antibody and subsequent horse-radish peroxidase based detection. The calculated molecular weight of a MBP-GID1A monomer is 81.6 kDa. **B.** Detected MBP-GID1A forms were quantified using a Fuji film Intelligent dark box-II and ImageGauge software. Quantification of monomeric (■) and total (○) MBP-GID1A for each MBP-GID1A concentration are plotted. The detected MBP-GID1A encompassing both monomeric and dimeric forms is also plotted (□).

The association and dissociation data of GID1A/GA_4 binding to $RGL1^{1-137}$ was fitted to a two state conformational change model:

$$A + B \underset{k_{off}}{\overset{k_{on}}{\rightleftharpoons}} AB \underset{k_{-2}}{\overset{k_2}{\rightleftharpoons}} AB^*$$

Where A is GID1A/GA_4, B is $RGL1^{1-137}$, and * indicates a bound conformational state that must revert prior to dissociation. Using adjusted active concentrations for 100 - 400 nM GID1A, the calculated k_{on} was 1.6×10^5 +/- 1.6×10^4 $M^{-1}s^{-1}$ and k_{off} 4.1×10^{-3} +/- 9.6×10^{-4} s^{-1}, while the constants for conformational change were $k_2 = 5.1 \times 10^{-3}$ +/- 5.5×10^{-4} s^{-1}, and $k\text{-}_2 = 3.8 \times 10^{-4}$ +/- 8.4×10^{-6} s^{-1}, for the forward and reverse directions, respectively (error value shows +/- one standard deviation) (Table 4.1). The overall equilibrium constant K was determined to be 5.3×10^8 +/- 1.5×10^8 M^{-1} representing a strong interaction. In summary, the kinetic data presented here model a two-step conformational transition of the N-terminal domain of DELLA proteins after initial binding to liganded GID1-like gibberellin receptors.

Table 4.1

Two-state conformational change model

GID1A	k_{on}	k_{off}	k_2	k_{-2}	Rmax†	K	Chi^{2} §
100 nM	1.6×10^{4}	3.7×10^{-3}	5.6×10^{-3}	3.7×10^{-4}	150	6.8×10^{7}	1.32
200 nM	1.7×10^{4}	3.5×10^{-3}	4.5×10^{-3}	3.8×10^{-4}	160	5.7×10^{7}	1.26
400 nM	1.2×10^{4}	5.3×10^{-3}	5.1×10^{-3}	3.9×10^{-4}	201	3.2×10^{7}	1.63
800 nM	8.8×10^{3}	6.7×10^{-3}	5.0×10^{-3}	3.8×10^{-4}	268	1.7×10^{7}	1.96
1600 nM	7.6×10^{3}	7.6×10^{-3}	4.5×10^{-3}	3.4×10^{-4}	315	1.4×10^{7}	3.21

Two-state conformational change model (active concentration)

GID1A	Adjusted	k_{on}	k_{off}	k_2	k_{-2}	Rmax†	K	Chi^{2}§
100 nM	10.5 nM	1.6×10^{5}	3.7×10^{-3}	5.6×10^{-3}	3.7×10^{-4}	150	6.5×10^{8}	1.32
200 nM	20.0 nM	1.7×10^{5}	3.5×10^{-3}	4.5×10^{-3}	3.8×10^{-4}	160	5.7×10^{8}	1.26
400 nM	36.3 nM	1.4×10^{5}	5.3×10^{-3}	5.1×10^{-3}	3.9×10^{-4}	201	3.6×10^{8}	1.63

Kinetic constants calculated using BiaEvaluation software version 3.1

Units: k_{on}, $M^{-1}s^{-1}$; k_{off},, s^{-1}; k_2, s; k_{-2}, s^{-1}; K, M^{-1}.

†: Rmax, calculated maximum binding capacity in response units.

§: Chi-square distribution of variance from model.

4.2 Gibberellin-dependent recruitment of SLY1 to RGL1

I have demonstrated that RGL1 exhibits a gibberellin-dependent interaction with GID1A through the conserved DELLA and TVHYNP motifs within the N-terminal DELLA domain, similar to interactions of other DELLA proteins previously reported. This interaction has been reported to be essential for gibberellin-induced DELLA protein degradation (Griffiths *et al.*, 2006; Ueguchi-Tanaka *et al.*, 2007). However, degradation also requires the F-box proteins GID2 or SLY1. I have further investigated the interactions of RGL1 with both GID1A and SLY1 *in vivo* using a yeast three-hybrid assay. As reported for the DELLA protein RGA, liganded GID1A primes RGL1 for interaction with SLY1 (Figure 4.12A,B) (Griffiths *et al.*, 2006). The GID1A/GA_3-dependent interaction between RGL1 and SLY1 as measured by yeast three-hybrid analysis, had a similar dose response to the gibberellins GA_3 and GA_4 as did the gibberellin-dependent interaction between GID1A and RGL1 (Figure 4.12C,D). Observed dose-response behaviour confirms that the gibberellin-dependent recruitment of SLY1 is sensitive to physiological levels of bioactive gibberellins, and that the affinity of GID1A for gibberellins is rate limiting in the recruitment of SLY1. To investigate whether GID1A recruits SLY1 through a direct physical interaction, both were introduced into a yeast two-hybrid system. GID1A and SLY1 show no direct interaction, neither in the presence of gibberellins, nor when a gain-of-function mutation of SLY1, $sly1^{E138K}$ was incorporated (Figure 4.12E) (Dill *et al.*, 2004; Fu *et al.*, 2004).

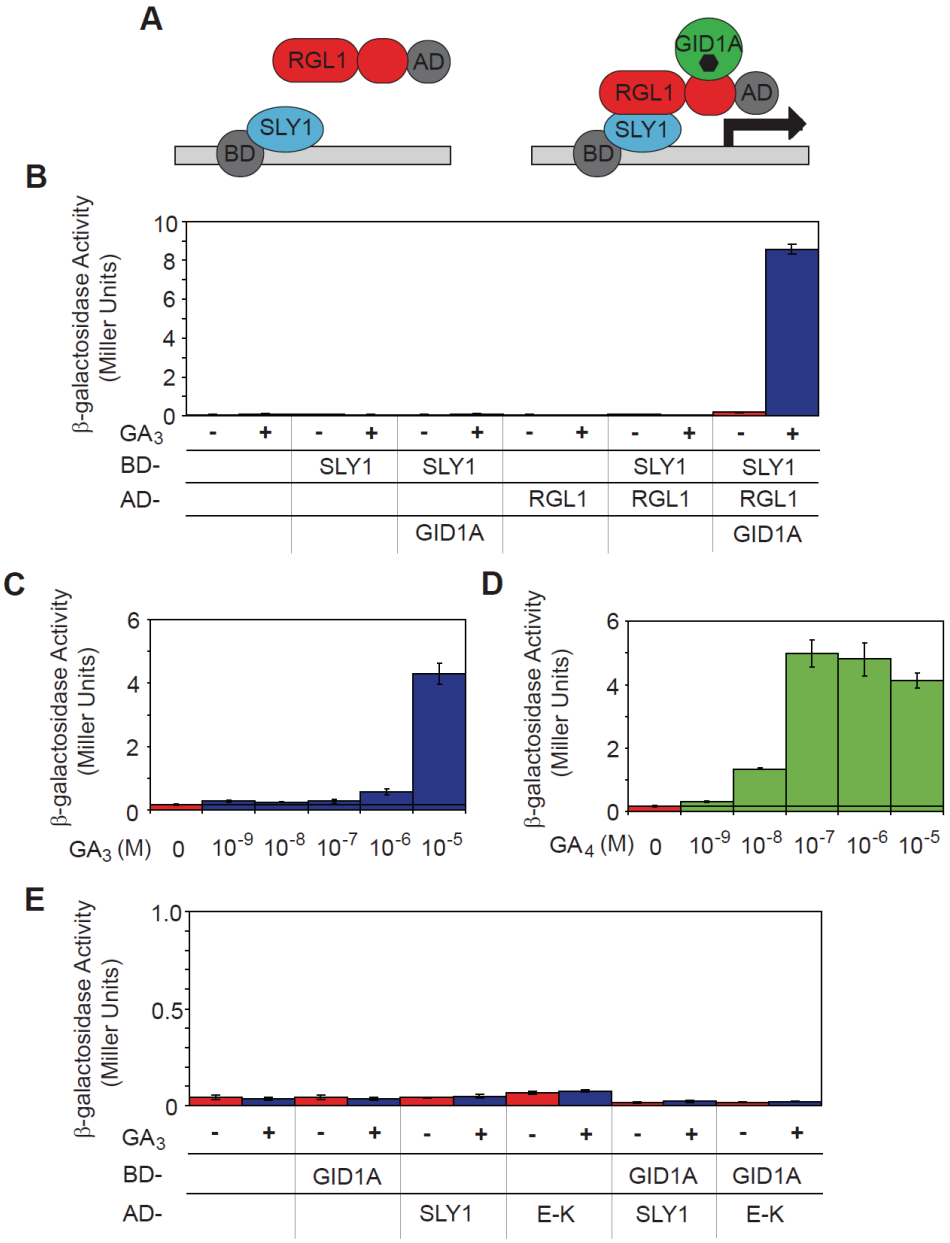

Figure 4.12. Gibberellin-dependent recruitment of SLY1 to RGL1. A. Schematic representation of the yeast three-hybrid system design for detection of an interaction between GID1A, RGL1 and SLY1. **A-E.** *LACZ* (β-galactosidase) reporter assays. **A.** Interaction between a GAL4 DNA binding domain (BD-) fusion of SLY1 and GAL4 activation domain (AD-) fusions of RGL1 in the absence or presence of co-expressed GID1A. Interactions were performed in the presence of either 0 or 100 µM gibberellin GA_3 **C-D.** Interaction between BD-SLY1, AD-RGL1, and GID1A in the presence of 1 nM - 10 µM gibberellins GA_3 (**C**) or GA_4 (**D**). **E.** Investigation for an interaction between a GAL4 DNA binding domain (BD-) fusion of GID1A and GAL4 activation domain (AD-) fusions of SLY1 in the absence or presence of gibberellin GA_3. Results are the averages of nine assays, with error bars showing +/- one standard deviation.

4.2.1 RGL1 inter-domain interactions

The three previously reported dwarf phenotype-inducing mutations reproduced in RGL1*:* *rgl1*$^{\Delta DELLA}$, *rgl1*$^{\Delta TVHYNP}$, and *rgl1*^{Q272R} were introduced into the yeast three-hybrid system (Buchanan, 2007; Itoh *et al.*, 2002; Koornneef *et al.*, 1985; Muangprom *et al.*, 2005; Peng *et al.*, 1997). As expected, deletion mutations of the key motifs in the N-terminal domain of RGL1, ΔDELLA, a 17-amino acid residue deletion of most of the conserved DELLA motif (Koornneef *et al.*, 1985; Peng *et al.*, 1997; Wen and Chang, 2002), and ΔTVHYNP, an 18-residue deletion of the TVHYNP motif (Itoh *et al.*, 2002) prevented binding of GID1A/GA_3 to RGL1 and recruitment of SLY1 (Figure 4.3; Figure 4.13).

The only known gibberellin-insensitive C-terminal domain DELLA protein mutation has been reported to block the weak interaction between RGA and SLY1 observed in yeast two-hybrid assays (Dill *et al.*, 2004; Muangprom *et al.*, 2005). I now show that this mutation, located in the C-terminal domain near the conserved VHIID motif, not only disrupted recruitment of SLY1 in the three-hybrid assay, but also that of dominant gain-of-function mutant sly1^{E138K} that exhibits an increased GID1A/GA_3-dependent and independent interactions with RGL1 (Figure 4.13), These results demonstrate that *rgl1*^{Q272R} mutation disrupts the interaction of RGL1 with SLY1 and most likely affects contact residues between RGL1 and SLY1.

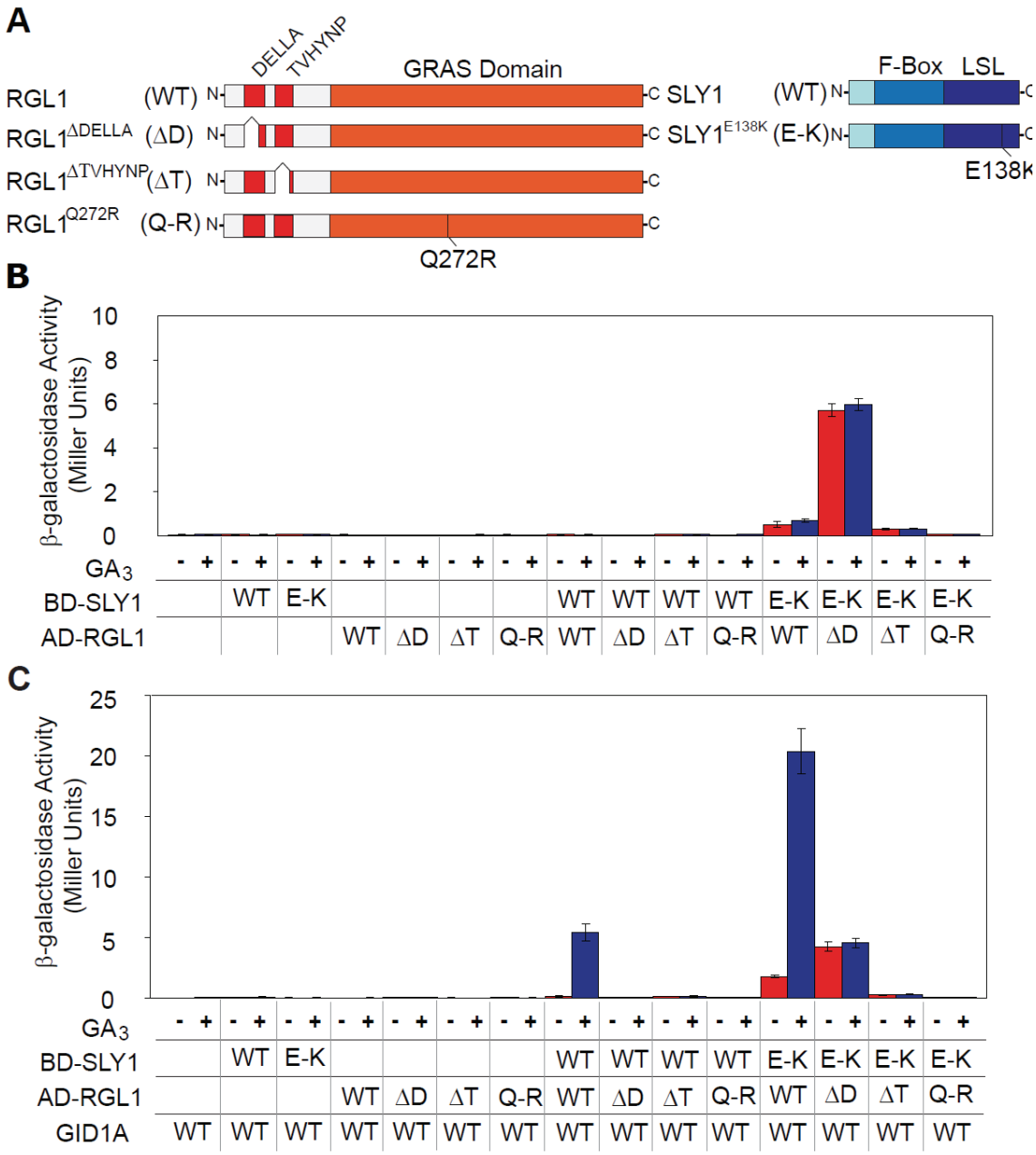

Figure 4.13. Domain analysis of the gibberellin/GID1A-dependent recruitment of SLY1 to RGL1. A. Schematic representation of the domain structure of RGL1 and SLY1, including investigated DELLA dwarfing mutations and SLY1 gain-of-function mutation. **B-C.** *LACZ* (β-galactosidase) reporter assays. **B.** Interaction between a GAL4 DNA binding domain (BD-) fusion of SLY1 or sly1^{E138K} (E-K) and GAL4 activation domain (AD-) fusions of RGL1 (WT), rgl1$^{\Delta DELLA}$ (ΔD), rgl1$^{\Delta TVHYNP}$ (ΔT), and rgl1^{Q272R} (Q-R). Assays were performed in the presence of either 0 or 100 μM gibberellin GA_3 **C.** Interactions as for B. in the presence of co-expressed GID1A. Results are the averages of nine assays, with error bars showing +/- one standard deviation.

The ΔDELLA, but not ΔTVHYNP of the N-terminal domain enhanced the gibberellin-independent interaction of RGL1 with sly1^{E138K} (Figure 4.12A). The E138→K mutation of SLY1 was originally isolated as a suppressor of *gai-1* (*gai*$^{\Delta DELLA}$) and has been shown to have increased affinity for several DELLA proteins relative to the wild-type SLY1 (Dill *et al.*, 2004; Fu *et al.*, 2004; Wilson and Somerville, 1995), However, my findings suggest that the increased binding of sly1^{E138K} mutant to rgl1$^{\Delta DELLA}$ is not only a result of increased affinity for the C-terminal domain of RGL1, but also that the absence of the DELLA motif of the N-terminal domain of RGL1 has an additive effect in the RGL1$^{\Delta DELLA}$- sly1^{E138K} interaction. This effect may be mediated by increasing accessibility of the C-terminal domain of RGL1 to sly1^{E138K}, possibly through disruption of an intramolecular N-C domain interaction of RGL1.

To investigate to possibility of an N-C domain interaction, the two domains of RGL1 were spatially separated through insertion of GFP in-frame between the two domains (RGL^{N}-GFP-RGL^{C}; Figure 4.14A) and effect of this separation on pair-wise and three-partite interactions between GID1A, RGL^{N}-GFP-RGL^{C} and SLY1 was investigated. This construct is predicted to separate the DELLA and GRAS domains of RGL1 by 20 Å, based on the crystal structure of GFP (PDB 1EMA; Ormö *et al*., 1996). When introduced into the yeast two-hybrid experiments, this construct was functional in gibberellin-dependent interactions between RGL^{N} and GID1A (Figure 4.14B). This is expected as the N-terminal DELLA domain is sufficient for interaction with GID1A (Griffiths *et al*., 2006, Ugeuchi-Tanaka *et* al., 2007).

If an N-C domain interaction is required for signalling events regulating SLY1 recruitment, then the spatial separation of the DELLA and GRAS domains should block the GID1A/GA_3-dependent recruitment of SLY1. Indeed, in the yeast three-hybrid system, the RGL^{N}-GFP-RGL^{C} GFP-interruption construct does not interact with SLY1 in the presence of GID1A and GA_3 (Figure 4.14C). This fusion protein is expressed, as shown by interaction with GID1A/GA_3, *S. cerevisiae* cell fluorescence and by immunoblot (data not shown). Intriguingly, RGL^{N}-GFP-RGL^{C} shows a GID1A/GA_3-dependent interaction with the dominant form of SLY1, sly1^{E138K} which binds wild-type RGL1 and rgl1$^{\Delta DELLA}$, but not rgl1$^{\Delta TVHYNP}$ (Figure 4.14C). This result shows that GID1A/GA_3-induced signalling can occur even though the DELLA and GRAS domains are spatially separated, albeit at a lower efficiency than in the wild-type RGL1.

Given that the GFP insertion does not completely block communication of the GID1A/GA_3 signal between the N- and C-domains, it is possible that the N-to-C interaction is intermolecular, rather than intramolecular, implying that DELLA proteins are dimers. DELLA proteins have been previously predicted to form dimers, based on the presence of Leucine-rich motifs (Itoh *et al*., 2002), however, dimerisation is yet to be clearly demonstrated.

An explanation for sly1^{E138K} binding to RGL^N-GFP-RGL^C regards the unstructured nature of the N-terminal DELLA domain. An unstructured N-terminal RGL1 domain will span hundreds of angstroms, far greater than the 20 Å introduced between the two domains through GFP insertion. However, upon interaction of the N-terminal domain with GID1A/GA_3 it takes on secondary and tertiary structure, greatly reducing the length and reach of this domain. An N-to-C domain interaction in RGL1 could have both inhibitory and stimulatory effect on the tri-partite interaction. The short Asp/Glu/Leu/Leu helix of the DELLA motif, that is not required for interaction of the N-terminal DELLA domain with GID1A/GA_3, could exhibit both an inhibitory effect in the absence of the liganded receptor and a stimulatory effect after receptor binding.

Supporting this model is the weaker GID1A/GA_3-independent and stronger GID1A/GA_3-dependent binding of sly1 ^{E138K} to wild-type RGL1 in comparison to rgl1$^{\Delta DELLA}$, and the absence of gibberellin-independent binding of sly1 ^{E138K} to RGL^N-GFP-RGL^C (Figure 4.14C). In the GID1A/GA_3-RGL^N-GFP-RGL^C state, the contribution of the Asp/Glu/Leu/Leu helix towards the structure of the SLY1 binding site would not be possible due to spatial distances. In this scenario, Asp/Glu/Leu/Leu-independent sly1^{E138K}, but not Asp/Glu/Leu/Leu-dependent SLY1 could bind to the C-domain, consistent with the yeast-three-hybrid results (Figure 4.14C). This model is discussed further in Chapter 6.

In summary, these findings demonstrate for the first time that the DELLA motif could be important for an RGL1 N- to C-domain intramolecular interaction, which in turn may regulate availability of the binding site for SLY1 present on DELLA proteins.

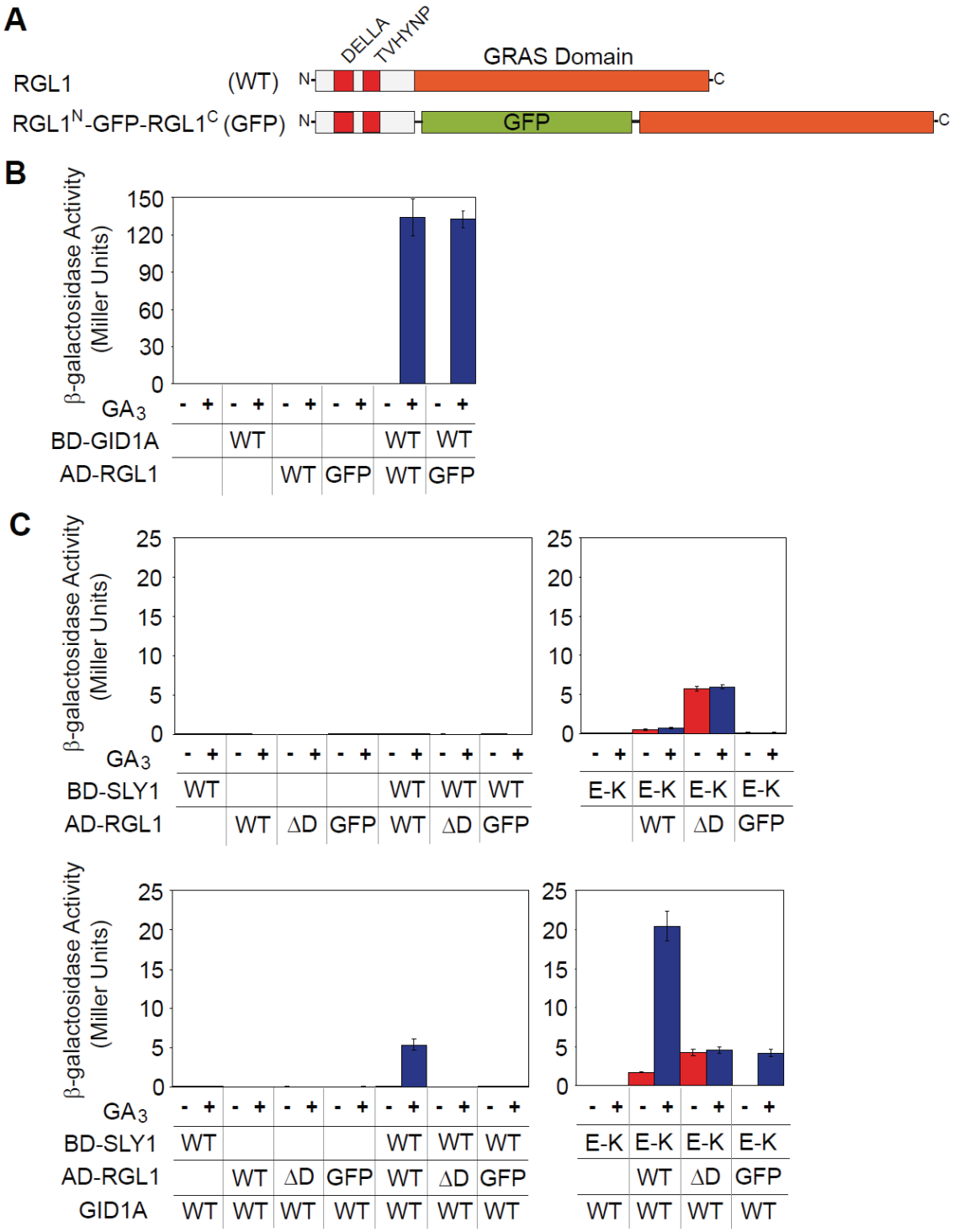
A
DELLA
TVHYNP
GRAS Domain
RGL1 (WT)
N
C
RGL1N-GFP-RGL1C (GFP)
GFP
B
β-galactosidase Activity (Miller Units)
150
120
90
60
30
0
GA3
BD-GID1A
AD-RGL1
WT
GFP
C
β-galactosidase Activity (Miller Units)
25
20
15
10
5
0
BD-SLY1
AD-RGL1
GID1A
ΔD
E-K

Figure 4.14. Spatial domain separation affects on gibberellin/GID1A-dependent recruitment of SLY1 to RGL1. A. Schematic representation of the domain structure of RGL1 and SLY1, including investigated DELLA dwarfing mutations and in-frame GFP insertion. **B-C.** *LACZ* (β-galactosidase) reporter assays. **B.** Interaction between a GAL4 DNA binding domain (BD-) fusion of GID1A and GAL4 activation domain (AD-) fusions of RGL1 (WT), $rgl1^{\Delta DELLA}$ (ΔD), and $RGL1^{N}$-GFP-$RGL1^{C}$ (GFP) **C.** Interaction between a GAL4 DNA binding domain (BD-) fusion of SLY1 or $sly1^{E138K}$ (E-K) and GAL4 activation domain (AD-) fusions of RGL1 in the presence or absence of co-expressed GID1A. Assays were performed in the presence of either 0 or 100 μM gibberellin GA_3. Results are the averages of nine assays, with error bars showing +/- one standard deviation.

4.3 Prediction of the surface accessibility of Q272

The absolutely conserved glutamine residue (RGL1 Q272) within the DELLA proteins is immediately downstream of the VHIID motif that defines the GRAS protein family. Assuming that residues with the highest conservation will cluster to regions within the core and binding sites of the tertiary structure, I aligned this region with all *A. thaliana* GRAS proteins to determine the conservation of the glutamine residue (Figure 4.15A). This region is almost absolutely conserved amongst DELLA proteins from multiple species including *A. thaliana*, grape, pea, rice, barley, wheat, and maize (DELLA alignment presented in Appendix B). However, amongst the GRAS proteins, of which only DELLA proteins have been shown to function in gibberellin signalling, this putative α-helix is not so highly conserved. Indeed, when this region is presented as a helical wheel, a representation of looking down the predicted helix, highly conserved non-polar residues cluster to one side (Figure 4.15B). In contrast the opposite face of the helix, including Q272, is poorly conserved and consists of primarily polar residues.

Although glutamine is the most common residue at the Q272 position, other GRAS proteins possess both negatively and positively charged residues at this position. Several *A. thaliana* GRAS proteins even encode arginine, the very residue exchanged in the Q272R mutation. Hence the polar face of this putative amphipathic α-helix is not well conserved, and therefore, likely forms a region on the surface of the GRAS proteins. The implication is that the Q272R mutation does not simply disrupt the C-terminal GRAS domain from folding correctly. This is supported by the fact that the C-terminal GRAS domain of the Q272R mutant is still functional as a repressor of gibberellin responses, leading to gibberellin-insensitivity (Muangprom *et al.*, 2005).

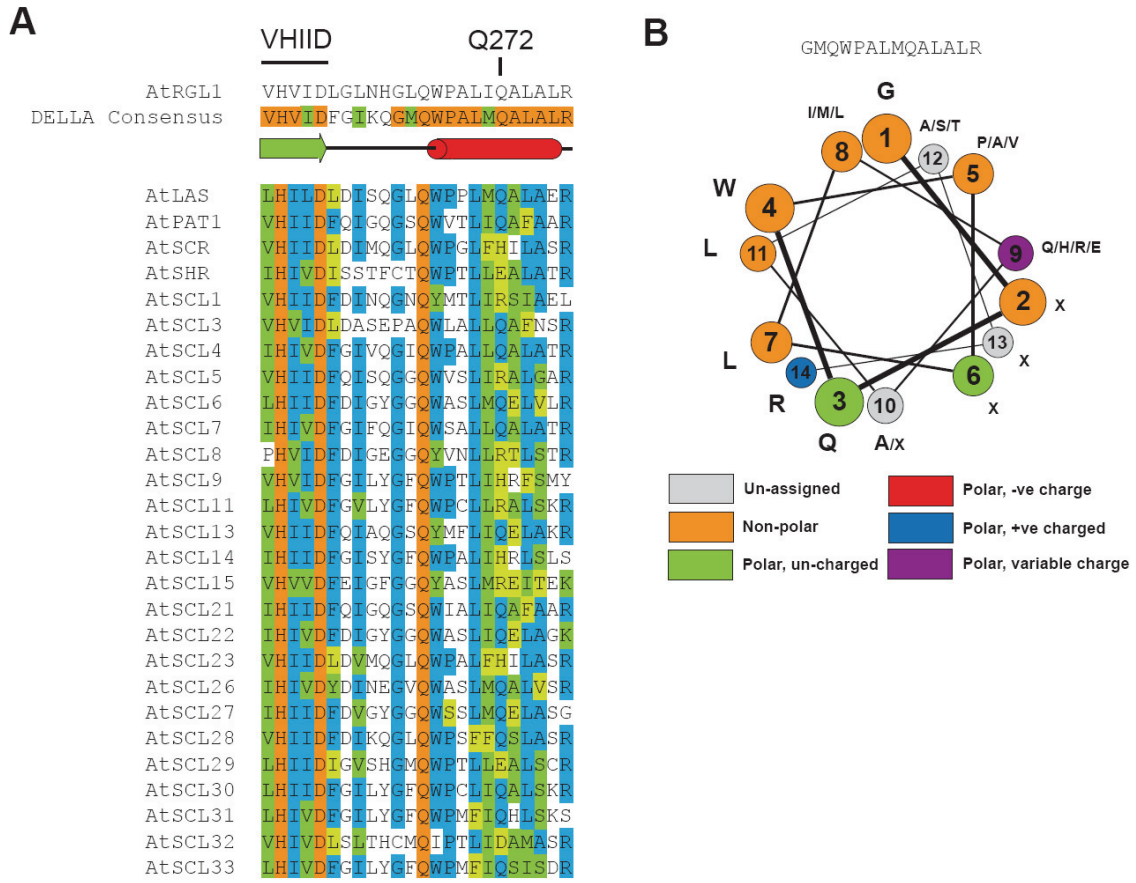

Figure 4.15. Conservation of the VHIID motif and downstream Q272 amongst *A. thaliana* GRAS proteins. A. AlignX alignment of the VHIID motif and downstream sequence of *A. thaliana* GRAS proteins, compared to the DELLA protein consensus sequence (alignment presented in Appendix B) (Vector NTI software, Invitrogen, California, USA). DELLA protein secondary structure, predicted using Jpred, is indicated below the DELLA consensus (full RGL1 secondary structure prediction presented in Appendix C) (Cole *et al.*, 2008). **B.** Helical wheel display of the predicted GMQWPALMQALAR α-helix, indicating conservation and characteristics of residues in the GRAS protein family.

4.3.1 Prediction of the RGL1 GRAS domain tertiary structure

There are currently no tertiary structures available for the GRAS domain of any DELLA or GRAS proteins. Using predictive analysis I present a putative tertiary structure for a core to the GRAS domain (Figure 4.16). This model was generated using the I-TASSER structure prediction algorithm. Instead of alignment of primary sequence to those of known high-resolution structures, the secondary structure is predicted and this aligned to similar patterns of secondary structure. The resulting model is then refined, giving several possible structures. In the presented model, similar in two out of five of the predicted models, the core of the GRAS domain forms a parallel β-sheet surrounded by amphipathic α-helices, a structure similar to methyltransferases (PDB entries 2AOT and 1RI5). The VHIID motif forms the central β-strand, consistent with its high homology amongst GRAS proteins. The highly conserved SAW motif also forms a terminal β-strand of the β-sheet, though in an anti-parallel direction. Other regions of the GRAS domain are excluded from the presented model as their structure was not well predicted. These regions likely form a second domain that sits atop the β-sheet, with the N-terminal DELLA domain extruding from the top. There are currently no algorithms that can predict protein tertiary structures with any reliability unless a similar crystal structure has previously been solved. As no structures of GRAS-like proteins have been solved, only very distantly related proteins can be used, resulting in a low confidence of predicted models. In support of this putative structure, all regions of secondary structure align well with regions that are highly conserved amongst DELLA proteins (Appendix B,C)

This predicted structure places the Q272 residue protruding into a possible binding site on the surface of the protein. With the long unstructured poly-S/T/V region spacing the DELLA and TVHYNP motifs from the GRAS domain, it may be possible for the DELLA motif to bind near the Q272 cleft formed by three α-helices, thus providing a mechanism by which this motif regulates SLY1 recruitment.

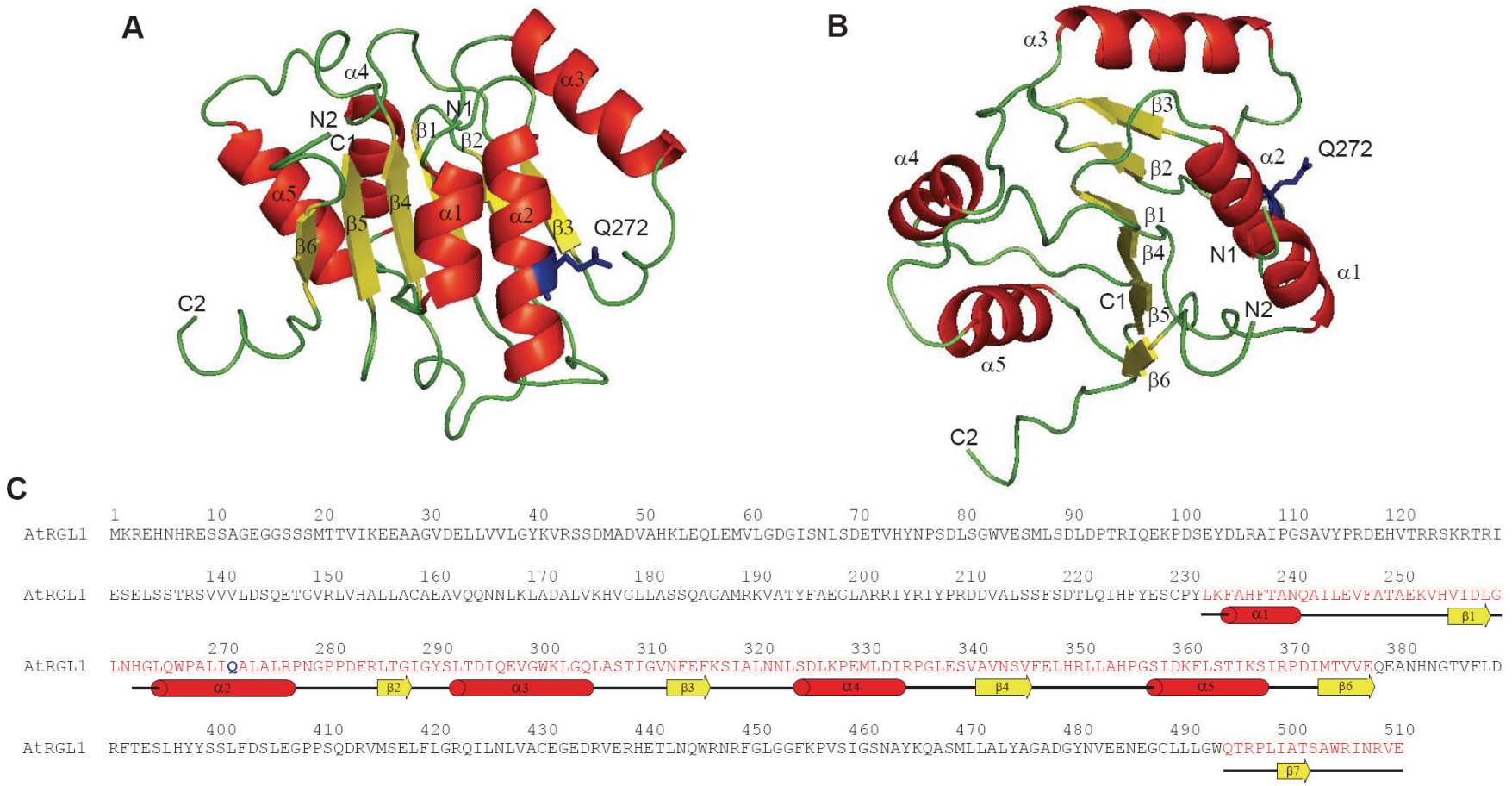

Figure 4.16. Prediction of the RGL1 GRAS domain tertiary structure. Predicted structure of a portion of the GRAS domain of RGL1, including the VHIID and SAW motif, obtained using I-TASSER (Wu *et al.*, 2007; Zhang, 2007, 2008). **A-B.** Side (A), and top (B) views of a predicted core domain. Q272 is indicated in blue. **C.** RGL1 sequence, indicating predicted region in red; corresponding secondary structure is symbolised below the sequence.

Chapter 5

Identification of novel RGL1-interacting proteins

Many of the mechanisms by which the DELLA proteins function in plant development have not yet been resolved. DELLA proteins have been shown to be destabilised in response to auxins, and stabilised in response to ethylene (Achard *et al.*, 2007a; Achard *et al.*, 2006; Fu and Harberd, 2003). Furthermore, only one case of DELLA-mediated transcriptional regulation has been described in detail (de Lucas *et al.*, 2008; Feng *et al.*, 2008).

These uncharacterised functions of the DELLA proteins are expected to be mediated through direct interactions with other signalling components. Therefore, one approach to reveal the mechanism by which DELLA protein function is mediated or regulated is to discover the identities of DELLA-interacting proteins.

I have performed affinity purification to isolate novel RGL1-interacting proteins from plant tissue, using the N-terminal DELLA domain as bait. A method for the affinity purification of two RGL1 interacting proteins was developed as part of my Masters thesis (Sheerin, 2005). As part of my doctoral thesis I have improved the efficiency and up-scaled the procedure to increase yields of purified proteins. These improvements have allowed the identification of two novel RGL1-interacting proteins using mass spectrometry fingerprinting.

5.1 Affinity purification of RGL1-interacting proteins

The DELLA protein RGL1 is expressed primarily in the inflorescence (Tyler *et al.*, 2004), hence this tissue is expected to be enriched in RGL1-interacting proteins. Furthermore, RGL1 has been shown to be localised exclusively to the nucleus, where all known interactions of DELLA proteins take place (Wen and Chang, 2002). Therefore, I attempted isolation of RGL1-interacting proteins from a nuclear protein fraction of wild-type *A. thaliana* inflorescence tissue.

Full length RGL1 could not be used as an affinity purification bait. This is due to the complete insolubility of recombinant fusions expressed in *E. coli*. Semi-soluble GST-fusions are misfolded, and were non-functional in binding either recombinant GID1A or SLY1 (data not shown). Therefore, the N-terminal DELLA domain of RGL1, $RGL1^{1-137}$, was expressed as a recombinant fusion to MBP and purified from *Escherichia coli*. This fusion was functionally active in binding gibberellin-liganded GID1A in *in vitro* experiments (Chapter 4). Furthermore, the N-terminal domain encompasses regions predicted to regulate gibberellin signal perception (Itoh *et al.*, 2002). Thus, use of the recombinant N-terminal domain of RGL1 as bait is a suitable design for the purification of interacting proteins that regulate DELLA protein stability.

Two proteins were purified from plant nuclear extract by their affinity for the N-terminal domain of RGL1, with apparent molecular weights of 24 and 64 kDa (Figure 5.1A). These two proteins were not isolated in control experiments, which were performed to determine non-specific binding to the sepharose matrix or MBP (Figure 5.1B). A number of other *A. thaliana* proteins were enriched by affinity purification, but in much smaller amounts than the 24 and 64 kDa proteins. These additional proteins were either non-specific for $RGL1^{1-137}$, or specificity could not be established due to mobilities similar to the MBP-tag in the control experiment. The reason for the release of immobilised MBP-tag during elution conditions is unknown (Figure 5.1B).

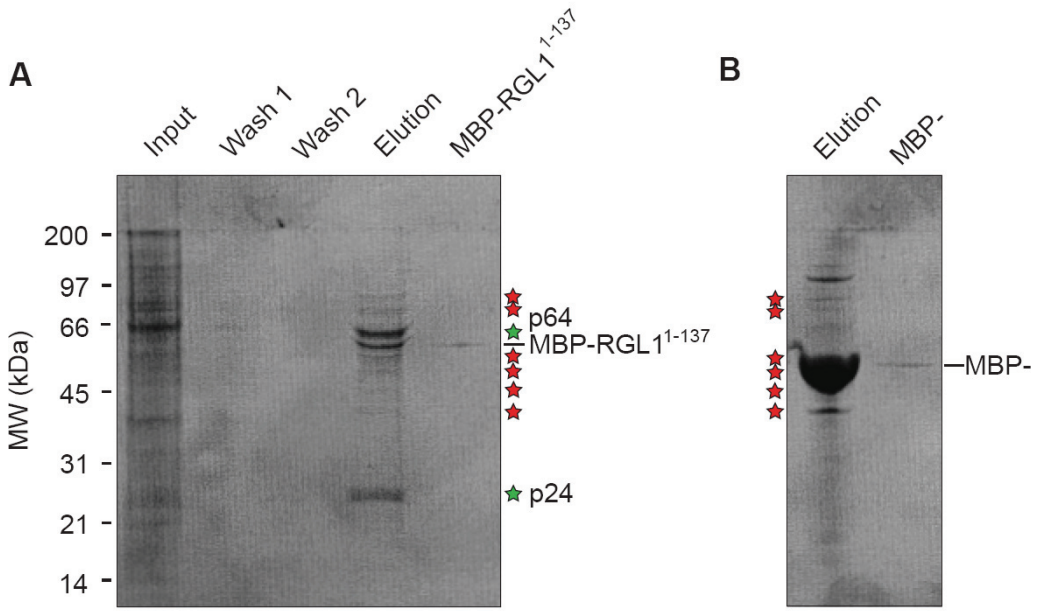

Figure 5.1. **Affinity purification of RGL1 N-terminal domain interacting proteins. A-B.** Isolation of nuclear proteins, through interaction with immobilised MBP-RGL1$^{1-137}$ (**A**), or control bait protein MBP-β-galactosidase-α (MBP-β-gal) (**B**). Nuclear proteins (input) were extracted from 10 g wild-type *A. thaliana* Col-0 inflorescence tissue. Proteins extracted from nuclei that bound to 200 µg of immobilised bait protein were eluted by boiling in SDS-PAGE loading buffer. Isolated proteins from both A and B were separated by SDS-PAGE on a single gel (lanes separated for clarity of labelling), and stained with SYPRO ruby gel stain. Purified recombinant bait proteins (MBP-RGL1$^{1-137}$ and MBP-, 2ng of each) indicate the size of immobilised bait proteins released from the matrix during elution. Red stars indicate eluted proteins that are not specific for RGL1$^{1-137}$. Green stars indicate eluted proteins p24 (24 kDa) and p64 (64 kDa) specific to RGL1$^{1-137}$. Lanes: input, nuclear extract, 0.2 % input volume; wash 1 and 2, initial and final (second) wash, 2 % of total volume; elution, eluted proteins, 50 % total volume.

5.2 Identification of isolated RGL1-interacting proteins

The two major isolated RGL1-sepecific interacting proteins, 24 kDa and 64 kDa, were analysed using tandem electrospray-ionisation/quadrapole mass spectrometry (LC-ESI MS/MS) at the Mass Spectrometry Facility, University of Auckland. Mass spectrometry data was analysed using MASCOT (Matrix Science, London, UK) to search the SwissProt database, and unassigned peptides were searched using NCBI and MSDB databases and *de novo* sequenced using PEAKS (a database of all possible peptides, Bioinformatics Solutions, Ontario, Canada).

The 24 kDa protein was assigned as *A. thaliana* At1g72610, GERMIN-LIKE PROTEIN-1 (GLP1; Table 5.1). Only three peptides were matched to GLP1; others originated from human keratin and trypsin self-cleavage products, and several peptides could not be matched to any protein in the database. Un-assigned peptides are either due to poor mass spectra data or are derived from a protein that is not predicted from genome sequences, recombinant Trypsin self-cleavage products, or are post-translationally modified peptides (either *in planta* or chemically). Other peptides expected for a tryptic digest of GLP1 are too large to be reliably identified using this method (greater in mass than the quality cut-off used in data analysis), and thus are not presented in the final peptide dataset.

GLP1 has a calculated molecular weight of 21.6 kDa, but *A. thaliana* derived endogenous GLP1 has been shown to exhibit an apparent molecular weight of 23 kDa, similar to that of the isolated p24 protein (Membre *et al.*, 2000). GLP1 is predicted to be post-translationally modified through *N*-glycosylation, which could account for the un-assigned peptides detected (Membre *et al.*, 2000). GLP1 is predicted to contain a typical signal sequence and hence is destined for export from the cytoplasm (SignalP, data not shown) (Emanuelsson *et al.*, 2007). Furthermore, the SVQDFCVANLK peptide detected cannot be generated by digestion with trypsin unless GLP1 was processed for secretion. This is in disagreement with the fact that this protein was isolated from nuclear extract. GLP1 has been shown to be present in the extracellular matrix, though a significant portion is within other cell fractions (Membre *et al.*, 2000). Therefore, there

are three possible explanations for the detection of GLP1: the peptide identification was wrong due to the low abundance of substrate protein; the nuclear extract was contaminated with other cellular fractions (*GLP1* is highly expressed); or indeed a portion of GLP1 is present within the nucleus and can interact with RGL1.

The second major protein isolated by interaction with the N-terminal domain of RGL1 that had a molecular weight of 64 kDa was assigned as At5g25980, THIOGLUCOSIDE GLUCOHYDROLASE-2 (TGG2; Table 5.2). Only two peptides were assigned to TGG2. There were several unassigned peptides, and these matched those unassigned for p24 and likely originated from recombinant Trypsin self-digestion. TGG2 also has a predicted signal sequence and a predicted localisation to the vacuole (SignalP, PSORT) (Emanuelsson *et al.*, 2007; Nakai and Kanehisa, 1991). *TGG2* is shown to be a highly expressed gene in microarray screens (AtGENexpress; Schmid *et al*., 2005). However, probes for *TGG2* cannot differentiate the adjacent duplicated *TGG1* (Barth and Jander, 2006). Indeed, TGG2 protein levels are reported to be low in comparison to the highly abundant TGG1 (Barth and Jander, 2006).

The isolation of GLP1 and TGG2 from the nuclear extract could be accounted for by contamination of nuclear extract with other cellular fractions or due to high abundance proteins being inadequately removed by washing during the purification. However, neither were purified in control experiments; suggesting that they do interact specifically with RGL1. Affinity purification procedures can isolate interacting proteins that have no biological relevance. Neither GLP1 nor TGG2 have yet been implicated in plant responses to gibberellin. GLP1 has no known function, whilst TGG2 is predicted to be a myrosinase: an enzyme that catabolises glucosinolates into toxic compounds in response to herbivores (Barth and Jander, 2006). Given that germin-like-proteins have been suggested to function in many plant functions including hormone signalling, I subjected this protein to further investigation to confirm a direct interaction with RGL1.

Table 5.1

Mass spectrometry analysis of RGL1-interacting protein p24

	Ion (m/z)[§]	Peptide[†]	Score[‡]
Trypsin, Pig			**91**
	421.78	VATVSLPR	47
	523.30	LSSPATLNSR	44
Keratin, Human			**235**
	517.28	TLLEGEESR	55
	533.29	AQYEDIAQK	28
	590.33	YEELQITAGR	59
	651.89	SLDLDSIIAEVK	61
	738.40	WELLQQVDTSTR	32
At1g72610, Arabidopsis			**101**
	328.72	LDLAPK	30
	617.82	AETPAGYPCIR	25
	640.85	SVQDFCVANLK	46
Unassigned			
	412.77	VAGDPLPR	-
	428.79	LATVLSPR	-
	435.79	VVTVSLPR	-
	633.35	-	-
	647.86	-	-
	769.35	-	-
	883.93	-	-
	897.95	-	-
	996.59	-	-

[§] Parent peptide mass/charge ratio.

[†] MS/MS determined peptide sequence.

[‡] Probability based scoring (Pappin *et al.*, 1993).

Table 5.2

Mass spectrometry analysis of RGL1-interacting protein p64

	Ion (m/z)[§]	Peptide[†]	Score[‡]
Trypsin, Pig			**86**
	421.78	VATVSLPR	47
	523.30	LSSPATLNSR	39
Keratin, Human			**51**
	517.28	TLLEGEESR	40
	738.40	WELLQQVDTSTR	11
At5g25980, Arabidopsis			**78**
	539.291	GYALGTDAPGR	62
	757.401	WFLPYDDTLESK	16
Unassigned			
	412.77	VAGDPLPR	-
	428.79	LATVLSPR	-
	435.79	VVTVSLPR	-

[§] Parent peptide mass/charge ratio.

[†] MS/MS determined peptide sequence.

[‡] Probability based scoring (Pappin *et al.*, 1993).

GLP1 is a member of the Germin-like protein family; a large protein family involved in enzymatic, structural, and cell signalling functions (Bernier and Berna, 2001). Tests for oxalate oxidase activity, a function of the originally isolated Germin protein, show GLP1 does not exhibit this enzymatic function (Membre *et al.*, 2000). GLP1 shares homology with several germin-like proteins that exhibit an affinity for auxins: the *Prunus persica* (peach) AUXIN BINDING PROTEIN-19A (ABP19A), -19B (ABP19B), and -20 (ABP20) (Figure 5.2) (Ohmiya *et al.*, 1998). Therefore, the interaction between GLP1 and RGL1 was investigated in a yeast two-hybrid assay to investigate a requirement for either gibberellins or auxins. GLP1 with or without a signal sequence did not interact with full length RGL1 in the presence or absence of either gibberellin GA_3 or the auxin indole acetic acid (IAA) (Figure 5.3). Similarly GLP1 did not show any interactions with the N-terminal domain of RGL1 (residues 1-137) in a yeast two-hybrid system (Figure 5.3). It is possible that GLP1 requires plant specific post-translational modifications to interact, or perhaps IAA is required and uptake of IAA by *S. cerevisiae* is limited (no yeast two-hybrid interactions for IAA-dependent interactions have been reported to my knowledge). Therefore this interaction may either be artefact of the affinity purification procedure, or could not be replicated in the yeast two-hybrid system.

In summary, two novel proteins that interact with the recombinant N-terminal domain of RGL1 have been identified: GLP1 and TGG2. However, whether the interaction between these proteins exists *in planta* and is of biological significance is yet to be determined.

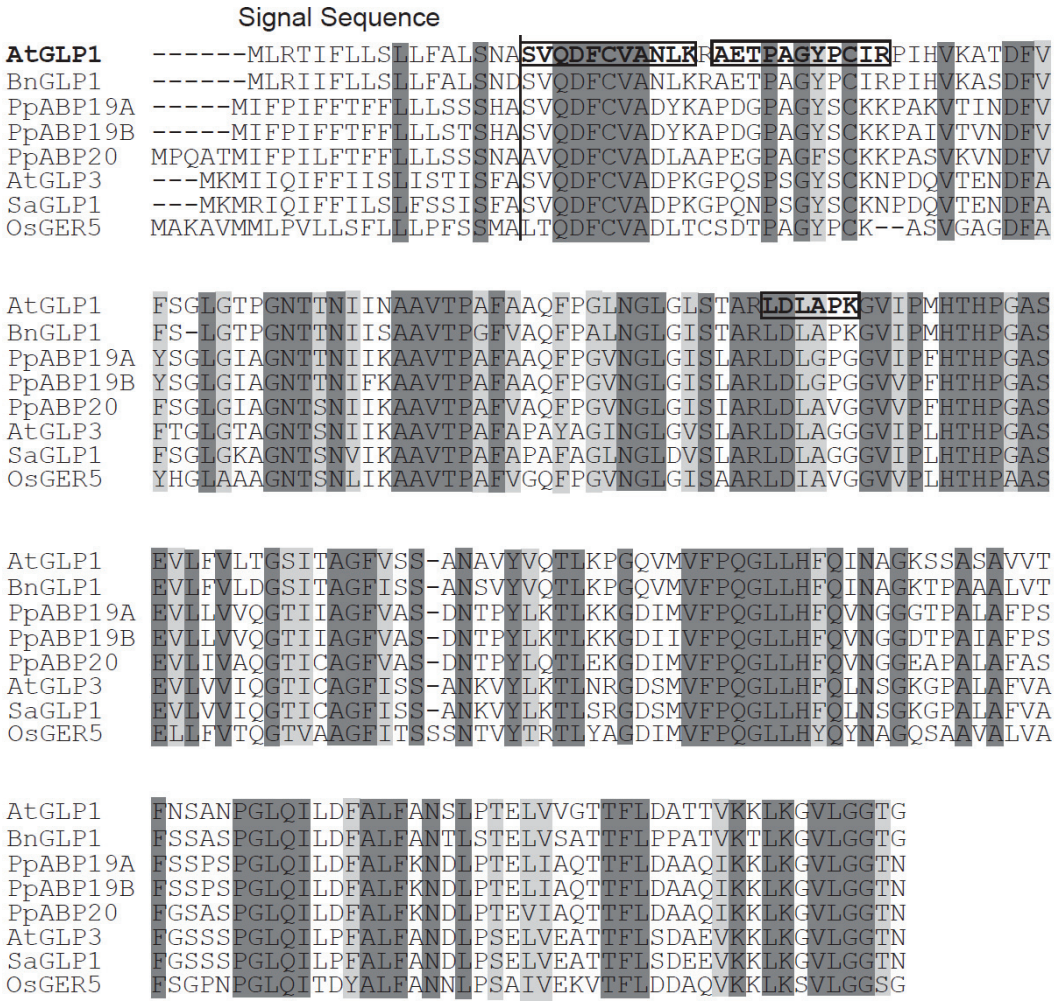

Figure 5.2. **Alignment of closely related GLP protein sequences**. ClustalW alignment of *A. thaliana* GLP1 and related Germin-like protein sequences with > 50% sequence identity (Larkin *et al.*, 2007). Signal sequence and cleavage site, indicated by a vertical line, were predicted using SignalP (Emanuelsson *et al.*, 2007). Peptides identified by mass spectrometry fingerprinting are boxed. Bn, *Brassica napus*; Pp, *Prunus persica*; Sa*, Sinapis alba*.

				+	IAA
			+		GA_3
BD-	AD-	-	-	-	
BD-p53	AD-T-antigen	60 mM	60 mM	60 mM	
BD-GLP1	AD-	-	-	-	
BD-GLP1 $^{\Delta SS}$	AD-	-	-	-	
BD-	AD-RGL1	-	-	-	
BD-	AD-RGL1 $^{1-137}$	-	-	-	
BD-GLP1	AD-RGL1	-	-	-	
BD-GLP1	AD-RGL1 $^{1-137}$	-	-	-	
BD-GLP1 $^{\Delta SS}$	AD-RGL1	-	-	-	
BD-GLP1 $^{\Delta SS}$	AD-RGL1 $^{1-137}$	-	-	-	

Figure 5.3. **Evaluating an *in vivo* GLP1:RGL1 interaction**. Yeast two-hybrid *HIS3* reporter assay for interaction between a GAL4 DNA binding domain fusion of GLP1 (BD-GLP1) and a GAL4 activation domain fusion of either full-length RGL1 (AD-RGL1) or the N-terminal domain of RGL1 (AD-RGL1$^{1-137}$). Interaction investigated by assaying for growth on minimal media supplemented with 0-60 mM of the histidine biosynthesis inhibitor 3-AT. Both full length GLP1 and GLP1 lacking the signal sequence (GLP$^{\Delta SS}$) were investigated. Experiment performed in the presence or absence of either 100 µM gibberellin GA_3 or 100 µM auxin indole-acetic acid (IAA). The well characterised p53-T-antgen interaction was used as a positive control for interaction.

Chapter 6

Discussion

6.1 Detection of endogenous *A. thaliana* DELLA proteins

The five *DELLA* genes encoded by *A. thaliana* have been reported to be differentially expressed throughout plant development (Lee *et al.*, 2002; Tyler *et al.*, 2004). Furthermore, they have been shown to be only partially redundant in function. All five are expressed within inflorescence tissues, yet in mutant lines lacking individual *DELLA* genes, only loss of either *RGA* or *RGL2* generates an apparent phenotype (Lee *et al.*, 2002). However, loss of multiple *DELLA* genes reveals that both *GAI* and *RGL1* also have functions in the repression of gibberellin responses in inflorescence tissues (Cheng *et al.*, 2004; Tyler *et al.*, 2004). In characterising a suite of anti-DELLA antibodies, I have shown that GAI, RGA, RGL1, and RGL2 can each be detected in extracts prepared from inflorescence tissue. The presence of the product of the poorly expressed RGL3 gene could not be confirmed, though it may be present at a very low level, as detected by the monoclonal antibody AD7.

Two forms of RGL1 were detected in extracts prepared from gibberellin-deficient *ga1-3 A. thaliana* lines. One form separated at the approximate molecular weight of RGL1 (56.7 kDa), the second having a slower mobility close to 62 kDa. This phenomenon was observed from multiple samplings of plant tissue. Therefore, it is unlikely that the slow mobility form originated from RGL2 contamination, but this cannot be excluded.

The two forms of RGL1 were detected differentially by the suite of anti-DELLA antibodies. The RGL1 specific antibody, AB8, could not detect the slow mobility form

of endogenous RGL1. Hence, I propose that 62 kDa form is post-translationally modified at or near the AB8 epitope. The DELLA proteins have been reported to be both phosphorylated and poly-Ubiquitinated (Dill *et al.*, 2004; Gomi *et al.*, 2004; Itoh *et al.*, 2005; Wang *et al.*, 2009). Due to the large (approximately 5 kDa) shift in mobility, the putative post-translational modification of RGL1 is unlikely to be phosphorylation. DELLA proteins are normally poly-ubiquitinated, targeting them for degradation. Therefore, it may be possible for RGL1 to undergo mono-ubiquitin-like modification. Mono-ubiquitination and mono-ubiquitin-like modifications of proteins can have roles in altering protein stability and function, rather than targeting for degradation (Hicke, 2001). Alternatively, DELLA proteins have been proposed as targets of the *O*-GlcNAc transferase SPINDLY (SPY), which would *O*-glucosylate serine and/or theronine residues.

The second unexpected observation whilst characterising anti-DELLA antibodies was an apparent substantial increase in abundance of RGL2 in extracts prepared from *A. thaliana* lines with the *rgl1-1* mutation. This could be explained by several possible events. RGL1 may affect the abundance of RGL2 through down regulation of *RGL2* expression, destabilisation of RGL2, or alteration of post-translational modifications of RGL2 protein. A more likely explanation is that the *rgl1-1* mutation results in developmental changes in the inflorescence over representing a stage where RGL2 accumulates. Indeed, the *A. thaliana* line retaining only individual functional DELLA genes in the gibberellin-deficient *ga1-3* background reveal possible roles of RGL1 (Cheng *et al.*, 2004). *RGL1* inhibits the formation of developing seed in the *ga1-3* background (Cheng *et al.*, 2004). As this is a site where *RGL2* is normally expressed, removal of *RGL1* may induce or otherwise alter this stage of development.

The expression pattern for *RGL2*, as determined by GUS staining of the *rgl2-5* T-DNA (transposon-DNA) insertion mutant, has been reported to the limited to the inflorescence, siliques, and germinating seeds (Lee *et al.*, 2002). Within these tissues *RGL2* is expressed in the sepals, stamen, and pistil, and in developing seeds within siliques. In comparison, *in situ* detection of *RGL1* expression reveals *RGL1* is limited to developing ovules and anthers, particularly associated with developing primordia and microsporogenesis (Wen and Chang, 2002). Therefore, as *RGL1* is normally involved in

the development of tissues where *RGL2* is expressed, the removal of *RGL1* could possibly generate tissues where RGL2 is abundant.

I did not directly investigate the phosphorylation state of endogenous *A. thaliana* DELLA proteins. However, the high-affinity RGL2 specific antibody BB7 appeared to bind poorly to the endogenous RGL2 extracted from inflorescence tissue. This protein was detected in abundance with other anti-DELLA monoclonal antibodies, suggesting that the BB7 epitope may be partially blocked. Therefore, it is likely that endogenous RGL2 is phosphorylated or otherwise post-translationally modified at or near the BB7 epitope. The BB7 epitope has not yet been mapped. However, in a similar fashion to AB8, BB7 binds outside either of the conserved DELLA or TVHYNP motifs (W. Jones, unpublished).

6.2 Contacts of the Asp/Glu/Leu/Leu α-helix of RGL1 are not essential for the GID1A/GA_4:RGL1 interaction

The high resolution tertiary structure of an N-terminal fragment of GAI in complex with gibberellin liganded GID1A has identified the contact residues between these two proteins (Murase *et al.*, 2008). The residues of the $GAI^{11\text{-}113}$ fragment that form direct contacts with GID1A/GA_4 are exclusively located within the conserved DELLA and TVHYNP motifs (Murase *et al.*, 2008). The involvement of both motifs is consistent with our *in vivo* interactions and previously published reports of interactions that involve N-terminal domain deletion mutants of DELLA proteins (Griffiths *et al.*, 2006; Itoh *et al.*, 2005). Since deletion mutations of the 17-residues of the DELLA motif and 18-residues of the TVHYNP motifs correspond to the only structured elements within the N-terminal domain, it could be expected that, in these deletion mutants, folding of the whole domain is disrupted.

The gibberellin-insensitive dwarfing mutations of *DELLA* genes isolated so far have contained mutations that extend beyond the DELLA pentapeptide (Peng *et al.*, 1999). One exception is a mutation of the GAI protein of *Vitis vinifera*, which contains a

Asp/Glu/Leu/Leu to Asp/Glu/Leu/His mutation and a gibberellin-insensitive phenotype (Boss and Thomas, 2002). The effect of this mutation upon the gibberellin-dependent interaction with GID1-family gibberellin receptors has not yet been studied. However, this mutation would place a polar residue within a hydrophobic pocket and therefore is likely to disturb the surface of the GID1/DELLA interface. Alternatively, the tertiary structure of DELLA protein subsets when in complex with liganded GID1-gibberellin receptors may be dissimilar.

Due to the possible secondary effects of deletion and replacement mutations, the interpretation of the effects on interactions must be taken with caution. This is why my analysis using competition with monoclonal antibodies that recognise separate sets of residues within the DELLA motif - Asp/Glu/Leu/Leu (6C8) and VLGYKVR (BC9) - was the only approach that could probe the requirement of contacts mediated by corresponding structural elements in the context of non-mutated DELLA proteins. The surprising outcome of this analysis is in that the αA helix (Asp/Glu/Leu/Leu) is not essential for the GID1A/GA_4:RGL1 interaction. The significance of this finding is in that the αA helix may possibly be available for interactions with unknown proteins whilst part of the complex with GID1A/GA_4. It is possible that this region forms weak transient interacts with GID1A, with the majority in the unbound state.

An alternative explanation for the observation that the Asp/Glu/Leu/Leu residues are not essential for interaction with GID1A/GA_4 is that for RGL1 the DELLV sequence varies slightly from the conserved DELLA sequence. Valine is bulkier and more hydrophobic than alanine. Furthermore, in the predicted structure of $RGL1^{1-137}$ modelled from the reported structure of GAI^{11-113} when in complex with GID1A/GA_4, the electron density of valine 36 overlaps with that of the side chain of glutamic acid 33. Hence, the structure of the N-terminal domain of RGL1 must differ slightly to that of GAI. What effects this will have on the conformation of the DELLV helix when RGL1 is in complex with liganded GID1A cannot be predicted.

6.3 The N-terminal DELLA domain of RGL1 undergoes conformational changes upon interaction with gibberellin-bound GID1A

The analysis of the gibberellin-dependent GID1A-C:RGL1$^{1-137}$ interaction in real time allowed visualisation of the effect of the two bioactive gibberellic acids on GID1A-C: RGL1$^{1-137}$ association/dissociation kinetics. Although GA_3 and GA_4 dramatically differ in their dissociation constants for GID1A-C (Nakajima *et al.*, 2006), I have shown that once gibberellins saturate GID1A-C, the liganded receptors demonstrate similar kinetics of association and dissociation with the N-terminal domain of RGL1 for both GA_3 and GA_4. This is in agreement with the high-resolution structures of the GID1A/GA/GAI$^{11-113}$ complex and GID1/GA whereby GA_3 and GA_4 induce identical conformational changes of the N-terminal extension of GID1A to form the platform to which the GAI binds (Murase *et al.*, 2008; Shimada *et al.*, 2008; Ueguchi-Tanaka *et al.*, 2007). My data shows, for recombinant proteins, that not only the structure of the GID1A/GA:DELLA complex, but also the kinetics of association and dissociation between liganded GID1A and DELLA proteins is largely independent to the bioactive gibberellin bound to the receptor.

The free N-terminal fragment of GAI (residues 11-113) has been proposed to exist as 100 % random coil, based on CD spectra (Murase *et al.*, 2008). Upon interaction with GID1A/GA_4, GAI$^{11-113}$ forms four α-helices (Murase *et al.*, 2008). Therefore, the fragment of N-domain of GAI must undergo structural changes upon interaction with GID1A/GA_4. No kinetic data has yet been available to describe these conformational changes for the N-terminal DELLA domains. Using deuterium exchange mass spectrometry to determine the solvent accessibility of the N-terminal DELLA domain of RGL1, I have shown that RGL1$^{1-137}$ is essentially unstructured in the absence of GID1A/GA_4, consistent with it being characterised as an intrinsically unstructured protein (Sun *et al*., 2010). I measured the association/dissociation kinetics of GID1A/GA_4 with the N-terminal domain of the DELLA protein RGL1 (residues 1-137). This data was fitted to models that predict at least two conformational states of the

GID1A/GA_4:$RGL1^{1-137}$ complex, reflecting a two-step folding process of the N-terminal DELLA domain upon binding to the liganded GID1A.

6.4 GID1A/GA_4 recruits SLY1 to RGL1 through alteration of the conformational state to RGL1

Using a yeast three-hybrid system to investigate the requirement of gibberellin-liganded GID1A for the interaction between RGL1 and the F-box protein SLY1, I have demonstrated a gibberellin-dependent mechanism for targeting RGL1 for degradation, in which the interaction of the RGL1 N-terminal domain with GID1A/GA "primes" the RGL1 C-domain for interaction with the F-box protein SLY1 This mechanism has also been reported for other DELLA proteins, including RGA, and the rice DELLA protein SLR1 in similar *in vivo* systems ((Griffiths *et al.*, 2006); M. Ueguchi-Tanaka unpublished).

I have shown that gain-of-function mutations, known to prevent gibberellin-dependent degradation of DELLA proteins, also prevented recruitment of SLY1 to RGL1. I included a C-terminal GRAS domain mutation that causes a dominant gibberellin-insensitive phenotype in my analyses. This dwarfing mutation, corresponding to Q272R in RGL1, was originally isolated from a DELLA protein of *Brassica rapa*. (Muangprom *et al.*, 2005). The RGL1 Q272-R point mutation within the C-terminal GRAS domain could disrupt protein-protein interactions through several possible mechanisms. If this residue forms an internal component of the GRAS domain, it could disrupt the entire folding of the DELLA protein. However, the Q272-R mutation is semi-conservative, both residues are of similar size, and although arginine is positively charged, glutamine is a polar residue. Furthermore, this mutation generates a gibberellin-insensitive phenotype (Muangprom *et al.*, 2005). Therefore, in this Q-R mutant the GRAS domain must fold correctly to function as a repressor of gibberellin responses.

The RGL1 Q272-R mutation lies close to the highly conserved VHIID motif that defines the GRAS protein family. However, the glutamine residue in question is not

well conserved. Indeed, several *A. thaliana* GRAS proteins possess arginine residues at this position. Furthermore, in predicted secondary and tertiary structures I have modelled for RGL1, this residue is likely exposed at the surface of the protein.

Of the other *A. thaliana* GRAS proteins, few have been studied. However the GRAS proteins SCARECROW (SCR) and SHORT ROOTS (SHR) have been studied in detail. Similar to the DELLA proteins, SCR and SHR associate with target gene promoters (Cui *et al.*, 2007). However, SCR has been shown to directly interact with SHR, and that this is of biological relevance. SHR function is inhibited by the direct binding of SCR, which sequesters it to the nucleus (Cui *et al.*, 2007). Importantly, the SCR:SHR interaction is mediated through the central region of SCR, including the VHIID and surrounding leucine-rich regions. Therefore, regions within this domain must form an interaction surface. Interestingly, the putative α-helix downstream of the VHIID motif is almost absolutely conserved between SCR, SHR, and the DELLA proteins. However, neither SCR nor SHR have a glutamine residue at the position of RGL1 Q272. Indeed SCR has a histidine, and SHR a glutamic acid. This information supports the hypothesis that the Q272R mutation does not disrupt the C-terminal GRAS domain.

The 17-residue DELLA motif deletion, that removes most of the αA helix, AB loop and αB helix (including DeLLaΦLxYxV), increased interaction of the C-terminal domain with the gain-of-function sly1^{E138K} mutation relative to the wild-type RGL1 in the absence of GID1A/GA_3. However, a deletion that removes most of the downstream GID1A-interacting helix-loop-helix motif (αC helix, CD loop and αD helix, including the conserved TVHYNP motif) abolishes interaction with sly1 ^{E138K}, indicating that this motif may not be engaged in regulation of accessibility to the SLY1 binding site.

To investigate further if the N-terminal DELLA domain mediates regulation of SLY1 recruitment through interactions with the C-terminal domain; I spatially separated the two domains of RGL1 through recombinant in-frame insertion of GFP. This resulted in disruption of the recruitment of SLY1, consistent with the involvement of N-C intramolecular interactions in gibberellin signalling. However, unexpectedly the GID1A/GA_3 dependent recruitment of the gain-of-function sly1^{E138K} mutant was not abolished, only reduced in strength relative to its recruitment by the wild-type RGL1. Although there are several explanations for this result, including mis-folding of the

GRAS domain or formation of putative dimers, this result may be due to the unstructured nature of the N-terminal DELLA domain.

The introduced GFP spacer is predicted to space the DELLA and GRAS domains of RGL1 by approximately 20 Å. However, in an unstructured conformation the N-terminal domain will greatly exceed this distance in length. If only a small region normally interacts with the GRAS domain, this will likely still occur in this fusion protein. Yet, upon GID1A/GA_3 associating with the DELLA domain, this region obtains secondary and tertiary structure, resulting in greatly reduced accessibility to the GRAS domain.

The recruitment of $sly1^{E138K}$, but not SLY1 could be explained by strong binding of $sly1^{E138K}$ to RGL1, reflected by its suppression of $rgl1^{\Delta DELLA}$ mutant. It is plausible that a region of the DELLA motif binds near the SLY1 binding site, regulating its conformation, forming three states of the SLY1 binding site: 1) DELLA motif actively repressing the SLY1 binding site; 2) DELLA motif unbound, SLY1 binding site in a partially open state (accessible to $sly1^{E138K}$); 3) GID1A/GA_4:DELLA complex bound, actively opening the SLY1 binding site. It is also possible that these states are formed in *trans* through head-to-tail dimerisation of RGL1.

Based on the data I have presented, I propose a model for operation of the DELLA protein switch, through transition between "closed" and "open" states. (Figure 6.1). In this model the N-terminal domain of RGL1 exists in a primarily unstructured state, except a small region of the DELLA motif (Asp/Glu/Leu/Leu) bound near the SLY1 binding site of the GRAS domain, forming the "closed" state. The "closed" state of RGL1 is able to bind to GID1A/GA_4, whilst the C-terminal domain of RGL1 is in a conformation where the SLY1 binding site is unavailable. On interaction of GID1A/GA_4 with the "closed" state, the N-terminal domain of RGL1 undergoes a major conformational change which in turn induces changes in the C-terminal domain, exposing the SLY1 binding site.

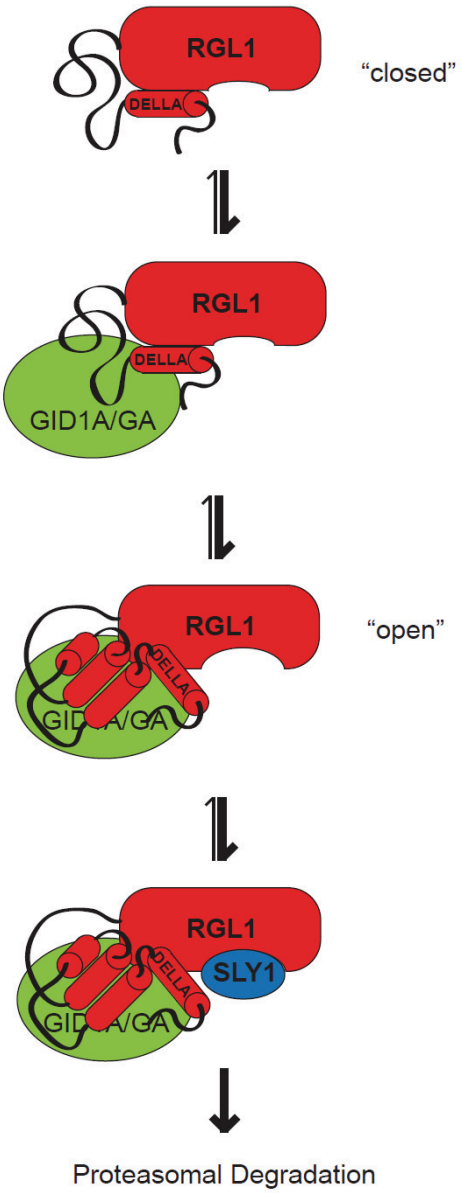

Figure 6.1. Proposed model of gibberellin-dependent recruitment of SLY1 to RGL1. RGL1 exists in a "closed" state where a region of the DELLA motif in the N-terminal domain is bound near the SLY1 binding site of the C-terminal GRAS domain. Upon binding bioactive gibberellin GID1A can bind to the primarily unstructured N-terminal domain. This induces the acquisition of secondary and tertiary structure of the N-terminal domain, including changes to the GRAS domain bound portion. This event in turn translates to structural changes in the GRAS domain, opening the SLY1 binding site, forming an "open" state.

In my *in vitro* interaction experiments, I observed the conformational changes within the N-terminal domain of RGL1 upon interaction with GID1A/GA_4 (Figure 6.1). These conformational changes are likely the trigger that induces “opening” of the C-terminal domain to expose the SLY1 binding site. In the "closed" state a region of the N-terminal domain of RGL1 is bound near to the SLY1 binding site, inducing a fully closed conformation, in which the DELLA motif plays the key role. The unstructured character of the N-terminal domain likely facilitates the conformational changes required to induce shifts in the conformational state of the SLY1 binding site.

In support of this model, the interaction of GID1-family gibberellin receptors with the DELLA proteins has been shown to overcome their inhibition of gibberellin-responses (Ariizumi *et al.*, 2008; Ueguchi-Tanaka *et al.*, 2008). In rice and *A. thaliana* backgrounds lacking functional F-box proteins (*gid2-1* and *sly1-10*), overexpression of GID1-family receptors rescued normal plant phenotypes (Ariizumi *et al.*, 2008; Ueguchi-Tanaka *et al.*, 2007). Thus, in the absence of DELLA protein degradation, the binding of liganded gibberellin receptors must alter the conformation of DELLA proteins in such a way as to prevent the C-terminal GRAS domain from interacting with transcription factors.

Similar inter-domain interactions have been reported for other proteins. The Na/proton exchanger NHERF1 consists of two functional PDZ domains and a C-terminal Ezrin binding motif (Cheng *et al.*, 2009). Nuclear magnetic resonance (NMR) analysis of the structure of this protein revealed that the Ezrin binding motif forms an α-helix that directly interacts with the second PDZ domain, thus mediating an inter-domain interaction. This interaction blocks the function of the protein, facilitating a self-regulatory function. Upon binding of Ezrin to the C-terminal motif, the PDZ domain is free to function. This describes a similar mechanism to that I have proposed for RGL1, where a mobile region within the protein has a dual binding function. The intramolecular interaction blocks an active or binding site on another domain of the protein, whereas interaction of the same domain with another signalling protein, releases the blocked site and allows its binding to the signalling targets.

The phosphorylation of DELLA proteins has been implicated in targeting these proteins for degradation (Fu *et al.*, 2004; Gomi *et al.*, 2004). The yeast three-hybrid results I

have shown here do not investigate any requirement of phosphorylation of RGL1 for SLY1 to interact, given that GID1A, RGL1 and SLY1 are not predicted to function as protein kinases. The DELLA proteins SLR1 and GAI extracted from tissue of rice and *A. thaliana*, respectively, have been shown to only interact with GST- fusions of the F-box proteins GID2 or SLY1 when phosphorylated, suggesting the involvement of a kinase (Fu *et al.*, 2004; Gomi *et al.*, 2004). It is possible that phosphorylation, or indeed other post-translational modifications, may alter the accessibility of the SLY1 binding site independently or cooperatively with GID1A. Alternatively, phosphorylation of particular residues may be able to induce a similar conformational change in DELLA proteins as I have proposed for the interaction of GID1A/GA_4 with the N- terminal domain of RGL1, but in response to other plant signalling molecules.

In summary, my analysis of GID1A/GA_4:RGL1:SLY1 interactions by yeast two/three hybrid system and interaction kinetics modelled from *in vitro* interactions are consistent with induction of a series of conformational changes within the N-terminal domain of RGL1. These changes are likely translated to the C-terminal domain conformational changes through intramolecular N-C interactions within RGL1, unmasking the SLY1 binding interface. I have also shown, using competition assays with monoclonal antibodies and intact N-terminal domain of DELLA protein RGL1, that the contacts mediated by AB loop and CD loop within the DELLA and TVHYNP motifs of RGL1 are essential for interaction with GID1A-C, whereas the contacts mediated by αA helix (Asp/Glu/Leu/Leu) within the DELLA motif are not.

6.5 Novel RGL1-interacting proteins

The thioglucoside glucohydrolase TGG2 I isolated through affinity-purification of RGL1 interacting proteins is one of two functionally redundant myrosinases involved in the breakdown of glucosinolates into toxic isothiocyanates (Barth and Jander, 2006). Neither TGG2, nor the highly similar TGG1 have yet been implicated in gibberellin signalling. Only recently have TGG1 and TGG2 been shown to function in ABA mediated stomatal closure, acting upstream of calcium efflux from the endoplasmic

reticulum (Islam *et al.*, 2009). TGG1 is highly expressed within guard cells, constituting up to 15 % of the total cell protein content and present within the proteomes of most cellular organelles (Zhao *et al.*, 2008). However, the myrosinase that I isolated as interacting with RGL1, TGG2, has not been detected as expressed within guard cells. Despite the vastly different expression levels, both TGG1 and TGG2 function redundantly in the regulation of stomatal opening (Islam *et al.*, 2009). Therefore, the site of myrosinase involvement in ABA signalling must localised to the site of any TGG2, and only a potion of the highly abundant TGG1.

Myrosinases have been shown to bind to several proteins known as myrosinase-binding proteins. These interacting partners normally function to either modify the enzymatic activity of the myrosinase, or to trigger aggregation for the formation of myrosin bodies in myrosin cells (Eriksson *et al.*, 2002; Lambrix *et al.*, 2001). Importantly, myrosinase-binding proteins have been found within *A. thaliana* nuclear proteome (Bae *et al.*, 2003). The presence of these proteins in the nuclear fraction implies that the myrosinases, including TGG1 and TGG2, could in part be nuclear localised. Therefore, it is possible that a portion of the protein is localised to the nucleus; able to interact with RGL1 and possibly other DELLA proteins. However, the exact role of TGG2 in phytohormone signalling is as yet unclear.

The phenotype of *tgg1-1*, *tgg2-1* double deletion mutants has been reported to be indistinguishable from wild-type (Barth and Jander, 2006). However, the responses of these plants to phytohormones have not yet been studied. Furthermore, a deletion mutant of the SNARE transport protein VACUOLAR MORPHOLOGY-3 (VAM3), specifically accumulates large amounts of both TGG1 and TGG2 (Ueda *et al.*, 2006). This mutant interestingly has a semi-dwarf phenotype with short internodes, though this may be due to aberrant accumulation of auxin in leaf tissues (Shirakawa *et al.*, 2009). Therefore, further experimentation is required to confirm the interaction between TGG2 and RGL1, and to establish a biological role.

The germin-like-protein, GLP1, was also isolated as a novel RGL1-interacting protein. Little is known of the functions of the germin-like-proteins, a sub-family of the germin class seed storage proteins and oxalate oxidase enzymes (Membre *et al.*, 2000). Although germin-like-proteins are predicted to be exported out of the cytoplasm, both

GLP3 and GLP5 have been detected within the *A. thaliana* nuclear proteome (Bae *et al.*, 2003). Germin-like-proteins have been implicated in hormone signalling, based on direct binding of phytohormones, but may also have many other roles within the plant cell (Membre *et al.*, 2000). Indeed several germin-like-proteins similar to GLP1, including peach auxin-binding-proteins 19 and 20, have been shown to bind auxins (Ohmiya *et al.*, 1998). However, a role in auxin signalling has not yet been established. If GLP1 is indeed an auxin binding protein, allowing it to interact with DELLA proteins, it may form an integral part of a pathway for auxin-induced DELLA protein sensitisation to degradation (Fu and Harberd, 2003).

The germin-like-proteins have also been identified in a gibberellin-binding fraction of plant proteins (Park *et al.*, 2005). Therefore, I investigated the requirement for both gibberellins and auxins upon the putative GLP1:RGL1 interaction. Neither the presence of the gibberellin GA_3, nor the auxin IAA, induced an interaction between GLP1 and RGL1 in a yeast two-hybrid system. It is highly likely that auxins are unable to enter yeast cells efficiently, as auxin transport requires an active transporter *in planta* (Baluska *et al.*, 2003). Furthermore, there have been no reports of an auxin-dependent interaction occurring in a yeast two-hybrid system to date.

Alternatively, correct *in planta* post-translational modifications of GLP1 may be necessary for an interaction to occur. Endogenous GLP1 extracted from the extracellular matrix has been shown to be *N*-glycosylated (Membre *et al.*, 1997; Membre *et al.*, 2000). Although the GLP1 I isolated was present in nuclear extract, the mass spectrometry fingerprinting data revealed that it had been processed for secretion, and so may be similarly glycosylated. Therefore, further confirmation of this interaction may need to be performed in *in planta* systems, such as a split-YFP interaction assay.

Conclusion and future directions

The purpose of this research was to increase understanding of how the DELLA plant regulatory proteins function. The first aim was to characterise the mechanism by which the GID1-family gibberellin receptors induce the recruitment of F-box class proteins to the DELLA protein, thus describing a mechanism for gibberellin-induced DELLA protein degradation. The second aim was to identify novel components that interact with the DELLA protein RGL1 that may be involved with its regulation and functions.

A procedure was developed for the extraction of endogenous DELLA proteins as part of this study. Furthermore, these extracts have been used to characterise a suite of anti-DELLA antibodies for endogenous DELLA proteins, and in doing so has shown that at least four of the five DELLA proteins are present in this tissue. This procedure was developed with the intent of immunoprecipitation of endogenous DELLA proteins, and will be suitable for such experiments. These may be used to study the post-translational modifications of endogenous DELLA proteins through mass spectrometry analysis. Alternatively, DELLA-containing complexes may be isolated and associated proteins identified. Furthermore, associated chromosomal fragments can be isolated through chromatin-immunoprecipitation, allowing the identification of targeted genetic elements.

Using both *in vitro* and *in vivo* techniques, this study has demonstrated that regions of both the conserved DELLA and TVHYNP motifs within the N-terminal domain of RGL1 are essential for an interaction with gibberellin-liganded GID1A to occur. Furthermore, antibody-mediated competition experiments revealed that the Asp/Glu/Leu/Leu residues of RGL1 are not essential for interaction with GID1A/GA_4.

This study also shows that the N-terminal domain of RGL1 is essentially unstructured in the absence of interacting partners. Furthermore, the kinetics of the interaction between this domain and GID1A/GA_4 *in vitro* were characterised by surface plasmon resonance. Kinetic data fitted to complex interaction models was consistent with a two-state conformational change model. This implies that the N-terminal domain of RGL1

undergoes conformational changes upon contact to GID1A/GA_4. The calculated kinetic constant, K, of 5.3 x 10^8 M^{-1} reflects a strong interaction.

This study has also demonstrated that the interaction of gibberellin-bound GID1A with the N-terminal domain of RGL1 is sufficient for induction of SLY1 binding in a yeast three-hybrid system. This data describes a nuclear-localised four-component switch for the perception of gibberellins. By incorporating DELLA gain-of-function mutations and spatial separation of the DELLA and GRAS domains into a yeast three-hybrid system, this study has shown that the N- and C- terminal domains of RGL1 likely interact. Based on these observations, a conformational change mediated mechanism is proposed by which the gibberellin receptor GID1A induces conformational changes within the DELLA motif, which in turn induce the opening of the SLY1 binding site. This mechanism could be regulated through post-translational modifications that control conformational changes within RGL1.

The proposed interaction between the N- and C- domains of RGL1 needs to be confirmed. This could be achieved by several methods. Residue replacement strategies may reveal exactly which residues or motifs are involved. This approach may also yield valuable information on mutations with potential for altered sensitivity to gibberellin-induced degradation. In particular, investigation of the effects of the DELL-DELH on the binding of GID1A/GA should reveal if this motif indeed has roles in inter-domain interactions. Furthermore, expression of the spatially separated domains of RGL1 in plant can be used to confirm the functionality of the protein as a repressor and its insensitivity to gibberellin-induced degradation. Techniques requiring recombinant protein are currently not possible due to insolubility of the full-length and C-terminal domains of DELLA proteins.

Using an affinity purification procedure developed as part of my Masters thesis, I isolated two novel RGL1-interacting proteins. These two proteins were identified to be GERMIN-LIKE-PROTEIN-1 (GLP1) and THIOGLUCOSIDE GLUCOHYDROLASE-2 (TGG2). Neither protein has yet been implicated in gibberellin signalling. Therefore, further confirmation of the interaction between these two proteins and RGL1 is required. If they do indeed interact, the biological relevance will also need to be determined.

Appendix A

Supporting kinetic analysis

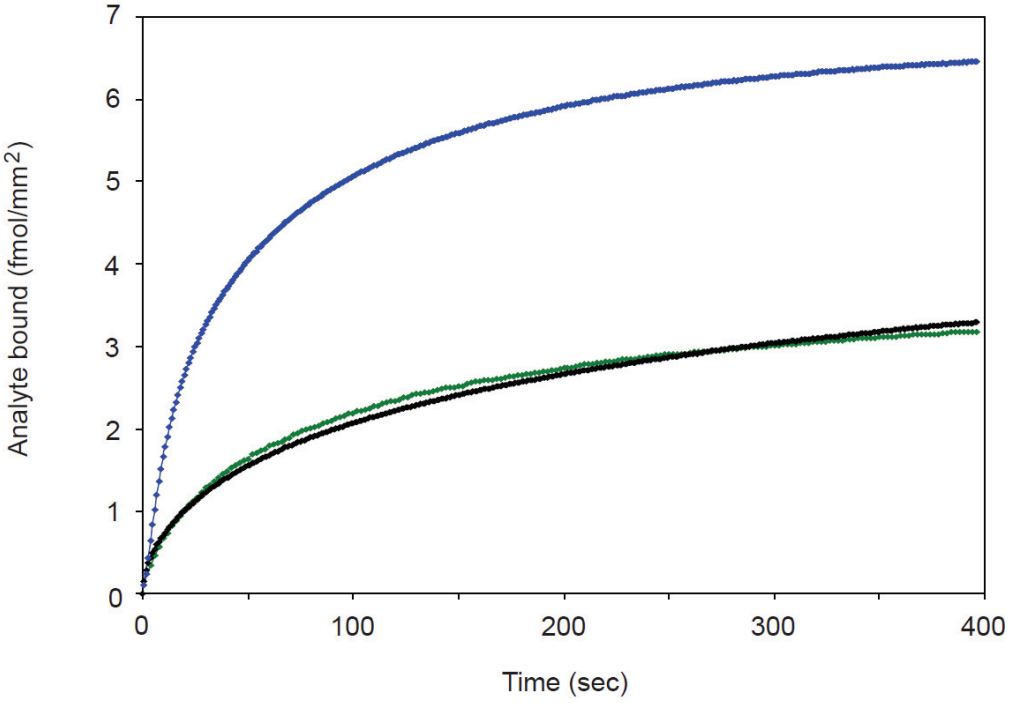

Figure A.1. Immobilised RGL1 N-terminal domain binding capacity.
Association of recombinant GID1A (green) or monoclonal antibodies BC9 (black) and AB8 (blue) with an immobilised N-terminal DELLA domain of RGL1 (residues 1-137). The bound mass from a continuous flow of 1600 nM GID1A or 500 nM BC9/AB8 during association (0-400 sec) was monitored by surface plasmon resonance. The interaction of GID1A was performed in the presence of 5 µM GA_4, incubated with GID1A for 30 min prior to the binding assay. The amount of GID1A, BC9 and AB8 bound is shown in fmol bound per mm^2 of surface area.

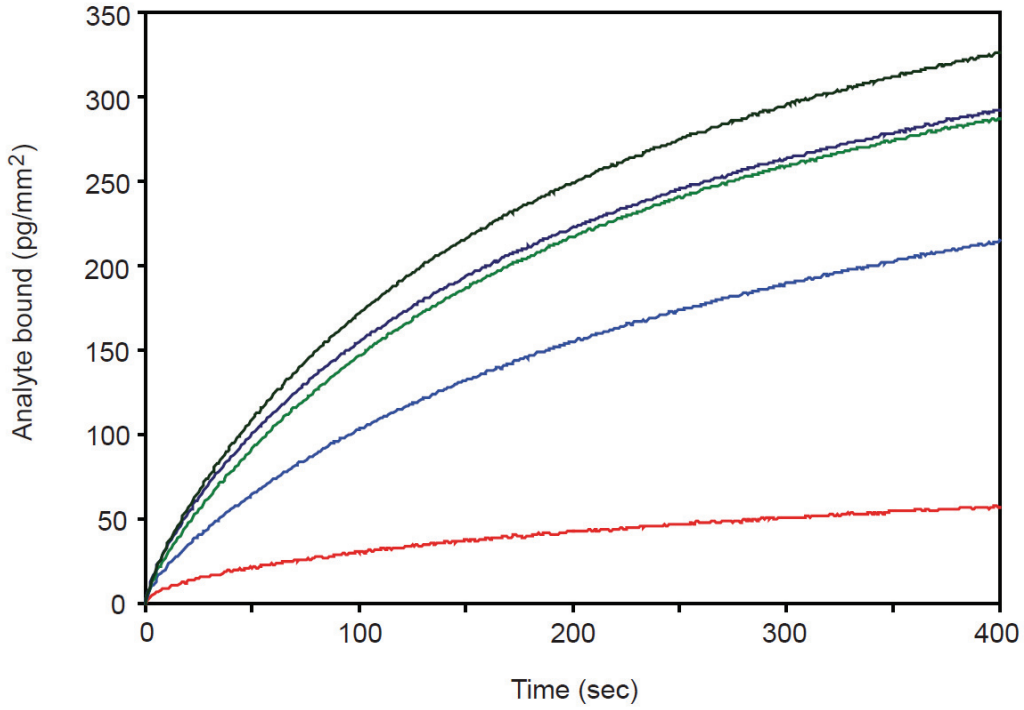

Figure A.2. Gibberellin saturation of GID1A. Association of recombinant GID1A with an immobilised N-terminal DELLA domain of RGL1 (residues 1-137). The bound mass from a continuous flow of 200 nM GID1A during association (0-400 sec) was monitored by surface plasmon resonance. Interactions were performed in the presence of either 5/100 µM GA_3 (blue/dark blue), 5/100 µM GA_4 (green/dark green), or no gibberellin (red). Gibberellins were incubated with GID1A for 30 min prior to the binding assays. The mass of GID1A is shown in pg bound per mm^2 of surface area.

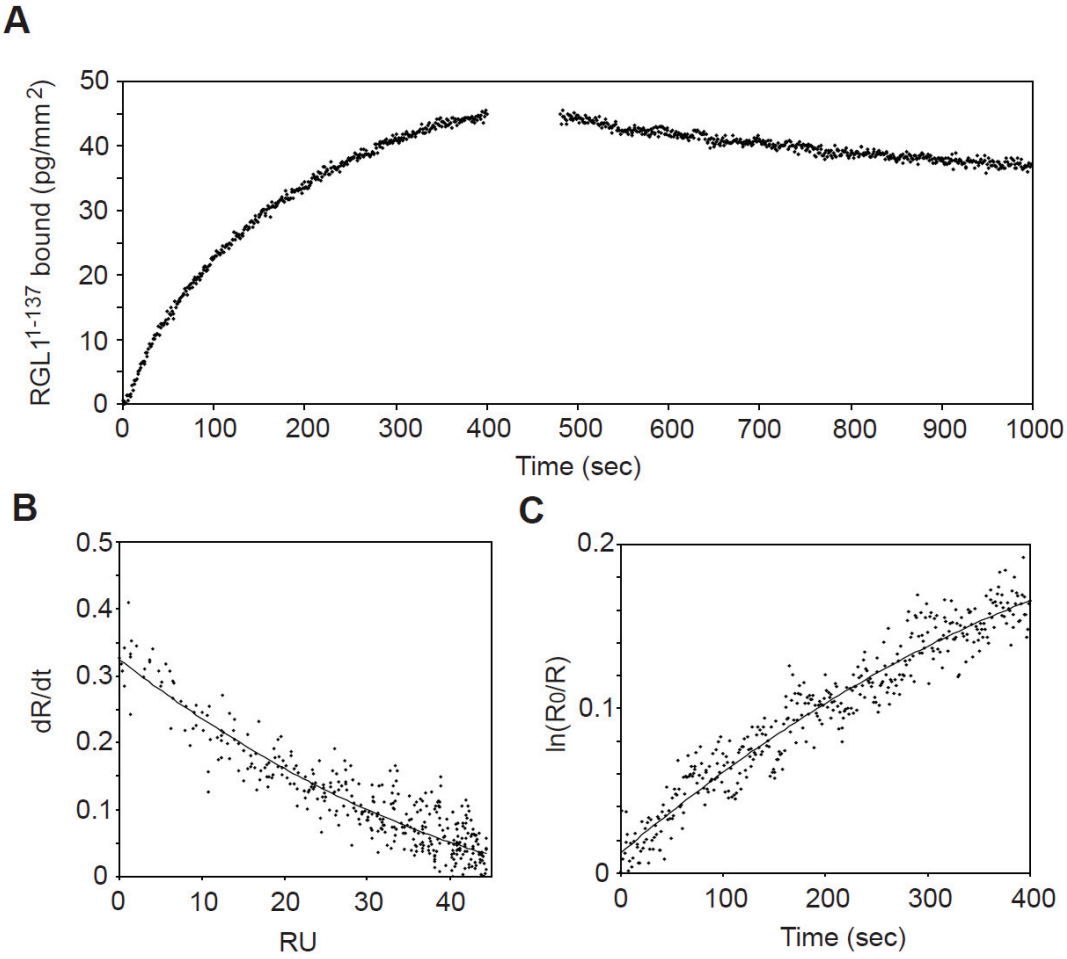

Figure A.3. Gibberellin-dependent binding of RGL1$^{1-137}$ to immobilised GID1A. **A.** Binding of purified recombinant RGL1$^{1-137}$ from a 1 µM solution to immobilised MBP-GID1A in the presence of gibberellin GA_4. Association 0-420 sec, dissociation 420-1000 sec. RGL1$^{1-137}$ prepared by rTEV protease cleavage form MBP- fusion and subsequent anion exchange chromatography. Dissociation of immobilised MBP-GID1A subtracted (approximately -15 pg/mm^2 at 400 sec, -28 pg/mm^2 at 1000 sec). 5 µM Gibberellin present in all solutions and running buffers. **B.** dR/dt *vs* R linearisation (Scatchard plot) of the association phase. **C.** ln(R0/R) *vs* time linearisation of the dissociation phase.

Appendix B

DELLA protein alignments

The full-length sequences for DELLA proteins from a range of plant species were aligned using AlignX (Vector NTI software, Invitrogen, California, USA). Absolutely conserved residues are highlighted in orange; highly conserved in blue; highly similar residues in green, and similar residues in yellow. The RGL1 gain-of-function mutants used in this thesis are displayed. The sequences of several DELLA gain-of function mutations are also displayed, indicating in-frame deletions or amino acid replacements. The *A. thaliana gai-1*, $rga^{\Delta 17}$; grape *gai-1*; rice $slr1^{\Delta DELLA}$, $slr1^{\Delta SPACE}$, $slr1^{\Delta TVHYNP}$, $slr1^{\Delta S/T/V}$; barley *sln1-d*; wheat *rht*, *rht-B1b*, *rht-D1b*; and maize *d8-MP*, have been previously described as semi-dominant gibberellin-insensitive mutations (Boss and Thomas, 2002; Chandler *et al.*, 2002; Itoh *et al.*, 2002; Peng *et al.*, 1997; Peng *et al.*, 1999; Weston *et al.*, 2008)

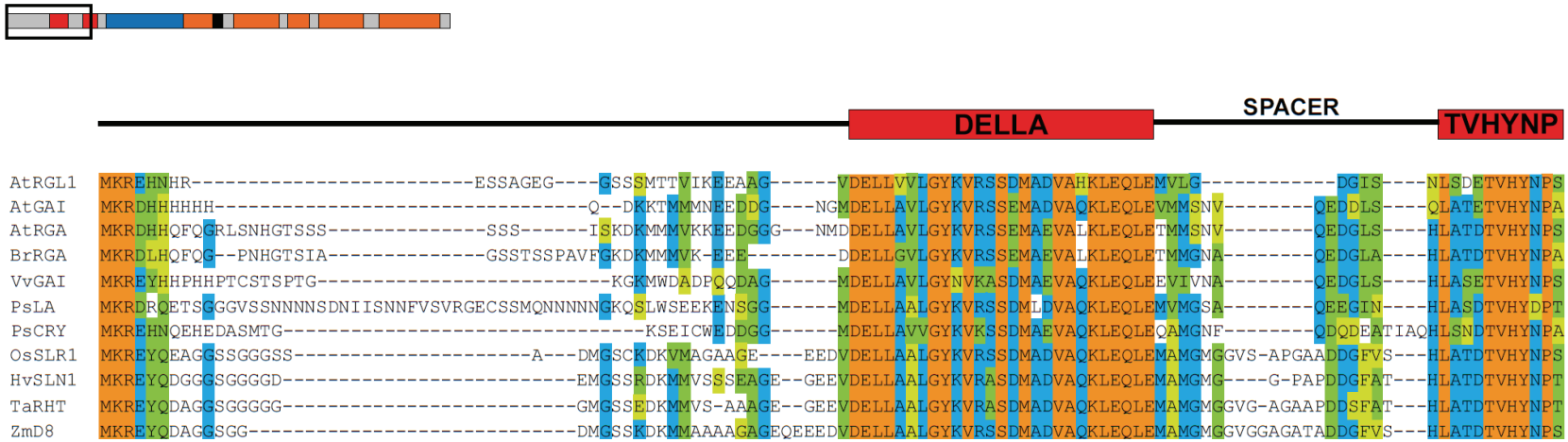
DELLA
SPACER
TVHYNP
AtRGL1
AtGAI
AtRGA
BrRGA
VvGAI
PsLA
PsCRY
OsSLR1
HvSLN1
TaRHT
ZmD8

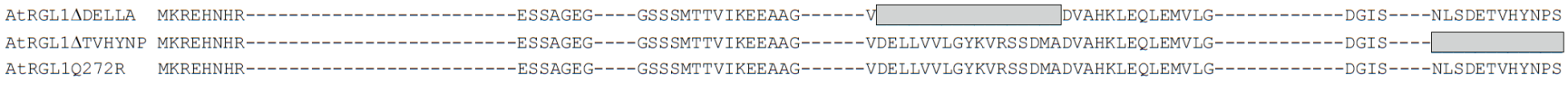
AtRGL1ΔDELLA
AtRGL1ΔTVHYNP
AtRGL1Q272R

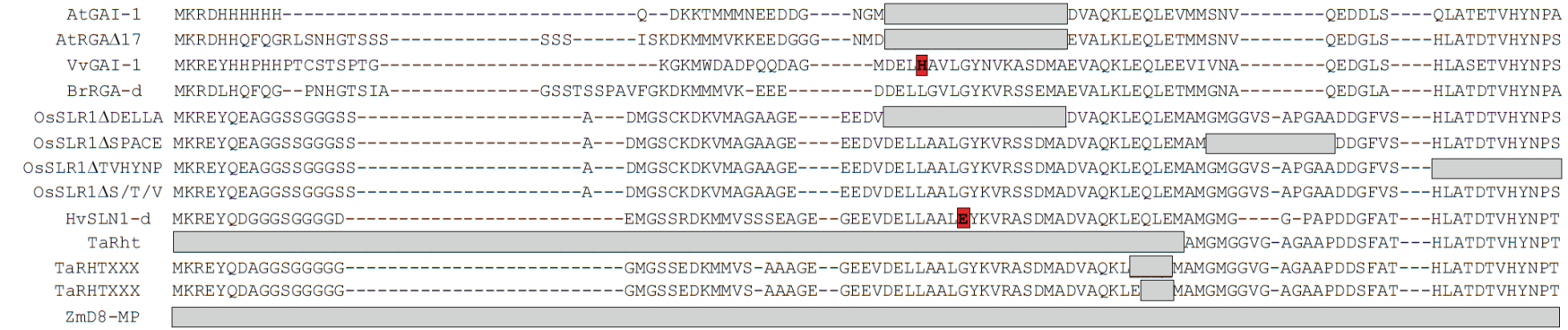
AtGAI-1
AtRGAΔ17
VvGAI-1
BrRGA-d
OsSLR1ΔDELLA
OsSLR1ΔSPACE
OsSLR1ΔTVHYNP
OsSLR1ΔS/T/V
HvSLN1-d
TaRht
TaRHTXXX
TaRHTXXX
ZmD8-MP

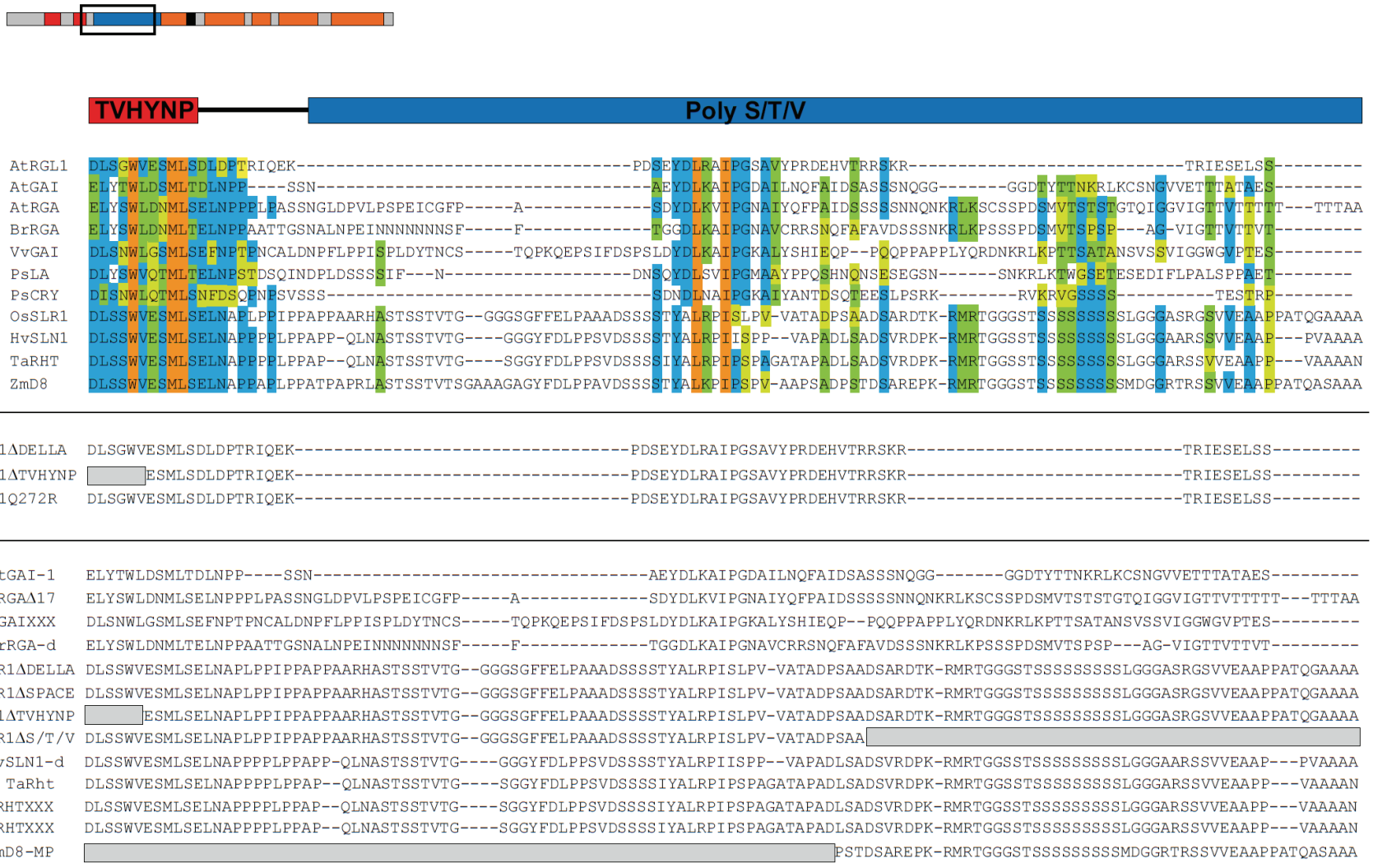
TVHYNP
Poly S/T/V
AtRGL1
AtGAI
AtRGA
BrRGA
VvGAI
PsLA
PsCRY
OsSLR1
HvSLN1
TaRHT
ZmD8
AtRGL1ΔDELLA
AtRGL1ΔTVHYNP
AtRGL1Q272R
AtGAI-1
AtRGAΔ17
VvGAIXXX
BrRGA-d
OsSLR1ΔDELLA
OsSLR1ΔSPACE
OsSLR1ΔTVHYNP
OsSLR1ΔS/T/V
HvSLN1-d
TaRht
TaRHTXXX
TaRHTXXX
ZmD8-MP

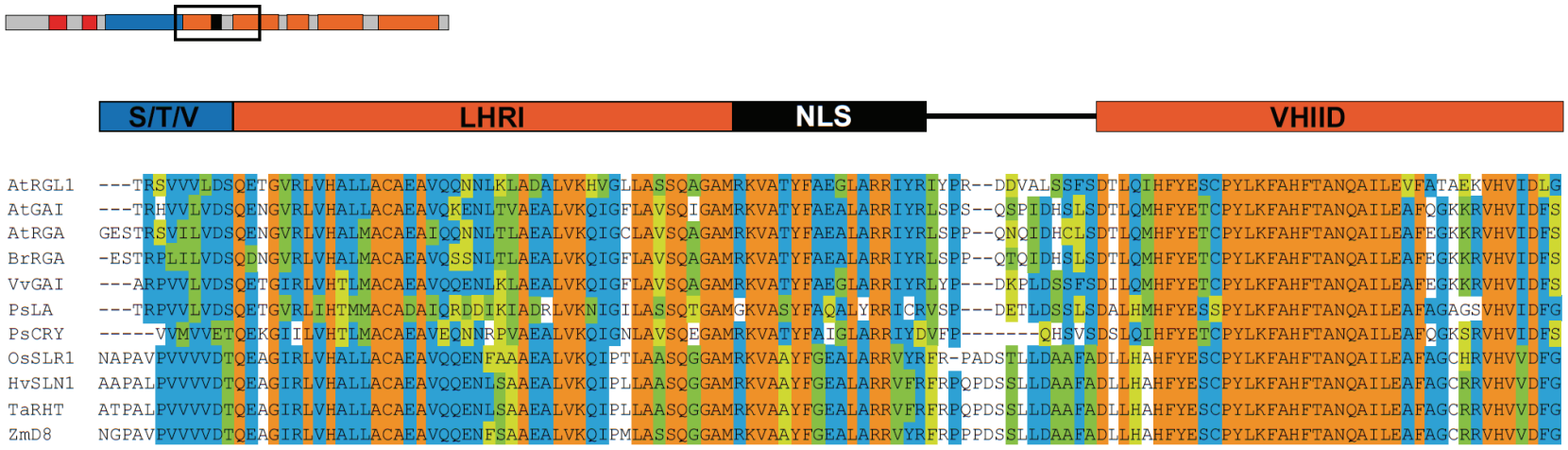


```
AtRGL1ΔDELLA  ---TRSVVVLDSQETGVRLVHALLACAEAVQQNNLKLADALVKHVGLLASSQAGAMRKVATYFAEGLARRIYRIYPR--DDVALSSFSDTLQIHFYESCPYLKFAHFTANQAILEVFATAEKVHVIDLG
AtRGL1ΔTVHYNP ---TRSVVVLDSQETGVRLVHALLACAEAVQQNNLKLADALVKHVGLLASSQAGAMRKVATYFAEGLARRIYRIYPR--DDVALSSFSDTLQIHFYESCPYLKFAHFTANQAILEVFATAEKVHVIDLG
AtRGL1Q272R   ---TRSVVVLDSQETGVRLVHALLACAEAVQQNNLKLADALVKHVGLLASSQAGAMRKVATYFAEGLARRIYRIYPR--DDVALSSFSDTLQIHFYESCPYLKFAHFTANQAILEVFATAEKVHVIDLG
```

```
AtGAI-1       ---TRHVVLVDSQENGVRLVHALLACAEAVQKENLTVAEALVKQIGFLAVSQIGAMRKVATYFAEALARRIYRLSPS--QSPIDHSLSDTLQMHFYETCPYLKFAHFTANQAILEAFQGKKRVHVIDFS
AtRGAΔ17      GESTRSVILVDSQENGVRLVHALMACAEAIQQNNLTLAEALVKQIGCLAVSQAGAMRKVATYFAEALARRIYRLSPP--QNQIDHCLSDTLQMHFYETCPYLKFAHFTANQAILEAFEGKKRVHVIDFS
VvGAIXXX      ---ARPVVLVDSQETGIRLVHTLMACAEAVQQENLKLAEALVKQIGFLAVSQAGAMRKVATYFAEGLARRIYRLYP---DKPLDSSFSDILQMHFYETCPYLKFAHFTANQAILEAFEGKKRVHVIDFS
BrRGA-d       -ESTRPLILVDSQDNGVRLVHALMACAEAVQSSNLTLAEALVKQIGFLAVSQAGAMRKVATYFAEALARRIYRLSPP--QTQIDHSLSDTLQMHFYETCPYLKFAHFTANQAILEAFEGKKRVHVIDFS
OsSLR1ΔDELLA NAPAVPVVVVDTQEAGIRLVHALLACAEAVQQENFAAAEALVKQIPTLAASQGGAMRKVAAYFGEALARRVYRFR-PADSTLLDAAFADLLHAHFYESCPYLKFAHFTANQAILEAFAGCHRVHVVDFG
OsSLR1ΔSPACE NAPAVPVVVVDTQEAGIRLVHALLACAEAVQQENFAAAEALVKQIPTLAASQGGAMRKVAAYFGEALARRVYRFR-PADSTLLDAAFADLLHAHFYESCPYLKFAHFTANQAILEAFAGCHRVHVVDFG
OsSLR1ΔTVHYNP NAPAVPVVVVDTQEAGIRLVHALLACAEAVQQENFAAAEALVKQIPTLAASQGGAMRKVAAYFGEALARRVYRFR-PADSTLLDAAFADLLHAHFYESCPYLKFAHFTANQAILEAFAGCHRVHVVDFG
OsSLR1ΔS/T/V [gap]LLACAEAVQQENFAAAEALVKQIPTLAASQGGAMRKVAAYFGEALARRVYRFR-PADSTLLDAAFADLLHAHFYESCPYLKFAHFTANQAILEAFAGCHRVHVVDFG
HvSLN1-d      AAPALPVVVVDTQEAGIRLVHALLACAEAVQQENLSAAEALVKQIPLLAASQGGAMRKVAAYFGEALARRVFRFRPQPDSSLLDAAFADLLHAHFYESCPYLKFAHFTANQAILEAFAGCRRVHVVDFG
TaRht         ATPALPVVVVDTQEAGIRLVHALLACAEAVQQENLSAAEALVKQIPLLAASQGGAMRKVAAYFGEALARRVFRFRPQPDSSLLDAAFADLLHAHFYESCPYLKFAHFTANQAILEAFAGCRRVHVVDFG
TaRHTXXX      ATPALPVVVVDTQEAGIRLVHALLACAEAVQQENLSAAEALVKQIPLLAASQGGAMRKVAAYFGEALARRVFRFRPQPDSSLLDAAFADLLHAHFYESCPYLKFAHFTANQAILEAFAGCRRVHVVDFG
TaRHTXXX      ATPALPVVVVDTQEAGIRLVHALLACAEAVQQENLSAAEALVKQIPLLAASQGGAMRKVAAYFGEALARRVFRFRPQPDSSLLDAAFADLLHAHFYESCPYLKFAHFTANQAILEAFAGCRRVHVVDFG
ZmD8-MP       NGPAVPVVVVDTQEAGIRLVHALLACAEAVQQENFSAAEALVKQIPMLASSQGGAMRKVAAYFGEALARRVYRFRPPPDSSLLDAAFADLLHAHFYESCPYLKFAHFTANQAILEAFAGCRRVHVVDFG
```

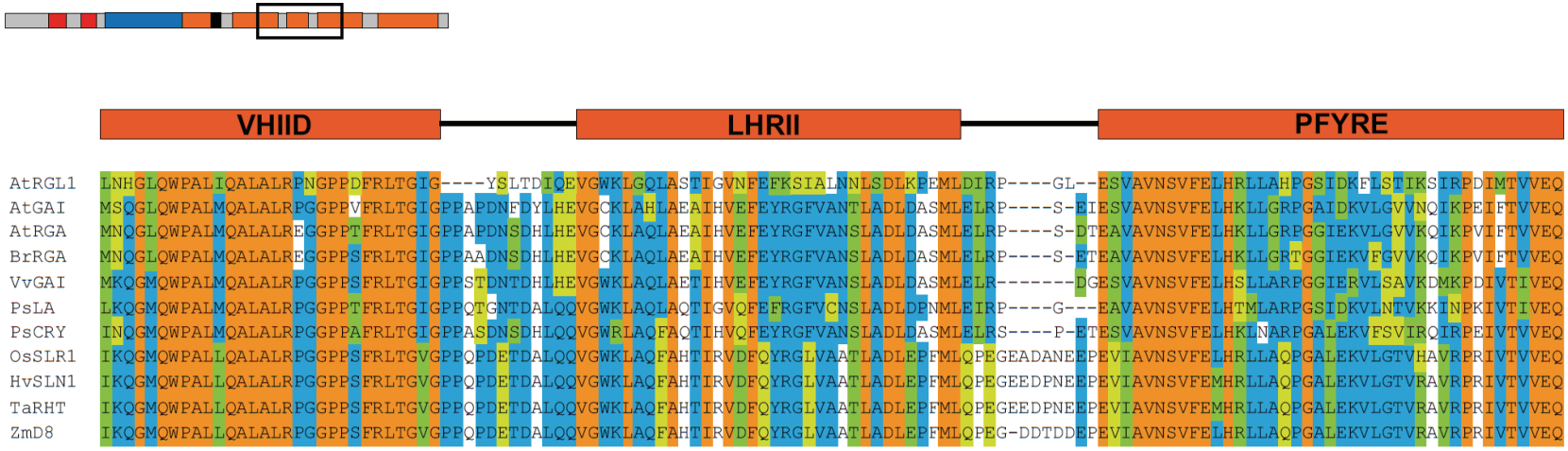

AtRGL1ΔDELLA LNHGLQWPALIQALALRPNGPPDFRLTGIG----YSLTDIQEVGWKLGQLASTIGVNFEFKSIALNNLSDLKPEMLDIRP----GL--ESVAVNSVFELHRLLAHPGSIDKFLSTIKSIRPDIMTVVEQ

AtRGL1ΔTVHYNP LNHGLQWPALIQALALRPNGPPDFRLTGIG----YSLTDIQEVGWKLGQLASTIGVNFEFKSIALNNLSDLKPEMLDIRP----GL--ESVAVNSVFELHRLLAHPGSIDKFLSTIKSIRPDIMTVVEQ

AtRGL1Q272R LNHGLQWPALIRALALRPNGPPDFRLTGIG----YSLTDIQEVGWKLGQLASTIGVNFEFKSIALNNLSDLKPEMLDIRP----GL--ESVAVNSVFELHRLLAHPGSIDKFLSTIKSIRPDIMTVVEQ

AtGAI-1 MSQGLQWPALMQALALRPGGPPVFRLTGIGPPAPDNFDYLHEVGCKLAHLAEAIHVEFEYRGFVANTLADLDASMLELRP----S-EIESVAVNSVFELHKLLGRPGAIDKVLGVVNQIKPEIFTVVEQ

AtRGAΔ17 MNQGLQWPALMQALALREGGPPTFRLTGIGPPAPDNSDHLHEVGCKLAQLAEAIHVEFEYRGFVANSLADLDASMLELRP----S-DTEAVAVNSVFELHKLLGRPGGIEKVLGVVKQIKPVIFTVVEQ

VvGAIXXX MKQGMQWPALMQALALRPGGPPSFRLTGIGPPSTDNTDHLHEVGWKLAQLAETIHVEFEYRGFVANSLADLDASMLELR-------DGESVAVNSVFELHSLLARPGGIERVLSAVKDMKPDIVTIVEQ

BrRGA-d MNQGLQWPALMRALALREGGPPSFRLTGIGPPAADNSDHLHEVGCKLAQLAEAIHVEFEYRGFVANSLADLDASMLELRP----S-ETEAVAVNSVFELHKLLGRTGGIEKVFGVVKQIKPVIFTVVEQ

OsSLR1ΔDELLA IKQGMQWPALLQALALRPGGPPSFRLTGVGPPQPDETDALQQVGWKLAQFAHTIRVDFQYRGLVAATLADLEPFMLQPEGEADANEEPEVIAVNSVFELHRLLAQPGALEKVLGTVHAVRPRIVTVVEQ

OsSLR1ΔSPACE IKQGMQWPALLQALALRPGGPPSFRLTGVGPPQPDETDALQQVGWKLAQFAHTIRVDFQYRGLVAATLADLEPFMLQPEGEADANEEPEVIAVNSVFELHRLLAQPGALEKVLGTVHAVRPRIVTVVEQ

OsSLR1ΔTVHYNP IKQGMQWPALLQALALRPGGPPSFRLTGVGPPQPDETDALQQVGWKLAQFAHTIRVDFQYRGLVAATLADLEPFMLQPEGEADANEEPEVIAVNSVFELHRLLAQPGALEKVLGTVHAVRPRIVTVVEQ

OsSLR1ΔS/T/V IKQGMQWPALLQALALRPGGPPSFRLTGVGPPQPDETDALQQVGWKLAQFAHTIRVDFQYRGLVAATLADLEPFMLQPEGEADANEEPEVIAVNSVFELHRLLAQPGALEKVLGTVHAVRPRIVTVVEQ

HvSLN1-d IKQGMQWPALLQALALRPGGPPSFRLTGVGPPQPDETDALQQVGWKLAQFAHTIRVDFQYRGLVAATLADLEPFMLQPEGEEDPNEEPEVIAVNSVFEMHRLLAQPGALEKVLGTVRAVRPRIVTVVEQ

TaRht IKQGMQWPALLQALALRPGGPPSFRLTGVGPPQPDETDALQQVGWKLAQFAHTIRVDFQYRGLVAATLADLEPFMLQPEGEEDPNEEPEVIAVNSVFEMHRLLAQPGALEKVLGTVRAVRPRIVTVVEQ

TaRHTXXX IKQGMQWPALLQALALRPGGPPSFRLTGVGPPQPDETDALQQVGWKLAQFAHTIRVDFQYRGLVAATLADLEPFMLQPEGEEDPNEEPEVIAVNSVFEMHRLLAQPGALEKVLGTVRAVRPRIVTVVEQ

TaRHTXXX IKQGMQWPALLQALALRPGGPPSFRLTGVGPPQPDETDALQQVGWKLAQFAHTIRVDFQYRGLVAATLADLEPFMLQPEGEEDPNEEPEVIAVNSVFEMHRLLAQPGALEKVLGTVRAVRPRIVTVVEQ

ZmD8-MP IKQGMQWPALLQALALRPGGPPSFRLTGVGPPQPDETDALQQVGWKLAQFAHTIRVDFQYRGLVAATLADLEPFMLQPEG-DDTDDEPEVIAVNSVFELHRLLAQPGALEKVLGTVRAVRPRIVTVVEQ

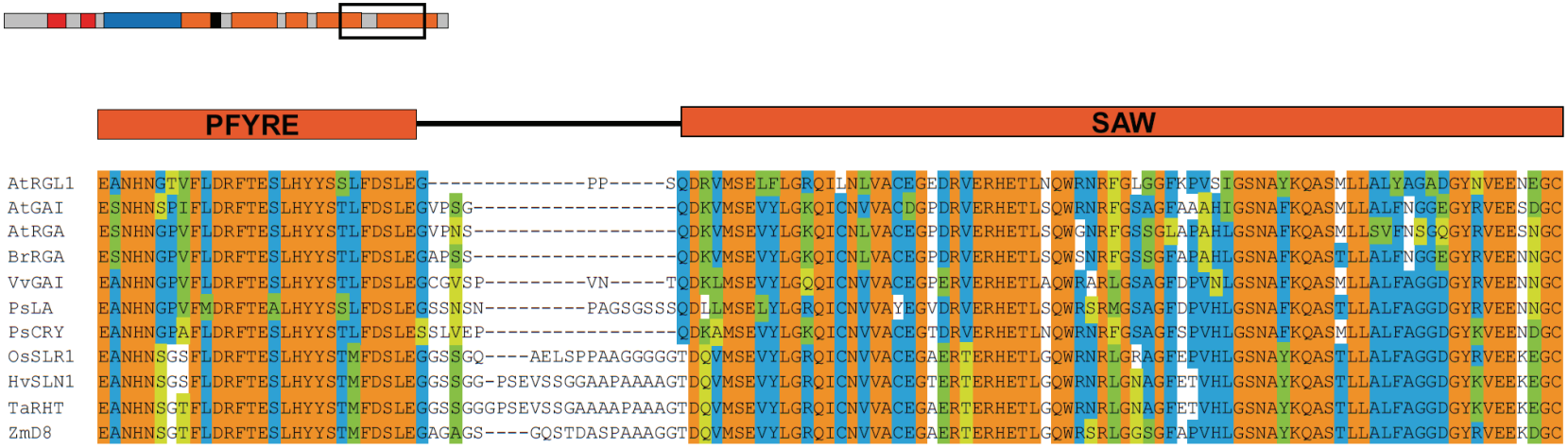
PFYRE
SAW
AtRGL1 EANHNGTVFLDRFTESLHYYSSLFDSLEG----------PP-----SQDRVMSELFLGRQILNLVACEGEDRVERHETLNQWRNRFGLGGFKPVSIGSNAYKQASMLLALYAGADGYNVEENEGC
AtGAI ESNHNSPIFLDRFTESLHYYSTLFDSLEGVPSG----------QDKVMSEVYLGKQICNVVACDGPDRVERHETLSQWRNRFGSAGFAAAHIGSNAFKQASMLLALFNGGEGYRVEESDGC
AtRGA ESNHNGPVFLDRFTESLHYYSTLFDSLEGVPNS----------QDKVMSEVYLGKQICNLVACEGPDRVERHETLSQWGNRFGSSGLAPAHLGSNAFKQASMLLSVFNSGQGYRVEESNGC
BrRGA ESNHNGPVFLDRFTESLHYYSTLFDSLEGAPSS----------QDKVMSEVYLGKQICNLVACEGPDRVERHETLSQWSNRFGSSGFAPAHLGSNAFKQASTLLALFNGGEGYRVEENNGC
VvGAI EANHNGPVFLDRFTESLHYYSTLFDSLEGCGVSP---------VN-----TQDKLMSEVYLGQQICNVVACEGPERVERHETLAQWRARLGSAGFDPVNLGSNAFKQASMLLALFAGGDGYRVEENNGC
PsLA EANHNGPVFMDRFTEALHYYSSLFDSLEGSSNSN---------PAGSGSSSQDLLMSELYLGRQICNVVAYEGVDRVERHETLSQWRSRMGSAGFDPVHLGSNAFKQASTLLALFAGGDGYRVEENNGC
PsCRY EANHNGPAFLDRFTESLHYYSTLFDSLESSLVEP----------QDKAMSEVYLGKQICNVVACEGTDRVERHETLNQWRNRFGSAGFSPVHLGSNAFKQASMLLALFAGGDGYKVEENDGC
OsSLR1 EANHNSGSFLDRFTESLHYYSTMFDSLEGGSSGQ----AELSPPAAGGGGGTDQVMSEVYLGRQICNVVACEGAERTERHETLGQWRNRLGRAGFEPVHLGSNAYKQASTLLALFAGGDGYRVEEKEGC
HvSLN1 EANHNSGSFLDRFTESLHYYSTMFDSLEGGSSGG-PSEVSSGGAAPAAAAGTDQVMSEVYLGRQICNVVACEGTERTERHETLGQWRNRLGNAGFETVHLGSNAYKQASTLLALFAGGDGYKVEEKEGC
TaRHT EANHNSGTFLDRFTESLHYYSTMFDSLEGGSSGGGPSEVSSGAAAAPAAAGTDQVMSEVYLGRQICNVVACEGAERTERHETLGQWRNRLGNAGFETVHLGSNAYKQASTLLALFAGGDGYKVEEKEGC
ZmD8 EANHNSGTFLDRFTESLHYYSTMFDSLEGAGAGS----GQSTDASPAAAGGTDQVMSEVYLGRQICNVVACEGAERTERHETLGQWRSRLGGSGFAPVHLGSNAYKQASTLLALFAGGDGYRVEEKDGC
AtRGL1ΔDELLA EANHNGTVFLDRFTESLHYYSSLFDSLEG----------PP-----SQDRVMSELFLGRQILNLVACEGEDRVERHETLNQWRNRFGLGGFKPVSIGSNAYKQASMLLALYAGADGYNVEENEGC
AtRGL1ΔTVHYNP EANHNGTVFLDRFTESLHYYSSLFDSLEG----------PP-----SQDRVMSELFLGRQILNLVACEGEDRVERHETLNQWRNRFGLGGFKPVSIGSNAYKQASMLLALYAGADGYNVEENEGC
AtRGL1Q272R EANHNGTVFLDRFTESLHYYSSLFDSLEG----------PP-----SQDRVMSELFLGRQILNLVACEGEDRVERHETLNQWRNRFGLGGFKPVSIGSNAYKQASMLLALYAGADGYNVEENEGC
AtGAI-1 ESNHNSPIFLDRFTESLHYYSTLFDSLEGVPSG----------QDKVMSEVYLGKQICNVVACDGPDRVERHETLSQWRNRFGSAGFAAAHIGSNAFKQASMLLALFNGGEGYRVEESDGC
AtRGAΔ17 ESNHNGPVFLDRFTESLHYYSTLFDSLEGVPNS----------QDKVMSEVYLGKQICNLVACEGPDRVERHETLSQWGNRFGSSGLAPAHLGSNAFKQASMLLSVFNSGQGYRVEESNGC
VvGAIXXX EANHNGPVFLDRFTESLHYYSTLFDSLEGCGVSP---------VN-----TQDKLMSEVYLGQQICNVVACEGPERVERHETLAQWRARLGSAGFDPVNLGSNAFKQASMLLALFAGGDGYRVEENNGC
BrRGA-d ESNHNGPVFLDRFTESLHYYSTLFDSLEGAPSS----------QDKVMSEVYLGKQICNLVACEGPDRVERHETLSQWSNRFGSSGFAPAHLGSNAFKQASTLLALFNGGEGYRVEENNGC
OsSLR1ΔDELLA EANHNSGSFLDRFTESLHYYSTMFDSLEGGSSGQ----AELSPPAAGGGGGTDQVMSEVYLGRQICNVVACEGAERTERHETLGQWRNRLGRAGFEPVHLGSNAYKQASTLLALFAGGDGYRVEEKEGC
OsSLR1ΔSPACE EANHNSGSFLDRFTESLHYYSTMFDSLEGGSSGQ----AELSPPAAGGGGGTDQVMSEVYLGRQICNVVACEGAERTERHETLGQWRNRLGRAGFEPVHLGSNAYKQASTLLALFAGGDGYRVEEKEGC
OsSLR1ΔTVHYNP EANHNSGSFLDRFTESLHYYSTMFDSLEGGSSGQ----AELSPPAAGGGGGTDQVMSEVYLGRQICNVVACEGAERTERHETLGQWRNRLGRAGFEPVHLGSNAYKQASTLLALFAGGDGYRVEEKEGC
OsSLR1ΔS/T/V EANHNSGSFLDRFTESLHYYSTMFDSLEGGSSGQ----AELSPPAAGGGGGTDQVMSEVYLGRQICNVVACEGAERTERHETLGQWRNRLGRAGFEPVHLGSNAYKQASTLLALFAGGDGYRVEEKEGC
HvSLN1-d EANHNSGSFLDRFTESLHYYSTMFDSLEGGSSGG-PSEVSSGGAAPAAAAGTDQVMSEVYLGRQICNVVACEGTERTERHETLGQWRNRLGNAGFETVHLGSNAYKQASTLLALFAGGDGYKVEEKEGC
TaRht EANHNSGTFLDRFTESLHYYSTMFDSLEGGSSGGGPSEVSSGAAAAPAAAGTDQVMSEVYLGRQICNVVACEGAERTERHETLGQWRNRLGNAGFETVHLGSNAYKQASTLLALFAGGDGYKVEEKEGC
TaRHTXXX EANHNSGTFLDRFTESLHYYSTMFDSLEGGSSGGGPSEVSSGAAAAPAAAGTDQVMSEVYLGRQICNVVACEGAERTERHETLGQWRNRLGNAGFETVHLGSNAYKQASTLLALFAGGDGYKVEEKEGC
TaRHTXXX EANHNSGTFLDRFTESLHYYSTMFDSLEGGSSGGGPSEVSSGAAAAPAAAGTDQVMSEVYLGRQICNVVACEGAERTERHETLGQWRNRLGNAGFETVHLGSNAYKQASTLLALFAGGDGYKVEEKEGC
ZmD8-MP EANHNSGTFLDRFTESLHYYSTMFDSLEGAGAGS----GQSTDASPAAAGGTDQVMSEVYLGRQICNVVACEGAERTERHETLGQWRSRLGGSGFAPVHLGSNAYKQASTLLALFAGGDGYRVEEKDGC


```
AtRGL1   LLLGWQTRPLIATSAWRINRVE----------
AtGAI    LMLGWHTRPLIATSAWKLSTN-----------
AtRGA    LMLGWHTRPLITTSAWKLSTAAY---------
BrRGA    LMLSWHTRPLITTSAWKLSAVH----------
VvGAI    LMLGWHTRPLIATSAWQLANKPALPSSTPASN
PsLA     LMLGWHTRSLIATSAWKLPLSESK--------
PsCRY    LMLGWHTRPLIATSAWKLAANSMVVSH-----
OsSLR1   LTLGWHTRPLIATSAWRVAAA-----------
HvSLN1   LTLGWHTRPLIATSAWRLAAP-----------
TaRHT    LTLGWHTRPLIATSAWRLAGP-----------
ZmD8     LTLGWHTRPLIATSAWRVAAAAAP--------
```

```
AtRGL1ΔDELLA   LLLGWQTRPLIATSAWRINRVE----------
AtRGL1ΔTVHYNP  LLLGWQTRPLIATSAWRINRVE----------
AtRGL1Q272R    LLLGWQTRPLIATSAWRINRVE----------
```

```
    AtGAI-1    LMLGWHTRPLIATSAWKLSTN-----------
   AtRGAΔ17    LMLGWHTRPLITTSAWKLSTAAY---------
    VvGAIXXX   LMLGWHTRPLIATSAWQLANKPALPSSTPASN
     BrRGA-d   LMLSWHTRPLITTSAWKLSAVH----------
 OsSLR1ΔDELLA  LTLGWHTRPLIATSAWRVAAA-----------
 OsSLR1ΔSPACE  LTLGWHTRPLIATSAWRVAAA-----------
OsSLR1ΔTVHYNP  LTLGWHTRPLIATSAWRVAAA-----------
 OsSLR1ΔS/T/V  LTLGWHTRPLIATSAWRVAAA-----------
    HvSLN1-d   LTLGWHTRPLIATSAWRLAAP-----------
      TaRht    LTLGWHTRPLIATSAWRLAGP-----------
   TaRHTXXX    LTLGWHTRPLIATSAWRLAGP-----------
   TaRHTXXX    LTLGWHTRPLIATSAWRLAGP-----------
    ZmD8-MP    LTLGWHTRPLIATSAWRVAAAAAP--------
```

Appendix C

RGL1 secondary structure prediction

The secondary structure of RGL1 was predicted using Jpred (Cole *et al.*, 2008). The DELLA consensus, showing absolutely conserved residues (orange), and highly conserved residues (green) is aligned below the full-length RGL1 sequence. Predicted secondary structure elements, α-helices are in red, β-strands in green, are displayed below the primary sequence. Residues that were predicted to be buried residues are indicated by B, based on prediction using a cut-off of < 25 % probability of surface exposure.

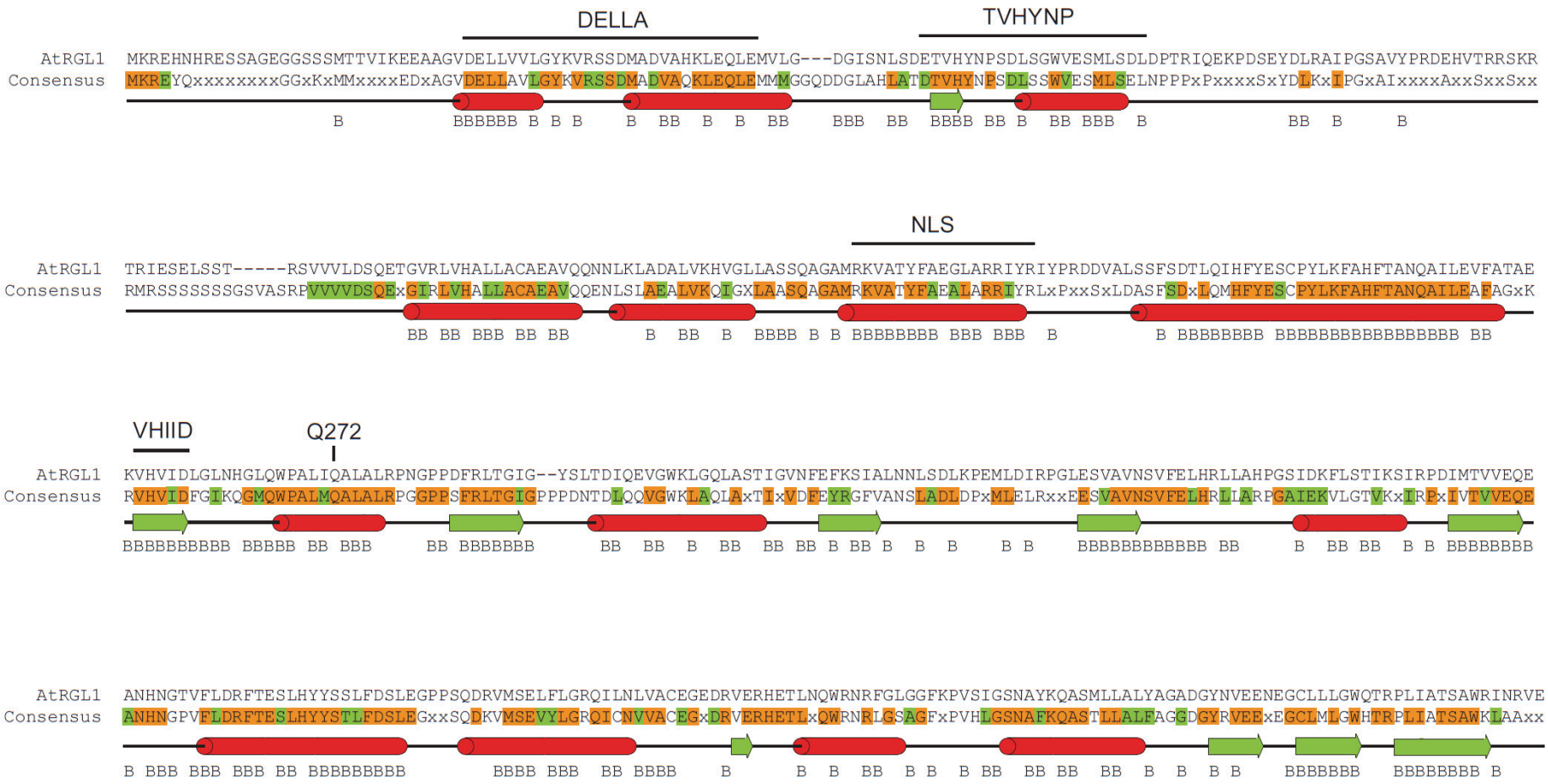
DELLA
TVHYNP
AtRGL1 MKREHNHRESSAGEGGSSSMTTVIKEEAAGVDELLVVLGYKVRSSDMADVAHKLEQLEMVLG---DGISNLSDETVHYNPSDLSGWVESMLSDLDPTRIQEKPDSEYDLRAIPGSAVYPRDEHVTRRSKR
Consensus MKREYQxxxxxxxxxGGxKxMMxxxxEDxAGVDELLAVLGYKVRSSDMADVAQKLEQLEMMMGGQDDGLAHLATDTVHYNPSDLSSWVESMLSELNPPPxPxxxxSxYDLKxIPGxAIxxxxAxxSxxSxx
NLS
AtRGL1 TRIESELSST-----RSVVVLDSQETGVRLVHALLACAEAVQQNNLKLADALVKHVGLLASSQAGAMRKVATYFAEGLARRIYRIYPRDDVALSSFSDTLQIHFYESCPYLKFAHFTANQAILEVFATAE
Consensus RMRSSSSSSSSGSVASRPVVVVDSQExGIRLVHALLACAEAVQQENLSLAEALVKQIGXLAASQAGAMRKVATYFAEAIARRIYRLxPxxSxLDASFSDxLQMHFYESCPYLKFAHFTANQAILEAFAGxK
VHIID
Q272
AtRGL1 KVHVIDLGLNHGLQWPALIQALALRPNGPPDFRLTGIG--YSLTDIQEVGWKLGQLASTIGVNFEFKSIALNNLSDLKPEMLDIRPGLESVAVNSVFELHRLLAHPGSIDKFLSTIKSIRPDIMTVVEQE
Consensus RVHVIDFGIKQGMQWPALMQALALRPGGPPSFRLTGIGPPPDNTDLQQVGWKLAQLAxTIxVDFEYRGFVANSLADLDPxMLELRxxEESVAVNSVFELHRLLARPGAIEKVLGTVKxIRPxIVTVVEQE
AtRGL1 ANHNGTVFLDRFTESLHYYSSLFDSLEGPPSQDRVMSELFLGRQILNLVACEGEDRVERHETLNQWRNRFGLGGFKPVSIGSNAYKQASMLLALYAGADGYNVEENEGCLLLGWQTRPLIATSAWRINRVE
Consensus ANHNGPVFLDRFTESLHYYSTLFDSLEGxxSQDKVMSEVYLGRQICNVVACEGxDRVERHETLxQWRNRLGSAGFxPVHLGSNAFKQASTLLALFAGGDGYRVEExEGCLMLGWHTRPLIATSAWKIAAxx

References

Achard, P., Herr, A., Baulcombe, D.C., and Harberd, N.P. (2004). Modulation of floral development by a gibberellin-regulated microRNA. Development *131*, 3357-3365.

Achard, P., Cheng, H., De Grauwe, L., Decat, J., Schoutteten, H., Moritz, T., Van der Straeten, D., Peng, J.R., and Harberd, N.P. (2006). Integration of plant responses to environmentally activated phytohormonal signals. Science *311*, 91-94.

Achard, P., Baghour, M., Chapple, A., Hedden, P., Van der Straeten, D., Genschik, P., Moritz, T., and Harberd, N.P. (2007a). The plant stress hormone ethylene controls floral transition via DELLA-dependent regulation of floral meristem-identity genes. Proceedings of the National Academy of Sciences of the United States of America *104*, 6484-6489.

Achard, P., Liao, L.L., Jiang, C.F., Desnos, T., Bartlett, J., Fu, X.D., and Harberd, N.P. (2007b). DELLAs contribute to plant photomorphogenesis. Plant Physiology *143*, 1163-1172.

Ali, S.A., and Steinkasserer, A. (1995). PCR-ligation-PCR mutagenesis - a protocol for creating gene fusions and mutations. Biotechniques *18*, 746-750.

Altschul, S.F., Gish, W., Miller, W., Myers, E.W., and Lipman, D.J. (1990). Basic local alignment search tool. Journal of Molecular Biology *215*, 403-410.

Amador, V., Monte, E., Garcia-Martinez, J.L., and Prat, S. (2001). Gibberellins signal nuclear import of PHOR1, a photoperiod-responsive protein with homology to Drosophila armadillo. Cell *106*, 343-354.

Aoyama, T., and Chua, N.H. (1997). A glucocorticoid-mediated transcriptional induction system in transgenic plants. Plant Journal *11*, 605-612.

Ariizumi, T., Murase, K., Sun, T.P., and Steber, C.M. (2008). Proteolysis-independent downregulation of DELLA repression in *Arabidopsis* by the gibberellin receptor GIBBERELLIN INSENSITIVE DWARF1. Plant Cell *20*, 2447-2459.

Arnold, K., Bordoli, L., Kopp, J., and Schwede, T. (2006). The SWISS-MODEL workspace: a web-based environment for protein structure homology modelling. Bioinformatics *22*, 195-201.

Aya, K., Ueguchi-Tanaka, M., Kondo, M., Hamada, K., Yano, K., Nishimura, M., and Matsuoka, M. (2009). Gibberellin modulates anther development in rice via the transcriptional regulation of GAMYB. Plant Cell *21*, 1453-1472.

Bae, M.S., Cho, E.J., Choi, E.Y., and Park, O.K. (2003). Analysis of the *Arabidopsis* nuclear proteome and its response to cold stress. Plant Journal *36*, 652-663.

Baluska, F., Samaj, J., and Menzel, D. (2003). Polar transport of auxin: carrier-mediated flux across the plasma membrane or neurotransmitter-like secretion? Trends in Cell Biology *13*, 282-285.

Barth, C., and Jander, G. (2006). *Arabidopsis* myrosinases TGG1 and TGG2 have redundant function in glucosinolate breakdown and insect defense. Plant Journal *46*, 549-562.

Bernier, F., and Berna, A. (2001). Germins and germin-like proteins: Plant do-all proteins. But what do they do exactly? Plant Physiology and Biochemistry *39*, 545-554.

Bethke, P.C., Hwang, Y.S., Zhu, T., and Jones, R.L. (2006). Global patterns of gene expression in the aleurone of wild-type and *dwarf1* mutant rice. Plant Physiology *140*, 484-498.

Boss, P.K., and Thomas, M.R. (2002). Association of dwarfism and floral induction with a grape 'green revolution' mutation. Nature *416*, 847-850.

Buchanan, J. (2007). Protein-protein interactions triggered by gibberellins. Honours dissertation. Institute of Molecular Biosciences (Palmerston North, Massey University).

Busk, P.K., and Pages, M. (1997). Microextraction of nuclear proteins from single maize embryos. Plant Molecular Biology Reporter *15*, 371-376.

Cao, D.N., Hussain, A., Cheng, H., and Peng, J.R. (2005). Loss of function of four *DELLA* genes leads to light- and gibberellin-independent seed germination in *Arabidopsis*. Planta *223*, 105-113.

Cao, D.N., Cheng, H., Wu, W., Soo, H.M., and Peng, J.R. (2006). Gibberellin mobilizes distinct DELLA-dependent transcriptomes to regulate seed germination and floral development in *Arabidopsis*. Plant Physiology *142*, 509-525.

Chandler, P.M., Marion-Poll, A., Ellis, M., and Gubler, F. (2002). Mutants at the *Slender1* locus of barley cv Himalaya. molecular and physiological characterization. Plant Physiology *129*, 181-190.

Chen, J.G., Pandey, S., Huang, J.R., Alonso, J.M., Ecker, J.R., Assmann, S.M., and Jones, A.M. (2004). GCR1 can act independently of heterotrimeric G-protein in response to brassinosteroids and gibberellins in Arabidopsis seed germination. Plant Physiology *135*, 907-915.

Cheng, H., Qin, L.J., Lee, S.C., Fu, X.D., Richards, D.E., Cao, D.N., Luo, D., Harberd, N.P., and Peng, J.R. (2004). Gibberellin regulates *Arabidopsis* floral development via suppression of DELLA protein function. Development *131*, 1055-1064.

Cheng, H., Li, J., Fazlieva, R., Dai, Z., Bu, Z., and Roder, H. (2009). Autoinhibitory interactions between the PDZ2 and C-terminal Domains in the scaffolding protein NHERF1. Structure *17*. 660-669.

Chiang, H.H., Hwang, I., and Goodman, H.M. (1995). Isolation of the *Arabidopsis GA4* locus. Plant Cell *7*, 195-201.

Cole, C., Barber, J.D., and Barton, G.J. (2008). The Jpred 3 secondary structure prediction server. Nucleic Acids Research *36*, W197-W201.

Cui, H.C., Levesque, M.P., Vernoux, T., Jung, J.W., Paquette, A.J., Gallagher, K.L., Wang, J.Y., Blilou, I., Scheres, B., and Benfey, P.N. (2007). An evolutionarily conserved mechanism delimiting SHR movement defines a single layer of endodermis in plants. Science *316*, 421-425.

de Lucas, M., Daviere, J.M., Rodriguez-Falcon, M., Pontin, M., Iglesias-Pedraz, J.M., Lorrain, S., Fankhauser, C., Blazquez, M.A., Titarenko, E., and Prat, S. (2008). A molecular framework for light and gibberellin control of cell elongation. Nature *451*, 480-486.

Dill, A., Jung, H.S., and Sun, T.P. (2001). The DELLA motif is essential for gibberellin-induced degradation of RGA. Proceedings of the National Academy of Sciences of the United States of America *98*, 14162-14167.

Dill, A., Thomas, S.G., Hu, J.H., Steber, C.M., and Sun, T.P. (2004). The *Arabidopsis* F-box protein SLEEPY1 targets gibberellin signaling repressors for gibberellin-induced degradation. Plant Cell *16*, 1392-1405.

Emanuelsson, O., Brunak, S., von Heijne, G., and Nielsen, H. (2007). Locating proteins in the cell using TargetP, SignalP and related tools. Nature Protocols *2*, 953-971.

Englander, J.J., Del Mar, C., Li, W., Englander, S.W., Kim, J.S., Stranz, D.D., Hamuro, Y., and Woods, V.L. (2003). Protein structure change studied by hydrogen-deuterium exchange, functional labeling, and mass spectrometry. Proceedings of the National Academy of Sciences of the United States of America *100*, 7057-7062.

Eriksson, S., Andreasson, E., Ekbom, B., Graner, G., Pontoppidan, B., Taipalensuu, J., Zhang, J.M., Rask, L., and Meijer, J. (2002). Complex formation of myrosinase isoenzymes in oilseed rape seeds are dependent on the presence of myrosinase-binding proteins. Plant Physiology *129*, 1592-1599.

Eriksson, S., Bohlenius, H., Moritz, T., and Nilsson, O. (2006). GA(4) is the active gibberellin in the regulation of *LEAFY* transcription and *Arabidopsis* floral initiation. Plant Cell *18*, 2172-2181.

Fei, H.M., Zhang, R.C., Pharis, R.P., and Sawhney, V.K. (2004). Pleiotropic effects of the *male sterile33* (*ms33*) mutation in *Arabidopsis* are associated with modifications in endogenous gibberellins, indole-3-acetic acid and abscisic acid. Planta *219*, 649-660.

Feilotter, H.E., Hannon, G.J., Ruddell, C.J., and Beach, D. (1994). Construction of an improved host strain for 2-hybrid screening. Nucleic Acids Research *22*, 1502-1503.

Feng, S.H., Martinez, C., Gusmaroli, G., Wang, Y., Zhou, J.L., Wang, F., Chen, L.Y., Yu, L., Iglesias-Pedraz, J.M., Kircher, S.*, et al.* (2008). Coordinated regulation of *Arabidopsis thaliana* development by light and gibberellins. Nature *451*, 475-479.

Fleck, B., and Harberd, N.P. (2002). Evidence that the *Arabidopsis* nuclear gibberellin signalling protein GAI is not destabilised by gibberellin. Plant Journal *32*, 935-947.

Fleet, C.M., and Sun, T.P. (2005). A DELLAcate balance: the role of gibberellin in plant morphogenesis. Current Opinion in Plant Biology *8*, 77-85.

Freemont, P.S. (2000). Ubiquitination: RING for destruction? Current Biology *10*, 84-87.

Fridborg, I., Kuusk, S., Moritz, T., and Sundberg, E. (1999). The *Arabidopsis* dwarf mutant *shi* exhibits reduced gibberellin responses conferred by overexpression of a new putative zinc finger protein. Plant Cell *11*, 1019-1031.

Fridborg, I., Kuusk, S., Robertson, M., and Sundberg, E. (2001). The *Arabidopsis* protein SHI represses gibberellin responses in *Arabidopsis* and barley. Plant Physiology *127*, 937-948.

Fu, X.D., Richards, D.E., Ait-Ali, T., Hynes, L.W., Ougham, H., Peng, J.R., and Harberd, N.P. (2002). Gibberellin-mediated proteasome-dependent degradation of the barley DELLA protein SLN1 repressor. Plant Cell *14*, 3191-3200.

Fu, X.D., and Harberd, N.P. (2003). Auxin promotes *Arabidopsis* root growth by modulating gibberellin response. Nature *421*, 740-743.

Fu, X.D., Richards, D.E., Fleck, B., Xie, D.X., Burton, N., and Harberd, N.P. (2004). The *Arabidopsis* mutant *sleepy1*(*gar2-1*) protein promotes plant growth by increasing the affinity of the SCFSLY1 E3 ubiquitin ligase for DELLA protein substrates. Plant Cell *16*, 1406-1418.

Gilroy, S., and Jones, R.L. (1994). Perception of gibberellin and abscisic-acid at the external face of the plasma-membrane of barley (Hordeum-vulgare L) aleurone protoplasts. Plant Physiology *104*, 1185-1192.

Gilroy, S. (1996). Signal transduction in barley aleurone protoplasts is calcium dependent and independent. Plant Cell *8*, 2193-2209.

Gomez-Cadenas, A., Zentella, R., Walker-Simmons, M.K., and Ho, T.H.D. (2001). Gibberellin/abscisic acid antagonism in barley aleurone cells: Site of action of the protein kinase PKABA1 in relation to gibberellin signaling molecules. Plant Cell *13*, 667-679.

Gomi, K., Sasaki, A., Itoh, H., Ueguchi-Tanaka, M., Ashikari, M., Kitano, H., and Matsuoka, M. (2004). GID2, an F-box subunit of the SCF E3 complex, specifically interacts with phosphorylated SLR1 protein and regulates the gibberellin-dependent degradation of SLR1 in rice. Plant Journal *37*, 626-634.

Griffiths, J., Murase, K., Rieu, I., Zentella, R., Zhang, Z.L., Powers, S.J., Gong, F., Phillips, A.L., Hedden, P., Sun, T.P.*, et al.* (2006). Genetic characterization and functional analysis of the GID1 gibberellin receptors in *Arabidopsis*. Plant Cell *18*, 3399-3414.

Gubler, F., Kalla, R., Roberts, J.K., and Jacobsen, J.V. (1995). Gibberellin-regulated expression of a MYB gene in barley aleurone cells - evidence for MYB transactivation of a high-pI alpha-amylase gene promoter. Plant Cell *7*, 1879-1891.

Gubler, F., Chandler, P.M., White, R.G., Llewellyn, D.J., and Jacobsen, J.V. (2002). Gibberellin signaling in barley aleurone cells. Control of *SLN1* and *GAMYB* expression. Plant Physiology *129*, 191-200.

Harberd, N.P., Belfield, E., and Yasumura, Y. (2009). The angiosperm gibberellin-GID1-DELLA growth regulatory mechanism: how an "inhibitor of an inhibitor" enables flexible response to fluctuating environments. Plant Cell *21*, 1328-1339.

Hardtke, C.S. (2003). Gibberellin signaling: GRASs growing roots. Current Biology *13*, 366-367.

Harlow, E., and Lane, D. (1988). Antibodies: A laboratory manual (Cold spring harbour, New York, Cold spring harbour laboratory press).

Hedden, P., and Phillips, A.L. (2000). Gibberellin metabolism: new insights revealed by the genes. Trends in Plant Science *5*, 523-530.

Hedden, P., Phillips, A.L., Rojas, M.C., Carrera, E., and Tudzynski, B. (2001). Gibberellin biosynthesis in plants and fungi: A case of convergent evolution? Journal of Plant Growth Regulation *20*, 319-331.

Hicke, L. (2001). Protein regulation by monoubiquitin. Nature Reviews Molecular Cell Biology *2*, 195-201.

Higuchi, R., Krummel, B., Saiki, R. (1988). A general method of *in vitro* preparation and specific mutagenesis of DNA fragments: study of protein and DNA interactions. Nucleic Acids Research *16*, 7351-7367.

Hou, X.L., Hu, W.W., Shen, L.S., Lee, L.Y.C., Tao, Z., Han, J.H., and Yu, H. (2008). Global identification of *DELLA* target genes during *Arabidopsis* flower development. Plant Physiology *147*, 1126-1142.

Hussain, A., Cao, D.N., Cheng, H., Wen, Z.L., and Peng, J.R. (2005). Identification of the conserved serine/threonine residues important for gibberellin-sensitivity of *Arabidopsis* RGL2 protein. Plant Journal *44*, 88-99.

Hussain, A., Cao, D.N., and Peng, J.R. (2007). Identification of conserved tyrosine residues important for gibberellin sensitivity of *Arabidopsis* RGL2 protein. Planta *226*, 475-483.

Ikeda, A., Ueguchi-Tanaka, M., Sonoda, Y., Kitano, H., Koshioka, M., Futsuhara, Y., Matsuoka, M., and Yamaguchi, J. (2001). *slender rice*, a constitutive gibberellin response mutant, is caused by a null mutation of the *SLR1* gene, an ortholog of the height-regulating gene *GAI*/*RGA*/*RHT*/*D8*. Plant Cell *13*, 999-1010.

Islam, M.M., Tani, C., Watanabe-Sugimoto, M., Uraji, M., Jahan, M.S., Masuda, C., Nakamura, Y., Mori, I.C., and Murata, Y. (2009). Myrosinases, TGG1 and TGG2, redundantly function in ABA and MeJA signaling in *Arabidopsis* guard cells. Plant and Cell Physiology *50*, 1171-1175.

Itoh, H., Tanaka-Ueguchi, M., Kawaide, H., Chen, X.B., Kamiya, Y., and Matsuoka, M. (1999). The gene encoding tobacco gibberellin 3 beta-hydroxylase is expressed at the site of GA action during stem elongation and flower organ development. Plant Journal *20*, 15-24.

Itoh, H., Ueguchi-Tanaka, M., Sentoku, N., Kitano, H., Matsuoka, M., and Kobayashi, M. (2001). Cloning and functional analysis of two gibberellin 3 beta-hydroxylase genes that are differently expressed during the growth of rice. Proceedings of the National Academy of Sciences of the United States of America *98*, 8909-8914.

Itoh, H., Ueguchi-Tanaka, M., Sato, Y., Ashikari, M., and Matsuoka, M. (2002). The gibberellin signaling pathway is regulated by the appearance and disappearance of SLENDER RICE1 in nuclei. Plant Cell *14*, 57-70.

Itoh, H., Sasaki, A., Ueguchi-Tanaka, M., Ishiyama, K., Kobayashi, M., Hasegawa, Y., Minami, E., Ashikari, M., and Matsuoka, M. (2005). Dissection of the phosphorylation of rice DELLA protein, SLENDER RICE1. Plant and Cell Physiology *46*, 1392-1399.

Iuchi, S., Suzuki, H., Kim, Y.C., Iuchi, A., Kuromori, T., Ueguchi-Tanaka, M., Asami, T., Yamaguchi, I., Matsuoka, M., Kobayashi, M.*, et al.* (2007). Multiple loss-of-function of *Arabidopsis* gibberellin receptor AtGID1s completely shuts down a gibberellin signal. Plant Journal *50*, 958-966.

Kaneko, M., Itoh, H., Inukai, Y., Sakamoto, T., Ueguchi-Tanaka, M., Ashikari, M., and Matsuoka, M. (2003). Where do gibberellin biosynthesis and gibberellin signaling occur in rice plants? Plant Journal *35*, 104-115.

Kaneko, M., Inukai, Y., Ueguchi-Tanaka, M., Itoh, H., Izawa, T., Kobayashi, Y., Hattori, T., Miyao, A., Hirochika, H., Ashikari, M.*, et al.* (2004). Loss-of-function mutations of the rice *GAMYB* gene impair alpha-amylase expression in aleurone and flower development. Plant Cell *16*, 33-44.

Karlsson, R., Michaelsson, A., and Mattsson, L. (1991). Kinetic-analysis of monoclonal antibody-antigen interactions with a new biosensor based analytical system. Journal of Immunological Methods *145*, 229-240.

Kato, C., Mizutani, T., Tamaki, H., Kumagai, H., Kamiya, T., Hirobe, A., Fujisawa, Y., Kato, H., and Iwasaki, Y. (2004). Characterization of heterotrimeric G protein complexes in rice plasma membrane. Plant Journal *38*, 320-331.

King, K.E., Moritz, T., and Harberd, N.P. (2001). Gibberellins are not required for normal stem growth in *Arabidopsis thaliana* in the absence of *GAI* and *RGA*. Genetics *159*, 767-776.

Kipreos, E.T., and Pagano, M. (2000). The F-box protein family. Genome Biology *1*, 30021-30027.

Koornneef, M., and Vanderveen, J.H. (1980). Induction and analysis of gibberellin sensitive mutants in *Arabidopsis-thaliana* (L) Heynh. Theoretical and Applied Genetics *58*, 257-263.

Koornneef, M., Elgersma, A., Hanhart, C.J., Vanloenenmartinet, E.P., Vanrijn, L., and Zeevaart, J.A.D. (1985). A gibberellin insensitive mutant of *Arabidopsis-thaliana*. Physiologia Plantarum *65*, 33-39.

Laemmli, U.K. (1970). Cleavage of structural proteins during assembly of head of bacteriophage-T4. Nature *227*, 680-685.

Lambrix, V., Reichelt, M., Mitchell-Olds, T., Kliebenstein, D.J., and Gershenzon, J. (2001). The *Arabidopsis* epithiospecifier protein promotes the hydrolysis of glucosinolates to nitriles and influences *Trichoplusia ni* herbivory. Plant Cell *13*, 2793-2807.

Larkin, M.A., Blackshields, G., Brown, N.P., Chenna, R., McGettigan, P.A., McWilliam, H., Valentin, F., Wallace, I.M., Wilm, A., Lopez, R.*, et al.* (2007). Clustal W and clustal X version 2.0. Bioinformatics *23*, 2947-2948.

Lee, S.C., Cheng, H., King, K.E., Wang, W.F., He, Y.W., Hussain, A., Lo, J., Harberd, N.P., and Peng, J.R. (2002). Gibberellin regulates *Arabidopsis* seed germination via *RGL2*, a *GAI*/*RGA*-like gene whose expression is up-regulated following imbibition. Genes & Development *16*, 646-658.

Li, L., Elledge, S.J., Peterson, C.A., Bales, E.S., and Legerski, R.J. (1994). Specific association between the human DNA-repair proteins XPA and ERCC1. Proceedings of the National Academy of Sciences of the United States of America *91*, 5012-5016.

Louvet, O., Doignon, F., and Crouzet, M. (1997). Stable DNA-binding yeast vector allowing high-bait expression for use in the two-hybrid system. Biotechniques *23*, 816-820.

Maymon, I., Greenboim-Wainberg, Y., Sagiv, S., Kieber, J.J., Moshelion, M., Olszewski, N., and Weiss, D. (2009). Cytosolic activity of SPINDLY implies the existence of a DELLA-independent gibberellin-response pathway. Plant Journal *58*, 979-988.

McCubbin, A.G., Ritchie, S.M., Swanson, S.J., and Gilroy, S. (2004). The calcium-dependent protein kinase HvCDPK1 mediates the gibberellic acid response of the barley aleurone through regulation of vacuolar function. Plant Journal *39*, 206-218.

McGinnis, K.M., Thomas, S.G., Soule, J.D., Strader, L.C., Zale, J.M., Sun, T.P., and Steber, C.M. (2003). The *Arabidopsis SLEEPY1* gene encodes a putative F-box subunit of an SCF E3 ubiquitin ligase. Plant Cell *15*, 1120-1130.

Membre, N., Berna, A., Neutelings, G., David, A., David, H., Staiger, D., Vasquez, J.S., Raynal, M., Delseny, M., and Bernier, F. (1997). cDNA sequence, genomic organization and differential expression of three *Arabidopsis* genes for germin oxalate oxidase-like proteins. Plant Molecular Biology *35*, 459-469.

Membre, N., Bernier, F., Staiger, D., and Berna, A. (2000). *Arabidopsis thaliana* germin-like proteins: common and specific features point to a variety of functions. Planta *211*, 345-354.

Millar, A.A., and Gubler, F. (2005). The *Arabidopsis GAMYB*-like genes, *MYB33* and *MYB65*, are MicroRNA-regulated genes that redundantly facilitate anther development. Plant Cell *17*, 705-721.

Mitchum, M.G., Yamaguchi, S., Hanada, A., Kuwahara, A., Yoshioka, Y., Kato, T., Tabata, S., Kamiya, Y., and Sun, T.P. (2006). Distinct and overlapping roles of two gibberellin 3-oxidases in *Arabidopsis* development. Plant Journal *45*, 804-818.

Monte, E., Amador, V., Russo, E., Martinez-Garcia, J., and Prat, S. (2003). PHOR1: A U-Box GA signaling component with a role in proteasome degradation? Journal of Plant Growth Regulation *22*, 152-162.

Morton, T.A., Myszka, D.G., and Chaiken, I.M. (1995). Interpreting complex binding-kinetics from optical biosensors - a comparison of analysis by linearization, the integrated rate-equation, and numerical-integration. Analytical Biochemistry *227*, 176-185.

Muangprom, A., Thomas, S.G., Sun, T.P., and Osborn, T.C. (2005). A novel dwarfing mutation in a green revolution gene from *Brassica rapa*. Plant Physiology *137*, 931-938.

Murase, K., Hirano, Y., Sun, T.P., and Hakoshima, T. (2008). Gibberellin-induced DELLA recognition by the gibberellin receptor GID1. Nature *456*, 459-463.

Murray, F., Kalla, R., Jacobsen, J., and Gubler, F. (2003). A role for HvGAMYB in anther development. Plant Journal *33*, 481-491.

Nakai, K., and Kanehisa, M. (1991). Expert system for predicting protein localization sites in gram-negative bacteria. Proteins-Structure Function and Genetics *11*, 95-110.

Nakajima, M., Shimada, A., Takashi, Y., Kim, Y.C., Park, S.H., Ueguchi-Tanaka, M., Suzuki, H., Katoh, E., Iuchi, S., Kobayashi, M*., et al.* (2006). Identification and characterization of *Arabidopsis* gibberellin receptors. Plant Journal *46*, 880-889.

Nanjo, Y., Asatsuma, S., Itoh, K., Hori, H., Mitsui, T., and Fujisawa, Y. (2004). Posttranscriptional regulation of alpha-amylase II-4 expression by gibberellin in germinating rice seeds. Plant Physiology and Biochemistry *42*, 477-484.

Nemhauser, J.L., Hong, F.X., and Chory, J. (2006). Different plant hormones regulate similar processes through largely nonoverlapping transcriptional responses. Cell *126*, 467-475.

O'Shannessy, D.J. (1994). Determination of kinetic rate and equilibrium binding constants for macromolecular interactions: a critique of the surface plasmon resonance literature. Current Opinion in Biotechnology *5*, 65-71.

Offermanns, S. (2003). G-proteins as transducers in transmembrane signalling. Progress in Biophysics & Molecular Biology *83*, 101-130.

Ogawa, M., Hanada, A., Yamauchi, Y., Kuwalhara, A., Kamiya, Y., and Yamaguchi, S. (2003). Gibberellin biosynthesis and response during *Arabidopsis* seed germination. Plant Cell *15*, 1591-1604.

Ohmiya, A., Tanaka, Y., Kadowaki, K., and Hayashi, T. (1998). Cloning of genes encoding auxin-binding proteins (ABP19/20) from peach: Significant peptide sequence similarity with germin-like proteins. Plant and Cell Physiology *39*, 492-499.

Ormö, M., Cubitt, A. B., Kallio, K., Gross, L. A., Tsien, R. Y., and Remington S. J. (1996). Crystal structure of the *Aequorea victoria* green fluorescent protein. Science *273*. 1392-1395.

Osterlund, T. (2001). Structure-function relationships of hormone-sensitive lipase. European Journal of Biochemistry *268*, 1899-1907.

Pappin, D.J.C., Hojrup, P., and Bleasby, A.J. (1993). Rapid identification of protein by peptide-mass fingerprinting. Current Biology *3*, 327-332.

Park, S.H., Nakajima, M., Hasegawa, M., and Yamaguchi, I. (2005). Similarities and differences between the characteristics of gibberellin-binding protein and gibberellin 2-oxidases in adzuki bean (*Vigna angularis*) seedlings. Bioscience Biotechnology and Biochemistry *69*, 1508-1514.

Peng, J.R., Carol, P., Richards, D.E., King, K.E., Cowling, R.J., Murphy, G.P., and Harberd, N.P. (1997). The *Arabidopsis GAI* gene defines a signaling pathway that negatively regulates gibberellin responses. Genes & Development *11*, 3194-3205.

Peng, J.R., Richards, D.E., Hartley, N.M., Murphy, G.P., Devos, K.M., Flintham, J.E., Beales, J., Fish, L.J., Worland, A.J., Pelica, F*., et al.* (1999). 'Green revolution' genes encode mutant gibberellin response modulators. Nature *400*, 256-261.

Penson, S.P., Schuurink, R.C., Fath, A., Gubler, F., Jacobsen, J.V., and Jones, R.L. (1996). cGMP is required for gibberellic acid-induced gene expression in barley aleurone. Plant Cell *8*, 2325-2333.

Phillips, A.L., Ward, D.A., Uknes, S., Appleford, N.E.J., Lange, T., Huttly, A.K., Gaskin, P., Graebe, J.E., and Hedden, P. (1995). Isolation and expression of 3 gibberellin 20-oxidase cDNA clones from *Arabidopsis*. Plant Physiology *108*, 1049-1057.

Pysh, L.D., Wysocka-Diller, J.W., Camilleri, C., Bouchez, D., and Benfey, P.N. (1999). The GRAS gene family in *Arabidopsis*: sequence characterization and basic expression analysis of the SCARECROW-LIKE genes. Plant Journal *18*, 111-119.

Richards, D.E., King, K.E., Ait-ali, T., and Harberd, N.P. (2001). How gibberellin regulates plant growth and development: a molecular genetic analysis of gibberellin signaling. Annual Review of Plant Physiology and Plant Molecular Biology *52*, 67-88.

Robertson, M. (2004). Two transcription factors are negative regulators of gibberellin response in the HvSPY-signaling pathway in barley aleurone. Plant Physiology *136*, 2747-2761.

Sambrook, J., and Russell, D. (2001). Molecular cloning: A laboratory manual, Third edn (Cold spring harbour, New York, Cold spring harbour laboratory press).

Sasaki, A., Itoh, H., Gomi, K., Ueguchi-Tanaka, M., Ishiyama, K., Kobayashi, M., Jeong, D.H., An, G., Kitano, H., Ashikari, M.*, et al.* (2003). Accumulation of phosphorylated repressor for gibberellin signaling in an F-box mutant. Science *299*, 1896-1898.

Schagger, H., and Von Jagow, G. (1987). Tricine sodium dodecyl-sulfate polyacrylamide-gel electrophoresis for the separation of proteins in the range from 1-kDa to 100-kDa. Analytical Biochemistry *166*, 368-379.

Schagger, H. (2001). Blue-native gels to isolate protein complexes from mitochondria. In Methods in Cell Biology, Vol 65 (San Diego, Academic Press Inc), pp. 231-244.

Schuurink, R.C., Chan, P.V., and Jones, R.L. (1996). Modulation of calmodulin mRNA and protein levels in barley aleurone. Plant Physiology *111*, 371-380.

Schmid, M., Davison, T.S., Henz, S.R., Pape, U.J., Demar, M., Vingron, M., Schölkopf, B., Weigel, D. and Lohmann, J.U. (2005). A gene expression map of *Arabidopsis thaliana* development. Nature Genetics *37*, 501-506.

Sheerin, D. (2005). Interactions of AtRGL1, a negative regulator of gibberellic acid signalling. MSc thesis. Institute of Molecular biosciences (Palmerston North, Massey University).

Shimada, A., Ueguchi-Tanaka, M., Sakamoto, T., Fujioka, S., Takatsuto, S., Yoshida, S., Sazuka, T., Ashikari, M., and Matsuoka, M. (2006). The rice *SPINDLY* gene functions as a negative regulator of gibberellin signaling by controlling the suppressive function of the DELLA protein, SLR1, and modulating brassinosteroid synthesis. Plant Journal *48*, 390-402.

Shimada, A., Ueguchi-Tanaka, M., Nakatsu, T., Nakajima, M., Naoe, Y., Ohmiya, H., Kato, H., and Matsuoka, M. (2008). Structural basis for gibberellin recognition by its receptor GID1. Nature *456*, 520-523.

Shirakawa, M., Ueda, H., Shimada, T., Nishiyama, C., and Hara-Nishimura, I. (2009). Vacuolar SNAREs function in the formation of the leaf vascular network by regulating auxin distribution. Plant and Cell Physiology *50*, 1319-1328.

Silverstone, A.L., Mak, P.Y.A., Martinez, E.C., and Sun, T.P. (1997). The new *RGA* locus encodes a negative regulator of gibberellin response in *Arabidopsis thaliana*. Genetics *146*, 1087-1099.

Silverstone, A.L., Ciampaglio, C.N., and Sun, T.P. (1998). The *Arabidopsis RGA* gene encodes a transcriptional regulator repressing the gibberellin signal transduction pathway. Plant Cell *10*, 155-169.

Silverstone, A.L., Jung, H.S., Dill, A., Kawaide, H., Kamiya, Y., and Sun, T.P. (2001). Repressing a repressor: Gibberellin-induced rapid reduction of the RGA protein in *Arabidopsis*. Plant Cell *13*, 1555-1565.

Silverstone, A.L., Tseng, T.S., Swain, S.M., Dill, A., Jeong, S.Y., Olszewski, N.E., and Sun, T.P. (2007). Functional analysis of SPINDLY in gibberellin signaling in *Arabidopsis*. Plant Physiology *143*, 987-1000.

Smyth, D.R., Bowman, J.L., and Meyerowitz, E.M. (1990). Early flower development in *Arabidopsis*. Plant Cell *2*, 755-767.

Strader, L.C., Ritchie, S., Soule, J.D., McGinnis, K.M., and Steber, C.M. (2004). Recessive-interfering mutations in the gibberellin signaling gene *SLEEPY1* are rescued by overexpression of its homologue, *SNEEZY*. Proceedings of the National Academy of Sciences of the United States of America *101*, 12771-12776.

Sun, X.L., Frearson, N., Kirk, C., Jones, W.T., Harvey, D., Rakonjac, J., Foster, T., and Al-Samarrai, T. (2008). An *E. coli* expression system optimized for DELLA proteins. Protein Expression and Purification *58*, 168-174.

Sun, X.L., Jones, W.T., Harvey, D., Edwards, P.J.B., Pascal, S.M., Kirk, C., Considine, T., Sheerin, D.J., Rakonjac, J., Oldfield, C.J.*, et al.* (2010). N-terminal domains of DELLA proteins are intrinsically unstructured in the absence of interaction with GID1/gibberellic acid receptors. Journal of Biological Chemistry *285*, 11557-11571.

Swain, S.M., Tseng, T.S., and Olszewski, N.E. (2001). Altered expression of SPINDLY affects gibberellin response and plant development. Plant Physiology *126*, 1174-1185.

Swain, S.M., Tseng, T.S., Thornton, T.M., Gopalraj, M., and Olszewski, N.E. (2002). SPINDLY is a nuclear-localized repressor of gibberellin signal transduction expressed throughout the plant. Plant Physiology *129*, 605-615.

Swain, S.M., Muller, A.J., and Singh, D.P. (2004). The *gar2* and *rga* alleles increase the growth of gibberellin-deficient pollen tubes in *Arabidopsis*. Plant Physiology *134*, 694-705.

Swain, S.M., and Singh, D.P. (2005). Tall tales from sly dwarves: novel functions of gibberellins in plant development. Trends in Plant Science *10*, 123-129.

Talon, M., Koornneef, M., and Zeevaart, J.A.D. (1990). Endogenous gibberellins in *Arabidopsis thaliana* and possible steps blocked in the biosynthetic pathways of the semidwarf *GA4* and *GA5* mutants. Proceedings of the National Academy of Sciences of the United States of America *87*, 7983-7987.

Thomas, S.G., Phillips, A.L., and Hedden, P. (1999). Molecular cloning and functional expression of gibberellin 2-oxidases, multifunctional enzymes involved in gibberellin deactivation. Proceedings of the National Academy of Sciences of the United States of America *96*, 4698-4703.

Tirode, F., Malaguti, C., Romero, F., Attar, R., Camonis, J., and Egly, J.M. (1997). A conditionally expressed third partner stabilizes or prevents the formation of a transcriptional activator in a three-hybrid system. Journal of Biological Chemistry *272*, 22995-22999.

Tsuji, H., Aya, K., Ueguchi-Tanaka, M., Shimada, Y., Nakazono, M., Watanabe, R., Nishizawa, N.K., Gomi, K., Shimada, A., Kitano, H.*, et al.* (2006). GAMYB controls different sets of genes and is differentially regulated by microRNA in aleurone cells and anthers. Plant Journal *47*, 427-444.

Tyler, L., Thomas, S.G., Hu, J.H., Dill, A., Alonso, J.M., Ecker, J.R., and Sun, T.P. (2004). DELLA proteins and gibberellin-regulated seed germination and floral development in *Arabidopsis*. Plant Physiology *135*, 1008-1019.

Ueda, H., Nishiyama, C., Shimada, T., Koumoto, Y., Hayashi, Y., Kondo, M., Takahashi, T., Ohtomo, I., Nishimura, M., and Hara-Nishimura, I. (2006). AtVAM3 is required for normal specification of idioblasts, myrosin cells. Plant and Cell Physiology *47*, 164-175.

Ueguchi-Tanaka, M., Fujisawa, Y., Kobayashi, M., Ashikari, M., Iwasaki, Y., Kitano, H., and Matsuoka, M. (2000). Rice dwarf mutant *d1*, which is defective in the alpha subunit of the heterotrimeric G protein, affects gibberellin signal transduction. Proceedings of the National Academy of Sciences of the United States of America *97*, 11638-11643.

Ueguchi-Tanaka, M., Ashikari, M., Nakajima, M., Itoh, H., Katoh, E., Kobayashi, M., Chow, T.Y., Hsing, Y.I.C., Kitano, H., Yamaguchi, I.*, et al.* (2005). *GIBBERELLIN INSENSITIVE DWARF1* encodes a soluble receptor for gibberellin. Nature *437*, 693-698.

Ueguchi-Tanaka, M., Nakajima, M., Katoh, E., Ohmiya, H., Asano, K., Saji, S., Xiang, H.Y., Ashikari, M., Kitano, H., Yamaguchi, I.*, et al.* (2007). Molecular interactions of a soluble gibberellin receptor, GID1, with a rice DELLA protein, SLR1, and gibberellin. Plant Cell *19*, 2140-2155.

Vriezen, W.H., Achard, P., Harberd, N.P., and Van der Straeten, D. (2004). Ethylene-mediated enhancement of apical hook formation in etiolated *Arabidopsis thaliana* seedlings is gibberellin dependent. Plant Journal *37*, 505-516.

Ueguchi-Tanaka, M., Hirano, K., Hasegawa, Y., Kitano, H., and Matsuoka, M. (2008). Release of the repressive activity of rice DELLA protein SLR1 by gibberellin does not require SLR1 degradation in the *gid2* mutant. Plant Cell *20*, 2437-2446.

Ullah, H., Chen, J.G., Wang, S.C., and Jones, A.M. (2002). Role of a heterotrimeric G protein in regulation of *Arabidopsis* seed germination. Plant Physiology *129*, 897-907.

Wang, F., Zhu, D.M., Huang, X., Li, S., Gong, Y.N., Yao, Q.F., Fu, X.D., Fan, L.M., and Deng, X.W. (2009). Biochemical insights on degradation of *Arabidopsis* DELLA proteins gained from a cell-free assay system. Plant Cell *21*, 2378-2390.

Washio, K., and Morikawa, M. (2006). Common mechanisms regulating expression of rice aleurone genes that contribute to the primary response for gibberellin. Biochimica Et Biophysica Acta-Gene Structure and Expression *1759*, 478-490.

Weiss, D., and Ori, N. (2007). Mechanisms of cross talk between gibberellin and other hormones. Plant Physiology *144*, 1240-1246.

Wen, C.K., and Chang, C. (2002). Arabidopsis *RGL1* encodes a negative regulator of gibberellin responses. Plant Cell *14*, 87-100.

Weston, D.E., Elliott, R.C., Lester, D.R., Rameau, C., Reid, J.B., Murfet, I.C., and Ross, J.J. (2008). The pea DELLA proteins LA and CRY are important regulators of gibberellin synthesis and root growth. Plant Physiology *147*, 199-205.

Weston, D.E., Reid, J.B., and Ross, J.J. (2009). Auxin regulation of gibberellin biosynthesis in the roots of pea (*Pisum sativum*). Functional Plant Biology *36*, 362-369.

Willige, B.C., Ghosh, S., Nill, C., Zourelidou, M., Dohmann, E.M.N., Maier, A., and Schwechheimer, C. (2007). The DELLA domain of GA INSENSITIVE mediates the interaction with the GA INSENSITIVE DWARF1A gibberellin receptor of *Arabidopsis*. Plant Cell *19*, 1209-1220.

Wilson, R.N., and Somerville, C.R. (1995). Phenotypic suppression of the gibberellin-insensitive mutant (*gai*) of *Arabidopsis*. Plant Physiology *108*, 495-502.

Wu, S.T., Skolnick, J., and Zhang, Y. (2007). *Ab initio* modeling of small proteins by iterative TASSER simulations. Bmc Biology *5*, 17

Xu, Y.L., Li, L., Wu, K.Q., Peeters, A.J.M., Gage, D.A., and Zeevaart, J.A.D. (1995). The *GA5* locus of *Arabidopsis thaliana* encodes a multifunctional gibberellin 20-oxidase - molecular cloning and functional expression. Proceedings of the National Academy of Sciences of the United States of America *92*, 6640-6644.

Yamaguchi, S., Smith, M.W., Brown, R.G.S., Kamiya, Y., and Sun, T.P. (1998). Phytochrome regulation and differential expression of gibberellin 3 beta-hydroxylase genes in germinating *Arabidopsis* seeds. Plant Cell *10*, 2115-2126.

Yang, Y.Y., Nagatani, A., Zhao, Y.J., Kang, B.J., Kendrick, R.E., and Kamiya, Y. (1995). Effects of gibberellins on seed germination of phytochrome-deficient mutants of *Arabidopsis thaliana*. Plant and Cell Physiology *36*, 1205-1211.

Yasumura, Y., Crumpton-Taylor, M., Fuentes, S., and Harberd, N.P. (2007). Step-by-step acquisition of the gibberellin-DELLA growth-regulatory mechanism during land-plant evolution. Current Biology *17*, 1225-1230.

Zentella, R., Zhang, Z.L., Park, M., Thomas, S.G., Endo, A., Murase, K., Fleet, C.M., Jikumaru, Y., Nambara, E., Kamiya, Y.*, et al.* (2007). Global analysis of DELLA direct targets in early gibberellin signaling in *Arabidopsis*. Plant Cell *19*, 3037-3057.

Zhang, Y. (2007). Template-based modeling and free modeling by I-TASSER in CASP7. Proteins-Structure Function and Bioinformatics *69*, 108-117.

Zhang, Y. (2008). I-TASSER server for protein 3D structure prediction. Bmc Bioinformatics *9*, 40

Zhao, Z.X., Zhang, W., Stanley, B.A., and Assmann, S.M. (2008). Functional proteomics of *Arabidopsis thaliana* guard cells uncovers new stomatal signaling pathways. Plant Cell *20*, 3210-3226.